FACTORS INFLUENCING STARCH CHAIN REALIGNMENT AND INTERACTIONS WITHIN THE AMORPHOUS AND CRYSTALLINE DOMAINS OF PULSE AND HIGH AMYLOSE MAIZE STARCHES ON ANNEALING

By

©Maaran Suntharamoorthy

A dissertation submitted to the

School of Graduate Studies

in partial fulfillment of the requirements for the degree of

Doctor of Philosophy

Department of Biochemistry

Memorial University of Newfoundland

October 2017

St. John's Newfoundland and Labrador Canada

This thesis work is dedicated to my former supervisor, Dr. R. Hoover, who, although no longer with us, continues to inspire by his perseverance and hardwork to the students he guided during his tenure

Abstract

The composition, morphology, structure and physicochemical properties of starches extracted from lablab bean, navy bean, rice bean, tepary bean and velvet bean were examined. Imaging techniques revealed the presence of cracks on granule surfaces and disorganized starch chains near the vicinity of the hilum in some starches. The starches exhibited wide variations with respect to granular size and specific surface area. Molecular order, molecular orientation (birefringence), double helical content, crystallinity, crystalline perfection and crystalline stability differed among the pulse starches. However, they exhibited similar amylopectin chain length distribution. The results showed that interplay among differences in molecular order, double helical content, relative crystallinity, amylose content, granule morphology and the extent of interactions between starch chains within the amorphous and crystalline domains, influenced thermal, rheological and digestibility properties. The factors underlying the susceptibility of pulse (including wrinkled pea) and Hylon®VII starches toward *in vitro* hydrolysis were studied. The rate and extent of hydrolysis were influenced by the structure of the native starches at different levels (molecular, supramolecular, granular) of granule organization, and by the extent of interaction among hydrolysed starch chains. Starches were modified by annealing treatment. Annealing increased the relative crystallinity and the onset (To) and melting (Tp) temperatures and decreased the gelatinization temperature range (Tc-To). The increase in Tp and decrease in Tc-To suggest that annealing improved double helix arrangement by decreasing heterogeneity within the crystalline lamellae. This study showed that the organization of starch chains

within the amorphous and crystalline domains of native starches influenced reorganization of starch chains on annealing. The extent of these changes differed between normal and high amylose starches due to the structural differences that exist in both amorphous and crystalline regions. The role of amorphous regions on annealing was studied using the approaches of partial acid hydrolysis and cross-linking with sodium trimetaphosphate and sodium tripolyphosphate. The results suggest that the amorphous regions contributed to the molecular mechanism of annealing by influencing the realignment of glucan chains in the crystalline regions.

Acknowledgements

It is with immense gratitude that I acknowledge the help and guidance of the late Dr. R Hoover throughout my program at MUN. During my period of study, he remained very supportive by encouraging my research, sharing his knowledge and experience, and preparing me to grow as a researcher. I also would like to express my special appreciation and thanks to Dr. R. Brown who took the role of my supervisor after the unfortunate passing of Dr. Hoover last year. Without his vital support and assistance, this thesis would not have been possible. Additionally, I would like to thank my committee members, Dr. V. Booth and Dr. D. Dave, for providing me extensive guidance and invaluable suggestions. I gratefully acknowledge the Department of Biochemistry, School of Graduate Studies and NSERC for the financial support to undertake my doctoral research.

I also am indebted to Dr. Q. Liu, Dr. E. Donner, Dr. V. Vamadevan, Dr. R. Waduge, Dr. M. Shaffer, Dr. C. Schnider, Dr. D. Davidson, Dr. D. Grant, Dr. W. Aylward and Mrs. S. Strowbridge, for their support in some of the analytical techniques during my research. I am particularly grateful for the assistance given by Dr. A. Yethiraj in using confocal and polarized microscopy. I specially thank Craig and Marie Codner for their technical assistance. I also would like to thank my lab mates, colleagues, and all the faculty and staff members of the Department of Biochemistry for their help and encouragement. Finally, I would like to thank my family and friends who have always stood by me in hard times. I owe my deepest gratitude to them for providing unconditional support and constant encouragement which helped me to realize my dream.

Table of contents

List of Figures

List of Tables

List of abbreviations

AAC	-	Apparent amylose content
AACC	-	American Association of Cereal Chemists
ADP	-	Adenosine diphosphate
ADP-Glc	-	Adenosine 5'-diphosphate-glucose
ae	-	Amylose extender
AGPase	-	ADP glucose pyrophosphorylase
AML	-	Amylose leaching
ANN	-	Annealing
ANOVA	-	Analysis of variance
APCLD	-	Amylopectin chain length distribution
APTS	-	8-amino-1, 3, 6-pyrenetrisulfonic acid
ATP	-	Adenosine triphosphate
ATR-FTIR	-	Attenuated total reflectance Fourier transform infrared spectroscopy
AUC	-	Area under the curve
BL	-	Bound lipid
^{13}C CP/MAS NMR	-	^{13}C cross-polarization magic angle spinning nuclear magnetic resonance
$\overline{CL}$	-	Average chain length
CL	-	Cross-linked
CLD	-	Chain length distribution
CL-ANN	-	Cross-linked and annealed
CLSM	-	Confocal laser scanning microscopy

dwb	-	Dry weight basis
DBE	-	Debranching enzyme
DHC	-	Double helical content
DMSO	-	Dimethyl sulfoxide
dp	-	Degree of polymerization
dp_n	-	Degree of polymerization by number
DS	-	Degree of substitution
DSC	-	Differential scanning calorimetry
DTGS	-	Deuterated triglycine sulfate
Dwb	-	Dry weight basis
EC	-	Enzyme Commission
eGI	-	Expected glycemic index
ELC	-	Extra-long unit chains
FFA	-	Free fatty acids
G-1-P	-	Glucose-1-phosphate
GBBS	-	Granule-bound starch synthase
GH	-	Glycoside hydrolase
GI	-	Glycemic index
GOPOD	-	Glucose oxidase/peroxidase
HPAEC-PAD	-	High performance anion exchange chromatography with pulsed amperometric detection
ΔH	-	Enthalpy of gelatinization
ΔH_R	-	Enthalpy of gelatinization (retrogradation)
HYVII	-	Hylon®VII

ICP-OES	-	Inductively coupled plasma-optical emission spectrometry
ISA	-	Isoamylase
LB	-	Lablab bean
LysoPL	-	Lysophospholipid
MG	-	Monoacylglycerol
Mw	-	Molecular weight
MSMP	-	Monostarch monophosphate
NB	-	Navy bean
NMR	-	Nuclear magnetic resonance
P-enzyme	-	Plastidal starch phosphorylase
3-PGA	-	3-phosphoglycerate
PLM	-	Polarized light microscopy
PPA	-	Porcine pancreatic α-amylase
PPi	-	Pyrophosphate
RB	-	Rice bean
RDS	-	Rapidly digestible starch
RE	-	Reaction efficiency
RS	-	Resistant starch
RVA	-	Rapid visco analyser
SANS	-	Small angle X-ray scattering
SAXS	-	Small angle nuclear scattering
sb	-	Starch weight basis
SBE	-	Starch branching enzyme

SCFA	-	Short chain fatty acids
SD	-	Starch damage
SDS	-	Slowly digestible starch
SEM	-	Scanning electron microscopy
SF	-	Swelling factor
SL	-	Surface lipid
SP	-	Swelling power
SS	-	Starch synthase
SSA	-	Specific surface area
STMP	-	Sodium trimetaphosphate
STPP	-	Sodium tripolyphosphate
SuSy	-	Sucrose synthase
%T	-	Percentage light transmission
TB	-	Tepary bean
Tc	-	Conclusion temperature of gelatinization
Tc-To	-	Gelatinization temperature range
Tg	-	Glass transition temperature
Tm	-	Peak minimum/melting temperature of gelatinization
TMS	-	Tetramethylsilane
To	-	Onset temperature of gelatinization
Tp	-	Peak temperature of gelatinization
TS	-	Total starch
UDP-glucose	-	Uridine diphosphate glucose

VB	-	Velvet bean
v/v	-	Volume/volume
WAXS	-	Wide angle X-ray diffraction
WP	-	Wrinkled pea
w/v	-	Weight/volume
w/w	-	Weight/weight
wx	-	Waxy
XRD	-	X-ray diffraction

Chapter 1

Introduction

1.1 Introduction and overview

Pulses, a subgroup of legumes, are the edible seeds of plants belonging to the *Fabaceae* (*Leguminoseae*) family which has 16,000–19,000 species in approximately 750 genera (Allen & Allen, 1981; Hoover *et al.*, 2010). Nutritionally, pulses are considered an important part of the human diet in many regions of the world since they are an inexpensive and rich source of protein, carbohydrate, dietary fiber, vitamins, minerals and phytochemicals (Jood *et al.*, 1988). Starch (22 % to 45 %, dry weight basis [dwb]) is the main storage carbohydrate in pulse seeds (Hoover *et al*., 2010). In contrast to most other starch sources, pulse starches exhibit a relatively low glycemic index due to their higher amylose content and strong interactions between the amylose chains. These factors contribute to the higher resistant starch content in addition to the dietary fiber and provides a high nutritional value (Tiwari & Singh, 2012). Resistant starch (RS) refers to the sum of starch and products of starch degradation that resist digestion as they pass through the gastrointestinal tract (stomach and small intestine) and are fermented in large intestine (Nugent, 2005). Thus, the potential health benefits of resistant starch are linked to prevention of colon cancer (Morita *et al.*, 1999; Bingham *et al.*, 2003), hypoglycemic effects (Raben *et al.*, 1994; Reader *et al.,* 1997), promoting beneficial microflora and colonic health (Brown *et al*., 1996; Topping & Clifton 2001), reduction of gallstone formation (Malhotra 1968; Birkett *et al*., 2000), hypocholesterolemic effects (Han *et al*., 2003; Martinez *et al*., 2004), inhibition of fat accumulation (Higgins *et al*., 2004) and increased absorption of minerals (Morais *et al*., 1996).

In terms of processing, pulse starches have been given lesser importance in starch based food products due to the emphasis placed on pulses as a protein source rather than a carbohydrate source. Structural and functional properties of cereal and tuber starches have been studied extensively and they are used in a wide range of applications in food and non-food industries. Pulse starches have not benefited from the kind of value-added research required for competitiveness on an international scale. Consequently, their use in both food and non-food sectors is limited. As a result, cereal and tuber starches continue to dominate world markets in food and non-food industries. A survey of the literature (Hoover *et al*., 2010) has shown that with the exception of a few starches, there is a dearth of information on the structure, physicochemical properties and nutritional fractions of pulse starches. Presently, the food industry is increasingly concerned with the potential to incorporate pulse starches into food products due to their high amylose content (35-80 , sb), resistance to shear thinning, rapid retrogradation and high resistant starch content (Singh, 2011). Based on current studies on the structure-property relationships among pulse starches, it was considered worthwhile to investigate the molecular structure and properties of under-utilized pulse starches, which have not been characterized with respect to composition, molecular structure, polymorphic composition, physicochemical properties and digestibility characteristics.

Starch is extensively used as an additive in many food applications, such as thickening, stabilizing, texturizing, gelling, encapsulation, moisture retention and shelflife extension. Most starches cannot be utilized in their native form for food and industrial applications due to their poor thermal stability, susceptibility to acid, low resistance to

shear stress and high tendency toward retrogradation (Singh *et al*., 2007). Consequently, starches must be modified to improve their positive attributes and/or to diminish their defects. Recognition of variation in structure and properties among these pulse starches would form the basis for further investigations to modify starch structure (Hoover *et al*., 2010). This could be achieved by altering the structural arrangement of the starch chains within the amorphous and crystalline domains by different modification techniques and could lead to a wider application for pulse starches that are currently not used in the food industry.

Starch modification techniques can be classified into four categories: physical, chemical, enzymatic and genetic modifications (Bemiller, 1997). Beyond genetic and agronomic variations in starches, the physicochemical properties of starches can be modified by means of physical and chemical modification techniques. Currently, there is great deal of interest in the use of physical modification techniques, such as annealing, which modifies the properties of starches without destroying their granular structure. Annealing refers to the treatment of starch granules in excess or at intermediate moisture contents and held at a temperature somewhat lower than its melting temperature for a specific period of time. Annealing improves starch functionality by inducing a structural reorganization of starch chains within the amorphous and crystalline domains (Tester & Debon, 2000), thereby increasing their stability– a desirable feature for thermally processed foods containing starch as an ingredient. Thus, a comparative study of native and annealed pulse starches may provide a deep insight into how the structural organi-zation of starch chains influences the functionality of these starches in food applications.

1.2 Starch - Introduction

Starch is produced by green plants for energy storage, and it is a major component of the human diet. Starch can be readily found in most plant tissues and storage organs, including leaves, grains, roots, tubers, shoots, fruits and pollen (Ballicora *et al*., 2004). The major sources of starch are cereal grains (maize, wheat, barley, sorghum, and oats), tubers and roots (potato, sweet potato, yam, cassava and taro), pulse seeds (beans, peas and lentils), and some immature fruits (mango and banana). Generally, starches from various botanical origins exhibit fundamental structural similarities, but they differ in the specific details of their microstructure and ultrastructure (Huber & BeMiller 2001). Globally, maize is the primary source of starch (over 77 %), followed by cassava (12 %), wheat (7 %), potato (4 %) and a lesser contribution by pulse and other starch sources (Waterschoot *et al*., 2015). Worldwide, the production of starch in 2000 was 48.5 million tons and was projected to increase to about 85 million tons by 2015 (LMC International, 2002; Waterschoot *et al*., 2015). The United States of America (USA) and the European Union (EU) are the largest producers and consumers of starch. The EU mainly produces wheat and potato starch, whereas the USA almost entirely produces maize starch (Mitchel & Bemiller, 2009; International Starch Institute, 2017). Outside these regions, a significant amount of cassava starch is produced, mainly in Southeast Asia, while pulse starch is produced mainly in Canada. Starch is utilized in a wide range of food and industrial applications due to its universal abundance, comparatively low cost and desirable functional properties in food and non-food products (Wurzburg, 1986; Jane, 1995). Food and non-food applications of starches are summarized in Table 1.1.

Table 1.1: Food and industrial (non-food) applications of native and modified starches.

Application area	Uses of native and modified starches
Food	Bakery products, batters and breading, beverages, confectionery, gravy and creams, syrups, fat mimetic, yoghurt, cheese and imitation cheese, meat binder, cereals and snacks, instant meals, dressings
Functional foods	Ingredient (e.g. slowly digestible starch [SDS], resistant starch [RS]), encapsulation
Pharmaceutical	Diluent, binder, drug delivery, dusting agent, encapsulant
Medical	Plasma extender/replacement (Hydroxyethyl starch plasma), Organ preservation, absorbent sanitary products, plasters and dressings
Biotechnology	Substrate for growing microorganisms
Fuel	Bioethanol
Adhesives	Hot-melt glues, stamps, book binding, envelopes, labels, wood adhesives, lamination, paper bags
Agrochemicals	Mulches, pesticide delivery, seed coatings
Cosmetics	Dusting powder, makeup, soap filler/extender, face cream, tooth paste
Detergents	Bio-surfactants, builders, bleaching agents, bleach activators
Paper	Binding, sizing, filler retention, paper coating, carbonless paper stilt material, disposable diapers
Plastics	Biodegradable filler
Biologically-degradable materials	Biodegradable plastic film (e.g. food packaging materials)
Textiles	Warp sizing, fabric finishing and printing, fire resistance
Ceramics	Filler
Metals	Foundry core binder, sintered metal additive, sand casting binder
Construction	Concrete block binder, paint filler, plywood/chipboard adhesive, asbestos, clay/lime stone binder, fire resistant wallboard, gypsum board binder
Purification	Flocculent for wastewater treatment
Mining	Viscosity modifier (oil), ore flotation, ore sedimentation, oil well drilling muds
Miscellaneous	Dry cell batteries, printed circuit boards, leather finishing

Adapted from (Galliard & Bowler 1987; Satin, 1998; Burrell, 2003; Davis *et al*., 2003)

1.3 Starch biosynthesis

The biosynthesis of starch involves not only the formation of complex glucan polymers, but also their arrangement into ordered three-dimensional polysaccharide structures within the granule (Martin & Smith, 1995). All higher plant starches are synthesized inside plastids (specialized subcellular organelles), and their functions depend on the plastid type and the plant tissue origin (Tetlow, 2011). Based on temporal and spatial differences in biosynthesis, starch can be categorized into two different types: transitory starches (leaf starch) and reserve starches (storage starch) (Radchuk *et al*., 2009; Li & Gilbert, 2016). In higher plants, transitory starch synthesis occurs in the chloroplasts of photosynthetic tissues during daytime photosynthesis, and then is degraded and transported to the amyloplasts of storage organs at night, where it is incorporated into reserve starch (Zeeman *et al*., 2007). Transitory starch significantly influences crop yield, but there is no direct effect on the fine structure of the reserve starch (Wu *et al*., 2014). Storage starch is produced in amyloplasts, a heterotrophic tissue that is located inside a specialized plastid.

Starch synthesis is a complex process involving many enzymes. Various isoforms of many starch metabolic enzymes can be found in both chloroplasts and amyloplasts, and their activity differs among plant species and botanical organs, contributing to the variation in starch structure (Li & Gilbert, 2016). The initial part of the pathway is confined to the cytosol area, and the latter part (final steps) is localized in the amyloplast (Keeling & Myers, 2010). The major enzymes involved in the synthesis of starch in the amyloplast are ADP glucose pyrophosphorylase (AGPase), starch synthases (SS, Enzyme

Commission (E.C) 2.1.1.21) starch-branching enzymes (SBEs, 1,4-α-glucan:1,4-α-glucan 6-glucosyl transferase; E.C. 2.4.1.18), starch debranching enzymes (DBEs, E.C. 3.2.1.41, and E.C. 3.2.1.68) and plastidal starch phosphorylase (P-enzyme, E.C. 2.4.1.1) (Jeon *et al*., 2010; Tetlow, 2011).

Sucrose (derived from photosynthesis) is the main form of carbohydrate transported and serves as an initial point of α-glucan deposition (Emes *et al*., 2003). In the cell cytosol, sucrose synthase (SuSy, EC 2.4.1.13), an enzyme, is responsible for the conversion of sucrose into uridine diphosphate glucose (UDP-glucose) and fructose. The resulting UDP-glucose is then converted to glucose -1-phosphate (G-1-P) by the enzyme, UDP-glucose pyrophosphorylase (EC 2.7.7.9) in the presence of pyrophosphate (PPi). G-1-P is then converted to G-6-P by phosphoglucomutase (EC 5.4.2.2). The G-6-P is translocated across the amyloplast membrane and is then converted to G-1-P by phosphoglucomutase. Adenosine 5'-diphosphate-glucose (ADP-Glc), the precursor of starch synthesis, is made in the amyloplast via AGPase. However, it is also reported that in cereals, ADP-Glc is made in the cytosol via a cytosolic form of AGPase (Beckles *et al.,* 2001). ADP-Glc transporter translocates cytosolic ADP-Glc into the amyloplasts for starch synthesis (Comparot-Moss & Denyer, 2009). Figure 1.1 illustrates the starch biosynthesis pathway that describes the conversion of ADP-Glc into starch using enzymes that are encoded by nuclear genes.

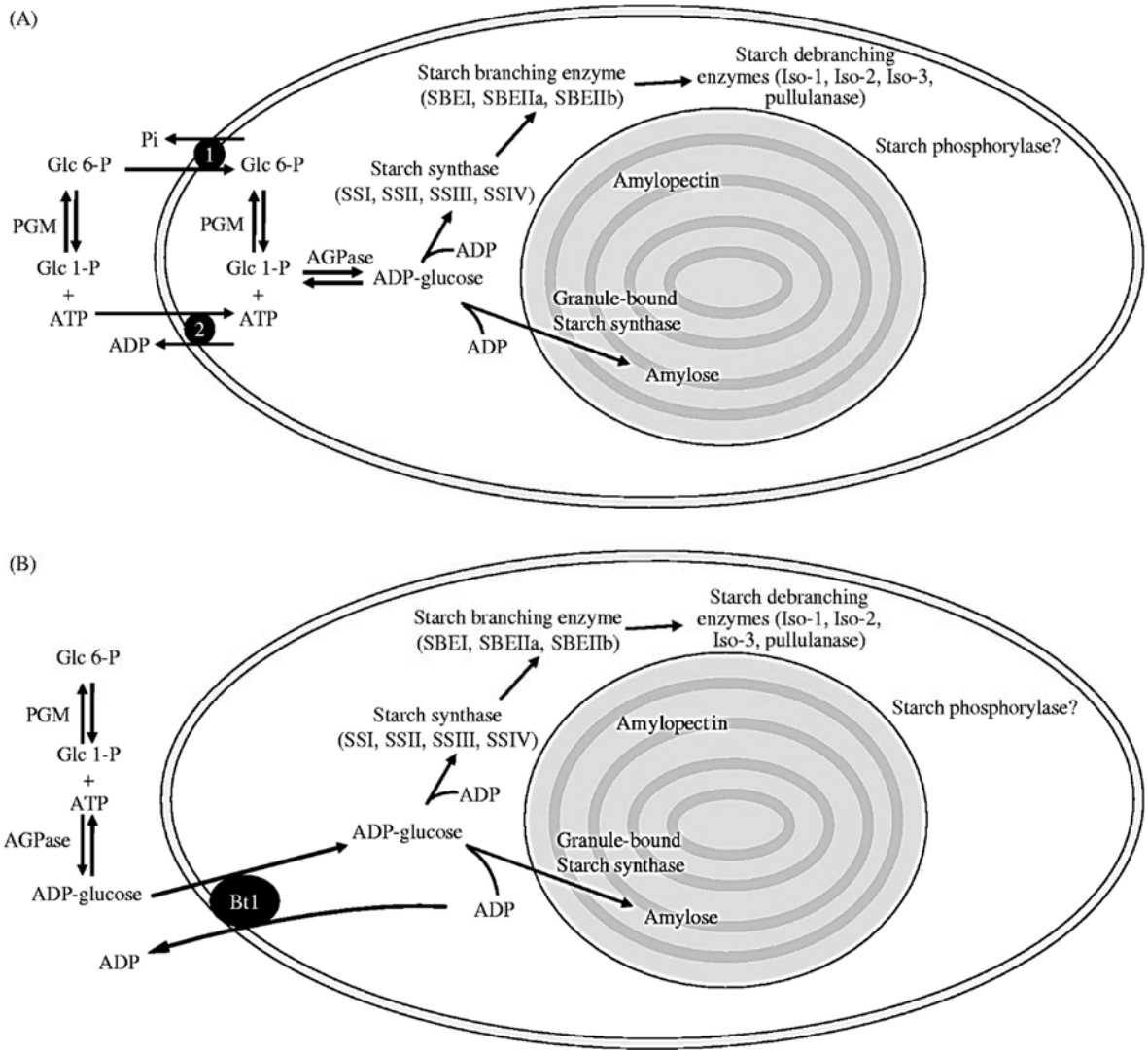

Figure 1.1: A diagram illustrating starch biosynthesis in the amyloplasts of seed storage tissue. A and B represent the starch biosynthesis pathways in the storage tissue of dicots and the endosperm of monocots, respectively. (Tetlow, 2011, Copyright Cambridge University Press, reproduced with permission).

1.3.1 ADP-Glc generation by ADP-glucose pyrophosphorylase

AGPase is the enzyme responsible for the production of ADP-Glc from sucrose, the soluble precursor and substrate for SSs. The AGPase reaction is the starting and rate controlling step in the biosynthesis of both transient starch in chloroplasts and storage starch in amyloplasts (Ball & Morell, 2003; Tetlow *et al*., 2004; Tetlow & Emes, 2014). The reaction scheme of AGPase is given below:

$$\text{Glucose-1-phosphate} + \text{ATP} \leftrightarrow \text{ADP-Glc} + \text{PPi}$$

In many species, AGPase is a key enzyme in the regulatory pathway and is sensitive to allosteric regulation by both phosphoglyceric acid/3-phosphoglycerate (3-PGA, an activator) and inorganic orthophosphate (Pi, inhibitor) (Ghosh & Preiss, 1966). The plant tissue, plastid type and subcellular location of enzymes (mainly in cereal endosperms) are the main factors influencing the relative sensitivity of the AGPases to these allosteric effects (Tetlow, 2011). Furthermore, AGPase plays an important role in crop yield, whereas the modification of this enzyme in different ways could result in increased/decreased content of starch (Wang *et al*., 1998).

1.3.2 The role of starch synthases on the elongation of glucan chain

Starch synthases are involved in the elongation of linear glucan chains during starch biosynthesis. SSs catalyse the transfer of a glucosyl unit of ADP-Glc (soluble precursor) to the non-reducing ends of pre-existing glucan chains forming new α(1→4) glycosidic bonds with the release of ADP (Tetlow, 2011). Generally, SSs can be categorized into two major groups: granule-bound SS (GBBS) and soluble SS. There are multiple isoforms of SS found in higher plants, some of which show differences in organ

specificity and temporal regulation, but their impact on overall activity in various tissues is still not fully understood (Wang *et al*., 1998). Mukerjea *et al*. (2009) suggested that SS adds the monomer to the end of glucan chains by a two-site insertion mechanism. GBSSI, GBSSII, SSI, SSII, SSIII and SSIV are the main isoforms of SS that are much conserved in higher plants (Tetlow, 2011). GBSS is involved in the elongation of maltooligosaccharides to form amylose molecules, whereas unit chains of amylopectin are synthesized by SS (Denyer *et al*., 1999; Jane, 2006).

1.3.3 Biosynthesis of amylose

The major isoform GBSSI is encoded by the *Waxy* (wx) locus in cereals and is responsible for the synthesis of amylose molecules (Shure *et al*., 1983). GBSSI is found in storage tissues completely within the granule matrix and its elimination in a number of mutants (maize, barley, pea, and wheat) results in an amylose-free or reduced amylose content in their endosperm starch (Jeon *et al*., 2010; Tetlow, 2011). Furthermore, GBSSI is also responsible for the elongation of extra-long unit chains (ELC) of amylopectin. Another form of GBSS, GBSSII, accounts for the synthesis of amylose in leaves and other non-storage tissues containing transient starch (Fujita & Taira, 1998; Vrinten & Nakamura, 2000).

1.3.4 Biosynthesis of amylopectin

The multiple isoforms of SS play a distinct role in amylopectin biosynthesis and their distribution in the plastid between the stroma and starch granules is influenced mainly by species, tissue and the developmental stage (Ball & Morell, 2003). It has been reported that SSI is principally responsible for the elongation of the shortest glucan chains

(degree of polymerization [dp]<10), whereas SSII and SSIII are responsible for the further extension of longer glucan chains (Commuri & Keeling, 2001; James *et al*., 2003). Two classes of SSII genes are identified in monocots: SSIIa and SSIIb. Several authors have reported that SSIIa plays an important role in the synthesis of intermediate side chains (dp 12-24) from pre-existing short chains, and its down regulation critically affects the amount and composition of starch in cereal endosperms (Nakamura, 2002; Morell *et al*., 2003). The inhibition of SSIIa (in monocots) and SSII (in dicots) activities results in decreased starch content, reduced amylopectin chain length and crystallinity, and alteration in the size and shape of starch granules (Morell, *et al*., 2003; Kosar-Hashemi *et al*., 2007). Furthermore, SSIII and SSIV have also been discovered and are believed to participate in starch granule initiation (Szydlowski *et al*., 2009). It has been proposed that SSIII is involved in the elongation of relatively long chains of amylopectin (dp >37), including the B2, B3 and B4 chains (see section 1.6.2.1) which interconnect the amylopectin clusters (James *et al*., 2003; Jeon *et al*., 2010). Maize SSIII mutants (*dull*) produce a subtle phenotype with a glassy and tarnished endosperm (Gao *et al*., 1998).

1.3.5 The action of starch branching enzymes on the branching of glucan chains

Starch branching enzymes form the α(1→6) branches by hydrolysing α(1→4) linkages within a chain and then transfering the released reducing ends to C6 hydroxyls to form new α(1→6) linkages (branched structure) between the reducing end of the 'cut' glucan chain and another glucose residue from the hydrolysed chain (Emes *et al*., 2003). Hernández *et al*. (2008) reported that the possible mechanisms in the action of SBEs include intra-chain transfer, inter-chain transfer and intra-chain cyclization. An inter-

chain reaction occurs via a glucan chain transfer to a different chain, whereas an intra-chain reaction takes place in a chain where the donor and the acceptor are in the same glucan chain. Intra-chain cyclization is also considered a specific intra-chain reaction, where the formation of cyclic glucan originates with a sequence of steps involving the splitting of an α(1→4) glycosidic linkage, and the subsequent transfer to the OH group at position 6 of a glucosyl unit of the same chain (Takata *et al*., 1996; Li & Gilbert, 2016). Existing branched chains can be extended by SS, and additional branches can be formed by branching enzymes (Burton *et al*., 1995). During the branching process, branches are not formed randomly; there is a minimum chain length required for the size of the transformed branch. The remaining branches are referred to as Xmin (7 residues) and Xo (6 residues), respectively (Nielsen *et al*., 2002; Wu *et al*., 2014).

Two major forms of SBE are identified based on their primary amino acid sequence in higher plants: SBE I (SBE B) and SBE II (SBE A). These isoforms differ in terms of the length of the glucan chain transferred, catalytic capacity and their substrate preference (Tetlow *et al*., 2004). The individual isoenzymes of SBE involve a distinctive role in amylopectin biosynthesis. SBE I has been shown to be associated with higher rates of branching of amylose chains, whereas SBE II transfers shorter glucan chains during branch formation and shows a higher affinity toward amylopectin compared to SBE I (Guan & Preiss, 1993; Takeda *et al*., 1993). The two SBE isoforms exhibit unique developmental time of their expression (peak activity) and a different length of amylose chain that is transferred (Smith *et al*., 1995). Burton *et al*. (1995) reported that in peas, the SBE II is highly active in early stages of embryo development, whereas the activity of

SBE I is observed later in embryo development. The activity of these enzymes greatly influences the synthesis of amylopectin at different stages of granule formation, and it changes from shorter to longer branch length.

Generally, a crystalline polymorphism of starch is determined by the chain length and the arrangement of amylopectin side chains. During the early stages of embryo development, SBE I is highly active and produces short side chains with a large number of branches leading to the formation of A-type starches. Eventually, the activity of SBE I decreases and SBE II activity increases at a later stage of embryo development; thus, it produces long side chains and initiates the B-type polymorph. Therefore, pea starches exhibit a mixed polymorphism: the central part of the granules is rich in B-type, while peripheral regions are mainly made up of A-type polymorphs (Wang *et al*., 2012).

1.3.6 The action of debranching enzymes (DBEs) on starch synthesis

There are two types of DBEs involved in starch synthesis: isoamylase-type (ISA, EC 3.2.1.68) and pullulanase-type (PUL, EC 3.2.1.41). Kubo *et al*. (1999) reported that ISA plays a predominant role in cereal endospores and PUL also can perform that same role. DBE efficiently catalyses the hydrolysis (debranching) of α(1→6) glycosidic bonds in amylopectin and releases the linear polymer chains. In starch biosynthesis, the exact role of SDE is not fully understood (Tetlow, 2011). Two different models have been proposed to describe the role of DBEs in starch synthesis and phytoglycogen accumulation. The 'glucan trimming' (pre-amylopectin) model proposes that glucan trimming is necessary for the assembling of amylopectin in an insoluble confined granular structure (Ball *et al*., 1996; Myers *et al*., 2000). It has been postulated that the

activity of DBE is responsible for the removal of pre-amylopectin branches (or improperly positioned branches) formed at the surface of immature starch granules to facilitate crystallization (Tetlow, 2011). Furthermore, the debranching action is necessary for the formation of double helices, which could facilitate glucan chain aggregation. Nielson *et al*. (2002) reported that numerous short chains are located on the surface of the immature granules and these observations further validate this model.

An alternative model for the role of DBE in starch synthesis holds that DBEs limit the availability (clearing) of soluble glucans which are not attached to the granule from the stroma. The removal of the substrates for the amylopectin synthesizing enzymes (SS and SBE) prevents the random/futile synthesis of glucan chains. Otherwise, these starch synthesizing enzymes produce phytoglycogen, which in turn reduces the rate of starch synthesis. A substantial accumulation of phytoglycogens is observed in DBE mutants at the expense of amylopectin and could be evidence for the model that explains the role of DBE in starch synthesis (Zeeman *et al*., 1998).

1.3.7 Starch phosphorylase

Two types of starch phosphorylases are found in plants: Pho1 and Pho2. The catalytic activity of these starch phosphorylases involves the reversible transfer of glucosyl units from glucose-1-phosphate (Glc-1-p) to the non-reducing end of α(1→4)-linked glucan polymers. Pho1 and Pho2 are found in the plastid and cytosol, respectively. Pho1 exhibits a higher affinity toward amylopectin and is inhibited by ADP-Glc (Dauvillée *et al*., 2000). Pho 1 plays an important role in storage starch biosynthesis by providing suitable substrates to other enzymes involved in starch biosynthesis.

Consequently, released Glc-1-p is reintroduced into the biosynthetic pathway of starch (Jeon *et al*., 2010).

1.4 Molecular architecture of starch

Starch has a complex structure with multiple levels of hierarchical organization made up of glucose polymers (Wu *et al*., 2014). Figure 1.2 illustrates the structure of starch in a rice grain with six levels of structural organization:

- Level 1, individual chains (0.1-1 nm): The lowest molecular level represents the distribution of individual linear chains that form the branches of macromolecules in starch. Each chain has a certain dp and their distribution is often termed as the chain-length distribution (CLD) (Dona *et al*., 2010). The amylopectin branches have an average dp of ~17-25, whereas amylose has a dp of ~200-700 (Wu *et al*., 2014).

- Level 2, whole starch molecules: This level represents all branched macromolecules, including amylose and amylopectin, which form the starch granule. The individual molecules can be characterized by molecular weight, size distribution and z-average radius of gyration. Compared to amylose, amylopectin is a highly branched structure and the branch chains are categorized into three distinct groups based on their branching pattern. The detailed structure of amylopectin is described in section 1.6.3.

- Level 3, lamellar structure: During starch biosynthesis, inter- and intra-molecular aggregations of polymer chains in the native state form the lamellar structure.

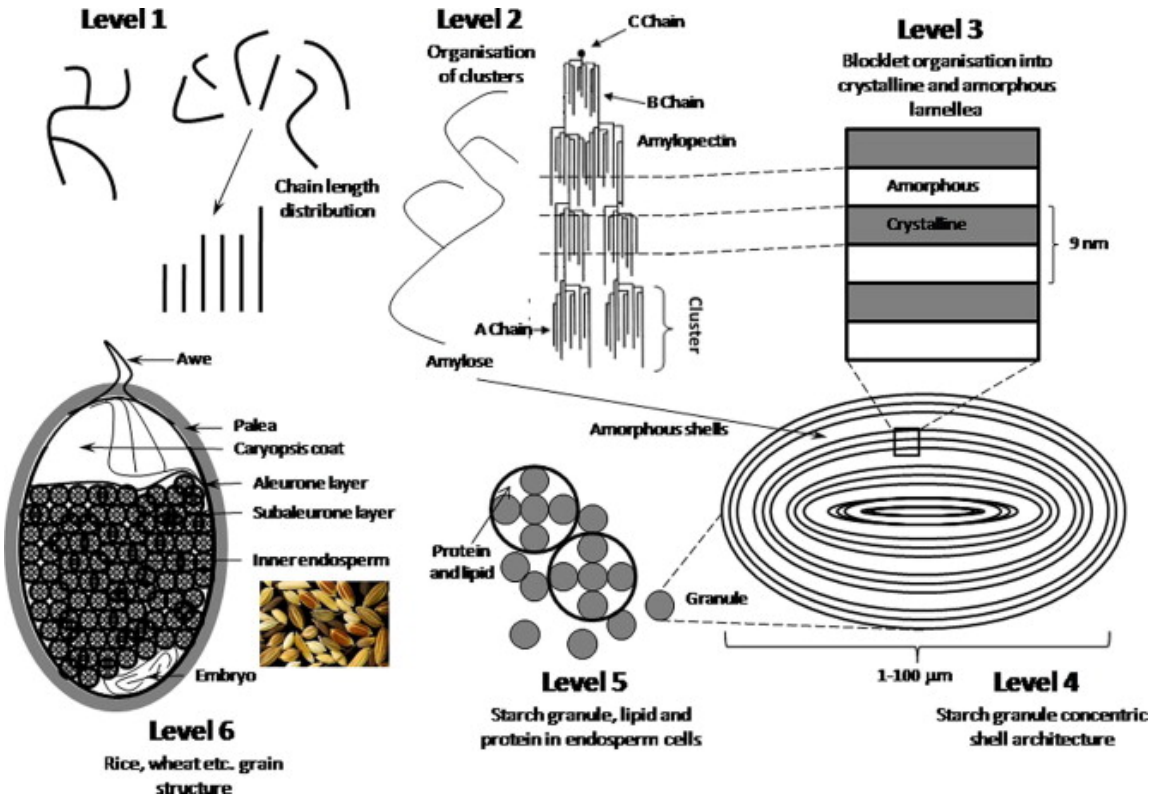

Figure 1.2: Schematic representation of six levels of organization of the rice starch granule/grain, (Dona *et al.*, 2010, Copyright Elsevier, reproduced with permission)

The dense packing of starch chains enables them to intertwine and form double helices. The double helices aggregate together and form crystallites. The parallel arrangement of double helices made up of exterior shorter chains of amylopectin form crystalline lamella. The branching points of amylopectin are mainly located in the amorphous lamellae (Dona *et al*., 2010). Generally, amylose molecules are present in either amorphous layers or complexed with lipids in native granules. Depending on the botanical origin, the thickness of crystalline lamella is 5-7 nm (Putaux *et al*., 2003).

- Level 4, starch granule with concentric cell architecture: The internal architecture of a starch granule is made up of concentric layers of growth rings (concentric shells) extending from the hilum toward the peripheral (surface) region. These concentric growth rings contain semi-crystalline radial regions of 100-400 nm in thickness and separated by amorphous regions. The alternative radial arrangement of crystalline and amorphous lamellae (lamellar structure) creates the semi-crystalline growth rings. Compared to crystalline regions, amorphous regions are loosely packed and contain the branching points of amylopectin and the disordered conformation of amylose and amylopectin molecules (Donald, 2004; Copeland *et al*., 2009; Wang & Copeland, 2015).

- Level 5, endosperm: The endosperm is the largest part of the seed where starch is stored as an energy reserve (James *et al*., 2003). In this level, starch granules are associated with proteins and lipids. These minor components are incorporated into

the granule during the synthesis of starch and have a significant impact on starch properties (Pérez & Bertoft, 2010).

- Level 6, whole grain: This level is comprised of all outer layers of the grain and the highest levels of structures including the hull (Dona *et al*., 2010).

1.5 Granule morphology, size and distribution

Starch granules exhibit a characteristic granule morphology depending on the botanical origin (Jane *et al*., 1994). The diameter of starch granules generally ranges from submicron to 200 μm, and shapes can be regular (oval, ellipsoidal, spherical, polyhedral, lenticular, kidney shape, etc.) or irregular (Buléon *et al*., 1998; Hoover, 2001; Singh *et al*., 2003; Alcázar-Alay & Meireles, 2015). Starch granules from cereals are usually relatively small, and spherical or polygonal in shape with a concentric hilum (Tester *et al*., 2004). High amylose maize starches have a larger population of rod-shaped filamentous granules (Perez & Bertoft, 2010). The majority of pulse starch granules are medium sized, and they are kidney-like or oval in shape with an elongated or starred hilum. However, spherical, round, elliptical and irregularly shaped granules also are common in pulse starches (Hoover & Ratnayake 2002; Zhou *et al*., 2004; Sandu & Lim, 2008; Hoover *et al*., 2010). In general, starch granules from tubers are large, ellipsoid or spherical in shape with an eccentric hilum (Hoover, 2001; Zhang *et al*., 2017).

The size distribution of native granules from different botanical sources can be uni-, bi- or polymodal. Most of the legumes, some cultivars of barley (waxy, normal) and potato (normal) have shown a tri-modal distribution, whereas maize (waxy, normal and high amylose), rice millet and potato (waxy) exhibit a unimodal distribution (Jane *et al*.,

1994; Singh *et al*., 2004; Tester *et al*., 2004; Hoover *et al*., 2010). Some cereal starch granules, including those of wheat, barley, oat and rye, exhibit two different size distributions (bimodal) and shapes. In these starches, the A-type is larger in size with a lenticular shape, whereas smaller B-type granules have a spherical shape (Tester *et al*., 2006).

Synthesis of starch granules is localized and granulses are usually produced individually in the amyloplast. In certain plants, more than one granule is initiated simultaneously in a single amyloplast and produces compound granules. Compound granules are mostly polyhedral and found in rice, waxy rice, oat and smooth pea starches (Pérez & Bertoft, 2010). However, the wrinkled pea has two or more fused sub-granules, generally referred to as semi-compound granules. The larger granules of wrinked pea starch exhibit extensive damage resulting in splitting and the exposure of the internal layering (Bertoft *et al*., 1993; Zhou *et al*., 2004).

Surface and internal cracks have been reported in corn, sorghum, potato, kidney bean, mung bean and faba bean starches (Hoover & Sosulski, 1985; van de Velde *et al*., 2002; Glaring *et al*., 2006; Ambigaipalan *et al*., 2011). The cracks could reflect the low granule integrity and/or the sub-optimal packing of glucan chains within the granule (Glaring *et al*., 2006). Surface pores, cavities and channels are topographical characteristics of some starch granules. Granular surfaces of pulse, tuber and root starches are generally smooth with no evidence of pores (pin holes), cracks or fissures (Jane *et al*., 1994; Hoover, 2001; Singh *et al*., 2004). Granules of corn, sorghum, rice, barley, tapioca

and millet starches have pores on their granular surface (Fannon *et al*., 1992; Bemiller, 1997; Jayakody & Hoover, 2002).

1.6 Molecular components of starch

Starch is a major polysaccharide reserve in plants and the second largest biomass on earth. It is deposited in the form of semi-crystalline granules in plant storage tissues. In the vast majority of native starches, amylose and amylopectin represent 98-99 % of the dry weight of the granules, with the remainder comprised of non-starch components (Copeland *et al*., 2009). The moisture content of native granules varies from 10-17% (w/w), depending on the botanical origin and extraction method (Wang & Copeland, 2015). The ratio of the two macromolecular components varies with the botanical origin of the starch, and the amylopectin component predominates in about 70-80 % of normal starches. In 'waxy' starches, amylopectin is the sole component or varies between 0-10 % (Buléon *et al*., 1998; Pérez & Bertoft, 2010). The amylose content of normal starches varies from 20-30 % of their dry weight. However, high amylose starches contain more than 40 % amylose and some mutant genotypes (*ae*[amylose extender] mutant) of maize, barley, rice and wrinkled pea starches contain up to 80 % amylose (Tester *et al*., 2004). A third component has been identified in high amylose maize and wrinkled pea starches, and referred to as intermediate material (Pérez & Bertoft, 2010). Apart from major molecular components, starch contains small quantities of other 'minor components', such as surface and integral proteins and lipids and a trace amount of minerals (calcium, magnesium, phosphorous, potassium and sodium) (Tester *et al*., 2004).

1.6.1 Fine structure of amylose

Amylose is essentially a linear polymer consisting almost entirely (99 %) of α(1→4) linked glucopyranose units with a few long chain α(1→6) linked branches (~1 %), and it differs in size and structure depending on the botanical origin (Buléon *et al*., 1998; Pérez & Bertoft, 2010). Amylose has a broad distribution of molecular weight (Mw) that varies from $1x10^5$ to $1x10^6$ (Buléon *et al*., 1998), with an average dp by number (dp_n) of 324-4920 (Yoshimoto *et al*., 2000; Tester *et al*., 2004). The majority of starches are comprised of a mixture of linear and branched amyloses with around 9-20 branch points per amylose molecule. In general, the amylose contains 3-11 chains per molecule and each chain carries approximately 200-700 glucose units, equivalent to a Mw of 32400-113400 (Morison & Karkales, 1990; Tester & Karkalas, 2002). Perez and Bertoft (2010) reported that, the molecular weight of branched amylose is higher compared to that of linear amylose, and the molar fraction of branched amylose varies from 0.1 to 0.7 in different starches.

Incomplete hydrolysis by β-amylase indicates that amylose molecules have branches (Hizukuri *et al*., 1981; Takeda *et al*., 1987). The enzyme, β-amylase, hydrolyses only α(1→4) linkages from the non-reducing ends, producing β-maltosyl units; its reaction pattern is restricted by α(1→6) linkages, whereas the linear molecules are completely converted into maltose units. However, β-amylolysis of amylose molecules produces maltose and β-limit dextrins (low Mw polymers with a certain degree of branching) (Banks & Greenwood, 1975; Buléon *et al*., 1998). Generally, the limit of β-amylolysis of amylose molecules is in the range of 72-95 %, while the limit for highly

branched amylopectin is in the range of 55-61 % (Takeda *et al*., 1986; Hizukuri *et al*., 1988).

1.6.1.1 Location of amylose

The location of amylose and its contribution to granular architecture is not entirely known. Initially, it was hypothesized that amylose is located in bundles among amylopectin clusters (Nikuni, 1978), based on the different properties exhibited by starch granules (such as dimethyl sulfoxide (DMSO) solubility, amylose leaching, iodine binding and formation of lipid complex (Immel & Lichtenthaler, 2000: Nuessli *et al*., 2003). Zobel (1988a) suggested that amylose is separated from the amylopectin fraction in normal maize starches, but interspersed with amylopectin in potato starches. However, a series of cross-linking studies on potato and corn starches demonstrated that amylose molecules exist as individual molecules. They are randomly interspersed among the amylopectin molecules and adjacent to or intertwined with amylopectin rather than grouped together in both the crystalline and amorphous regions (Jane *et al*., 1992). Jenkins and Donald (1995) investigated the effect of varying amylose content on the internal structure of maize, barley and pea starches using small angle x-ray diffraction techniques. These authors suggested that the co-crystallization of amylose with amylopectin chains and the penetration of amylose tie chains into the amorphous lamellae disrupt the packing of amylopectin chains within the crystalline lamellae (Figure 1.3 b & c).

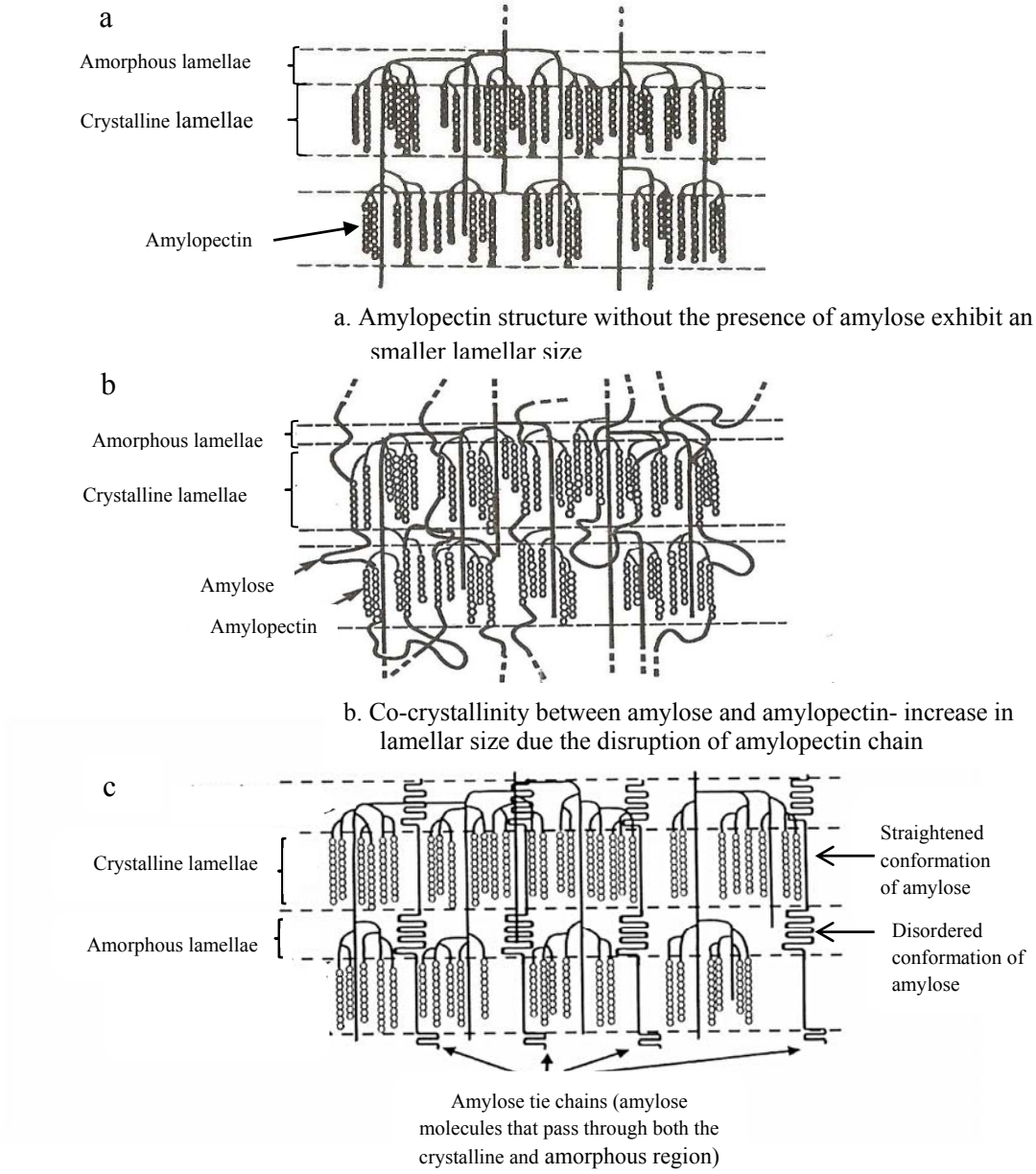

Figure 1.3: Schematic representation of the localization of amylose chains within the amylopectin clusters**.** a, b (Jenkins and Donald, 1995, Copyright Elsevier reproduced with permission) & c (adapted from Yuryev *et al*., 2007).

Based on chemical surface gelatinization studies, potato and normal maize starches exhibit an enrichment of amylose in the peripheral regions compared to the central (core) regions of the granules (Jane & Shen, 1993). In contrast, Tatge *et al*. (1999) proposed that amylose is largely confined to a central region of transgenic potato granules and synthesized within the matrix formed by amylopectin chains. Based on the acid degradation of pea starches, Wang *et al*. (2012) proposed a model in which amylose is mainly concentrated in the central region of the granule, whereas amylopectin predominantly exists in the outer regions of the granules interspersed with some amylose molecules.

The location of amylose was visualized by enzyme gold labelling, combined with iodine staining of potato and maize starches, and 8-amino-1,3,6-pyrenetrisulfonic acid (APTS) staining of potato starches, indicated that amylose is confined to the amorphous regions around the hilum (Atkin *et al*., 1999; Blennow *et al*., 2003; Glaring *et al*., 2006). On the basis of iodine binding and X-ray diffraction (XRD) analysis, Saiban and Seetharaman (2010) reported that amylose in maize starches is localized mainly within the amorphous regions independent of the amylopectin crystallites, while in potato starch, amylose chains are co-crystallized with the external chains of amylopectin. The presence of amylose in the amorphous and/or crystalline region is dependent on the botanical origin (Oates, 1997).

1.6.1.2 Amylose-inclusion complex

Amylose has the characteristic features to form inclusion complexes with a variety of inorganic and organic complexing agents. In the helical conformation, the inner surface

is built up by methylene groups (-CH_2- groups) and glycosidic oxygen atoms, forming a hydrophobic cavity, while all of the polar glycosyl hydroxyl groups are positioned at the outer surface of the helix (Whittam *et al*., 1989; Cui & Oates 1999). Amylose undergoes a coil to helical transformation in the presence of suitable complexing agents, such as DMSO, potassium hydroxide, polyiodide ions, lipids and alcohols (Buléon *et al*., 1998). The size of the complexing agent residing within the amylose helix determines the inner diameter of the helix and the number (typically six, seven or eight) of glucose residues per-turn (Biliaderis & Galloway, 1989; Helbert & Chanzy, 1994).

The amylose-complex formation is mainly driven by hydrophobic interactions, whereby the hydrophobic ligand is transferred to the helical cavity of an amylose chain from the polar (water) to the non-polar environment (Whittam, *et al*., 1989; Fanta *et al*., 1999). Intramolecular bonds (such as van der Waals forces and hydrogen bonds) occur between the consecutive turns of the helices and the intermolecular forces between amylose and the ligands stabilize the amylose-ligand complex (Godet *et al*., 1993). In the amylose-lipid complex, the aliphatic part (hydrocarbon chain) of the lipid is included inside the lipophilic core of the amylose helix, while the polar group of the lipid molecule lies outside of the helical cavity (Carlson *et al*., 1979; Godet *et al*., 1995). It has been shown that amylose-lipid complex formation is influenced by amylose chain length, pH of the medium, ligand concentration and solubility, chain length and unsaturation, lipid type (mono-/di-acylglycerols of fatty acids), and complexation temperature (Hahn & Hood, 1987; Morrison 1988; Godet *et al.*, 1995; Ozcan & Jackson, 2002; Tufvesson *et al*., 2003; Tang & Copeland, 2007).

1.6.2 Amylopectin

Compared to amylose, amylopectin is a much larger and extensively branched molecule with an average Mw of 1×10^7 - 1×10^9. It is composed of linear chains of α(1→4) linked D-glucopyranose units interconnected at the branching points through α(1→6) linkages (Buléon *et al*., 1998). The dp_n varies in the range of 9,600-15,900, but typically it comprises three major groups, with dp_n values of 13,400-26,500, 4,400-8,400 and 700-2,100 (Takeda *et al*., 2003). The molecular size, structure and poly-dispersity of the molecule is largely influenced by the botanical origin of the starch.

Several models/depictions have been proposed to explain the structure and the organization of the unit chains in amylopectin. Currently, two major structural models are widely accepted; 1) the cluster model (French, 1972; Nikuni, 1978) with polymodal chain length distribution (Hizukuri, 1986), which is referred to as the traditional model; and 2) the building block backbone model (Pérez & Bertoft, 2010). The major difference between these models is the different visualization of chain organization within an amylopectin molecule (Chauhan & Seetharaman, 2013).

1.6.2.1 Cluster model of amylopectin

The cluster model of amylopectin describes the clusters that are packed together, forming alternating amorphous and crystalline layers in starch (Robin, 1974). The short chains (less than 36 glucosyl units) are organized into clusters and the clusters are interconnected by long chains. Based on the chain length and their pattern of substitution, the amylopectin unit chains are classified as A, B and C chains (Hizukuri, 1986) (Figure 1.4).

The A-chains are the shortest (dp 6-12), unsubstituted and linked through a single α(1→6) linkage to the rest of the amylopectin molecule. B chains carry one or several other chains (A- and/or B-chains) and are connected via α(1→6) linkages. B chains are further classified into B_1, B_2, B_3 and B_4 (one to four clusters) based on the chain length and the number of clusters they span (Hizukuri, 1986). Each amylopectin molecule carries a C-chain, which contains the sole reducing group at the end, with a size ranging from 10 to 130 glucose units (Hizukuri, 1986; Hanashiro *et al*., 1996). According to the cluster model some 'B' chains are long enough to traverse both crystalline and amorphous segments.

Amylopectin exhibits an average chain length ($\overline{CL}$) of 18-27 glucose units (Takeda *et al*., 2003). A chains and B chains build a single cluster and their external segments form the double helices that crystalize into crystalline lamellae. Their branching points are located in the amorphous lamellae (Pérez & Bertoft, 2010). The B chains that are located within a single cluster are referred as B1 chains, where clusters are interconnected through long, amylopectin branch chains (B2 – B4). The B2 chains are involved in the interconnection of two clusters, whereas B3 and B4 chains participate in the inter linkage of three and four clusters, respectively (Hizukuri, 1986; Bertoft et al., 2008). According to the cluster model, some B chains are long enough to traverse both crystalline and amorphous segments.

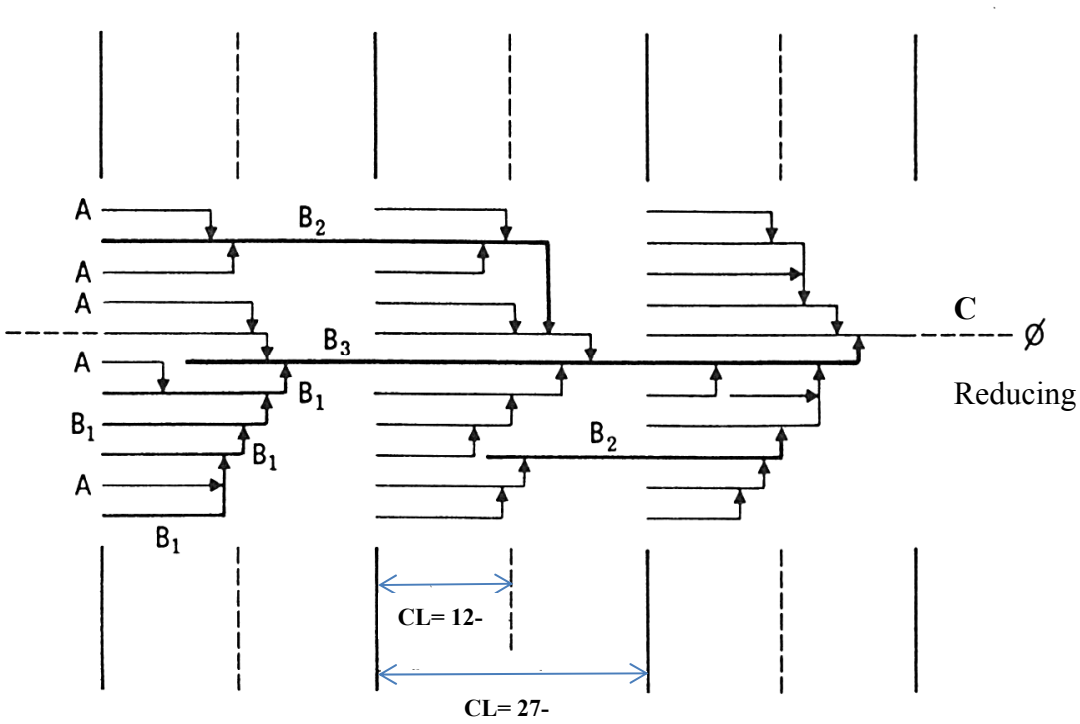

Figure 1.4: A cluster model of amylopectin; CL- chain length (dp) (Hizukuri, 1986, Copyright Elsevier, used with permission and adapted).

1.6.2.2 Building block backbone model

The building block backbone model proposes that clusters are formed by smaller structural units referred to as building blocks (Vamadevan & Bertoft, 2015). These units are made up of 10 or more chains with an average internal chain length (segments between branches) of 1-3 glucose residues. A backbone (longer chain containing more than 35 glucose units) together with the branched building blocks, that are smaller than clusters, splayed (helices not arranged in a crystalline array) along the backbone chain build up the basic structural unit of amylopectin (Pérez & Bertoft, 2010).

1.6.2.3 Starch crystallinity and polymorphism

Starch is a semi-crystalline polymer comprised of different polymorphic types with varying degrees of crystallinity. The crystalline structure of a starch granule is mainly influenced by the structural elements of amylopectin (Jane *et al*., 2006). The crystalline lamellae are mainly formed by the double helices of amylopectin side chains that are packed into different polymorphic forms identified by characteristic XRD patterns (Figure 1.5). Three types of polymorphic forms are identified in starches from different botanical origins, known as types A, B and C. These polymorphic types are characterized by the specific diffraction angles resulting from the degree of order of amylopectin double helices and the CL of amylopectin (Hizukuri *et al*., 1983).

The A- and B-type polymorphic forms are identical with respect to helical structure. Nevertheless, the packing of these double helices within the A-type is relatively compact with a low proportion of water (4 water molecules per 12 glucose residues), whereas the double helices are loosely packed in the B-type, creating a more open

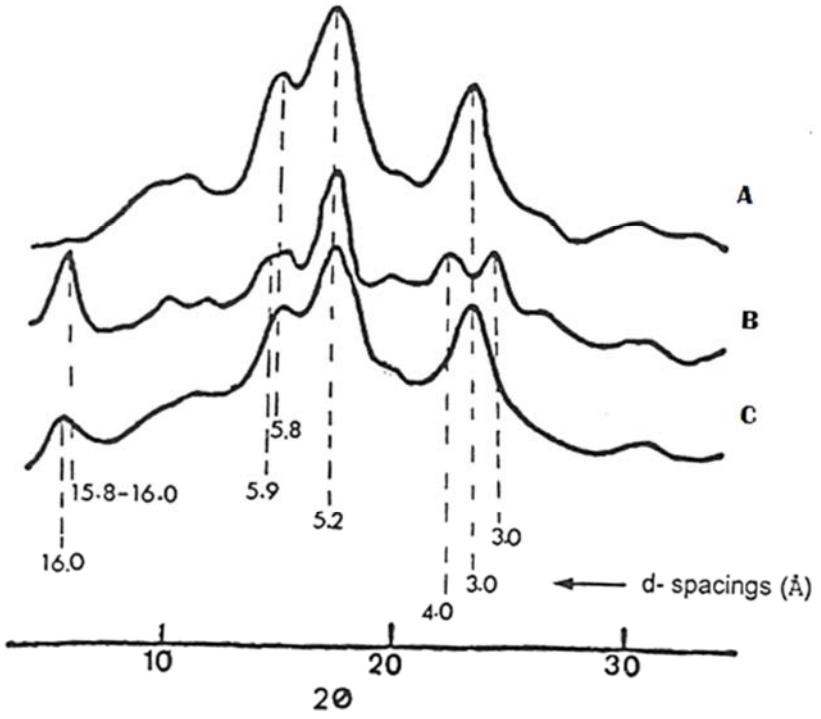

Figure 1.5: Characteristic X-ray diffraction patterns of A-, B- and C-type starches with their specific d-spacings. (Zobel, 1988b, Copyright John Wiley and Sons, used with permission and adapted).

structure containing a hydrated helical core (36 water molecules per 12 glucose residues) (Jane *et al*., 1997). The starch crystals exhibit differences in the geometry of the unit cells; A-type polymorphic starch has a monoclinic unit cell and B-type polymorphic starch has a hexagonal unit cell (Imberty & Perez, 1988) as shown in Figure 1.6. The C-type polymorphic starch is a mixture of A- and B forms (Gernat *et al*., 1990). It is considered to be an intermediate between A- and B-type polymorphic forms in packing density and structure (Hoover *et al*., 2010). Another polymorph found is the V-type (often associated with A-, B- or C- types), which is formed by the single left-handed amylose helices complexed with lipids, other organic solvents and polyiodide (Gallant *et al*., 1997; Lopez-Rubio *et al*., 2008).

The A-type polymorphs are found in cereal starches and some legume starches, while B-type polymorphs are found in tuber, root, high amylose and retrograded starches (Biliaderis, 1998; Buléon *et al*., 1998). The C-type polymorph is a characteristic feature of most pulse starches and is also found in some root and tuber starches with a different proportion of A- and B- type polymorphs (Wang *et al*., 1998; Jane, 2006). A-type polymorphic starch is mainly comprised of a larger proportion of short amylopectin branch chains (CL<19.7), but B-type polymorphic starch contains more long branch chains, including B2, B3 and other long chains (CL≥ 21.6).

C- type polymorphic starches contain different proportions of short and long chains (CL ≥ 20.3, ≤ 21.3) (Hizukuri *et al*., 1983; Jane *et al*., 2006). Yashinoto *et al*. (2000) reported that high amylose starches contain a relatively higher proportion of long chains of amylopectin.

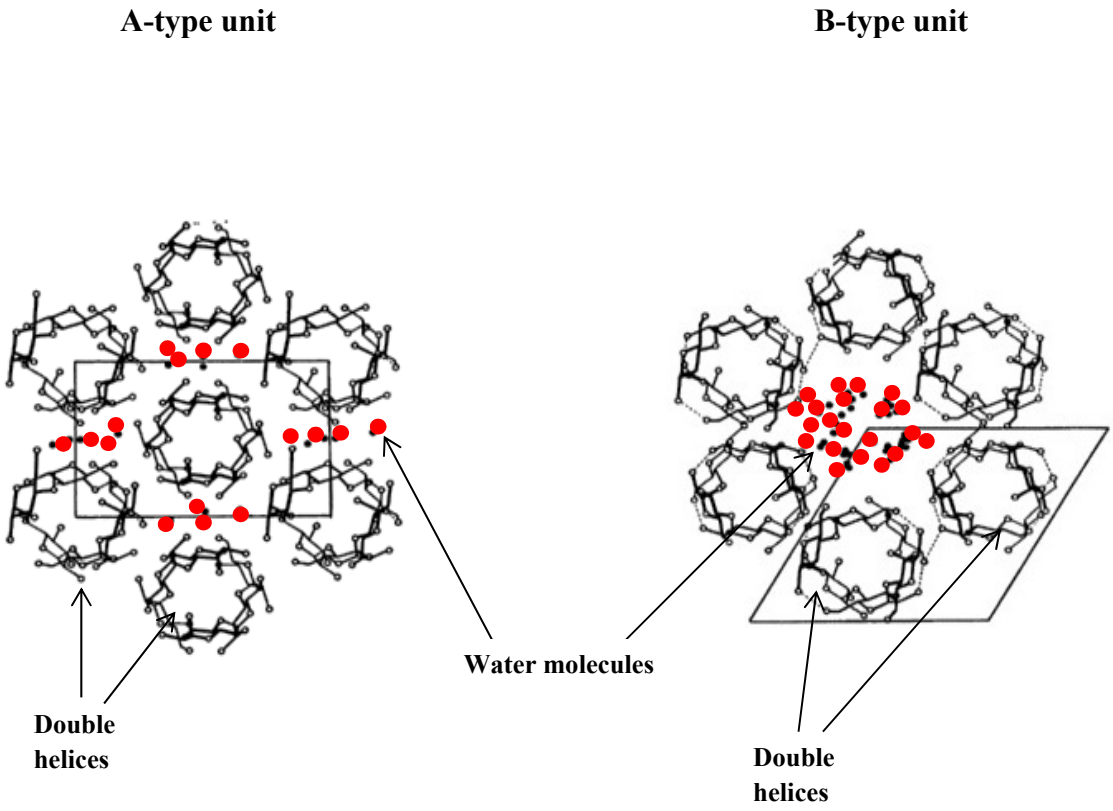

Figure 1.6: Double helices arrangement of A-type (monoclinic unit cell) and B-type (hexagonal unit cell) crystallites in starch (dots indicate water molecules). (Wu & Sarko, 1978, Copyright Elsevier, reproduced with permission).

The ratio of the long to short chain branches has a significant impact on the shape of the amylopectin molecule (conical vs cylindrical shape), which influences the packing arrangement of the granular interior and in turn affects the morphology and size of the granule (Jane, 2007).

Jane *et al*. (1997) proposed that the α(1→6) branch points of A-type polymorphic starches are scattered in both amorphous and crystalline regions, whereas in B-type starches most branch points are located in the amorphous regions, as shown in Figure 1.7. Studies on native maize starches with different amylose contents have revealed that crystal type is largely influenced by the amylose content. A change in polymorphic form from A through C to B was observed to be associated with a decrease in crystallinity, but an increase in apparent amylose content (Cheetham & Tao, 1998). Bogracheva *et al*. (1998) reported that pea starches contain both A- & B-type polymorphs. The B-type polymorphs are arranged centrally, while the A-type polymorphs are located in the peripheral regions of the granule.

The crystallinity of native starch ranges between 15-45 % depending on the botanical origin, hydration level and characterization technique (Zobel, 1988a; Buléon *et al*., 1998; Lopez-Rubio *et al*., 2008). In pulse starches, the crystallinity ranges from 17-34 % and the proportion of the B-polymorphic content varies from 22.1-92.2 % (Zhou *et al.*, 2004; Jayakody., 2007; Sandu & Lim, 2008). The degree of crystallinity is often calculated as the percentage of the crystalline regions with respect to the total area including both the amorphous and crystalline regions of the starch.

Solid state nuclear magnetic resonance (NMR) can be useful in the characterization of starch and it provides information about molecular organization at shorter distant scales (individual helices) than those probed by XRD, which detects only those double helices that are packed in crystalline arrays (Gilbert *et al*., 2012). Furthermore, the existence of helical structures within granular starch has been extensively studied using ^{13}C NMR. These methods reveal the existence of single and double helical amylose and amylopectin structures, co-complexes of amylose and amylopectin, and V-amylose-lipid complexes (Tamaki *et al*., 1998; Paris *et al*., 1999; Bogracheva *et al*., 2001; Yusuph *et al*., 2003). Starches belong to different botanical origins, and within a given species, may exhibit differences in double helical content (DHC). These differences may be due to the fact that not all of the exterior chains of amylopectin participate in the formation of double helices and non-helical forming regions also exist within amylopectin (Tester *et al*., 2004). Tester and Morrison (1990b) suggested that amylopectin is the major crystalline component in starch granules, where amylose acts as a diluent to amylopectin. In some cases, amylose molecules also form double helices, particularly in high amylose starches, and are organized in the crystalline arrays (Shi *et al*., 1998; Tester & Debon, 2000).

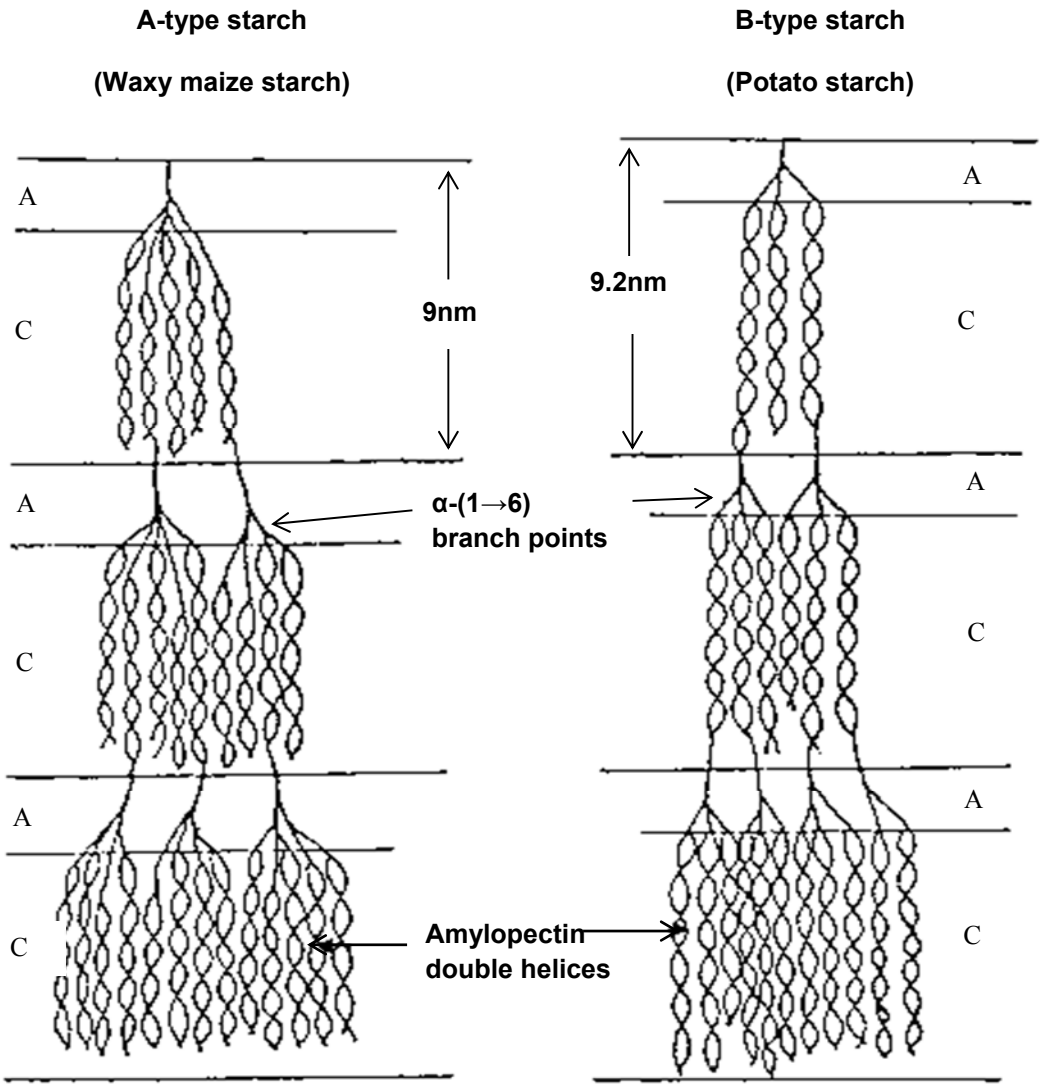

Figure 1.7: Proposed models for branching patterns of A- and B-type starches (Jane *et al*., 1997, Copyright Elsevier, reproduced with permission).

1.7 Minor components

1.7.1 Starch lipids

The endogenous lipid composition and lipid contentvary with starch botanical origin (Morrison, 1988). In native granules, lipids can be found on the surface of granules and thus they are called surface lipids, whereas those found within the starch granules are so-called internal or bound lipids (Morrison, 1981). The surface lipids mainly include triacylglycerols, followed by glycolipids, phospholipids and free fatty acids, while bound lipids are largely monoacylglycerols with a major fraction of lysophospholipids (lysoPL) and free fatty acids (FFA) (Morrison, 1981; Vasanthan & Hoover, 1992a). The lipids (surface and internal) are present in the form of free components as well as those bound to the starch macromolecular components, either attached via ionic or hydrogen bonding with the hydroxyl groups of the glucan chains or in the form of amylose-lipid complexes (Morrison, 1988; Vasanthan & Hoover, 1992b; Morrison, 1995). Surface and bound lipids differ in terms of their extractability from the starch granules using common lipid solvents. Free lipids are easily extractable with cold solvents (chloroform and methanol) at ambient temperatures, and bound lipids can be extracted using hot aqueous alcohol (*n*-propanol-water) (Vasanthan & Hoover, 1992b).

The total lipid (surface and bound) content of starches has been reported to range from 0.7-1.2 % (by weight) in cereals, 0.01-1.4 % in pulses and 0.08-0.2 % in tuber and root starches (Takahashi & Seib, 1988; Haase & Shi, 1991; Vasanthan & Hoover, 1992a; Huang *et al*., 2007). In contrast to tubers and pulse starches, cereal starches contain a substantial amount of FFA and lysoPL with the level positively correlated with the

amylose content, and the lysoPL may contribute up to ~2 % of starch weight in high amylose starches (Tester *et al*., 2004). Lysophosphatidylcholine is predominantly found in cereal starches (maize and wheat), along with palmitic and linolenic acids (Buléon *et al*., 1998). Morrison (1995) reported that the amount of lipid-complexed amylose incereal starches varied from ~15-55 % of the amylose fraction.

1.7.2 Protein

Starch purity is often stated as protein content. The protein content of purified starches varies from trace amounts (<0.1) to 0.7 % by weight (Biliaderis *et al*., 1981). In common with starch lipids, proteins are present on the granule surfaces and within the interior matrix (integral protein) of the granule (Baldwin, 2001). Surface proteins can be readily extracted at temperatures below the gelatinization temperature, whereas integral proteins require a temperature near or above the gelatinization temperature (Ellis *et al*., 1998). The starch granule associated proteins may be present together with lipids on the granule surface (Skerritt *et al*., 1990; Baldwin, 2001; Han & Hamaker, 2002). The presence and nature of the protein associated with the starch granule influence physicochemical properties and have the potential to moderate the starch functionality (Han *et al*., 2002; Israkarn *et al*., 2007)

1.7.3 Phosphorous

Phosphorous is one of the non-carbohydrate constituents found in most starches. Phosphorous is present in the form of internal phospholipids, phosphate monoesters and inorganic phosphates in various starches. Phosphorous in cereal starches exists mainly within phospholipids, whereas in root, tuber and pulse starches, it is found primarily as

phosphate monoesters (Hizukuri *et al*., 1970; Lim *et al*., 1994; McPherson & Jane, 1999). The phosphate monoesters are formed during starch biosynthesis and the level of phosphorylation varies with the botanical origin of starch (Blennow *et al*., 2002). Tuber starches contain predominantly starch mono phosphate esters (0.2-0.4 %), whereas cereal starches contain a minute amount of phosphate monoesters compared to their phospholipid content (0.02-0.06 %) (Blennow *et al*., 2002; Singh *et al*., 2003). The phosphorous content of legume starches has been reported to range from 0.004 to 0.01 % (Kasemsuwan & Jane, 1996; Ambigaipalan, *et al*., 2011). In native starches, phosphate monoesters are confined primarily to the amylopectin fraction and are found at the C-2, C-3 and C-6 positions of the glycosyl units (Lim *et al*., 1994; Kasemsuwan & Jane, 1996).

Surface gelatinization studies have shown that phosphorous in potato starch is more concentrated in the granule core than in peripheral regions and smaller granules contain a greater phosphate content than large granules (Jane & Shen, 1993; Nielsen *et al*., 1994). The nature of the phosphorous present in starch granules produces different effects on pasting properties. Starches with a high phosphate monoester content increase paste clarity and paste viscosity in potato starches, whereas higher phospholipid contents produce pastes with low paste clarity and viscosity (Singh *et al*., 2003; Jane, 2009).

1.8 Starch properties

1.8.1 Granular swelling and amylose leaching

Native starch granules are generally insoluble in cold water. When starch granules are heated in the presence of excess water, the crystalline structure is disrupted by

increased hydrogen bonding between water molecules and the hydroxyl groups exposed on the amylose and amylopectin molecules (Srichuwong *et al*., 2005b). These changes facilitate granular swelling and an increase in granule size. The hydration and swelling of starch contribute to amylopectin-amylose phase separation and loss of crystallinity (Conde-Petit *et al*., 2001), which is accompanied by leaching of glucan components from the granules. Amylose, with a lower molecular weight diffuses out at a lower temperature, while higher molecular weight fractions leach at a higher temperature (Gomand *et al*., 2010). Leaching of amylose molecules from the swollen starch granules is denoted as amylose leaching (Whistler & BeMiller, 1997). Granular swelling is associated primarily with amylopectin content and amylose acts as a diluent and restricts the swelling (Singh *et al*., 2003).

The granular swelling and amylose leaching of starch illustrate the extent of glucan chain interactions (amylose-amylose, amylose-amylopectin, amylopectin-amylopectin) within the amorphous and crystalline regions and the packing arrangement of the glucan chain within the crystalline lamella (Ratnayake *et al*., 2002; Gomand, 2010). The extent of this interaction is influenced by the amylose to amylopectin ratio and the characteristics of each molecule, including the degree of polymerization, length and degree of branching of amylopectin, molecular weight, and molecular conformation (Sasaki & Matsuki, 1998; Hoover, 2001; Ratnayake *et al*., 2002; Gomand, 2010). Furthermore, granule size, non-carbohydrate constituents such as proteins, phospholipids, monoacylglycerol and phosphate monoesters, starch modifications imposed by chemical and physical methods and heating temperature all have been shown to influence granular

swelling and amylose leaching from starch granules (Tester & Morrison, 1990a; Hoover & Vasanthan, 1994a; Hoover & Vasanthan, 1994b; Roach & Hoseney, 1995; Wang & Seib, 1996; Lindeboom *et al*., 2004; Srichuwong *et al*., 2005b).

The degree of granular swelling has been studied using two different methods: swelling power (SP), which represents the ratio of wet weight of the sediment gel (volume of swollen granules) to its dry weight, and swelling factor (SF), which measures the ratio of the volume of sediment gel to the volume of dry starch granules (Vamadevan & Bertoft, 2015). The SP measures both the intra-granular and inter-granular water, whereas SF represents only the water that enters the granule and thus contributes to the increase in volume upon heating (mainly intra-granular water) (Tester & Morrison 1990a; Tester & Morrison 1990b). Starches from pulses, roots and tubers generally display single-stage swelling, whereas normal cereal starches exhibit two-stage swelling (Hoover, 2001; Hoover & Sosulski, 1986; Langton & Hermansson, 1989). In general, granular swelling increases with an increase in temperature up to a certain limit, and the extent of granular swelling decreases with an increase in amylose content (waxy > normal > high amylose). Restricted swelling was observed in high amylose maize, potato and pulse starches (Debet & Gidley, 2006; Hoover *et al*., 2010; Srichuwong *et al*., 2005b).

1.8.2 Gelatinization

When starch is heated in the presence of excess water, it undergoes an order to disorder irreversible phase transition referred as gelatinization (Wang & Copeland, 2013). It is generally accepted that the following processestake place during gelatinization: water initially enters the amorphous growth rings of starch granules, hydrates and initiates a

certain degree of swelling, crystallite melting, loss of optical birefringence, uptake of heat and thermal motion. The solvation causes disruption of molecular order (rupture of crystalline regions), unravelling, dissociation of double helices and leaching of amylose followed by leaching of amylopectin (Atwell *et al*., 1988; Cooke & Gidley, 1992; Jenkins & Donald, 1998). According to Colonna and Buleon (2009), four different steps are involved in the process of gelatinization: 1) cleavage of bonds between starch chains (endothermic); 2) formation of new hydrogen bonds between starch and the solvent (exothermic); 3) unravelling (helix to coil transition) of amylopectin double helices (endothermic); and 4) the development of amylose lipid complexes.

Waigh *et al*. (2000) have suggested that gelatinization is due to the interplay between self-assembly and the disruption of starch structure during heating. The lamellae in starch consist of a backbone, side chain and double helices. The distinctive property of a given starch is governed by the degree of mobility of lamellar components coupled with the helix to coil transformation. Starch gelatinization has been described with a liquid-crystalline model (Figure 1.8), where the amylopectin molecules may have the structure of a side-chain liquid crystalline polymer (Waigh *et al*., 2000). In this model, depending on the water content and heating rate, gelatinization occurs as a result of helix to coil transition and the transformation of amylopectin helices from a rigid (glass) nematic phase to a plasticized smectic phase. In the nematic state, amylopectin helices are not organized into lamellae, whereas in the smectic state, the double helices are aligned into lamellae with a 9 nm inter-lamellar spacing.

a) Low water content (<5 % w/w)

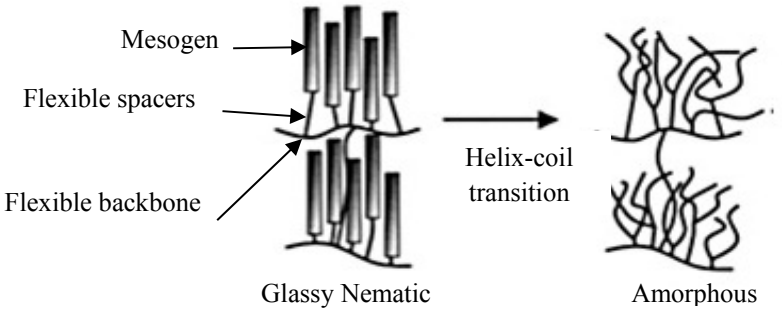

b) Intermediate water content (>5 %, <40 % w/w)

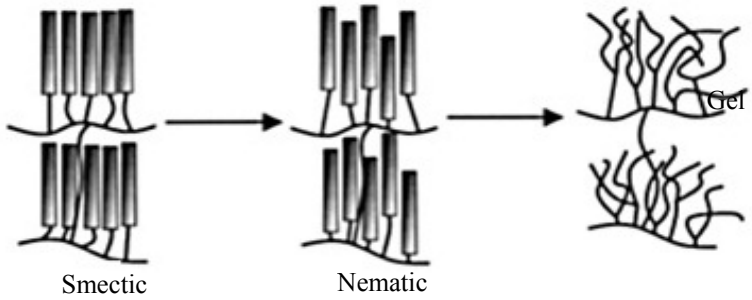

c) Excess water content (>40 % w/w)

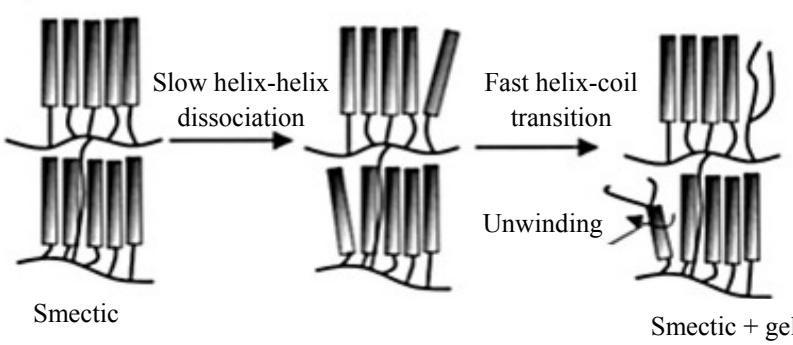

Figure 1.8: Liquid crystalline model of starch gelatinization (Waigh *et al*., 2000, Copyright Elsevier, reproduced with permission).

At low water content (< 5 %, w/w), the amylopectin helices are in a glassy nematic state. Upon heating, the single peak of a differential scanning calorimetry (DSC) endotherm corresponds to the helix to coil transition. Intermediate water contents (from 5 to 40 %, w/w) consist of two steps in their breakdown and possess two endothermic peaks (biphasic peak). The first peak is due to the rearrangement and dislocation between amylopectin double helices, which leads to a phase transition of a smectic to nematic phase. The nematic phase is the helix to coil transition, where the amylopectin double helices unravel irreversibly. In excess water (>40 %, w/w), the lamellar break-up and disentanglement of double helices occur at the same point as a result of the unstable nature of free unassociated helices (Waigh *et al*., 2000).

The phase transition and structural changes occurring during starch gelatinization have been investigated extensively using a variety of techniques, including DSC, SAXS (small angle X-ray scattering), WAXS (wide angle X-ray scattering), NMR, FTIR (Fourier transform infrared spectroscopy), SANS (small angle neutron scattering), small angle light scattering and microscopy (electron microscopy, light microscopy) (Jane *et al.*, 1992; Jenkins & Donald, 1998; Biliaderis, 2009; Wang & Copeland, 2013). DSC has proven to be a most valuable and sensitive tool to elucidate starch gelatinization (Wang & Copeland, 2013). DSC measures energy changes (heat released or absorbed) in a material during phase transitions or reactions. In the gelatinization process, DSC is used to determine the gelatinization transition temperatures (onset, To; midpoint, Tp; conclusion, Tc) and the energy absorbed (enthalpy of gelatinization, ΔH) by the starch-water system. The gelatinization and swelling properties of starches have been shown to be influenced

by the molecular structure of amylopectin (chain length distribution, molecular weight, degree of phosphorylation, branching frequency and polydispersity), starch composition (ratio of amylose to amylopectin, amylose lipid complex), internal granule structure (crystalline to amorphous ratio) and starch damage (Donovan, 1979; Tester & Morrison, 1990a; Tester *et al*., 1993; Eliasson & Gudmundsson, 1996; Sasaki *et al*., 2000; Hoover & Ratnayake, 2002; Vamadevan *et al*., 2013).

In addition to these endodenous traits, the presence of solvents and solutes (sugars, salts, alcohols and lipids), physical and chemical modifications (annealing, heat moisture treatment, acid hydrolysis, hydroxypropylation and acetylation), defatting, growth conditions, extraction procedures, water content and heating rate also affect the gelatinization properties of starches (Evans & Haisman, 1982; Eliasson & Kim, 1992; Tester & Debon, 2000; Waigh *et al*., 2000; Atichokudomchai *et al*., 2002a,b; Jayakody & Hoover, 2008; Hoover, 2010).

1.8.3 Pasting characteristics

Pasting is the process that takes place after gelatinization, which includes the following steps: granular swelling, exudation of molecular components (primarily amylose) from the granule and eventual disintegration of the starch granules (Atwell *et al*., 1988). The plasticization effect of water and heating destabilizes the hydrogen bonds holding the crystalline structure of amylopectin and forms new hydrogen bonds between water molecules and amylopectin chains which lead to hydration and granular swelling. Consequently, the swollen granules become more susceptible to shear disintegration and amylose starts to leach out from the granules, which increases the viscosity of the starch

paste (Joshi *et al*., 2013). Starch paste consists of a continuous phase of solubilized amylose and amylopectin network, and a discontinuous phase of granule ghosts and fragments (granule remnants) (Whistler & Bemiller, 1997).

The pasting profiles of starch-water mixtures are monitored continuously under constant stirring with a programmed heating and cooling cycle using a rapid visco analyser (RVA), which measures the change in viscosity consistently as a function of temperature and time (Mariotti *et al*., 2005). A typical RVA profile of starch describes the pasting behaviour in three phases: 1) a controlled heating phase, increasing the suspension temperature to 95°C; 2) an isothermal phase – holding the suspension at 95°C; and 3) a controlled cooling phase, decreasing the suspended temperature to 50°C.

Starch suspensions typically show a viscosity increase to a maximum level (peak viscosity) due to gelatinization and swelling of granules, followed by a decrease to a minimum value caused by shear-induced disintegration of swollen granules. The difference between the peak and minimum viscosity at 95°C is referred to as 'breakdown'. As the starch paste cools, leached amylose molecules form a three-dimensional gel network, which increases the viscosity from the minimum to a final value referred to as cold paste viscosity. A 'setback' is defined by the difference between cold paste viscosity and the minimum viscosity at 95°C (Deffenbaugh *et al*., 1989; Copeland *et al*., 2009). The peak time and peak viscosity values indicate the water binding capacity and susceptibility to disintegration of starch granules. The extent of setback is mainly influenced by the amylose content (Varavinit *et al*., 2003; Copeland *et al*., 2009). Pasting properties are influenced by the starch source, granule size, amylose content, amylose

content, extent of granular swelling and amylose leaching, presence of phosphate monoesters and lipids, friction between swollen granules, structure of amylopectin, and presence of solutes (Ziegler *et al*., 1993; Hoover & Vasanthan, 1994a; Jacobs *et al*., 1996; Hermansson & Svegmark, 1996; Jane, *et al*., 1999; Ao & Jane, 2007).

1.8.4 Retrogradation

Starch retrogradation is a process that occurs upon cooling of the gelatinized starch paste, where the starch chains begin to reassociate and lead to the formation of an ordered structure through hydrogen bonding (Hoover, 2010). During retrogradation, linear amylose molecules reassociate and form double helices of 40-70 glucose units (Jane & Robyt, 1989), while amylopectin molecules re-crystallize through the association of their outermost branches (Singh *et al*., 2003).

Starch retrogradation is considered a non-equilibrium, thermo-reversible recrystallization process which occurs in three successive steps: nucleation (formation of crystal nuclei), propagation (crystal growth from the nuclei formed during nucleation) and maturation (Silverio *et al*., 2000; Ambigaipalan *et al*., 2013). It has been shown that the rates of both nucleation and propagation steps are influenced by storage temperature (Silverio *et al*., 2000; Vandeputte *et al*., 2003). The nucleation rate increases with a decrease in temperature (below Tg), whereas the extent of propagation increases with an increase in temperature (up to To) (Eerlingen *et al*., 1993; Silverio *et al*., 2000).

During retrogradation, the gelation of solubilized amylose chains proceeds at a faster rate than the recrystallization of highly branched amylopectin molecules (Miles *et al*., 1985). Starches with higher amylose or intermediate material content exhibit a greater

tendency toward retrogradation. However, starches with longer amylopectin chains (tuber and pulse starches) retrograde faster compared to those with a shorter average chain length of amylopectin (cereal starch) (Fredriksson *et al*., 1998; Silverio *et al*., 2000; Vamadevan & Bertoft, 2015).

Retrogradation involves an increase in the crystallinity, gel strength, exudation of water (syneresis) and gel network formation changing molecular turbidity and appearance of the 'B' type polymorphic forms (Hoover, 1995; Mua & Jackson, 1998). Pulse starches retrograde to a high extent in comparison with cereal and tuber starches, due to the higher amylose content and/or differences in molecular structure (Hoover, 2010). Generally, retrogradation is not desirable in foods containing starch, because it affects the quality, acceptability and shelflife during storage (Biliaderis, 1991).

1.8.5 Acid hydrolysis

Acid hydrolysis has been used to modify the starch granule structure and produce thin-boiling starches for food and industrial uses (Hoover, 2000). Acid-modified starches are prepared by treating a starch slurry (~30-40 %) with dilute mineral acid (suphuric acid or hydrochloric acid) at a temperature below the gelatinization temperature (25-60°C) for a certain period of time (Wurzburg, 1986). The remaining starch residue after prolonged acid hydrolysis at room temperature is known as Naegeli dextrin (treatment with 15 % H_2SO_4) or lintnerized starch (treatment with 7.5 % w/v HCl). Lintnerized starches possess a high-molecular weight fraction, whereas Nageli dextrins are composed mainly of a mixture of linear and branched low-molecular-weight fractions of dextrins (Hoover, 2000; Robin, 1974). During acid hydrolysis, the hydronium ion (H_3O^+) carries out an

electrophilic attack on the glycosidic oxygen atom and the electrons in one of the carbon-oxygen bonds transfer to the oxygen atom to form a carbocation. The high energy, unstable carbocation intermediate then quickly reacts with water, leading to regeneration of a hydroxyl group (Hoover, 2000). The mechanism of acid hydrolysis is outlined in Figure 1.9.

All starches exhibit two distinct phases of hydrolysis. A relatively rapid hydrolysis rate is observed during the first eight days, followed by a slower rate after 9-12 days. During acid hydrolysis, the bulky amorphous and inter-crystalline regions of the granule are hydrolysed initially, followed by a slower rate of hydrolysis of the crystalline regions (Biliaderis *et al*., 1981; Hoover, 2000; Genkina *et al*., 2009; Kim *et al*., 2012). Amorphous regions within starch granules are more susceptible to acid attack due to the loose packing of starch chains compared to crystalline regions. Two different hypotheses have been proposed to explain the slower rate of the crystalline region: 1) the dense packing of starch chains within the starch crystallites restricts the rapid penetration of H_3O^+ into these regions; and 2) the conformational changes of D-glucopyranosyl units (chair to half-chair) required for the electrophilic attack of H_3O^+ on the glycosidic oxygen are restricted due to immobilization of starch chains within the crystallites. The majority of the glucosidic oxygens are buried inside the double helical arrangement and thus their accessibility to H_3O^+ ions is restricted (Kainuma & French, 1971; Jayakody & Hoover, 2002).

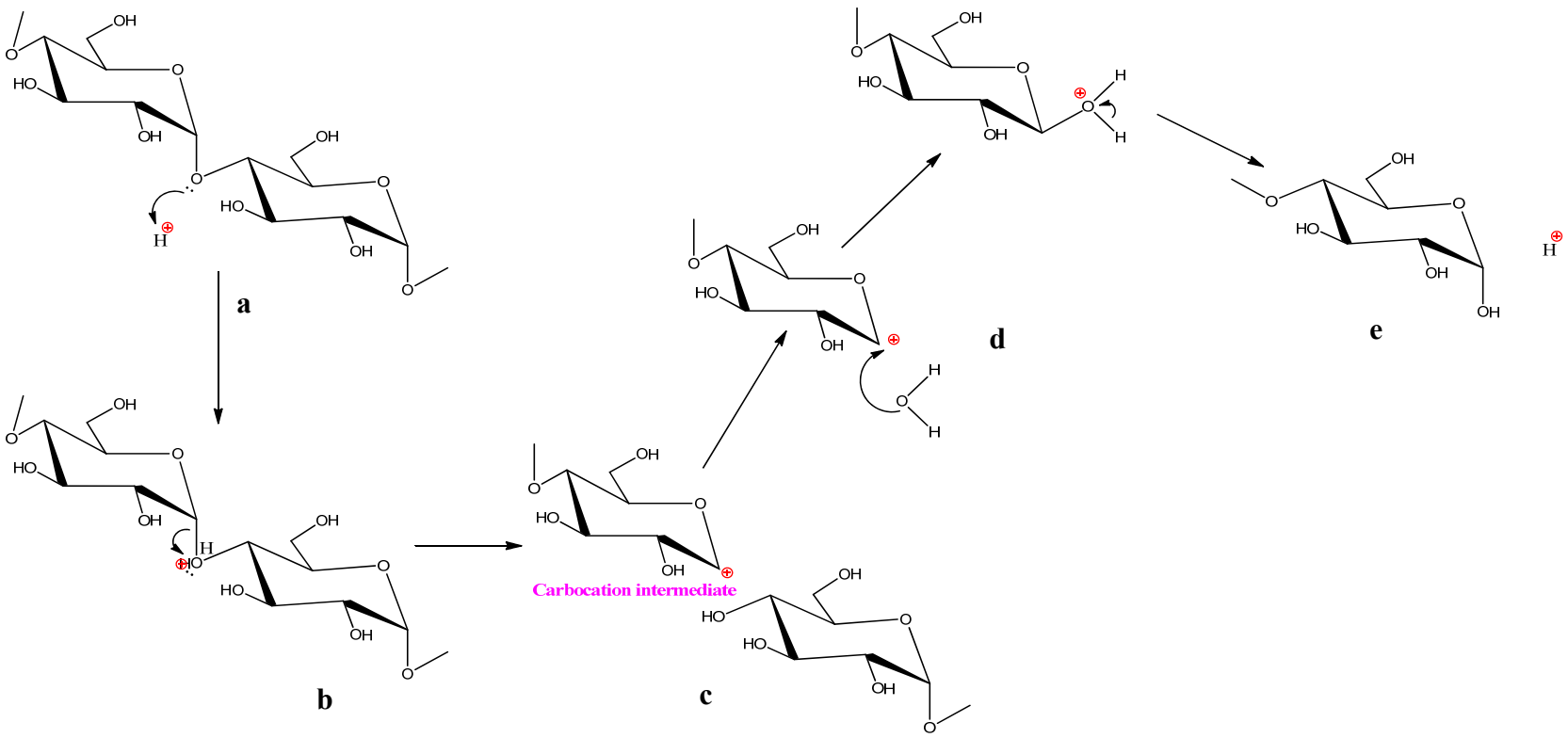

Figure 1.9: Mechanism of acid hydrolysis of starch (Adapted from Hoover 2000).

a. Electrophilic attack of H^+ on the oxygen atom of the α(1→4) glycosidic linkage

b. Electrons in one of the C=O bonds moves to the oxygen atom

c. Formation of unstable, high-energy carbocation intermediate

d. Reaction with water

Factors which influence the rate and extent of hydrolysis among starches include: 1) granular size; 2) extent of glucan chain interactions (within the amorphous and crystalline domains of the granule); 3) starch composition (amylose content and amylose-lipid complexes); 4) presence of pores and cracks on the granule surface; 5) distribution of α(1→6) branch points between the amorphous and crystalline regions; and 6) degree of packing of the double helices within crystallites (Morrison *et al*., 1993a; Jane *et al*., 1997; Hoover, 2000; Jayakody & Hoover, 2002). Acid hydrolysis of starch proceeds randomly, cleaving both α(1→4) and α(1→6) bonds and shortening the chain length with the progress of hydrolysis. Acid modification increases the gelatinization temperature, gelatinization temperature range, solubility of starch, gel strength and retrogradation rate and decreases the viscosity of starch (Shi & Seib, 1992; Kim & Ahn, 1996; Atichokudomchai *et al*., 2002a,b; Singh *et al*., 2009).

1.8.6 Enzyme hydrolysis

Enzyme-catalysed hydrolysis has been used as an investigative tool to study the ultrastructure of starch granules (Oates, 1997). Amylases are the most industrially applied starch degrading enzymes used to produce modified starches and hydrolysed products such as sweeteners and syrups. Amylolytic enzymes are generally referred to as glycoside hydrolases (GHs), a group of enzymes that catalyses the hydrolysis of α(1→4) and/or α(1→6) glycosidic bonds in starch and related oligo- or polysaccharides. The apha-amylase (EC 3.2.1.1) is an endo-acting enzyme that randomly internally hydrolyses α(1→4) glycosidic bonds and bypasses α(1→6) branch points of the glucan chains, producing linear and branched oligosaccharides of various chain lengths and α-limit dextrins containing α(1→6) bonds. Glucoamylase or amyloglucosidase (EC 3.2.1.3) is an exo-acting enzyme that depolymerizes both

α(1→4) and α(1→6) glycosidic bonds from the non-reducing ends of the starch polymer chains, yielding the complete conversion of starch into glucose units (Sujka & Jamroz, 2007). Pullulanase and isoamylase, referred to as debranching enzymes, hydrolyse only α(1→6) bonds, thus removing the branch chains of the glucan chains. Beta-amylase is also an exo-acting enzyme that hydrolyses only (1-4) linkages from the non-reducing ends of the glucan chains and produces β-maltose and β-limit dextrins (Goesaert *et al*., 2009). Alpha-amylases have been produced from various sources, including plants, bacteria, fungi, animals and humans. The α-amylases from different sources differ in their action patterns and size of binding site (Robyt & French, 1963; Robyt & French, 1967; Robyt & French, 1970; Klein & Foreman, 1980; Ryan *et al.,* 2006).

The enzymatic hydrolysis of starch granules involves several steps, which include the diffusion of enzymes to the solid surface area and then inside the granules, followed by adsorption of the enzyme onto the substrate and subsequent catalytic reaction (Gallant *et al*., 1992; Sujka & Jamroz, 2007). In general, the initial hydrolysis takes place on the surface of the granule, depending on the starch source. The hydrolysis of starch by α-amylase involves an enzyme in solution reacting on a solid substrate, whereas the critical kinetic parameters are the accessibility of the enzyme to the surface area of the substrate and the extent of enzyme adsorption onto the surface (Bertoft & Manelius, 1992).

Based on microscopic observations, different forms of enzymatic attack on starch granular surfaces have been reported (Zhang *et al*., 2006a,b; Apinan *et al*., 2007). Depending on the enzyme and type of starch, an enzyme can either erode the entire granule surface or the susceptible zones become pitted during the hydrolysis, a

process called exo-corrosion. Expansion of pits and the formation of digest channels at specific points on the surface toward the hilum (center) regions of the granules are referred to as endo-corrosion (Gallant *et al*., 1992; Zhang *et al*., 2006a; Copeland *et al*., 2009; Dona *et al*., 2010). Smaller granules have a large surface area per unit mass that facilitates diffusion and adsorption of enzymes which in turn increase the catalytic reaction; they hydrolyse faster compared to larger granules (Dhital *et al*., 2010).

Native granules are hydrolysed to a lesser extent than those of gelatinized (processed) starch. The gelatinization process disrupts the crystalline structure and causes a decrease or loss of polymer chain interactions, such as double helices or amylose-lipid complexes, which in turn facilitates the accessibility of enzyme toward substrates to a large extent (Blazek & Gilbert, 2010). Starch chains with limited mobility (either complexed or crystallized) are less susceptible to enzymatic hydrolysis because their constituent glucose units are more firmly organized into a specific configuration. This restricts the accessibility of amylases to unwind the double helices of the starch chains (Oates, 1997).

Crystalline polymorphic forms are an important factor in determining the rate and extent of enzymatic hydrolysis, but the susceptibility of a different polymorphism toward hydrolysis is still in dispute. Copeland *et al*. (2009) reported that A-type polymorphs are more resistant to enzymatic hydrolysis compared to B-type polymorphs. However, several authors have suggested that A-type crystals are more susceptible to amylolysis (Jane *et al*., 1997; Planchot *et al*., 1997; Srichuwong *et al*., 2005a). Jane *et al*. (1997) have shown that in the interior crystalline structures of A-type starches, the α(1→6) branch points are dispersed in both crystalline and amorphous regions. Furthermore, a larger proportion of short A chains (smaller

double helices) in the crystalline regions led them to be more susceptible to amylolysis. In contrast, B-type starches contain more α(1→6) branch points in the amorphous regions and fewer short branch chains, which results in a superior crystalline structure that resists amylolysis (Zhou *et al*., 2004). Studies on field pea starches have shown that the increase in the B-polymorphic content reduces the extent of amylolysis (Ratnayake *et al*., 2001). Gerard *et al*. (2001) have suggested that the arrangement and the orientation of B-type crystallites within the granule could be a factor that makes them less susceptible to α-amylolysis.

The presence of pores and channels in A-type starches (Fannon *et al*., 1992; Huber & BeMiller, 2000; Jane, 2006) facilitates the diffusion of enzymes to the granular interior with an enlargement of the surface pores. The enzymes hydrolyse these starch granules using an 'inside-out' pathway, where the concurrent hydrolysis takes place from the less organized hilum region toward the peripheral regions with a preferential hydrolysis of amorphous regions prior to ordered crystalline regions (Gallant *et al*., 1992; Blazek & Gilbert, 2010). Starches with B- and C-type polymorphs are less favorable to the 'inside-out' digestion pattern since they do not possess surface pores and channels. Thus, the digestion takes place from the outer resistant surface of those granules and the hydrolysis pattern is referred as 'exo-pitting' (Gallant *et al*., 1992; Planchot *et al*., 1995). However, Zhang *et al.* (2006a) have proposed that irrespective of the crystalline type, both the amorphous and crystalline regions are evenly digested through a mechanism called the 'side by side' mechanism. Furthermore, the glucan chains that do not participate in the crystalline formation may not be free and mobile; also, the tight packing of those chains adjacent to the crystalline regions inhibit hydrolysis (Zhang *et al*., 2006a,b; Dhital *et al*., 2010).

Tester *et al.* (2006) have shown that the extent of hydrolysis by α-amylase is inversely related to the amylose content of the native starch. For instance, waxy maize is hydrolysed faster compared to normal and high amylose maize starches. The rate and extent of amylolysis of native starch granules is influenced by many factors, including the starch botanical origin, granule structure and morphology, supramolecular structure, molecular structure (amylose to amylopectin ratio, fine structure of amylose and amylopectin), chemical composition, enzyme specificity and hydrolysed products (malto oligosaccharides) (Colonna *et al*., 1988; Hoover & Zhou, 2003; Copeland *et al*., 2009; Dhital *et al*., 2010; Blazek & Copeland, 2010).

The *in vitro* digestion pattern of different starches has been investigated using α-amylase (porcine pancreatic α-amylase) and amyloglucosidase (Englyst *et al*., 1996). The rate of hydrolysis is predominantly influenced by α-amylase, while amyloglucosidase mainly converts the hydrolysed products (maltose, maltotriose) of α-amylase into glucose units to prevent product inhibition of α-amylase activity. Therefore, the digestibilities of native starches are mainly controlled by α-amylase, and the direct influence of amyloglucosidase on hydrolysing starch chains is limited (Kimura & Robyt, 1995; Zhang *et al*., 2006a).

1.8.7 Starch nutritional fractions

Starch is an important part of the human diet and it serves as a major source of glucose. Depending on the rate and extent of digestion of starches in the gastrointestinal tract, the postprandial blood glucose levels and corresponding insulin response can be varied (Dhital *et al*., 2017). The concept of glycemic index (GI) was introduced to categorize foods based on their effect on postprandial blood glucose response. The GI is defined as the area under the glycemic response curve (AUC)

after the ingestion of the test product, expressed as the percentage of the corresponding area after ingestion of an equicarbohydrate portion of a reference food (Jenkins *et al*., 1981). Based on GI values, foods are categorized into three groups: high GI (GI>70), intermediate/medium GI (56-69) and low GI (GI<55) (Brand *et al*., 1991).

For nutritional purposes, Englyst *et al*. (1992) designed a study to classify starches based on the kinetics of *in vitro* digestion. In this study, porcine pancreatic α-amylase and fungal amyloglucosidase were used instead of human α-amylase and mucosal α-glucosidase for simulating gastrointestinal conditions, and glucose release was measured at different time intervals. Based on this study, starch nutritional fractions are identified. Starch that is digested into glucose within 20 min and is correlated to a high glycemic index is referred to as rapidly digestible starch (RDS). As an energy source, RDS is rapidly digested and absorbed in the duodenum and proximal part of the small intestine, leading to a rapid increase of plasma glucose and insulin levels (Englyst *et al*., 1992; Zhang & Hamaker, 2009; Lee *et al*., 2013).

In general, the RDS content of cereal starch (2.5-90.0 %) is greater compared to legume (3.0-21.0 %) and tuber (0.1-21 %) starches. Zhang *et al*. (2006b) have reported that starches with a higher proportion of short A chains are more susceptible to enzyme-catalysed hydrolysis, leading to higher levels of RDS. The A chains with a dp of 5-10 are too short to form double helices and disrupt the crystalline structure, which causes the crystalline defects (Zhang *et al*., 2006b). Consumption of foods that are rich in RDS leads to a substantial fluctuation of plasma glucose levels and causes high stress on the regulatory system of glucose homeostasis. Consequently, high levels of RDS have been shown to increase the risk of diabetes, cardiovascular disease

and obesity (Wolever & Bolognesi, 1996; Ludwig *et al*., 1999; Ludwig, 2002; Zhang *et al*., 2006b).

In contrast, slowly digestible starch (SDS) is fully digested into glucose during a prolonged digestion period (20-120 min) at a slower rate compared to RDS (Wolf *et al*., 1999; Zhang *et al*., 2008). However, both RDS and SDS are nutritionally considered as glycemic starches (Englyst *et al*., 1992). SDS is digested slowly through the small intestine with a moderate glycemic and insulinemic response and prolonged release of glucose (Zhang & Hamaker, 2009). The portion of starch that is not digested after 120 min is termed resistant starch (RS) (Englyst *et al*., 1992). In contrast to RDS and SDS, RS is not digested in the upper gastrointestinal tract, and is fermented by microorganisms in the colon to produce short chain fatty acids (SCFA) including acetic, propionic and butyric acids (Barry *et al., 1995*; Cummings *et al*., 1996; Perera *et al*., 2010).

In addition to potential health benefits, RS is considered a functional ingredient. As a source of dietary fiber, RS has a lower impact on the sensory properties of foods compared to traditional sources of fibers such as whole grains, fruits or bran (Fuentes-Zaragoza *et al*., 2010; Perera *et al*., 2010). Furthermore, the desirable properties of RS, including swelling capacity, formation of gel, increase in viscosity and water binding capacity, make it a useful functional ingredient in a variety of food products (Nugent, 2005; Sajilata *et al*., 2006; Augustin *et al*., 2008). The RS content of cereal and pulse starches differ with the molecular composition (amylose and amylopectin) and their chain lengths (Zhang & Hamaker, 2009).

Resistant starch is divided into four major types based on the nature of their enzyme resistance and starch structure: RS type 1 (RS1), RS type 2 (RS2), RS type 3 (RS3) and RS type 4 (RS4) (Englyst *et al*., 1992; Eerlingen & Delcour, 1995). RS1 represents the physically inaccessible starch trapped within whole plant cells with undamaged cell walls or within food matrices (e.g. partially milled grains, legume seeds and pasta) (Brown 2004; Sajilata *et al*., 2006). This type of RS is unavailable to digestive enzymes, since gastrointestinal tract enzymes are incapable of degrading the cell wall components (cellulose, hemicellulose, lignin and other constituents) (Leszczyñski, 2004). The presence of intact cell walls contributes to the RS content of legumes. The physical or chemical treatments (e.g. grinding and proteolysis) that can destroy the physical barriers of foods affect the RS1 content (Fardet *et al*., 1998).

Resistant starch type 2 represents raw starch granules that are resistant to enzymatic digestion due to the structural organization (compact structure) in their native state. RS2 is found in starches with B- or C-type polymorphic structures such as raw potato starch, green banana and high amylose maize starches (Jane *et al*., 2003; Brown, 2004). Some food applications, such as thermal processing methods, significantly reduce the RS2 content, while hydrothermal treatments (annealing and heat moisture treatment) can be used to increase the RS levels, particularly in high amylose starches (Kishida *et al*. 2001; Liu *et al.,* 2007).

Resistant starch type 3 comprises the retrograded starch formed during the cooling of gelatinized starch resulting from food processing operations. The starch granule is completely hydrated during the formation of RS3. The presence of lipids affects the double helical association of amylose molecules during retrogradation, where lipid molecules form an inclusive complex with amylose and reduce the

interaction between amylose chains. Therefore, the formation of a crystalline structure will be disrupted, which in turn lowers the resistant starch content (RS3) resulting from retrogradation (Leszczyñski, 2004). Partial acid hydrolysis, multiple freeze-thaw cycles and selected debranching of starches increase the rate and extent of retrogradation of thermally processed foods, which in turn increases the RS3 content (Brumovsky & Thompson, 2001; Lehmann *et al*., 2002; Chung *et al*., 2003; Hasjim & Jane, 2009).

Resistant starch type 4 represents the starches that are chemically modified to improve the functional characteristics of starches. Various types of chemical modification techniques, including etherification, esterification and cross-linking, are used to introduce new functional groups into the starch chains; these functional groups can prevent enzymatic digestion by hindering the accessibility of enzymes to glycosidic bonds. Furthermore, new additional bonds other than α(1→4) and α(1→6) are formed during chemical modification (Leszczyñski, 2004; Sajilata *et al*., 2006).

In addition to these four types of RS, amylose-lipid complexes are also considered an additional type of resistant starch as they are resistant to amylolysis. Amylose-lipid complexes are categorized as RS5 (Hasjim *et al*., 2010; Ai *et al*., 2013).

1.9 Annealing

Annealing (ANN) is a physical modification technique that involves treating starch granules in the presence of heat and water. During the process of ANN, starch granules treated in excess (>60 %, w/w) or intermediate (40 %, w/w) water content are subjected to a temperature exceeding the glass transition temperature (Tg) but below

the onset temperature (To) of gelatinization for a certain period of time (Jacobs & Delcour, 1998; Tester & Debon 2000; Jayakody & Hoover 2008). Tg is defined as the temperature at which the amorphous domains of the starch granules are modified from a rigid glassy to a mobile rubbery state when treated with heat in the presence of solvents like water/glycerol (Tester & Debon, 2000).

Starch is a semi-crystalline polymer, where the double helices are intact and do not have an optimal side by side arrangement in their unhydrated native state. This is because of the varying lengths of radial and tangential branches, and this state is referred to as a nematic state (Figure 1.10 a) (Waigh *et al*., 1996; Perry & Donald, 2000). During annealing, the amorphous portion of the starch granule has the ability to imbibe water which results in plasticization. The amorphous region is glassy and immobile prior to hydration; the mobility of the amorphous region increases and causes the vibrational movement of tangential and radial chains in amorphous and crystalline domains. Increasing the ANN temperature and excess water are two important factors that can drive the rate of hydration and increase the glucan chain mobility. This restricts the side by side movement of double helices and forms the smectic type structure (Figure 1.10 b) (Jayakody & Hoover, 2008; Perry & Donald, 2000).

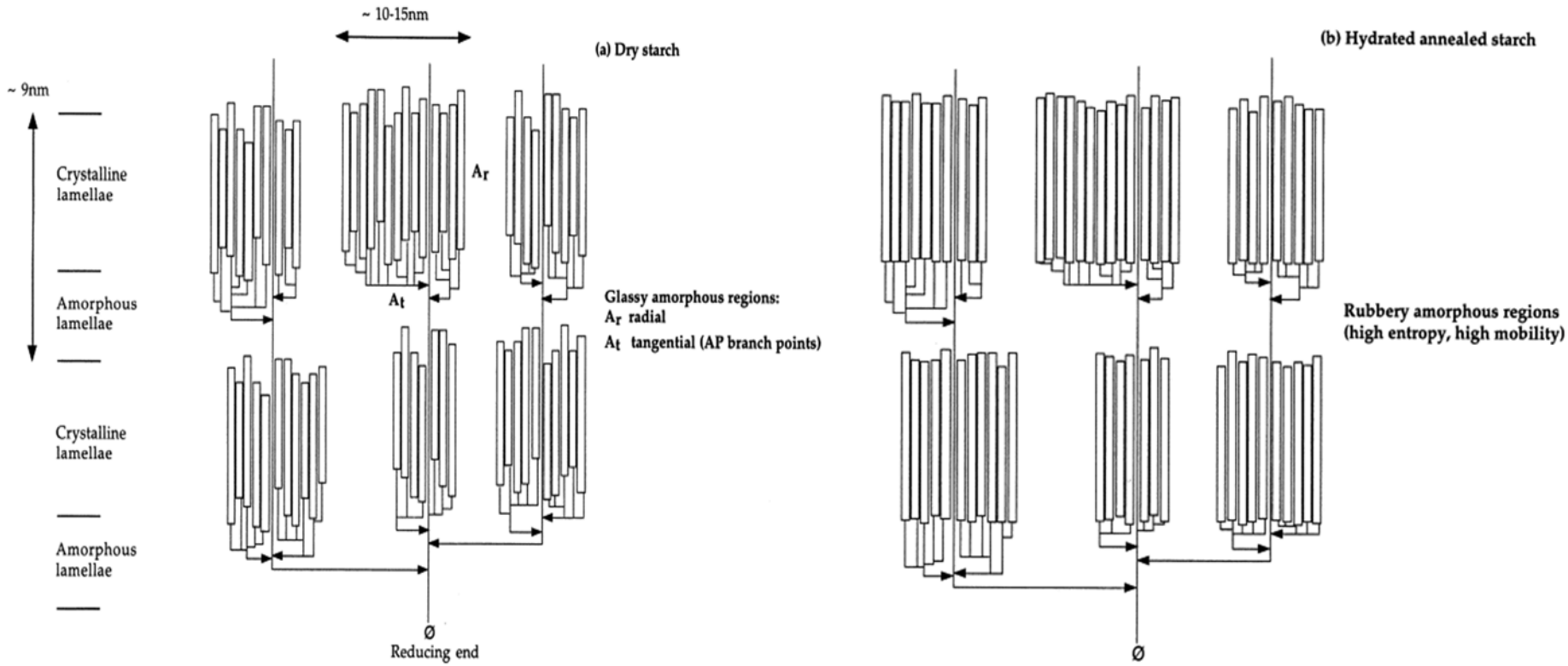

Figure 1.10: (a) Diagram illustrating the impact of hydration and subsequent ANN on semi-crystalline lamellae (the rectangles represent the amylopectin double helices): a) dry starch with glassy amorphous regions; (b) hydrated annealed starch with rubbery amorphous regions. (Tester *et al*. 2000, reproduced with permission from Elsevier).

As ANN progresses, the organization of starch chains and double helices of amylopectin become more organized and arranged in an ordered structure (Gomes *et al*., 2005; Zavareze & Dias, 2011).

1.9.1 Effect of annealing on granule morphology

The majority of studies have shown that there is a general lack of significant visible changes to the granule morphology (size or shape) or the birefringence pattern between native and annealed starches. However, a few studies have reported a decreased birefringence at granule centers, agglomeration/fusion of the granules, increased or decreased size of the granule, increased roughness, indentation or fissures at granule surfaces, and/or increased pore size after ANN (Nakazawa & Wang, 2003; Kiseleva *et al.*, 2005; Waduge *et al.*, 2006; Liu *et al.*, 2009; Dias *et al.*, 2010; Singh *et al.*, 2011; Rocha *et al.*, 2012; Wang *et al.*, 2013).

1.9.2 Effect of annealing on starch structure

On a supra-molecular level, annealed starches retain their native crystalline packing arrangement, since sub-gelatinization temperatures are commonly employed in ANN treatments. In most studies, the crystalline polymorphic patterns of different starches remained unchanged upon ANN (Hoover & Vasanthan, 1994a; Ozcan & Jackson, 2003; Vermeylen *et al*., 2006). However, a few studies have reported that a partial polymorphic transformation (B-/C-type to A-type) occurred during an extended period of ANN treatment (Genkina *et al*., 2004; Waduge *et al*., 2006). This transformation is energetically favorable for a more stable crystalline structure (type-A). In contrast to A-type starches, the impact of ANN on the crystalline structure is more pronounced in B-type starches (Muhrbeck & Wischmann, 1998).

The intensity of X-ray diffraction and/or relative crystallinity of starches from different botanical origins either remain unchanged (Chung *et al*., 2009a; Rocha *et al*., 2011; Wang *et al*., 2013), increased (Hoover & Vasanthan, 1994a; Jacobs *et al*., 1998; Vermeylen *et al*., 2006; Waduge *et al*., 2006; Rocha *et al*., 2012) or decreased (Jayakody *et al*., 2009; Dias *et al*., 2010) on ANN. The observed changes in starch crystallinity are mainly influenced by starch source and the treatment conditions during the ANN process. The extent of these changes reflects the balance between crystallite disruption, reorientation and subsequent recrystallization (Vermeylen *et al*., 2006). The increase in crystallinity may arise from the interplay of several factors, such as increased crystallite size and perfection of crystallites, formation of new crystallites between glucan chains, crystallite reorientation and amylopectin content (Vermeylen *et al*., 2006; Waduge *et al*., 2006; Lan *et al*., 2008; Rocha *et al*., 2011; Rocha *et al*., 2012). Gomes *et al*. (2004) observed a reduced intensity of the crystallinity peak in annealed starches. They suggested that the formation of new amylose-lipid complexes does not take part in the increase in helical order, which is mainly associated with interactions between amylose and amylopectin chains. Furthermore, the ordered and compact packing of the double helices is indicated by a reduced inter-crystalline spacing upon ANN.

On a molecular level, ANN increases the mobility of the glucan chains within amorphous lamella regions and the amylopectin double helical chain-segments in crystalline lamella regions. It facilitates the double helices to align into a more ordered structure within the crystalline lamella and leads to the crystallite perfection of existing crystallites (Kiseleva *et al*., 2004; Vermeylen *et al*., 2006; Gomand *et al*., 2012; BeMiller & Huber, 2015). Native starch possesses crystallites of different

stabilities. ANN disrupts the weak crystallites and facilitates the subsequent recrystallization and realignment of new or existing crystallites, which in turn increases molecular interactions between starch chains and results in more homogenous crystallites within the granule (Tester *et al*., 1998; Tester & Debon, 2000; Rocha *et al.*, 2011; Rocha *et al.*, 2012; Vamadevan *et al*., 2013).

Several authors have suggested that ANN does not increase the number of double helices in normal and waxy starches, whereas it facilitates lengthening of the double helices by twisting ends of the chains (Tester & Debon, 2000; Genkina *et al*., 2004; Kiseleva *et al*., 2005; Vamadevan *et al*., 2014). In high amylose starches, ANN induces the formation of new double helices and various chain interactions between the glucan chains (amylose-amylose, amylose-amylopecin, amylopectin-amylopectin) (Tester & Debon, 2000; Lin *et al*., 2009; Gomand *et al*., 2012). Based on small-angle X-ray scattering studies, Gomand *et al*. (2012) reported that ANN increases crystalline stability via crystal thickening, which is associated with the increased co-crystallization of amylose and amylopectin chains in high amylose potato starch. In waxy starches, crystal stability is increased by a reduction in crystal surface energy (γ). The reduction in crystal surface energy on ANN may be involved with the relaxation of conformationally constrained chains at the crystal border. Furthermore, the movement of amylopectin chains and/or their branch points, moving away from the amorphous-crystalline interface toward the granular amorphous regions (Gomand *et al*., 2002), lead to a very disordered nanomorphology (compartmentalization-like structures) on ANN (Knutson, 1990; Tester *et al.*, 2000; Gomand *et al.*, 2012).

In the amorphous regions, ANN-induced changes include the preferential hydration of amorphous regions, mobility of starch chains and the conversion of

amorphous amylose into structured helical forms. The structural changes occurring during the ANN treatment in both amorphous and crystalline regions lead to a decrease in mobility with restricted plasticisation and destabilization effects on starch crystallites, which, in turn, increases the Tg of the annealed starch (increase in the glassy nature) (Seow & Teo, 1993; Tester & Debon, 2000). Therefore, ANN induced changes within both crystalline and amorphous regions greatly influence the physicochemical properties of starch (BeMiller & Huber, 2015).

1.9.3 Effect of annealing on granular swelling and amylose leaching

Many researchers have shown that ANN reduces granular swelling in cereal, tuber and pulse starches (Jayakody *et al*., 2009; Chung *et al*., 2009a; Chung *et al*., 2010; Dias *et al*., 2010; Liu *et al*., 2009; Jyothi *et al*., 2011; Olu-Owolabi *et al*., 2011; Singh *et al*., 2011; Simsek *et al*., 2012; Yadav *et al*., 2013; Song *et al*., 2014). The extent of swelling reduction for these starches has been attributed to the interplay of the following factors: 1) amylose content; 2) increased crystalline perfection and decreased dehydration of amorphous regions; 3) extent of interaction between amylose-amylose and/or amylopectin-amylopectin interactions; 4) fine structure of amylopectin; 5) extended intra-granular binding forces and strengthening of the granule; and 6) presence of amylose lipid complexes (Hoover & Vasanthan, 1994a; Jacobs *et al*., 1995; Jacobs *et al*., 1998; Tester *et al*., 1998; Tester *et al*., 2000; Waduge *et al*., 2006).

Annealing has been shown to reduce amylose leaching at all temperatures below 100^{o}C in cereal, tuber and pulse starches compared to their native counterparts (Jacobs *et al*., 1995; Jayakody *et al*., 2009; Chung *et al*., 2010; Song *et al*., 2014). The extent of this reduction is influenced by the following factors: 1) restricted granular

swelling; 2) strong interactions between amylose-amylose and/or amylose-amylopectin; 3) formation of new amylose lipid complexes; and 4) the molecular size of amylose molecules (Hoover & Vasanthan, 1994a; Tester & Debon, 2000; Waduge *et al*., 2006). However, a few cereal starches (wheat, certain cultivars of barley) exhibit increased amylose leaching on ANN (Jacobs *et al*., 1995; Waduge *et al*., 2006).

1.9.4 Effect of annealing on starch gelatinization

It has been well recognized that ANN increases the onset temperature of gelatinization (To), peak temperature (Tp), and conclusion temperature (Tc), and narrows the gelatinization temperature range (Tc-To), irrespective of the starch source (Chung *et al*., 2009a; Chung *et al*., 2010; Rocha *et al*., 2012; Simsek *et al*., 2012; Wang *et al*., 2013; Vamadevan *et al*., 2013). Following ANN, the enthalpy of gelatinization (ΔH) has been reported to either increase (Nakazawa & Wang, 2003; Genkina *et al*., 2004; Kiseleva *et al*., 2004; Kiseleva *et al*., 2005; Waduge *et al*., 2006; Chung *et al*., 2010) or remain unchanged (Wang *et al*., 1997; Muhrbeck & Wischmann, 1998; Vermeylen *et al*., 2006; Wang *et al*., 2014). However, a few authors have reported that ΔH decreased on ANN (Chung *et al*., 2009b; Siswoyo & Morita, 2010; Gomand *et al*., 2012; Song *et al*., 2014).

The extent of the increase in gelatinization temperatures has been shown to be more pronounced for To and less for Tc, since the weakest crystallites melt at To (Wang *et al*., 1997; Nakazawa & Wang, 2003). The increase in gelatinization temperatures is associated with the extent of crystallite perfection of a native starch. The weakest crystallites are more susceptible to crystallite perfection upon ANN in comparison to crystals having higher stability (often Tc) (Jacobs *et al*., 1998).

Furthermore, it is also related to an increase in crystal size and the presence of fewer crystal defects (Gomand *et al*., 2012; Vamadevan *et al*., 2013). Gomand *et al*. (2012) reported that in a three-step ANN of high amylose mutant potato starch, the greatest stepwise increase in To was observed in the third ANN step. Whereas a greatest increase in To was observed in the first ANN step of waxy potatato starch and the lowest impact on subsequent steps. High amylose starches generally exhibit a high degree of stacking order with lower crystallinity due to higher amylose content whereas, waxy starches possess a higher degree of native crystalline order and thus the least changes were observed in the subsequent steps (Gomand *et al*., 2012). Post ANN polymer chain interactions and crystallite perfection lead to an increase in Tg, which in turn raises the gelatinization temperatures (To, Tp and Tc) of annealed starches (Jayakody & Hoover, 2008). Generally, starch crystallite perfection is represented by Tp values (Tester, 1997). The increase in Tp and decrease in Tc-To indicate that ANN improves the double helical arrangement by decreasing the heterogeneity and cooperative melting of crystallites within the crystalline lamellae (Jacobs & Delcour, 1998).

The marginal differences in ΔH pre- and post-ANN suggest that either the absence of crystallite melting and subsequent (re)formation or the crystallite melting is compensated by the recrystallization (Gomand *et al*., 2012), Where ΔH represents the disruption of H-bonds within and between the double helices displayed by the amylopectin endotherm. The increase in ΔH mainly observed in high amylose starches on post ANN could be attributed to the lengthening of amylopectin double helices by twisting of chain ends, enhanced double helix register, co-crystallization of amylose tie chains with the amylopectin exterior chains and the formation of new

double helices between amylose chains (Genkina *et al*., 2007; Jayakody & Hoover, 2008; Gomand *et al*., 2012; Vamadevan *et al*., 2013). Whereas the decrease in ΔH indicates that a partial melting of amylopectin crystallites with a lack of influence from recrystallization and the disruption of crystalline order is likely to occur at higher temperatures (Siswoyo & Morita, 2010). ANN temperature, which is set close to the To of native starch, has a more profound effect on starch structure and thus increases the gelatinization temperatures of annealed starches compared to their native counterparts (Knutson, 1990; Tester & Debon, 2000).

1.9.5 Effect of annealing on pasting properties

Regarding pasting properties, several authors have reported that annealed starches generally exhibit an increased pasting temperature, pasting time and thermal stability (Adebowale *et al*., 2009; Dias *et al*., 2010; Simsek *et al*., 2012; Yadav *et al*., 2013; Song, *et al*., 2014; Chen *et al*., 2014). It is also reported that ANN reduces the peak viscosity and final viscosity (viscosity at the end of a cooling cycle) (Stute, 1992; Adebowale *et al*., 2009; Simsek *et al*., 2012; Yadav *et al*., 2013; Chen *et al*., 2014; Song, *et al*., 2014). Reduced granular swelling and amylose leaching is reflected in the decrease in peak viscosity and greater shear resistance on ANN (Hoover & Vasanthan, 1994a; Jacobs *et al*., 1995). However, Jacobs *et al*. (1996) reported that the increase in peak and final viscosity of wheat starch on ANN was attributed to an increase in granule rigidity and resistance to shear. Several authors have demonstrated that the increase in pasting temperature can be attributed to an increase in crystalline stability as a result of reorganization of polymer chains and strengthening of intra granular bonds in starch granules which require more thermal energy for structural disintegration (Adebowale *et al*., 2005; Zavareze & Dias, 2011). Based on previous

studies, the effect of ANN on starch pasting properties is largely influenced by the structural characteristics of starch granules and analytical conditions such as paddle speed, starch to water ratio, heating and cooling rates, etc. (Zavareze & Dias, 2011).

1.9.6 Effect of annealing on acid hydrolysis

The susceptibility of annealed starches to acid hydrolysis has been shown to be influenced by the starch source, ANN conditions, method (single, double or multi step), type of acid, temperature and concentration of acid (Jacobs *et al*., 1998; Nakazawa & Wang, 2003; Jayakody & Hoover, 2008). Hoover and Vasanthan (1994a) reported that single step ANN decreased the acid susceptibility of wheat, potato and lentil starches, but increased it in oat starch. Jayakody *et al*. (2009) also showed that annealed yam starches are hydrolysed to a lesser extent than their native counterpart. However, Waduge *et al*. (2006) reported that the difference in acid hydrolysis between native and annealed barley starch was marginal. Various theories have been put forward to explain the susceptibility of annealed starches to acid hydrolysis. It has been reported that the extent of the decrease in acid hydrolysis on ANN has been attributed to the interplay of the following factors: 1) perfection of starch crystallites; 2) formation of amylose double helices and increased interactions between starch chains; 3) formation of amylose lipid complexes; and 4) reduced accessibility to the α(1→6) branch points (embedded within the crystallites) (Hoover & Vasanthan, 1994a; Jacobs *et al*., 1998; Nakazawa & Wang, 2003; Waduge *et al*., 2006).

Several studies have reported that the increase in acid hydrolysis on ANN is a reflection of the following factors: 1) starch chains in the amorphous regions become more concentrated as a result of crystalline perfection; 2) void areas form in the

crystalline regions which facilitates the penetration of H_3O^+; and 3) branch linkages of the imperfect double helices become more perfect as a consequence of enhanced crystalline structure (Nakazawa & Wang, 2003; Tester & Debon, 2000; Jayakody *et al.*, 2009). A marginal difference in the second phase of hydrolysis is linked with an unchanged double helical content (DHC) and the limited ordering of crystallites in the crystalline regions (Tester & Debon, 2000; Nakazawa & Wang, 2003). These studies suggested that the impact of ANN on the rapid and slow phases of acid hydrolysis is influenced to a larger extent by the changes occurring within the crystalline lamellae (Waduge *et al*., 2006)

1.9.7 Effect of annealing on in vitro digestibility

Although the impact of ANN on enzyme-catalysed hydrolysis has been investigated by several researchers, the findings are conflicting, which makes it difficult to interpret the exact outcomes (BeMiller & Huber, 2015). Jayakody and Hoover (2008) suggested that the variations in susceptibility of starches toward enzyme-catalysed hydrolysis is mainly due the differences in starch source (botanical origin and varietal differences), ANN treatment conditions (temperature, duration, moisture condition and number of ANN steps), enzymes (source, purity and concentration) and the duration of hydrolysis. Alpha-amylase from various sources, including bacterial α-amylase, fungal α-amylase, fungal amyloglucosidase, porcine pancreatic α-amylase, and porcine pancreatin (mixture of α-amylase, lipase and protease), have been used in many studies to compare the effect of ANN on *in vitro* digestibility. Several studies have shown that ANN increases the susceptibility toward porcine pancreatic α-amylase pancreatin in pulse starches (pinto bean, black bean, lentil, field pea and navy bean), cereal starches (normal, waxy and high amylose corn,

waxy, normal and high amylose rice, waxy wheat, oat), tuber and root starches (cassava, Peruvian carrot, potato) and sago starch (Hoover & Vasanthan, 1994a; Wang *et al*., 1997; Jacobs *et al*., 1997; Lan *et al*., 2008; Dias *et al*., 2010; Rocha *et al*., 2011; Rocha *et al*., 2012; Zeng *et al*., 2015). However, ANN decreased the extent of hydrolysis in wheat, cassava, sweet potato, arrowroot, breadfruit and potato starches (Hoover & Vasanthan, 1994a; Jacobs *et al*., 1997; Siswoyo & Morita, 2010; Jyothi *et al*., 2011).

The impact of ANN on starch nutritional fractions (RDS, SDS and RS) has been studied with the combined action of α-amylase and amyloglucosidase. The extent of changes in each fraction on ANN compared to their native counterparts differs with starch source, treatment conditions and the method used to determine the nutritional fractions. The structural changes occurring during ANN are considered to increase the SDS and RS fractions while reducing the RDS content, where the crystallite perfection and the enhanced interactions between glucan chains restrict the enzyme accessibility upon ANN. However, the increase in RDS levels with a substantial reduction in SDS and RS levels is associated with the formation of more porous structures (mainly in cereal starches) on granular surfaces, which could negate the effect of other structural barriers and thereby facilitate the accessibility of enzymes to the granular interior (Wang *et al*., 1997; Jayakody & Hoover, 2008; Chung *et al*., 2009b). Wang *et al*. (2014) reported that the increase in the SDS content was attributed to the slight disruption of crystalline lamellae and/or conformational changes, i.e. a slight dissociation of double helices. Pulse starches exhibited an increase in RS content upon ANN (Chung *et al*., 2009b).

1.10 Problem statement

A survey of the literature shows that there is limited information available on pulse starch structure at various levels of structural organization (granular, supramolecular and molecular). Consequently, the interpretation of variation in properties among pulse starches and factors influencing the susceptibility of pulse starches toward acid and enzyme-catalysed hydrolysis, rate and extent of retrogradation, polymorphic composition and starch nutritional fractions becomes difficult. It is therefore crucial to study and investigate the structure-property relationships of pulse starches.

Amylolysis of pulse starches has been shown to be lower compared to cereal starches in both *in vitro* and *in vivo* studies (Faki *et al.*, 1983; Socorro *et al.*, 1989; Schweizer *et al.*, 1990; Tovar *et al*., 1991; Frias *et al*., 1998). Pulse starches exhibit a wide variation in amylose content, crystallinity, polymorphic composition, and organization of starch chains and their association within the granule interior. In comparison with cereal and tuber starches, pulse starches are better substrates for α-amylolysis due to the following reasons: 1) an absence of fissures or pores on the granule surface; 2) the absence or trace quantities of phosphate monoesters; 3) a low amount of associated lipid; and 4) similarity in granule size (Hoover & Sosulski, 1991; Davydova *et al*., 1995; Hoover & Zhou, 2003). Thus, a comparative study of the susceptibility toward enzymatic hydrolysis would provide a better understanding about the factors that control the accessibility of amylolytic enzymes into the granule interior of pulse starches.

However, factors influencing differences in amylolysis have not yet been explained satisfactorily. Furthermore, the susceptibilities of pulse starches toward *in*

vitro amylolysis reported in the literature cannot be compared due to differences in enzyme source (bacterial, fungal, pancreatic), enzyme concentration and hydrolysis time. Pulse starch digestibility has been investigated using: 1) porcine pancreatic α-amylase (PPA), which is an endo-acting enzyme that cleaves mainly α-(1→4) linkages producing maltose and maltotriose; 2) pancreatin, which has an α-amylase activity; and 3) amyloglucosidase, which is an exo-acting enzyme that cleaves both α-(1→4) and α-(1→6) linkages and converts the products of α-amylase digestion into glucose (Weill *et al*., 1954; Robyt & French, 1967; Robyt, 1984; Woolnough *et al*., 2010). Zhang, *et al*. (2013) have reported that there is an apparent synergism in the action of α-amylase and amyloglucosidase, particularly when hydrolysing starches in their native state. A survey of the literature has shown that differences in hydrolysis patterns among pulse starches have been explained mainly in terms of differences in their morphology, composition and structure (Singh, 2011). However, there is limited information on changes to granule morphology, crystallinity, molecular order, DHC, polymorphic content, X-ray pattern and apparent amylose content during the progress of hydrolysis**.** Consequently, it is difficult to interpret differences in the rate and extent of amylolysis among pulse starches. Understanding these factors is essential for explaining the rate and extent of digestibility, which would enable food processors to optimize reaction conditions for modifying pulse starch structure to a level that could improve the health-related quality of pulse-starch-based foods.

In order to extend the range of applications in the food sector, pulse starches have to be modified to enhance their thermal stability, resistance to shear thinning and repeated freeze-thaw stability. Presently, there is considerable interest in pulse starches that are physically modified to improve their functionality and suitability for

use in food applications. Annealing is a hydrothermal treatment that results in the molecular reorganization of glucan chains due, to the increase in amylose and amylopectin mobility in the presence of water (or other plasticizers) (Jacobs *et al.*, 1998). The molecular reorganization leads to an increase in gelatinization temperature, narrowing of the gelatinization temperature range and increase in granular stability (Jacobs & Delcour, 1998). However, the type and extent of change has been shown to vary with botanical origin, starch composition and annealing treatment conditions (Hoover & Jayakody, 2008; BeMiller & Huber, 2015). The impact of annealing on the physicochemical properties of normal and high amylose starches have been compared without first ensuring that these starches had reached their optimum level of crystalline perfection under the given experimental conditions. For instance, in comparison to normal starches, high amylose starches may require a longer treatment time to achieve crystalline perfection. This is because of the slower uptake of water into the amorphous lamellae and improper alignment of a large proportion of double helices in the crystalline lamellae.

Several studies on starch annealing were carried out earlier and most of the work is focused on starch characterization prior to and after annealing treatment. Although many studies were performed on elucidating the nature of granular organization on the basis of structural changes occurring during annealing treatment, efforts at attempting to unravel the factors that govern the molecular mechanisms of annealing were not very successful and information in that area is still extremely limited (Tester *et al*., 1998; Kiseleva *et al*., 2004; Kiseleva *et al*., 2005; Alvani *et al.*, 2012; Vamadevan *et al*., 2014). Furthermore, post-annealing structural changes have been explained based on the increased crystallinity and perfection of starch crystallites

due to an optimal packing of double helices and/or lengthening of the double helices of amylopectin chains inside the starch granule (Tester & Debon, 2000; Genkina *et al*., 2004). A few studies have reported that annealing promotes new interactions between starch chains (amylose/amylose, amylose/amylopectin and/or amylopectin/amylopectin) (Hoover & Vasanthan, 1994a; Lin *et al*., 2009; Gomand *et al*., 2012). The extent of crystalline perfection and starch chain interactions that occurs during annealing varies depending on the starch botanical origin and prevailing annealing conditions. Although the structural changes occurring as a result of annealing have been described earlier, the mechanism of annealing is still in contention.

Annealing can be used as an investigative tool to understand the organization and segmental flexibility of glucan chains in pulse starches varying in of amylose content. In addition, it also is important to determine normal and high amylose (40-80 %) starches from different botanical origins (particularly pulse and cereal starches) exhibit similar types of structural changes upon annealing. It also would be worthwhile to analyse whether increases in crystalline stability on annealing are influenced by the changes within the amorphous regions.

The amorphous regions are mainly occupied with amylose chains, branch points of amylopectin molecules and amylose-lipid complexes, especially in high amylose starches. In high amylose starches, part of the amylose fraction is interspersed (co-crystallized) with amylopectin chains. In addition, the amylose chains that pass through both the amorphous and crystalline lamellae (amylose tie chains), the long B chains that are interspersed into the crystalline lamellae and the higher proportion of intermediate chains also contribute to crystalline defects in the

starch granules (Yuryev *et al*., 2004; Koroteeva *et al*., 2007; Genkina *et al*., 2007). Therefore, the presence of the above crystalline defects influence the structural rearrangement and the perfection of crystallites within the crystalline lamellae during the annealing process. Thus, it is necessary to investigate the crystalline defects present in high amylose starches. Limited information is available on the contributions made by amorphous regions of normal and high amylose starches to the structural changes. Detailed studies have not been conducted to investigate the contributions made by amorphous regions to the structural changes within the crystalline lamellae in normal and high amylose starches during the annealing treatment. Furthermore, the proportion of the amorphous region varies with the starch source, and the packing arrangement of amylose chains would be different for starches with the same amylose content. Some authors have suggested that amorphous regions become rigid after annealing treatment (Tester & Debon, 2000, Vamadevan *et al*., 2013). However, no experimental evidence is available to substantiate this claim. Therefore, emphasis must also be placed on the following to understand the mechanism of annealing in normal and high amylose starches: 1) investigation of the relationship between the native starch structure and annealing induced structural changes; 2) understanding how crystalline defects (mainly prevalent in high amylose starches) impact the extent of realignment and perfection of double helices within the crystalline lamella; and 3) the role of amorphous regions on annealing.

1.11 Hypothesis and objectives

The hypotheses and objectives of my thesis research are outlined below:

Hypothesis 1: The variation in granule morphology, composition and structure of pulse starches impacts their thermal, rheological and digestibility properties.

Objective 1: To determine the morphology, composition and structure (granular, supramolecular, and molecular levels) of pulse starches and their impact on thermal, rheological and digestibility properties (Chapter 3.1).

Hypothesis 2: The starches from the different pulse species used in this study differ widely with respect to morphology, amylose content and structural organization within the amorphous and crystalline regions in their native state. Consequently, the above differences will influence the rate and extent of hydrolysis and the molecular rearrangement of the starch chains that occur during *in vitro* digestion (Chapter 3.2).

Objective 2: a) To compare *in vitro* digestion behavior of granular pulse and high amylose maize starches varying in polymorphic composition (A and B polymorphic forms), granule morphology and composition; b) to understand whether amylose content *per se* and/or the packing density of amylose chains within the granule interior play a role in influencing the rate and extent of hydrolysis; and c) to monitor changes to granule morphology, structure and thermal properties of residues obtained at different time intervals of hydrolysis (Chapter 3.2).

Hypothesis 3: Structural changes which occur within the amorphous and crystalline domains upon annealing will be influenced by the structural

differences that exist among the starches in their native state. These structural changes will exert an influence on the physicochemical properties of starches.

Objective 3: To elucidate the structural changes (at molecular and supramolecular levels) that occur within the amorphous and crystalline domains in pulse and high amylose maize starches on annealing and their effect on physicochemical properties (Chapter 3.3).

Hypothesis 4: Amorphous regions contribute to the structural changes (double helical alignment) within the crystalline lamellae on annealing. The partial removal of amorphous regions will decrease the extent of crystalline perfection on annealing.

Objective 4: To determine the effect of partial erosion of the amorphous regions on the extent of crystalline perfection upon annealing and to understand the extent to which amorphous regions in the above starches contribute to annealing-induced structural changes within the crystalline lamella (Chapter 3.4.1).

Hypothesis 5: Cross-linked starches will not respond to annealing to the same extent as their native counterparts with respect to the extent of crystalline perfection.

Objective 5: To study the impact of cross-linking on the extent of crystalline perfection before and after annealing (Chapter 3.4.2).

1.12 Research outline

This section provides an overview of the study design using a flow diagram to address the specific of objectives (section 1.11) of this study.

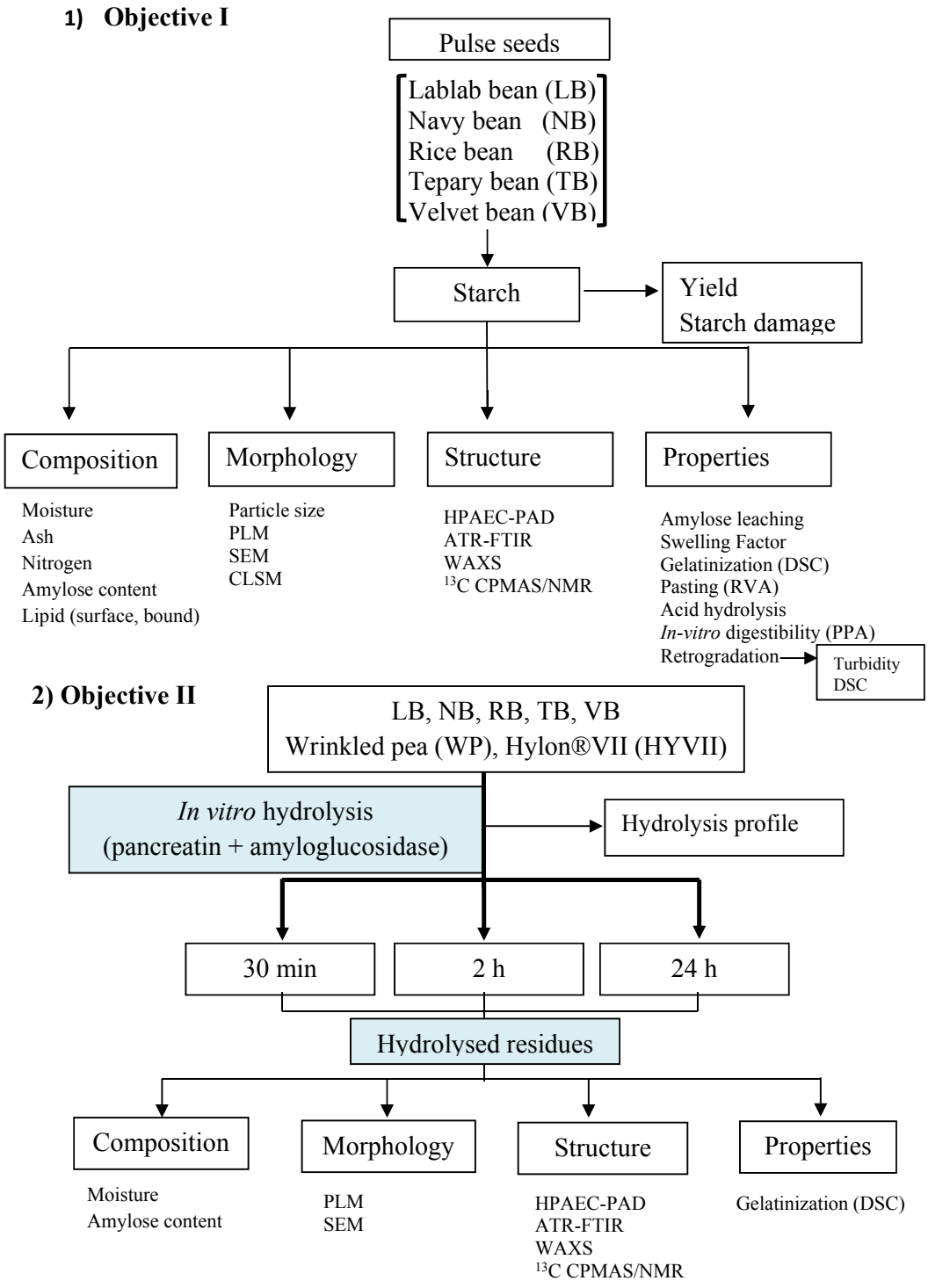

PLM- polarized light microscopy; SEM- scanning electron microscopy; CLSM- confocal laser scaning microscopy; HPEAC- high performance anion exchange chromatography with pulse amperometric detection; ATR-FTIR- attenuated total reflectance Fourier transform infrared spectroscopy; WAXS- wide angle X-ray diffraction; ^{13}C CPMAS/NMR- ^{13}C cross polarization magic angle spinning nuclear magnetic resonance spectroscopy; DSC- differential scanning calorimetry; RVA- rapid visco analyser; PPA- porcine pancreatic α-amylase

3) Objective III

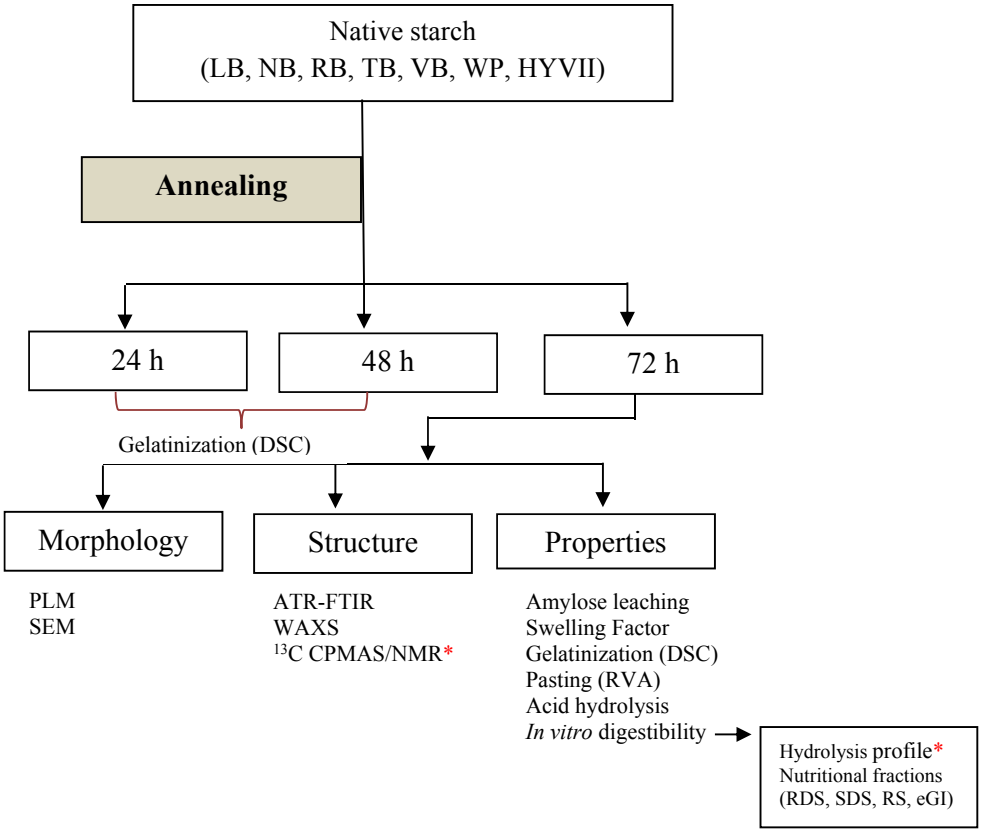

4) Objective IV

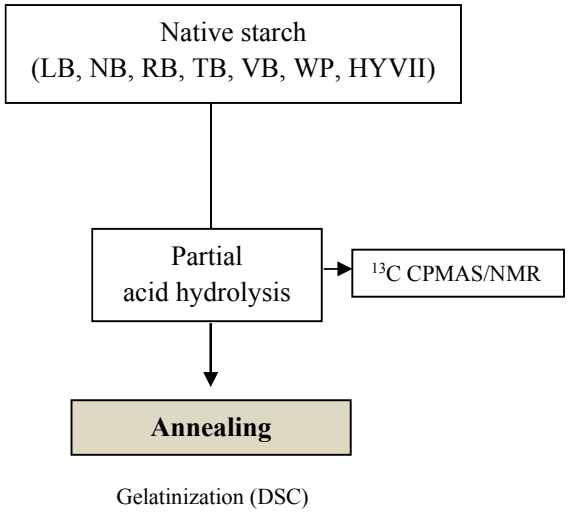

5) Objective V

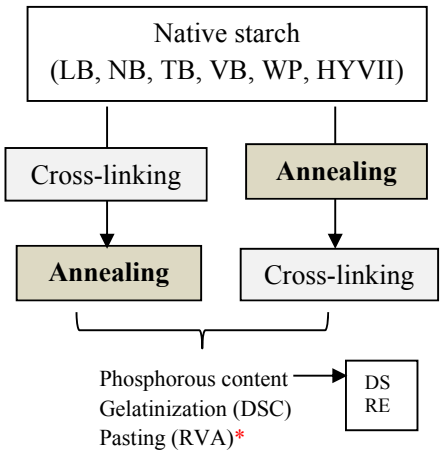

*Not included in this thesis

RDS- rapidly digestible starch; SDS- slowly digestible starch; RS- resistant starch, eGI- expected glycemic index; DS- degree of substitution; RE- reaction efficiency

Chapter 2

Material and methods

2.1 Materials

Starch sources: Seed of lablab bean (*Lablab purpureus* L.), rice bean (*Vigna umbellate* (Thunb.)), tepary bean (*Phaseolus acutifolius* (Jacq.)) and velvet bean (*Mucana deeringiana* (Bort) Merr.) was obtained from Shivalik Seeds Corporation (Dehradun, Uttarakhand, India). Navy bean (*Phaseolus vulgaris* L.) was obtained from the Harrow Research and Development Centre – Agriculture and Agri-Food Canada (Harrow, ON, Canada). Wrinkled pea (*Pisum sativum* L.) seed was provided by the Crop Development Centre at the University of Saskatchewan (Saskatoon, SK, Canada). High amylose maize starch (Hylon®VII) was purchased from National Starch & Chemical Company (Bridgewater, NJ, USA).

Enzymes and reagents: Pancreatin from porcine pancreas (cat. no. P-1625, activity ≥3× USP/g), crystalline porcine pancreatic α-amylase (type 1A, 1,333 U/mg protein), amyloglucosidase (300 U/mL) from *Aspergillus niger*, and α-amylase (157 U/mg protein) from *Aspergillus oryzae* were purchased from Sigma-Aldrich (St. Louis, MO, USA). A glucose oxidase–peroxidase assay kit (K-GLUC), total starch assay kit (K-TSTA) and isoamylase from *Pseudomonas* sp. (500 U/mL**)** were purchased from Megazyme International Ireland Ltd. (Bray, Wicklow, Ireland). APTS and sodium cyanoborohydride were obtained from Molecular Probes (Eugene, OR, USA). All chemicals and solvents were of ACS certified grade.

2.2 Methods

2.2.1 Starch isolation and purification

Pulse starches were extracted from the pulse seeds using the wet milling procedure described by Hoover and Sosulski (1985), with a few modifications. A sample of pulse seed (50 g) was steeped in 250 mL of 0.01 % (w/v) sodium metabisulfite for 36 h at 35°C. The swollen seeds were dehulled and the cotyledons were thoroughly rinsed with deionized water. The softened cotyledons were blended with sufficient deionized water (cotyledon/water 1:3, v/v) using a waring commercial blender (Dynamics Corporation of America, Greenwich, CT, USA) at low speed for 3 min, and the slurry was washed with an additional water rinse through cheese cloth. The cheese cloth containing the coarse fibrous material was re-blended with sufficient deionized water (~150 mL) and then re-screened with cheese cloth. This step was repeated twice and the filtrates were combined. The filtrate was then passed through a 210 μm polypropylene sieve, followed by a 70 μm nylon sieve, and then allowed to sediment at room temperature for 18 h. The liquid was decanted, and the sediment was re-suspended in excess 0.2 % (pH-12.7) sodium hydroxide solution (sediment/sodium hydroxide 1:2, v/v) and allowed to sediment at room temperature for 3 h. The brown layer of the supernatant was removed and this step was repeated multiple times until white sediment of starch was obtained. The resulting starch was rinsed with deionized water (~400 mL) and filtered through a 70 μm nylon screen to remove the larger particles. The starch slurry was then neutralized to pH 7.0 with 0.2 % hydrochloric acid. The neutralized starch slurry was filtered through Whatman No.4 filter paper on a Buchner funnel and thoroughly washed on the filter with deionized water (~200 mL). The resulting filter cake was oven dried at 30°C for 2 days. The dried starch was

gently ground using a mortar and pestle and passed through a 60-mesh (250 μm) screen.

2.2.2 Chemical composition

2.2.2.1 Moisture content

The moisture contents of starch samples were determined using AACC method 44-15A (American Association of Cereal Chemists, 2000). Empty aluminum moisture pans with lids were placed in a preheated forced air oven (Isotemp® 615G, Fisher Scientific, Pittsburgh, PA, USA) at 130 ± 1°C for 1 h and then cooled in a desiccator containing active silica gel desiccant for 1 h prior to analysis. Samples of 2 g were weighed into the pre-weighed moisture pans, and then samples were placed in the oven and dried at 130 ± 1°C for 1 h with the lids placed under the respective pans. The samples were then removed, covered with lids and transferred to the desiccator. The weight of the samples was measured after they reached room temperature. Three replicates were used for each determination and the moisture content was calculated as the percentage of weight loss of the initial sample using the following equation:

$$Moisture\ (percent) = \frac{W1-W2}{W1-W0} X\ 100 \qquad (2.1)$$

where, Wo is the weight of the moisture pan and lid (g), W_1 is the weight of sample, moisture pan and lid before drying (g), and W_2 is the weight of sample in the pan and lid after drying (g).

2.2.2.2 Determination of ash content

The ash contents of native starches were determined using AACC method 08-17 (American Association of Cereal Chemists, 2000). The crucibles were placed in a pre-heated (550°C) muffle furnace (Lab Heat, Blue Island, IL, USA) for 2 h, cooled in

a desiccator containing active silica gel desiccant for 45 min and then weighed. Starch samples (5 g) were transferred into pre-weighed dry crucibles, charred using a flame until the samples were carbonised and then placed in the muffle furnace (550°C) for 16 h until a light grey ash was obtained. The crucibles were cooled to room temperature in a desiccator and weighed. The ash content was calculated as the percentage weight of remaining material as follows:

$$Ash\ (percent) = \frac{W_2 - W_0}{W_1 - W_0} \times 100 \quad (2.2)$$

where, W_0 is the weight of the empty crucible and lid (g), W_1 is the weight of sample, crucible and lid (g), and W_2 is the weight of ash, crucible and lid (g).

2.2.2.3 Determination of nitrogen content

The nitrogen content of native starches was quantitatively analysed using the Micro Kjeldahl method, the 46-13 AACC method (American Association of Cereal Chemists, 2000) with a few modifications. Samples (300 mg, dry weight basis (dwb)) were weighed on nitrogen-free papers and placed in digestion tubes of a Büchi 430 (Büchi Laboratoriums-Technik AG, Flawill, Switzerland) digestion unit. Catalyst (2 Kjeltabs M pellets (Fisher Scientific, Fair Lawn, NJ, USA)) and concentrated H_2SO_4 (98 %, 20 mL) were added. The samples were digested until a clear yellow solution was obtained. After digestion, the samples were cooled, diluted with 50 mL of deionized water and then 40 % (w/w) sodium hydroxide (100 mL) was added. The released ammonia was steam distilled using a Büchi 321 distillation unit and collected into 4 % (w/v) boric acid (50 mL) containing 12 drops (~0.6 mL) of end point indicator (N-point indicator, Sigma-Aldrich, St. Louis, MO, USA). The distillation process was carried out until 150 mL of distillate were collected. By titrating against

0.05 N sulphuric acid, the amount of ammonia in the distillate was determined. The percentage of nitrogen was calculated using the following equation:

$$Nitrogen\ (percent) = \frac{(V_1 - V_2) \times N \times 14.0067}{W} \times 100 \quad (2.3)$$

where V_1 is the volume (mL) of sulphuric acid to titrate sample, V_2 is the volume (mL) of sulphuric acid to titrate blank, N is the normality of sulphuric acid, and W is the sample weight (g, dwb).

2.2.2.4 Determination of apparent amylose content

The amylose content of starches was determined according to the procedure outlined by Hoover and Ratnayake (2004). Starch (20 mg, dwb) was weighed into a round bottom screw cap tube and solubilized in 90 % dimethylsulfoxide/water (8 mL). The contents were vigorously vortexed and the tubes were left for 15 min at 85°C with intermittent mixing at 5 min intervals in a water bath. After cooling to room temperature (~45 min), the contents were diluted to 25 mL in a volumetric flask with deionized water. An aliquot (1 mL) of the diluted solution was added to 40 mL of deionized water and 5 mL of I_2/KI solution (2.5 mM I_2 and 6.5 mM KI) and vortexed. The final volume was made up to 50 mL with deionized water in a volumetric flask. The mixture was kept in the dark for 15 min at room temperature. The absorbance was read at 600 nm using a UV-visible spectrophotometer (LKB Novaspec-4049 spectrophotometer, LKB Biochrom Ltd., Cambridge, England). In order to avoid over-estimation of amylose content, a calibration curve was established using mixtures of pure amylose and amylopectin, fractioned from normal potato starch, over the range 0 to 100 % (Appendix I).

2.2.2.5 Determination of lipid content

Surface and bound lipid content of the native starch samples were determined by the procedure outlined by Vasanthan and Hoover (1992a) and the amount of extracted lipid was expressed as a percentage of the initial sample weight.

2.2.2.5.1 Surface lipid

Surface lipids were extracted at ambient temperature (25-27°C) by the addition of 100 mL of chloroform/methanol (2:1, v/v) to the starch sample (5 g, dwb). The contents were mixed under vigorous agitation using a magnetic stirrer for 1 h. The solution was filtered through Whatman No.4 filter paper into a 250 mL round bottomed flask. The residue was washed out thoroughly with small portions of chloroform/methanol solution and then retained for bound lipid extraction. The solvent mixture containing lipid was then evaporated to dryness using a rotary evaporator (Rotovapor-R110, Büchi Laboratorimus-Technik AG, Flawill, Switzerland). The Bligh and Dyer (1959) method was used to purify crude lipid extracts before quantification.

2.2.2.5.2 Bound lipid

Bound lipids were extracted using the residue from the chloroform/methanol extraction. The residue was transferred into a cellulose extraction thimble and refluxed with *n*-propanol/water (3:1, v/v) in a Soxhlet apparatus at 85°C for 7 h. The extracted lipid with solvent was then evaporated to dryness using a rotary evaporator. The method of Bligh and Dyer (1959) was used to purify the crude lipid extracts before quantification.

2.2.2.5.3 Crude lipid purification (Bligh and Dyer method, 1959)

The crude lipid extracts from surface and bound lipid extractions were washed using chloroform/methanol/water (1:2:0.8, v/v/v), thoroughly mixed and then transferred to a separatory funnel. Chloroform and water were then added to form a biphasic layer at room temperature. The chloroform layer containing the purified lipid was withdrawn into a pre-weighed round bottomed flask. Then evaporated to dryness in the rotary evaporator. The round bottomed flask with the purified lipid was then placed into forced-air oven and dried at 60°C for 1 h, then cooled in a desiccator containing active silica gel desiccant for 45 min and then weighed. Lipid content was calculated using the formula given below:

$$Lipid\ (percent) = \frac{W_2 - W_1}{W_0} \times 100 \qquad (2.4)$$

where, W_o is the sample weight (g, dwb), W_1 is the weight of the round bottomed flask (g), and W_2 is the weight of the round bottomed flask and lipid after drying (g).

2.2.2.6 Estimation of starch damage

Starch damage was estimated using an enzyme digestion procedure, following the AACC standard method 76-30A (American Association of Cereal Chemists, 2000). Starch samples (1 g, dwb) were measured into a 125 mL Erlenmeyer flask and then 50 mg of fungal amylase from *Aspergillus oryzae* (157 units/mg protein) was added. Acetate buffer (pH 4.6, 45 mL) at 30°C was added to the Erylenmeyer flask and the contents were mixed with a glass rod to obtain a uniform suspension. The acetate buffer was prepared by diluting 4.1 g of anhydrous sodium acetate and 3 mL of glacial acetic acid in 1 L of deionized water. The pH was adjusted to the range of 4.6 to 4.8. The contents were incubated at 30°C in a water bath for 15 min. At the end

of incubation, the enzyme reaction was terminated by adding 3 mL of 3.68 N sulphuric acid and 2 mL of 12 % sodium tungstate solution, respectively. The contents were mixed thoroughly and allowed to stand for 2 min and then filtered through Whatman No. 4 filter paper. The initial few drops of filtrate were discarded and the amount of reducing sugar was determined using the method outlined by Bruner (1964). A calibration curve was derived from standard maltose solutions. The reagent blank was prepared using the same procedure without starch. Starch damage was estimated using the following equation:

$$Starch\ damage\ (percent) = \frac{M \times 1.64}{W \times 1.05} \times 100 \quad (2.5)$$

where, M is the mg of maltose equivalents in the digest, W is the mg starch (dwb), 1.05 is the molecular weight conversion of starch to maltose, and 1.64 is the reciprocal of the mean percentage maltose yield from gelatinized starch. The latter is an empirical factor which assumes that under the conditions of the experiment, 61 % of starch is converted to maltose.

2.2.2.6.1 Determination of reducing value

The soluble carbohydrate content was determined according to the method of Bruner (1964). A 3, 5-dinitrosalicylic acid (DNS) solution was prepared by dissolving 2 g of DNS in warm (~70°C) 1 N sodium hydroxide. The contents were dissolved by rapid stirring for 3 min and the final volume was made to 100 mL with deionized water. Then, the solution was filtered through a medium porosity fritted glass filter and stored in an amber bottle at room temperature. For the determination of soluble sugar content, an aliquot of the sample (1 mL) was pipetted into a screw cap tube containing 2 mL of chilled DNS solution kept in an ice-water bath for 2-3 min. The

reaction mixture was then diluted to 4 mL with deionized water. The contents were vortexed and the tubes were kept in an ice-water bath until thoroughly chilled. The tubes were then heated in a boiling water bath for exactly 5 min for colour development with intermittent mixing. Tubes were returned to an ice-water bath until thoroughly chilled. Prior to color measurement, the final volume was adjusted to 12 mL with deionized water and the contents were mixed by rapid swirling. Depending on the reducing sugar content, the absorbance was read using a UV-visible spectrophotometer (Novaspec-4049 spectrophotometer, LKB Biochrom Ltd., Cambridge, England) against a reagent blank. The relative absorbance corresponding to maltose concentrations ranging from 0.58 to 14.0 μM and 4.2 to 92.5 μM were measured at 540 and 590 nm, respectively. A calibration curve was generated from standard maltose solutions (5 mg/mL for 540 nm and 36 mg/mL for 590 nm) (Appendix II). The apparent sugar content was estimated from the appropriate regression equation of the standard curves.

2.2.3 Granule morphology and particle size distribution

2.2.3.1 Starch granule size distribution

For measurements of granule size, a laser particle size analyser (Fritsch NanoTec "analysette 22", Idar-Oberstein, Germany) supplied with Fritch MaS software was employed. The starch samples were suspended in water at ~7 % (w/w). Refractive indices of starch and water (as the dispersant) were 1.52 and 1.31, respectively. The laser obscuration in all the measurements was maintained between from 7-10 %. Particle size distribution was expressed in terms of 10th percentile [d(0.1)], median [d(0.5)], 90th percentile [d(0.9)] and surface weighted mean [D(3,2)]. The average size of a granule was expressed in terms of surface weighted mean value,

referring to the diameter of a sphere that has the same volume/surface area ratio. This was used to calculate the specific surface area (m^2/g) with the assumption of spherical granules having a uniform density (1,500 kg/m^3). Specific surface area (SSA) was calculated from median using the equation shown below:

$$Specific\ surface\ area\ (m^2/g) = \frac{6}{1.5 \times surface\ weighted\ mean} \quad (2.6)$$

2.2.3.2 Light microscopy

Starch suspensions (in 1:1 v/v water:glycerol) were observed under bright field and cross-polarized light using a binocular microscope (Eclipse 80i microscope, Nikon INC, Melville, NY, USA) equipped with real time viewing software (Q-capture PRO^T, Surrey, BC, Canada). For the image capture, a QImaging digital camera (QICAM fast 1394, BC, Canada) was used.

2.2.3.3 Scanning electron microscopy (SEM)

Granular morphologies of starch samples were examined using a scanning electron microscope (FEI MLA 650 FEG, Brisbane, Australia) at an accelerating potential of 20 kV. The dried starch samples were thinly spread onto circular aluminum stubs with double-sided carbon adhesive tape and then carbon coated in a vacuum chamber.

2.2.3.4 Confocal laser scanning microscopy (CLSM)

In order to visualize the distribution of amylose and amylopectin, starch granules were stained with 8-Amino-1,3,6-pyrenetrisulfonic acid (APTS) according to the procedure outlined by Blennow *et al*. (2003). Starch samples (10-15 mg) were stained in 10 μL of freshly made APTS solution (20 mM APTS in 15 % acetic acid) and 10 μL of 1M sodium cyanoborohydride at 30°C for 15 h (Appendix III). The APTS-stained starch granules were thoroughly washed five times with deionized

water to remove the excess dye. The stained granules were finally suspended in 0.5 mL of 50 % glycerol and then observed under a confocal laser scanning microscope (ECLIPSE 80i microscope, Nikon INC, Melville, NY, USA) equipped with a 40x/1.3 oil objective lens. The excitation wavelength obtained with the diode laser was 488 nm. Laser power capacity and master gain were adjusted to maximum saturation. Images of optical sections of starch granules were taken and processed using the EZ-C1 3.8 software (Nikon INC, Melville, NY, USA).

2.2.4 Starch structure

2.2.4.1 Determination of amylopectin chain length distribution

Amylopectin chain length distribution of starches was determined by high performance anion exchange chromatography with pulsed amperometric detection (HPAEC-PAD), as described by Liu *et al*., 2007. The dispersion of starch (5 mg/mL) was carried out using 2 mL of 90 % dimethyl sulfoxide/water by stirring in a boiling water bath for 20 min and then cooling to room temperature. The contents were mixed with 6 mL of methanol, vortexed and placed in an ice water bath for 30 min. The resulting pellet was recovered by centrifugation (1,000 ×g for 12 min), and then dispersed in 2 mL of 50 mM sodium acetate buffer (pH 3.5) by stirring in a boiling water bath for 20 min. The contents were equilibrated at 37°C and then 5 µL of isoamylase (500 U/mL) was added. The sample was incubated at 37°C with gentle stirring for 22 h and the reaction was inactivated by placing the tube in a boiling water bath for 10 min. Aliquots (200 µL) containing debranched amylopectin chains were cooled and then diluted with 150 mM NaOH (2 mL). The content of the tube was filtered through a nylon syringe filter (0.45 µm) and injected into the HPAEC-PAD system using a 50 µL sample loop. The anion-exchange chromatography was carried

out in a system consisting of a Dionex DX 600 equipped with an ED50 electrochemical detector with a gold working electrode, GP50 gradient pump, LC30 chromatography oven and AS40 automated sampler (Dionex Corporation, Sunnyvale, CA, USA).

A standard triple potential waveform was applied, with the following periods and pulse potentials: T1 = 0.40 s, with 0.20 s sampling time, E1 = 0.05 V; T2 = 0.20 s, E2 = 0.75 V; T3 = 0.40 s, E3 = -0.15 V. Data were collected and analysed using Chromeleon software, version 6.50 (Dionex). The weight fractions of dp 6-12, 13-24, 25-36 and 37-58 were measured based on the area of peaks. The average chain length also was calculated. Eluents A and B were prepared in deionized water with helium sparging; eluent A was 500 mM sodium acetate in 150 mM sodium hydroxide, and eluent B was 150 mM sodium hydroxide. The separation of linear components was performed on a Dionex CarboPac^{TM} PA1 column (Dionex) with gradient elution: 0 min, 40 % eluent A; 5 min, 60 % eluent A; 45 min, 80 % eluent A at a column temperature of 26°C and the flow rate was set to 1 mL/min. A guard column (CarboPac^{TM} PA1) was installed in front of the analytical column.

2.2.4.2 Determination of short range molecular order by attenuated total reflectance Fourier transform infrared spectroscopy (ATR-FTIR)

Short range molecular order was determined using a Digilab FTS 7000 spectrometer (Digilab USA, Randolph, MA, USA) equipped with a thermoelectrically cooled deuterated triglycine sulfate (DTGS) detector using an attenuated total reflectance (ATR) accessory. For each measurement, 128 scans with a 4 cm^{-1} spectral resolution were co-added, before Fourier transform. An empty cell was used to obtain the background spectrum. Starch samples were mounted on the crystal in the sample

compartment. Original spectra were baseline corrected by subtracting a two-point linear function touching 1,200 and 800 cm^{-1} and then deconvoluted by using Win-IR Pro software (Bio-Rad, Mississauga, ON, Canada). A half-band width of 15 cm^{-1} and a resolution enhancement factor of 1.5 with Bessel apodization were employed. Intensity measurements at selective wavelengths (1,016, 1,022 and 1,047 cm^{-1}) were performed on the deconvoluted spectra by recording the peak heights of the absorbance bands from the base line. IR absorbance values for each spectrum at 1,016, 1,022 and 1,047 cm^{-1} were calculated per sample after baseline correction and deconvolution to estimate the degree of order of starch granules near the granule surface.

2.2.4.3 Wide angle X-ray diffraction (WAXS)

Relative crystallinity (RC) and polymorphic composition (proportion of A- and B-type unit cells) were determined using a Rigaku Ultima IV X-ray diffractometer (Rigaku Americas, The Woodlands, TX, USA) with operating conditions of target voltage at 40 kV, current at 44 mA, scanning range of 3–35° 2θ, scan speed of 1.00°/min, step time of 0.95, divergence slit width of 0.5°, scatter slit width of 0.5°, sampling width of 0.03°, and receiving slit width of 0.3 mm. The moisture content of the starches was adjusted to ~21-23 % by storing in a desiccator over saturated K_2SO_4 solutions (a_w=0.97) at room temperature for 14-21 days prior to X-ray diffraction measurements. The IGOR pro 6.1 software (WaveMetrics Inc., Lake Oswego, OR, USA) was used to calculate the relative crystallinity (%) by a curve fitting procedure as described by Lopez-Rubio *et al*. (2008). A Gaussian function was used for curve fitting (Appendix IV).

2.2.4.3.1 Determination of B-polymorphic composition

The proportion of B-polymorphic compositions of the samples was estimated by the method of Davydova *et al*. (1995). A series of starch mixtures was prepared with different proportions of pure potato starch (B-type, 0-100 %) and pure waxy corn starch (A-type, 100-0 %). Moisture content was adjusted to ~20 %. The diffractogram of each mixture was obtained and the ratio of peak area at 5.54° 2θ to the total crystalline area was calculated. A calibration curve was derived by plotting the B-polymorphic content versus the corresponding ratio of peak area at 5.54° 2θ to the total crystalline area.

2.2.4.4 ^{13}C Cross polarization magic angle spinning nuclear magnetic resonance spectroscopy (^{13}C CP/MAS NMR)

The solid state ^{13}C CP/MAS NMR spectra were recorded using a Bruker AVANCE II 14.1T (600 MHz) NMR spectrometer (Billerica, MA, USA) operating at frequencies of 600.33 MHz for ^{1}H and 150.96 MHz for ^{13}C.The data interpretation was performed with Bruker Topspin 2.0 and MestRe Nova (Mestrelab research SL, Santiago De Compostela, Spain). Experiments were performed using a Bruker 3.2 mm MAS probe (triple-tuned probe HCN (D) or ^{1}H/^{19}F/^{13}C). The samples were stored in a desiccator over saturated K_2SO_4 solutions (a_w=0.98) at room temperature (25°C) for 14-21 days and the moisture content was adjusted to 21-23 %. The samples were spun at 20 kHz and the temperature was maintained constant at 25°C. The cross-polarization contact time was 2 ms for all experiments and the Hartmann-Hahn condition was 62.5 kHz. Scans (1,024) were collected with a 3 s recycling delay at the magic angle (54.7°). ^{13}C chemical shifts were referenced to tetramethylsilane (TMS) with adamantane as an external secondary reference. The ^{13}C CP/MAS NMR spectra were peak fitted by using DMfit #20110512 software available on the

NMR@CEMHTI website (http://nmr.cemhti.cnrs-orleans.fr/dmfit/). The spectral analysis involved the decomposition of the native starch spectrum into its respective amorphous (single chain components) and ordered sub spectra (double helical components, DHC). The percentage of DHC was calculated as described by Tan et al. (2007). The ordered sub-spectrum was acquired by subtracting the sub-spectrum of the amorphous portion from the native starch spectrum (Appendix V). Within a starch sample, the relative proportions of amorphous, single helical and double helical components were estimated by comparing the area of the C1 signal in the ordered sub-spectrum relative to the area of the C1 signal. DHC of starch was calculated using the equation shown below:

$$Double\ helix\ (percent) = \frac{Area\ for\ the\ C1\ signals\ in\ the\ ordered\ subspectrum}{Area\ for\ the\ C1\ signals\ in\ the\ native\ spectrum} \times 100 \quad (2.7)$$

2.2.5 Starch properties

2.2.5.1 Swelling factor (SF)

The SFs of starches were determined by the method of Tester and Morrison (1990). This method accounts only for the intragranular water and therefore corresponds to the true swelling factor at a given temperature. Starch samples (50 mg, dwb) were weighed into screw cap tubes, 5 mL of deionized water was added to each and tubes were vortexed. SF was determined in the temperature range of 60-90°C. The tubes were placed in a shaking water bath at a particular temperature for 30 min, intermittently inverted several times and then cooled rapidly to 20°C in an ice water bath. After cooling, 0.5 mL of blue dextran (Pharmacia Mw 2×10^6, 5 mg/mL) was added, and the contents were mixed by inverting the tubes multiple times. The tubes were then centrifuged at 1,500 ×g for 10 min and the absorbance value of the supernatant was measured at 620 nm. A reference sample was prepared using the

same procedure without starch. The SF value represents the ratio of the volume of the swollen starch granules to the volume of the dry starch. Calculation of SF was based on starch weight corrected for moisture content, assuming a density of 1.4 g/mL.

Free or interstitial-plus-supernatant water (FW) is given by:

$$FW\ (mL) = 5.5(A_R/A_S) - 0.5 \quad (2.8)$$

Ar and As represent the absorbance values of the reference and sample, respectively.

The initial volume of the starch (V_O) of weight W (mg) is

$$V_0\ (mL) = W/1400 \quad (2.9)$$

and the volume of absorbed intragranular water (V_1) is thus

$$V_1 = 5.0 - FW \quad (2.10)$$

Hence, the volume of the swollen starch granules (V_2) is

$$V_2 = V_0 + V_1 \quad \text{and} \quad (2.11)$$

$$SF = V_2/V_0 \quad (2.12)$$

Therefore, SF can be expressed by the single equation shown below:

$$SF = 1 + \{(7700/w) \times [(A_s - A_r)/A_s]\} \quad (2.13)$$

2.2.5.2 Amylose leaching (AML)

Starch samples (20 mg, dwb) in water (10 mL) were heated at a temperature range of 60-90°C in volume-calibrated sealed tubes for 30 min; the contents were mixed every 5 min to re-suspend the starch slurry. The tubes then were cooled to ambient temperature (25-27°C) and centrifuged at 2,000 ×g for 10 min. The

supernatant liquid (1 mL) was taken and its amylose content was determined according to the procedure outlined by Hoover and Ratnayake (2004). Amylose leaching was reported as the percentage of amylose leached per 100 g of dry starch. The reference sample was prepared using the same procedure without starch.

2.2.5.3 Differential scanning calorimetry (DSC)

DSC measurements of starch samples were carried out using a Mettler Toledo differential scanning calorimeter (DSC1/700/630/GC200; Greifensee, Switzerland) equipped with a thermal analysis data station and data recording software (STAR@ SW 9.20). Starch (3 mg, dwb) was weighed accurately into an aluminum DSC pan, and then deionized water (11 μL) was added directly to the starch using a microsyringe. The pans were hermetically sealed, reweighed and kept overnight at room temperature to attain an even distribution of water prior to DSC analysis. The scanning temperature range was 30-120 or 20-110 at a heating rate of 10°C/min. The instrument was calibrated using indium as a standard. In all measurements, an empty aluminum pan was used as a reference. During the scans, the space surrounding the sample chamber was flushed with dry nitrogen to avoid condensation. The DSC endotherm of gelatinization was characterized by To, Tp, Tc, melting interval (Tc-To) and ΔH. The enthalpy of gelatinization (ΔH) was determined by numerical integration of the area between the thermogram and a base line under the peak and was expressed in terms of Joules per gram (J/g) of dry starch. Three replicates per sample were analysed.

To study the retrogradation characteristics, starch (3 mg) and deionized water (11 μL) were added in the DSC pans, which were then sealed, reweighed and left overnight at room temperature. DSC runs were performed from 20 to 110°C at a

heating rate of 10°C/min. The heated pans were then cooled to room temperature and stored at 4°C for 1 day and then at 25°C for 2 to 25 days. After this time period, the pans were left to equilibrate for 1 h at room temperature and then rescanned under the operating conditions described above. An empty pan was used as reference. The transition temperatures (To, Tp, Tc) and enthalpy of retrogradation (ΔH_r) were determined from the retrogradation endotherm.

2.2.5.4 Pasting properties

Pasting properties of starch samples were analysed using a rapid visco analyzer (Model RVA-4, Newport Scientific Pty. Ltd., Warriewood, NSW, Australia) according to method 76-21 of the AACC (American Association of Cereal Chemists, 2000). Each starch sample (3 or 2.5 g, corrected to 14 % moisture content) was added with 25 mL of deionized water to prepare the starch suspension. The starch suspension was stirred at 960 rpm for the first 10 s, then 160 rpm for the remainder of the experiment. Starch suspensions were kept at 50°C for 1 min, heated to 95°C at 6°C/min, held at 95°C for 5 min, cooled to 50°C at 6°C/min, and then held at 50°C for 2 min. The peak viscosity (PV), viscosity at trough (minimum viscosity, MV), and final viscosity (FV) were determined. The breakdown (BV, refers to PV minus MV) and setback (SB, refers to FV minus MV) were calculated.

2.2.5.5 Turbidity Measurements

A 2 % aqueous suspension (200 mL) of starch near neutral pH was prepared and immersed in a boiling water bath for 1 h with continuous gentle stirring, and then cooled for 50 min at 25°C. The turbidity of the suspension was determined by measuring transmittance at 640 nm using a UV-visible spectrophotometer (Spectronic 601, Milton Roy Company, Rochester, NY, USA) against a water blank. The turbidity development was followed by storing the remaining starch pastes for 1 day in a

refrigerator at 4°C followed by 2-20 days at 25°C. Freshly gelatinized (day 0) and stored (24 h at 4°C) starch pastes of tepary bean and lablab bean were freeze-dried and their morphology was examined by scanning electron microscopy under the conditions described for native starches.

2.2.5.6 Acid hydrolysis

Starch samples were suspended in 2.2 M hydrochloric acid (1 g, dwb, 40 mL) at 35°C in a shaking water bath (G76D, New Brunswick Scientific, Edison, NJ, USA) for a period ranging from 0-25 days. The contents were gently vortexed every day in order to resuspend the deposited starch granules. Aliquots (1 mL) taken at specific time intervals were then neutralized with 2.2 M sodium hydroxide and centrifuged (2,000 ×g) for 10 min. An aliquot of the supernatant was analyzed for the solubilized carbohydrates by Bruner's method (1964). The relative absorbances corresponding to D-glucose concentrations ranging from 0.55 to 13.88 μM and 4 to 88 μM were measured at 540 and 590 nm, respectively. A calibration curve was generated from standard glucose solutions (2.5 mg/mL for 540 nm and 18 mg/mL for 590 nm) (Appendix VI). The degree of hydrolysis was reported by expressing the solubilized carbohydrates (Jane & Robyt, 1984) as a percentage of the initial dry starch.

2.2.5.6.1 Preparation of acid thinned starches

The native starches (1g, dwb) were lintnerised by suspending in 2.2 N hydrochloric acid (40 mL) at 35 °C for 1.5, 3, 6, 12, 24, and 72 h in a shaking water bath (G76D, New Brunswick Scientific, Edison, NJ, USA). After hydrolysis, undissolved residues were recovered by centrifugation (2,000 ×g, 12 min) and then washed three times with deionized water. Suspensions were neutralized with 0.1 M sodium hydroxide, centrifuged and washed twice with deionized water to remove

sodium chloride. The resultant pellet was resuspended in acetone. The mixture was then centrifuged (2,000 ×g, 12 min) and the pellet was air-dried at room temperature. The dried samples were grounded using a mortar and sieved through a 60-mesh (250 μm) screen. The control for each starch source was prepared without acid, but subjected to the above experimental conditions; control samples were run concurrently.

2.2.6 Starch digestibility

2.2.6.1 Enzymatic hydrolysis by porcine pancreatic α-amylase

A crystalline suspension of porcine pancreatic α-amylase (PPA) in 2.9 M saturated sodium chloride containing 3 mM calcium chloride was used for enzymatic digestibility studies on native starches. Pulse starches (20 mg) were suspended in deionized water (5 mL) and then 4 mL of phosphate buffer (100 mM, pH 6.9) containing sodium chloride (6 mM) was added. The slurry was then gently vortexed and pre-warmed for 30 min at 37°C before the addition of PPA suspension (12 units/mg of starch). The samples were analysed after 3, 6, 9, 12, 24, 48 and 72 h of incubation at a constant temperature (37°C) in a shaking water bath (New Brunswick Scientific, G76D, Edison, NJ, USA). Aliquots (1 mL) were taken at specific time intervals and the digestion reaction was stopped by adding 2 mL of 95 % ethanol and centrifuged (2,000 ×g) for 5 min. Aliquots of the supernatant were analysed for reducing sugar content according to the Bruner's method (1964). A calibration curve was derived from standard maltose solutions (5 mg/mL for 540 nm and 36 mg/mL for 590 nm). The controls for each starch source were prepared without enzyme, but subjected to the above experimental conditions; control samples were run concurrently. The degree of hydrolysis was calculated to determine the amount of

reducing sugars released in the supernatant, expressed as mg maltose equivalents released per 100 mg of dry starch (Bruner, 1964). The degree of hydrolysis was calculated using the equation shown below:

$$Degree\ of\ hydrolysis\ (percent) = \frac{Released\ reducing\ sugar\ as\ maltose\ (mg) \times 0.95}{Initial\ starch\ weight\ (mg)} \times 100 \quad (2.14)$$

2.2.6.2 *In vitro* starch digestibility and expected glycemic index (eGI)

The *in vitro* digestibility of starches was determined following method 32–40 of the AACC (American Association of Cereal Chemists, 2000). Granular starches (100 mg) were incubated with pancreatin (10 mg) from porcine pancreas and amyloglucosidase (12 U) in 4 mL of sodium maleate buffer (100 mM, pH 6.0) at 37°C with continuous shaking (200 strokes/min) for 30 min to 30 h. Enzyme solutions were freshly prepared prior to each digestion. After incubation, aliquots (0.1 mL) were withdrawn at specific time intervals, and mixed with 4 mL of aqueous ethanol (80 %) to stop the enzyme activity. Then, the contents were centrifuged at 2,000 ×g for 10 min. Aliquots of the supernatant were analysed for glucose content using a glucose oxidase–peroxidase assay kit (K-GLUC) and data were converted to starch content by multiplying by 0.9 (the stoichiometric constant for starch from glucose contents). Starch hydrolysed was expressed as a percentage of the initial dry starch weight.

Starch fractions were classified based on the rate of hydrolysis: rapidly digestible starch (RDS, digested within 30 min), slowly digestible starch (SDS, digested between 30 min and 16 h) and resistant starch (RS, undigested after 16 h) (Chung *et al*., 2008). Resistant starch was calculated by subtracting both RDS and SDS fractions from the total starch (TS) content. The total starch content of each

starch was determined by the total starch assay kit (K-TSTA). Total starch was reported as a percentage on a dry weight basis.

The hydrolysis index (HI) was reported as the total glucose released from the starch compared to that amount of glucose released from a standard material (white bread) (Granfeldt *et al*., 1992). It was calculated as the relation between the area under the hydrolysis curve (AUC, 0 - 16 h) of each starch sample and the corresponding area obtained from white bread, expressed as a percentage. The expected glycemic index (eGI) was estimated using the equation as described by Granfeldt *et al*. (1992). eGI was determined from HI using the equation shown below:

$$eGI = 8.198 + 0.862\ HI \tag{2.15}$$

The residues (of undigested starch) obtained at various time intervals of hydrolysis (30 min, 2 h, and 24 h) were washed three times with deionized water and then centrifuged (2,000 ×g) for 12 min; the resultant pellet was resuspended in acetone. The mixture was then centrifuged (2,000 ×g) for 12 min and the pellet air-dried at room temperature. The controls for each starch source were prepared without enzyme, but subjected to the above experimental conditions; control samples were run concurrently.

2.2.6.2.1 Determination of glucose content (glucose oxidase–peroxidase assay)

A concentrated glucose oxidase-peroxidase (GOPOD) reagent buffer [1.0 M, pH 7.4, *p*-hydroxybenzoic acid and sodium azide (0.4 %, w/v)] was diluted to 1 L with deionized water. Then, the GOPOD reagent enzymes (>12000 U, glucose oxidase plus peroxidase) were dissolved in 20 mL of freshly prepared GOPOD buffer and transferred to the bottle containing the remainder of the GOPOD buffer solution.

Aliquots (100 μL) of the supernatant containing glucose plus GOPOD reagent (3 mL) were incubated at 50°C for 20 min. Finally, the absorbance (ΔA) of sample was measured at 510 nm against a reagent blank. Glucose content was determined using the following formula:

$$Glucose\ (\mu g\ /0.1\ mL) = \frac{\Delta A\ sample}{\Delta A\ glucose\ standard\ (100\ \mu g)} \times 100 \qquad (2.16)$$

2.2.7 Starch modification

2.2.7.1 Annealing

Starch slurries (1:4, w/w, starch (dwb): water) were incubated in sealed glass containers in an incubator for 24, 48 or 72 h at 10°C below the onset gelatinization temperature of their native counterparts. At the chosen annealing temperature, excessive melting of the crystallite is avoided. After the incubation period, the annealed samples were centrifuged (2,000 ×g) for 10 min at room temperature and supernatant was decanted (no amylose or soluble carbohydrates were detected in the supernatant). The annealed starches were washed twice with deionized water and acetone, and recovered by centrifugation (2,000 ×g) for 10 min. The samples were then air dried for 30 h. In the text, 24H_ANN, 48H_ANN and 72H_ANN represents the time of incubation at 10°C below the onset gelatinization temperature for each sample subjected to annealing treatment. Native starch samples subjected to 72 h of annealing treatment were used to determine the structure and properties of annealed starches.

Acid thinned and cross-linked starches were annealed by incubating starch suspensions (1:4, w/w, starch (dwb): water) for 72 h at 6°C below the onset gelatinization temperature. After the incubation period, samples were centrifuged,

washed twice with deionized water and acetone, and recovered by centrifugation. The samples were then air dried, ground and screened through a 60- mesh (250 μm) sieve.

2.2.7.2 Cross-linking

Starches cross-linked with sodium trimetaphosphate (STMP) and sodium tripolyphosphate (STPP) were prepared according to the procedure outlined by Woo and Seib (2002), with a few modifications. Starch samples (50 g, dwb) were mixed in deionized water (70 mL) containing STMP [5.9 g, 11.9 %, starch weight basis (sb)], STPP (0.06 g, 0.12 %, sb) and sodium sulfate (5.0g, 10 %, sb) at room temperature. The pH of the slurry was adjusted to 11.5 with 0.5 M sodium hydroxide and the contents were stirred continuously to avoid gelatinization of the starch. The slurry was then warmed to 45°C and kept at this temperature for 3 h in a shaking water bath; the contents were stirred at 10 min intervals during the 3 h reaction period. After the reaction period, the slurry was neutralized to pH 6.5 with 0.5 M hydrochloric acid. The cross-linked starch was recovered by centrifugation, washed with deionized water multiple times (7X, 125 mL) and dried at 30°C in forced-air oven. The dried samples were ground using a mortar and pestle and sieved through a 60-mesh (250 μm) screen. The controls for each starch source were prepared without STMP/STPP, but subjected to the cross-linking conditions; control samples were run concurrently.

2.2.7.2.1 Determination of degree of substitution and reaction efficiency

The phosphorus contents of control and cross-linked starches were determined using inductively coupled plasma-optical emission spectrometry (ICP-OES, Optima 5300 DV, Perkin Elmer, Waltham, MA, USA). The starch samples were prepared according to modified methods of Anderson (1996) and Hong *et al*. (2015). Starch samples (50 mg, dwb) were weighed into hard glass screw-cap tubes (calibrated at the

10 mL level) and 1.0 mL of 70 % (v/v) nitric acid was added. The tubes were then heated for 3 h at 140°C in an oil water bath. The contents were cooled to room temperature and diluted with MilliQ water to a final volume of 10 mL. All measurements were performed in triplicate. The degree of substitution (DS) was estimated on the basis of the amount (in g) of incorporated phosphorus in 100 g of starch. The incorporated phosphorus (in g) results in a difference in the level of phosphorous (ΔP) in cross-linked and control samples. The DS of cross-linked starches were calculated using the following equation described by Paschall, (1964):

$$DS = \frac{162 \times np}{100 - 102 \times np} = \frac{162 \times \Delta P}{3100 - 102 \times \Delta p} \quad (2.17)$$

Where, nP is the moles of incorporated phosphorus in 100 g starch (np = ΔP/31), 162 is the molecular weight of anhydroglucose, 100 is the dry starch sample weight (in g), and 102 is the molecular weight of $NaPO_3^{2-}$.

The reaction efficiency (RE) was calculated by the ratio of the actual DS to the theoretical DS. The theoretical DS was calculated with the assumption that all STMP reagents added would have reacted with starch. The RE was calculated as follows (Kweon *et al*., 1996):

$$RE = \frac{actual\ degree\ of\ substitution}{mole\ of\ phosphorous\ in\ STMP \frac{added}{drystarch} weight\ (g)} \times 100 \quad (2.18)$$

2.2.8 Statistical analysis

Analytical determinations for the samples were done in triplicate using samples from a single biological lot. Mean values and standard deviations were reported for all data. An independent sample test was used to determine the differences between two groups. A one-way analysis of variance (ANOVA) was performed to determine differences between more than pairs of groups and the mean

separation was analysed using Turkey's HSD test ($p < 0.05$). Analyses were performed using SPSS 16.0 for Windows (SPSS Inc., Chicago, IL, USA).

Chapter 3

Results and Discussion

3.1 Composition, structure, morphology and physicochemical properties of lablab bean, navy bean, rice bean, tepary bean and velvet bean starches

3.1.1 Composition

Data on the yield and composition of pulse starches are presented in Table 3.1. The purity of the starches was judged on the basis of composition [low nitrogen (0.02 to 0.13 %) and low ash (0.06 to 0.58 %)] and microscopic observation (absence of any adhering protein) (Figures 3.1k-o). The yield on a whole seed basis of pure starch was 20.6 to 29.9 % (Table 3.1); this was in the range reported for other pulse starches, being 12.3 to 49.3 % (Hoover *et al*., 2010). The nitrogen content was from 0.02 to 0.13 % (Table 3.1). The low nitrogen content indicated the absence of proteins or lipids associated with endosperm proteins. The free and bound lipids ranged from 0.03 to 1.2 %, and 0.40 to 0.52 %, respectively (Table 3.1). The apparent amylose content was 22.1 to 32.1 % (Table 3.1); this was within the range reported for other pulse starches, being 11.6 to 65.0 % (Hoover *et al*., 2010). Minimal damage was observed for all starches.

3.1.2 Granule characteristics

The birefringence patterns of the pulse starches are presented in Figure 3.1. The birefringence patterns (interference cross known as “maltese cross”) under polarized light reflects the radial arrangement of amylopectin crystallites within the granule at right angles to the surface with their single reducing end group toward the hilum. The hilum at the center of the maltese cross is the original growing point of the granule. Birefringence implies that there is a high degree of molecular orientation,

Table 3.1: Chemical composition (%) of pulse starches[1]

Starch source	Yield	Ash	Nitrogen	Apparent amylose content [2]	Starch damage	Lipid	
						Surface [3]	Bound [4]
Lablab bean	29.9±0.5[a]	0.14±0.00[a]	0.04±0.01[a]	32.1±0.3[a]	0.004±0.001[a]	0.10±0.02[ab]	0.44±0.03[ab]
Navy bean	24.3±0.3[b]	0.35±0.07[b]	0.06±0.01[ac]	26.5±0.2[b]	0.007±0.001[b]	0.05±0.01[a]	0.51±0.01[a]
Rice bean	20.6±0.6[c]	0.58±0.00[c]	0.13±0.01[b]	22.1±0.3[c]	0.011±0.001[c]	0.03±0.02[a]	0.52±0.03[a]
Tepary bean	27.9±0.4[a]	0.11±0.04[a]	0.02±0.02[a]	30.0±0.2[d]	0.005±0.001[ab]	0.12±0.02[b]	0.50±0.01[a]
Velvet bean	25.2±0.4[b]	0.06±0.10[a]	0.05±0.01[a]	27.9±0.4[e]	0.007±0.000[ab]	0.08±0.01[ab]	0.40±0.01[b]

[1]All data represent the mean of triplicates. Values followed by different superscripts in each column for each starch source are significantly different ($P < 0.05$) by Tukey's HSD test.

[2]Determined by iodine binding without removal of free and bound lipids.

[3]Lipid extracted from the starch by chloroform–methanol (CM) 2:1(v/v) at 25°C (mainly free lipids).

[4]Lipid extracted by hot 1-propanol:water (PW) 3:1(v/v) from the residue left after CM extraction (mainly bound lipids).

Figure 3.1: Granule morphology of pulse starches. (*a-e*): Polarized light microscopy (× 200) of lablab bean (*a*), navy bean (*b*), rice bean (*c*), tepary bean (*d*), and velvet bean (*e*). Arrows 1, 2, and 3 represent maltese cross (intensities and patterns), voids, and quadrants, respectively. *(f-j)*: Bright field microscopy (× 400) of lablab bean (*f*), navy bean (*g*), rice bean (*h*), tepary bean (*i*), and velvet bean (*j*). Arrow 4 indicates different types of surface cracks. *(k-o)*: Scanning electron microscopy (× 10,000) of lablab bean (*k*), navy bean (*l*), rice bean (*m*), tepary bean (*n*), and velvet bean (*o*). *(p-t)*: Confocal laser scaning microscopy (× 600) of lablab bean (*p*), navy bean (*q*), rice bean (*r*), tepary bean (*s*), and velvet bean (*t*). Arrows 5 and 6 represent the intensity of APTS flouresence in the hilum and peripheral regions, respectively. The dark central cracked region of tepary bean is indicated by arrow 7 (in panel *s*).

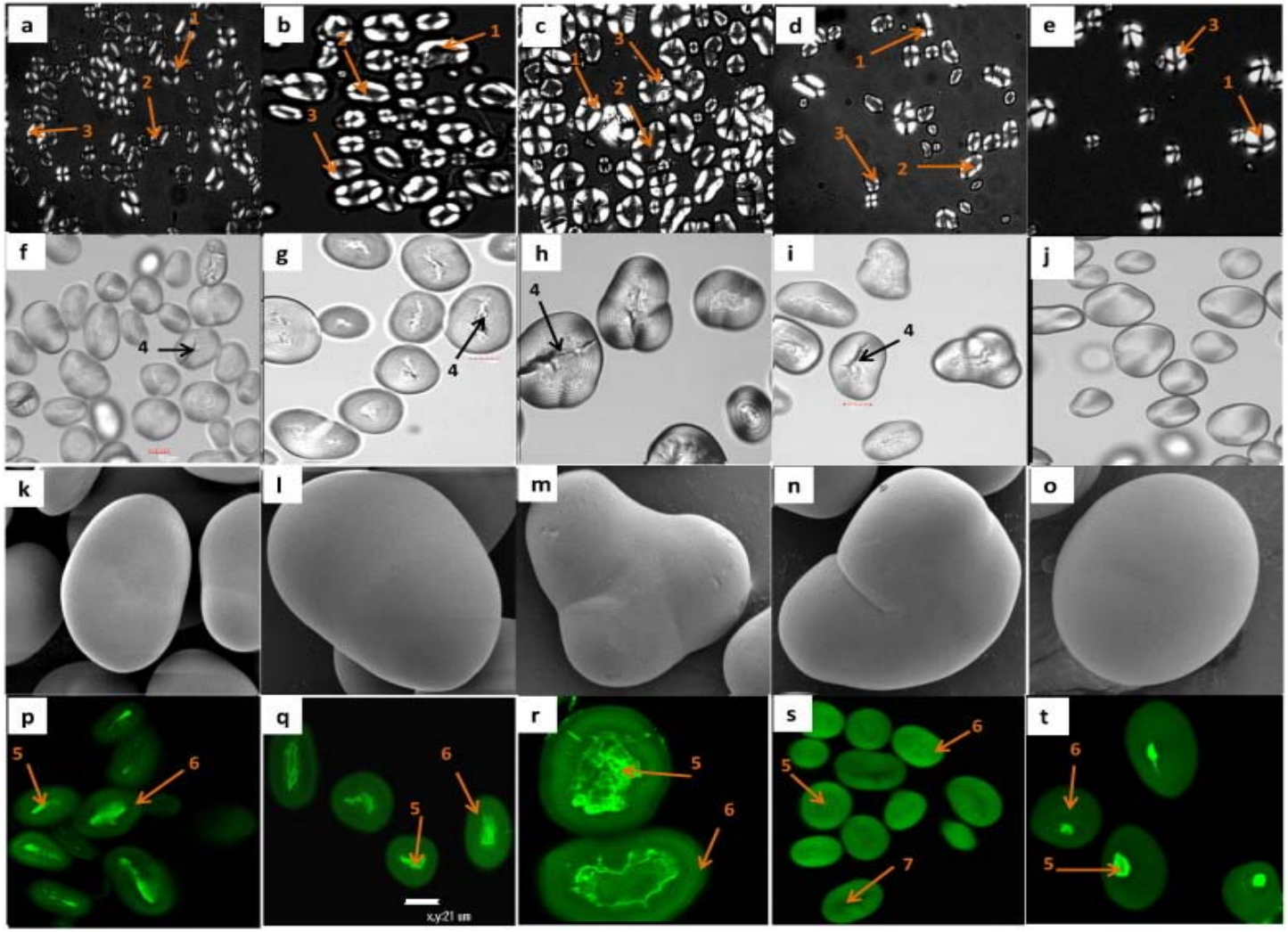
a
b
c
d
e
f
g
h
i
j
k
l
m
n
o
p
q
r
s
t
xy21 sm

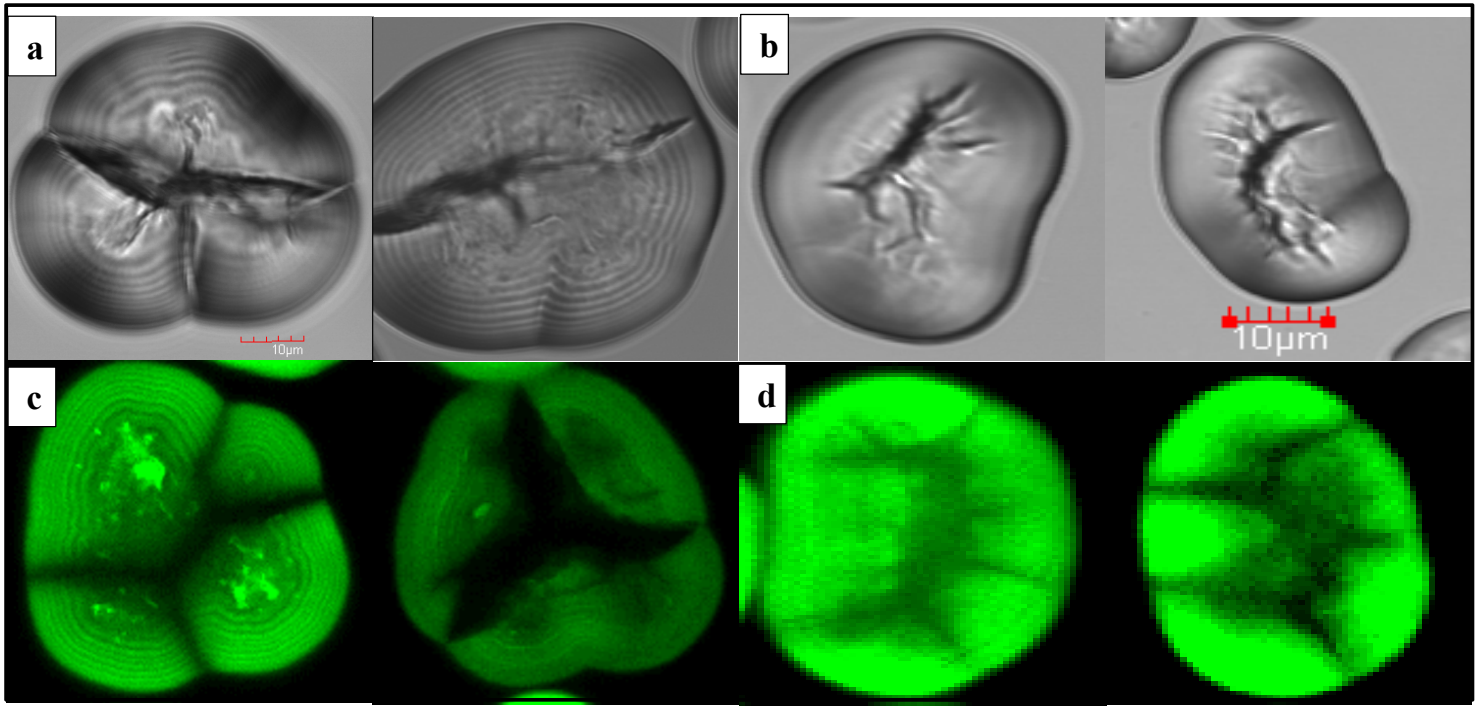

Figure 3.2: *(a-b)*: Cracking pattern in rice bean *(a)* and tepary bean *(b)* starches visualized by bright field microscopy (× 600).

(c-d): Cracking pattern in rice bean *(c)* and tepary bean *(d)* starches visualized by confocal laser scanning microscopy (× 600).

without reference to the three-dimensional crystalline order. All granules of velvet bean (VB) (Figure 3.1e) exhibited strong birefringence (reflected in compactly packed quadrants [depicted by arrow 1]). This is indicative that amylopectin crystallites in all VB granules exhibit a similar molecular orientation. However, in navy bean (NB, Figure 3.1b), rice bean (RB, Figure 3.1c) and tepary bean (TB, Figure 3.1d), some granules exhibited strong birefringence, whereas others exhibited weak birefringence with large voids (arrow 2) at the granule center and less compactly packed quadrants (arrow 3). Voids and disorganized quadrants were more pronounced in RB (Figure 3.1c). However, in lablab bean (LB), weak birefringence intensity was observed in many of its granules (Figure 3.1a). This could be attributed to lower amylopectin content (Table 3.1) and/or disordered AP chains in LB.

Bright field microscopy showed the presence of cracks on granules of RB (Figure 3.1h), NB (Figure 3.1g), TB (Figure 3.1i) and LB (Figure 3.1f). The extent of cracking among granules of each starch source followed the order: RB>TB>NB>LB. A larger magnification of the cracking pattern in RB and TB is illustrated in Figure 3.2. Cracks were not seen among VB granules (Figure 3.1j). Cracks have also been reported in other pulses (Ambigaipalan *et al*., 2011) and transgenically modified potato starches (Blennow *et al*., 2003). Cracks have been attributed to low granule integrity resulting from sub-optimal packing of amylopectin double helices (Blennow *et al*., 2003). Bright field microscopy showed wide variations in granule shape (oval, round, elongated, elliptical and multilobed) and size among starches (Figure 3.1k-o). Growth rings were clearly visible among granules of RB (Figure 3.1m) and NB (Figure 3.1l), but were hardly discernible in granules of VB (Figure 3.1o), LB (Figure 3.1k) and TB (Figure 3.1n). Scanning electron microscopy which provides

topographical data on the exposed surfaces of the starch granules showed smooth surfaces on VB, and some indentations on NB, RB, LB and TB (Figure 3.1k-o). These features were more pronounced in RB (Figure 3.1m).

CLSM images of LB (Figure 3.1p), NB (Figure 3.1q) and RB (Figure 3.1r) showed that the region surrounding the elongated hilum was intensely stained, and in RB, staining occurred in different locations near the vicinity of the hilum (Figure 3.1r). This suggests that cracks in RB granules (Figures 3.1r and 3.2a) may have disorganized the arrangement of starch chains surrounding the hilum region. However, in LB, NB and RB, the peripheral regions (arrow 6) were moderately stained compared to their hilum regions (Figures 3. 1p,1q,1r). Growth rings were not visible in LB (Figure 3.1p) and NB (Figure 3.1q) but were clearly visualized in RB (Figure 3.1r). In TB (Figure 3.1s), some granules exhibited intense staining in both the vicinity of the elongated hilum (arrow 5) and peripheral regions (arrow 6), whereas in other granules, the hilum region was stain free (arrow 7) with the peripheral regions moderately stained. VB differed from the above starches, with respect to the shape of the hilum (which appeared as an intensely stained small dot) (Figure 3.1t). VB exhibited moderately stained peripheral regions and growth rings compared to its hilum regions (Figure 3.1t). Bright fluorescence near the vicinity of the hilum region is indicative of a high concentration of amylose, since amylose is more heavily labelled with APTS than in amylopectin because it contains a higher molar ratio of reducing ends per glucose residue than does amylopectin (Blennow *et al*., 2003). The bright fluorescence in the hilum region could also reflect the presence of a higher concentration of amylopectin reducing ends (Blennow *et al*., 2003). The CLSM

images suggest that in all the starches, there is a high concentration of reducing ends near the hilum region.

3.1.3 Particle size analysis

Particle size analysis of the pulse starches are presented in Table 3.2. The arithmetic mean diameter and specific surface area followed the order: RB>NB>VB>LB~TB and TB~LB>VB>NB>RB, respectively. RB starch granules showed the highest mean granule diameter (42.9 μm) and widest granule size distribution, while LB and TB had the smallest mean granule diameter (21.9 μm) and the smallest granule size distribution. No comparison is possible with the granule dimensions of pulse starches reported in the literature (Hoover *et al*., 2010) due to the following reasons: 1) the width and length of starch granules have been solely obtained from scanning electron micrographs, 2) in many cases, the dimensions reported do not specify whether the width or length was measured; and 3) lack of data on surface area.

3.1.4 Amylopectin chain length distribution (APCLD)

The amylopectin chain length distribution of pulse starches are presented in Table 3.3. The normalized APCLD and the average chain length ($\overline{CL}$) of the debranched AP of the pulse starches showed marginal differences among the starches. The proportion of chains with dp 6-12 (18.0-21.3), dp 13-24 (50.9-55.0), dp 25-36 (15.6-18.5), dp 37-50 (9.3-10.8) and $\overline{CL}$ (20.6-21.3) were in the range reported for grass pea, smooth pea, mung bean and lentil starches (Hoover *et al*., 2010).

Table 3.2: Particle size analysis of pulse starches[1]

Starch source	Arithmetic mean diameter (µm)	d(0.1) (µm)[3]	d(0.5) (µm)[3]	d(0.9) (µm)[3]	Surface weighted mean D(3,2)[4]	Specific surface area (m^2/g)[5]	Elongation[6]
Lablab bean	21.9±0.1^{ad}	4.6±0.0^{a}	22.4±0.0^{a}	33.8±0.4^{a}	10.4±0.0^{a}	0.38±0.00^{a}	1.5±0.00^{ab}
Navy bean	30.8±0.1^{b}	10.1±0.3^{b}	30.1±0.1^{b}	46.9±0.1^{b}	13.4±0.1^{b}	0.30±0.00^{b}	1.3±0.00^{a}
Rice bean	42.9±3.0^{c}	19.0±0.0^{c}	41.1±0.1^{c}	59.8±0.4^{c}	17.4±0.1^{c}	0.23±0.00^{c}	1.4±0.00^{ab}
Tepary bean	21.9±1.0^{d}	6.2±0.1^{d}	21.6±0.1^{d}	32.5±0.0^{d}	10.3±0.1^{a}	0.39±0.00^{a}	1.6±0.16^{ab}
Velvet bean	28.4±1.0^{b}	7.8±0.5^{e}	27.9±0.1^{e}	42.6±0.5^{e}	12.3±0.0^{d}	0.33±0.00^{d}	1.4±0.00^{ab}

[1]All data represent the mean of triplicates. Values followed by different superscripts in each column for each starch source are significantly different ($P < 0.05$) by Turkey's HSD test.

[3,4]Particle size is defined in terms of 10th percentile [d(0.1)], median [d(0.5)], 90th percentile [d(0.9)] and surface weighted mean [D(3,2)]. Surface weighted mean is an average of particle size.

[5]Specific surface area (SSA) was calculated from the median (Riley *et al*., 2006) using the equation shown below (where 6 is a constant for spherical particles). Specific surface area (m^2/g) = $\frac{6}{1.5 \times \text{surface weighted mean}}$.

[6]Represents average length to breadth of a particle.

Table 3.3: Amylopectin chain length distribution of pulse starches determined by high performance anion exchange chromatography with pulsed amperometric detection (HPAEC-PAD)[1]

Starch source	Degree of polymerization[2] (dp) %				
	6-12	**13-24**	**25-36**	**37-50**	**$\overline{CL}$ [3]**
Lablab bean	18.8±1.1^{a}	55.0±0.5^{a}	15.6±0.4^{a}	10.6±0.2^{a}	20.8±0.2^{ab}
Navy bean	19.2±0.6^{a}	52.9±1.3^{ab}	17.1±0.5^{ab}	10.8±0.2^{a}	21.1±0.1^{ab}
Rice bean	21.3±1.0^{a}	51.4±0.9^{b}	17.3±0.4^{b}	10.0±0.3^{ab}	20.7±0.0^{a}
Tepary bean	21.2±1.3^{a}	50.9±1.1^{b}	18.5±0.1^{b}	9.3±0.1^{b}	20.6±0.1^{a}
Velvet bean	18.0±1.0^{a}	53.0±0.2^{ab}	18.4±0.5^{b}	10.7±0.3^{a}	21.3±0.2^{b}

[1]All data represent the mean of triplicates. Values followed by different superscripts in each column for each starch source are significantly different ($P < 0.05$) by Turkey's HSD test.

[2]dp_n: indicates degree of polymerization. Total relative area was used to calculate the percent distribution.

[3]Average chain length ($\overline{CL}$) was calculated using Σ ($dp_n \times$ peak area)/Σ (peak $area_n$).

3.1.5 Attenuated total reflectance Fourier transform infrared spectroscopy (ATR-FTIR)

The ATR-FTIR spectral data is presented in Table 3.4. The ATR-FTIR spectrum of starch has been shown to be sensitive to changes in structure on a molecular level (based on short range order) (van Soest, *et al*., 1995; Sevenou, *et al*., 2002). Short range order reflects double helical order as opposed to long range order, which is related to the packing of double helices (detected by X-ray diffraction). The penetration depth of the IR beam is about 2 μm. Thus, molecular organization investigated by ATR-FTIR is limited to regions near the granular surface (Sevenou, *et al*., 2002). The ATR-FTIR absorbance at 1048 cm^{-1} is related to crystallinity because this band increases with crystallinity, whereas the band at 1016 cm^{-1} has been attributed to vibrational modes (van Soest, *et al*., 1995) within the amorphous domains of starch granules; this band has been observed to decrease with an increase with crystallinity. Thus, the ratio 1048 cm^{-1}/1016 cm^{-1} has been used to express the amount of ordered crystalline domains to amorphous domains in starches. The 1048 cm^{-1}/1016 cm^{-1} ratio of the assessed bean starches followed the order VB>TB~RB~NB>LB (Table 3.4). This is indicative of double helices near the vicinity of the granule surface are better aligned in VB compared to LB. The ratios obtained were within the previously reported range of 0.886 to 0.938 for faba bean, black bean and pinto bean starches (Ambigaipalan *et al*., 2011), but it was much higher than that reported for pea starch (0.751) and lentil starch (0.765) (Chung *et al*., 2010).

Table 3.4: FTIR intensity ratio (1048 cm^{-1}/1016 cm^{-1}), relative crystallinity, double helical content and B-polymorphic content of pulse starches.

Starch source	FTIR ratio 1048/1016 cm^{-1}	Relative crystallinity (%)	Double helical content (%)	B-polymorphic content (%)
Lablab bean	0.813±0.000[a]	19.9[a]	34.1[b]	9.3
Navy bean	0.860±0.005[b]	20.7[a]	25.8[a]	0
Rice bean	0.867±0.001[b]	23.8[b]	31.1[c]	0
Tepary bean	0.860±0.001[b]	21.4[a]	37.8[d]	0
Velvet bean	0.901±0.005[c]	26.5[c]	37.2[d]	0

The maximum standard deviations for double helical content (NMR measurements) and relative crystallinity calculations were ±0.6 % and ±0.9 %, respectively.

Values followed by different superscripts in each column for each starch source are significantly different ($P < 0.05$) by Tukey's HSD test.

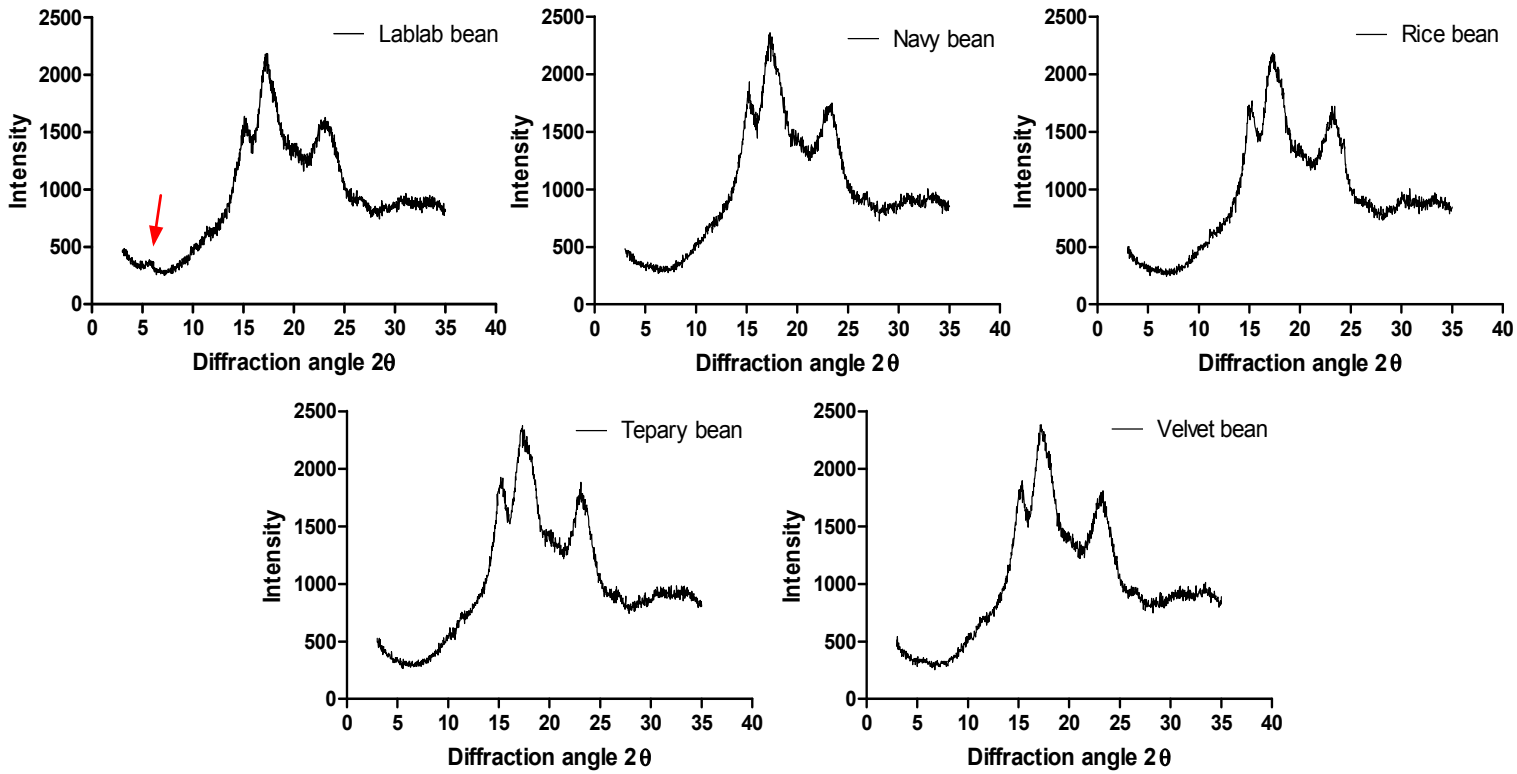

Figure 3.3: X-ray diffraction patterns of pulse starches. The arrow in the lablab bean panel shows the peak characteristic of B-type crystallites.

3.1.6 Wide angle X-ray diffraction (WAXS)

Pulse starches generally exhibit a 'C' type X-ray pattern, characterized by a weak peak at 2θ = 5.4 and strong peaks at 17.5 and 23° 2θ. Gernat *et al.* (1990) have shown that the C-type polymorph is a mixture of 'A' and 'B' unit cells, and that pulse starches contain pure 'A' and 'B' polymorphs in varying proportions. The WAXS patterns of the pulse starches are presented in Figure 3.3. LB starch exhibited a mixed A+B type pattern [due to the presence of 'B' type unit cells (9.3 %, Table 3.4)] with a peak centred at 5.5° 2θ, which is typical of pure B-type starches, whereas all other starches exhibited a pure A-type pattern (Figure 3.3). The relative crystallinity (RC) of the starches ranged from 19.9-26.5 % (VB>RB>TB~NB~LB, Table 3.4). These values were within the previously reported range of 17.0-34.0 % for other pulse starches (Hoover *et al.,* 2010). Differences in RC among starches could reflect differences in: 1) amylopectin content, 2) APCLD, 3) crystallite size; and 4) different orientations of double helices within the crystalline domains (Ambigaipalan, *et al.,* 2011). Difference in RC among the starches (Table 3.4) cannot be attributed to differences in the amylopectin content and the crystallite size for the following reasons: 1) higher amylopectin content (Table 3.1) was not associated with higher RC (Table 3.4); 2) APCLD and $\overline{CL}$ did not differ significantly ($p<0.05$) among the starches; and 3) nearly similar crystal size, indicated by very marginal differences in the sharpness of the X-ray spectrum (Figure 3.3). Thus, the higher RC of VB is probably due to stronger interaction between double helices within the crystalline lamella and/or better orientation of the crystallites to the X-ray beam. It was interesting to observe that molecular order (VB>RB>TB~NB~LB) closely paralleled the crystalline order (VB>RB>TB~NB~LB).

3.1.7 ^{13}C cross polarization magic angle spinning nuclear magnetic resonance spectroscopy (^{13}C CP/MAS NMR)

The DHC of the pulse starches (TP>VB>LB>RB>NB), determined by ^{13}C CP/MAS NMR, is presented in Table 3.4. DHC ranged from 25.8 to 37.8 %. A DHC of 39.7 % has been reported for pea starch (Bogracheva *et al.,* 2001). The DHC could represent double helices formed between outer branches (A and B1 chains) of amylopectin, amylose-amylopectin and/or amylose-amylose. Double helices in starch granules have been shown to be present in a crystalline and/or non-crystalline array (Morrison *et al*., 1993a; Morrison *et al*., 1993b). In the pulse starches, the DHC (25.8-37.8 %, Table 3.4) was much higher than their RC (19.9-26.5 %, Table 3.4), suggesting that not all helical conformations are involved in starch crystallites.

3.1.8 Differential scanning calorimetry (DSC)

The gelatinization temperatures (To, Tp and Tc), gelatinization temperature range (Tc-To) and ΔH are presented in Table 3.5. To, Tp and Tc represent crystalline stability, whereas ΔH represents melting of amylopectin based crystals with potential contributions from both crystal packing and helix melting enthalpies (Lopez-Rubio, *et al.,* 2008). The starches differed significantly ($p<0.05$) with respect to To (in the order of VB>TB>NB>RB~LB) and Tp (in the order of VB>NB>TB>RB>LB). Differences in Tc among the starches (except RB and VB) were not significant. Tc-To followed the order LB~RB~NB>TB>VB. The higher To of VB is indicative that its crystallites have a higher degree of stability (reflects closer packing of amylopectin crystallites within the crystalline lamella) and/or a lesser amount of structural defects. Structural defects in crystallites have been shown to occur if amylose chains pass through both the crystalline and the amorphous layer (Genkina, *et al.,* 2007), and if long chains of amylopectin are interspersed into the crystalline lamella (Koroteeva *et al.,* 2007).

Table 3.5: Gelatinization parameters of pulse starches as determined by differential scanning calorimetry[1]

Starch source	Gelatinization transition parameters (°C)				Enthalpy[4] (J/g)
	To[2]	Tp[2]	Tc[2]	(Tc-To)[3]	
Lablab bean	62.6±0.2^{a}	67.9±0.1^{a}	81.9±0.0^{ab}	19.3±0.2^{a}	10.5±0.2^{ab}
Navy bean	65.8±0.4^{b}	73.6±0.1^{b}	81.9±0.0^{ab}	16.1±0.4^{bc}	9.6±0.3^{a}
Rice bean	62.7±0.2^{a}	68.8±0.1^{c}	81.0±0.9^{a}	18.3±0.8^{ab}	11.3±0.3^{b}
Tepary bean	66.9±0.0^{c}	71.4±0.1^{d}	82.5±0.6^{ab}	15.6±0.6^{c}	10.1±0.2^{ab}
Velvet bean	72.4±0.0^{d}	77.2±0.3^{e}	83.7±0.7^{b}	11.2±0.7^{d}	10.6±0.2^{ab}

[1]All data represent the mean of triplicates. Values followed by different superscripts in each column for each starch source are significantly different ($P < 0.05$) by Tukey's HSD test. Starch: water ratio (1:3 w/w, dwb)

[2]To, Tp, Tc represents the onset, peak, and end temperatures, respectively.

[3](Tc-To) represents the gelatinization temperature range.

[4]Gelatinization enthalpy expressed in J/g of dry starch (amylopectin basis).

The lower Tc-To of VB suggests that VB crystallites have a higher degree of crystalline perfection (which reflects better alignment of double helices within the crystalline lamella) than those of the other starches. The higher degree of crystalline perfection also may partly explain the higher RC of VB. The order of crystalline perfection (VB>TB>NB~RB~LB) did not exactly parallel the RC order (VB>RB>TB~NB~LB, Table 3.4). This was not surprising, since RC differences among starches are influenced not only by crystallite perfection, but also by how well the crystallites are oriented towards the incoming X-ray beam. There was no significant difference ($p<0.05$) in ΔH among the starches of LB, TB and VB (Table 3.5). However, NB and RB starches showed a significant difference in their ΔH. This suggests that crystalline perfection has no influence on ΔH. For instance, VB, with a higher degree of crystalline perfection, exhibited a ΔH value similar to that of the other starches. This indicates that the extent of hydrogen bonding within and among double helices is the same in all of the starches. Consequently, no differences can be expected with respect to the magnitude of the thermal energy (ΔH) required to separate amylopectin double helices from their lamellar crystallites during gelatinization. Differences in gelatinization parameters among the starches cannot be attributed to amylopectin chain length or to amylopectin content, since there was marginal difference in APCLD. Furthermore, differences in amylopectin content (RB>NB>VB>TB>LB, Table 3.1) did not parallel differences in gelatinization parameters. The gelatinization parameters were within the range reported for other pulse starches (Hoover *et al*., 2010).

3.1.9 Swelling factor (SF)

The SFs of the pulse starches in the temperature range of 60 to 85°C is presented in Figure 3.4a. Swelling factor differences among starches have been shown to be influenced by bound lipid content (Sasaki & Matsuki, 1998), amylose content (Sasaki & Matsuki, 1998), amylopectin structure (Sasaki & Matsuki, 1998), extent of interaction between starch chains in the native granule (Ambigaipalan, *et al.,* 2011), and granule crystallinity (Ambigaipalan, *et al.,* 2011). Comparative studies on non-waxy and waxy cereal starches have shown that swelling is primarily a property of amylopectin and that amylose is a diluent (Tester & Morrison, 1990b; Morrison, *et al.,* 1993b).

Swelling factor differences (Figure 3.4a) among the starches were significant only between 60-80°C, in the order of TB>LB>RB>NB>VB. However, at 85°C, differences in SF among the starches were marginal. SF differences cannot be explained in terms of APCLD or bound lipid content (Table 3.1), since differences among the starches with regard to the above two factors were not significant ($p<0.05$). The differences in SF between LB and TB starches (TB>LB) in the temperature range 60-80°C may reflect higher granule integrity in TB due to higher DHC (Table 3.4). This seems plausible, since differences between TB and LB with respect to amylopectin content (Table 3.1) and RC (Table 3.4) were marginal. SF differences in the range 60-80°C between RB and NB (RB>NB) starches reflect the higher amylopectin content (Table 3.1), higher DHC (Table 3.4), larger granule size (Table 3.2) and the presence of a larger number of cracked (Figure 3.1h, arrow 4) granules. Cracking would facilitate rapid diffusion of water into the amorphous regions in RB.

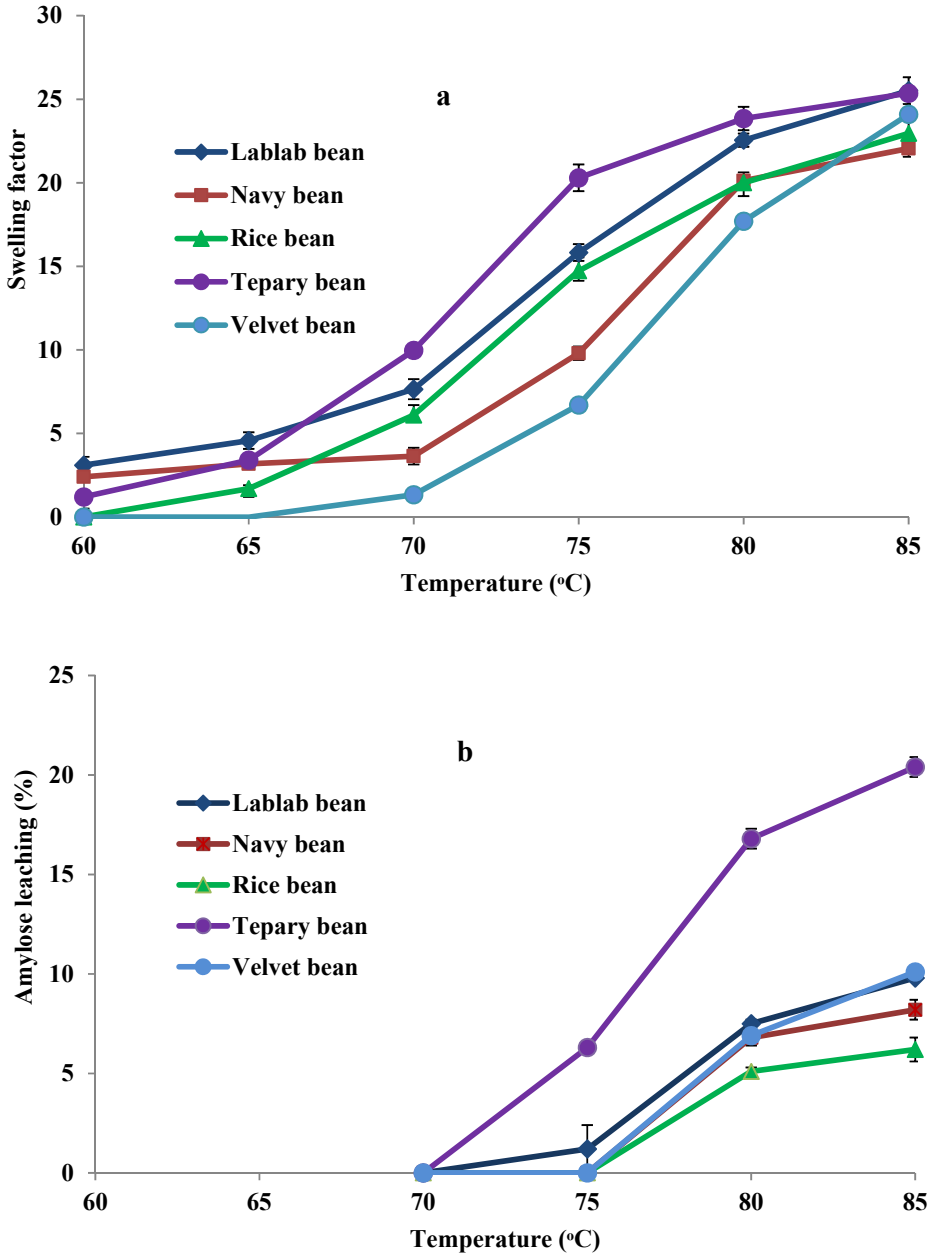

Figure 3.4: Swelling factor *(a)* and amylose leaching *(b)* of native pulse starches over the temperature range of 60-85°C.

The SF of VB is much lower than that of the other starches due to its higher RC and molecular order (Table 3.4). The above data suggest that differences in SF among the starches reflect the interplay among amylopectin content, RC, DHC, granule size and surface characteristics. The SF (22.1-25.5) of the pulsee starches at 85°C was similar to that for black bean (25.0) (Ambigaipalan, *et al.,* 2011) and pinto bean (21.0) (Ambigaipalan, *et al.,* 2011), but much higher than that for pea (17.9), lentil (16.8), navy bean (11.8) and chick pea (18.0) starches (Hoover *et al.,* 2010).

3.1.10 Amylose leaching (AML)

Data for AML are presented in Figure 3.4b. AML in the temperature range of 70 to 85°C followed the order TB>LB~VB~NB>RB. AML has been shown to be influenced by the interplay between amylose content and the extent to which amylose-amylopectin and amylose-amylose chains are associated within the granule interior (Ambigaipalan, *et al.,* 2011). Differences in AML between TB and LB (TB>LB) are indicative of weaker interactions between amylose-amylose and amylose-amylopectin chains within native granules of TB. This seems plausible, since the differences in amylose content (Table 3.1) between TB (30 % amylose) and LB (32.9 % amylose) was too small to account for the large difference in AML between these starches. Weaker interactions between amylose-amylose and amylose-amylopectin chains in TB also may have influenced SF differences (TB>LB) between these starches (Figure 3.4a). Marginal differences in AML among LB, VB and NB reflect the interplay between variations in amylose content (LB, 32.9 %; VB, 27.9 %; and NB, 26.1 %) and the extent of interactions between amylose-amylose and amylose-amylopectin chains. It is likely that the relatively low extent of AML (Figure 3.4b) in RB can be attributed to the amylose content of RB being much lower (22 %, Table 3.1) than that

of other starches (26.0-32.9 %, Table 3.1). AML at 80°C in TB, LB, VB, NB and RB was within the range reported for other pulse starches, being 4.5-28.5 % (Ambigaipalan, *et al.,* 2011).

3.1.11 Acid hydrolysis

The susceptibility of starches toward hydrolysis by 2.2 M hydrochloric acid is presented in Figure 3.5. Acid hydrolysis consists of two stages: an initial fast step (due to hydrolysis of the amorphous regions) which generally occurs during the first 9-12 days of hydrolysis, followed by a second slower rate (due to hydrolysis of the cryatalline regions) (Hoover, 2000). Differences in the extent of acid hydrolysis among starches have been attributed to differences in granule size, amount of bound lipids, APCLD, proportion of B-type unit cells and double helical order within the crystalline lamella (Gerard *et al.,* 2002; Ambigaipalan *et al.,* 2011). Differences in hydrolysis among the starches during the first 9 days of hydrolysis (Figure 3.5) were marginal. This suggests that the arrangement of starch chains (packing density) within the bulk amorphous and intercrystalline amorphous regions were similar in all starches. Beyond the 9th day, the hydrolysis curve was continued to increase in all starches and indicating that the starch chains in the crystalline region were also susceptible to acid hydrolysis. The faster rate of hydrolysis between the 9th and 15th day observed with LB and RB starches can be attributed to rapid penetration of H_3O^+ via the cracks on the granule surface (Figure 3.1f,h) and/or the presence of disorganized double helical arrangement (Table 3.4) within the crystalline lamella. This would facilitate the accesibilty of H_3O^+ on α(1→4) and α (1→6) linkages located within the crystalline lamella of LB and RB starches.

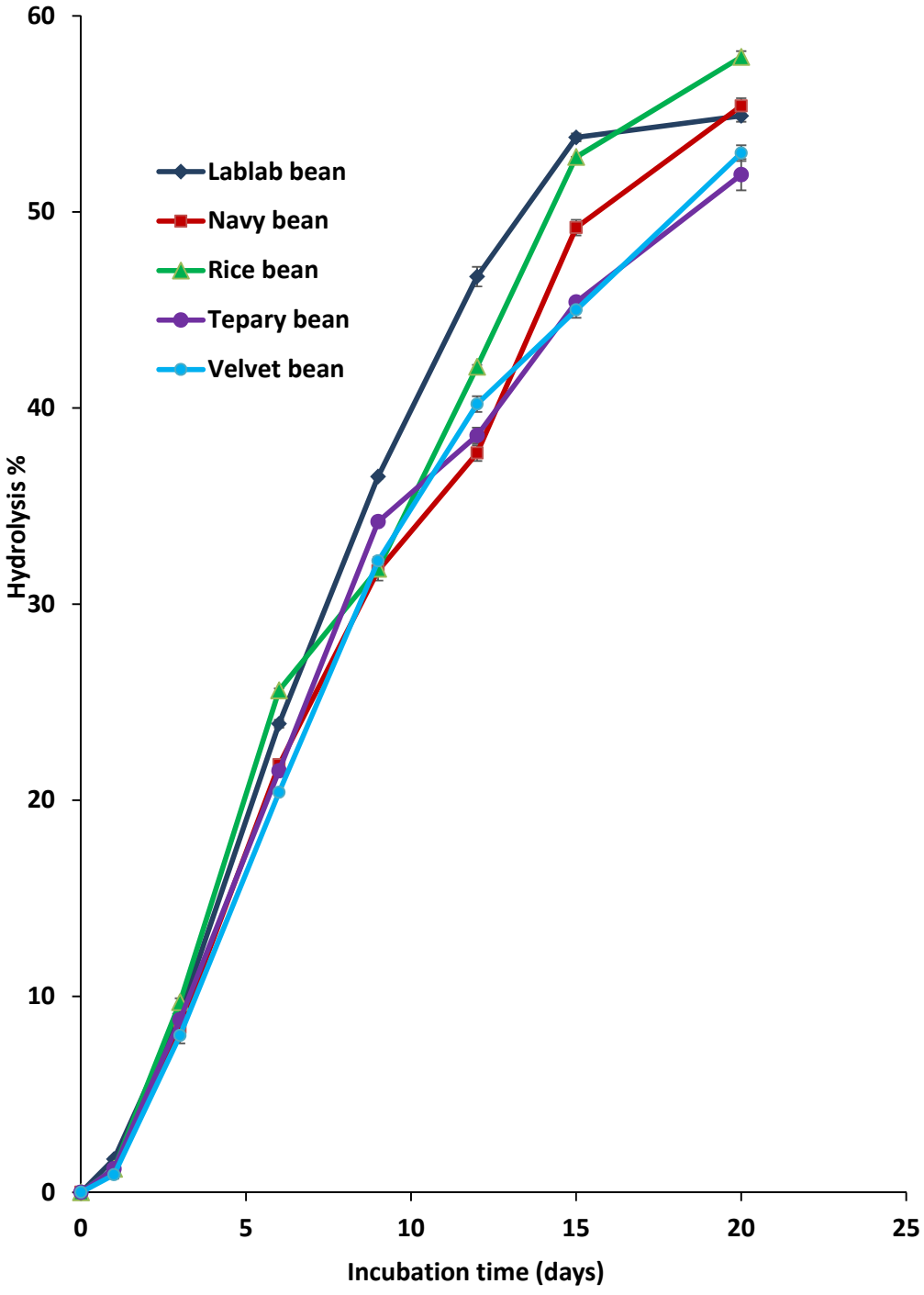

Figure 3.5: Acid hydrolysis (2.2 M hydrochloric acid, 35°C) profiles of pulse starches.

In contrast to RB starch, the susceptibility of LB starch toward acid hydrolysis could be attributed to the molecular order of LB at the granular surface, the RC (Table 3.4) being lower than that of the other starches and the presence of B-type unit cells. The lower molecular order on the granule surface facilitates faster diffusion of H_3O^+ into the crystalline domains and leads to a greater extent of hydrolysis. In starches containing B-type unit cells, the α(1→6) linkages are solely occupied within the amorphous domains, whereas in A-type starches, the α(1→6) linkages are located within both the amorphous and crystalline domains (Jane *et al.,* 1997). Consequently, α (1→6) linkages of LB will be more susceptible to acid hydrolysis, since in the other starches that contain only 'A' type unit cells, α (1→6) linkages are embedded in the crystallites, and hence will be less susceptible to acid hydrolysis. The higher resistance of VB and TB starches toward acid hydrolysis (Figure 3.5) could be attributed to their molecular order (double helical content, Table 3.4) being higher than those of the other starches. The above data suggest that differences in hydrolysis among RB and NB reflect the interplay among differences with respect to 1) molecular order [RB (0.867)>NB (0.860)]; 2) RC [RB (23.8 %)>NB (20.7 %)]; and 3) the presence of surface cracks on granule surfaces (RB>NB). APCLD, surface area and bound lipid content cannot be considered as factors influencing the extent of acid hydrolysis among these starches for the following reasons: 1) similarity in APCLD (Table 3.3); 2) the difference in surface area (Table 3.2) between RB (0.23 m^2/g) and NB (0.30 m^2/g) did not translate into NB being hydrolysed to a greater extent than RB; and 3) the absence of any significant difference ($p<0.05$) in bound lipid content (Table 3.1) among the starches. Differences in acid hydrolysis among pulse starches mainly

reflect the interplay between differences in granule surface characteristics and extent of double helical order within the crystalline lamellae.

3.1.12 *In vitro* digestibility by porcine pancreatic α-amylase (PPA)

Differences in digestibility among and within species of native starches have been attributed to the interplay of several factors such as granule size, extent of molecular association between starch chains, amylose content, branch chain length distribution of amylopectin, degree of crystallinity, polymorphic composition, granular pores, cracks on the granule surface, channels within the granules, and surface area (Hoover & Zhou, 2003; Zhang *et al*., 2006a,b). The *in vitro* enzyme-catalysed hydrolysis of pulse starches, monitored by measuring the release of maltose from starch by the action of PPA at specific intervals during hydrolysis, is presented in Figure 3.6. The amount of starch hydrolysed from the granules after 72 h of digestion ranged between 20.7 % and 67.9 % (Figure 3.6). The most readily hydrolysed starches were TB (60.7 %) and RB (67.9 %), whereas the most resistant starch was VB (20.7 %). LB and NB were hydrolysed to the extent of 35.4 % and 31.7 %, respectively. The hydrolysis curves (Figure 3.6) showed that in both RB and TB, the first 48 h of hydrolysis was characterized by a steeply increasing concentration of maltose, after which the rate of hydrolysis transitioned to a slower rate in TB, but continued to rise steeply in RB. The hydrolysis rates were lower for NB, LB and VB. The extent and rate of hydrolysis followed the order of LB>NB>VB. The rate of hydrolysis did not exhibit a plateau, even after 72 h of hydrolysis for LB, NB and VB starhes.

The higher extent of hydrolysis (Figure 3.6) seen with RB and TB (with RB>TB) could be attributed to the presence of cracks (with RB having more than TB)

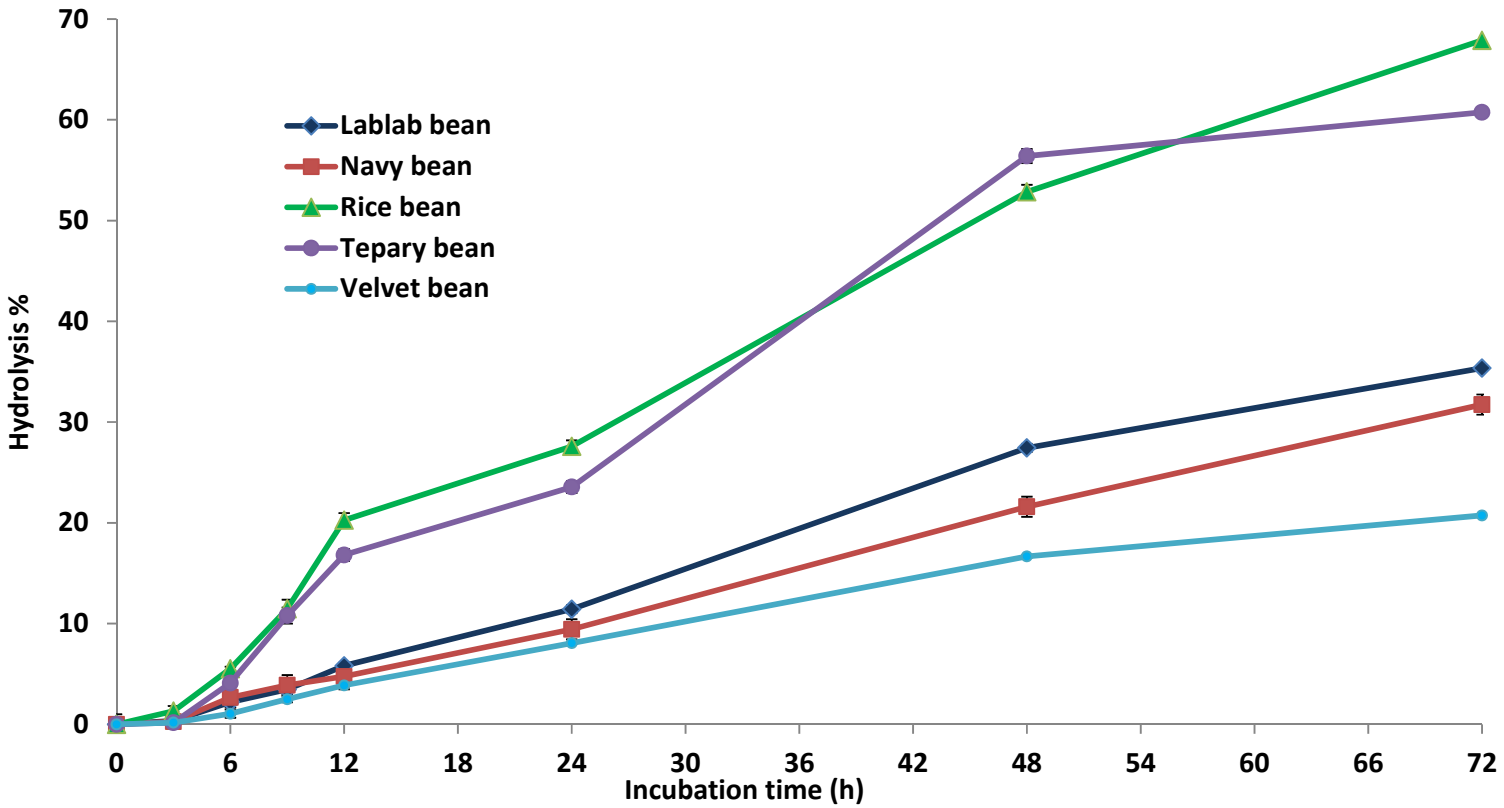

Figure 3.6: *In vitro* digestibility profile of native pulse starches subjected to enzyme-catalysed hydrolysis by porcine pancreatic α-amylase at 37°C.

on their granular surfaces (Figures 3.1h and 3.1i), which may have facilitated rapid penetration of PPA into the amorphous growth rings, and then into the amorphous and crystalline regions of the semi-crystalline growth rings, resulting in destruction of the lamellar structure. The double helical conformation has been shown to hinder enzyme-catalysed hydrolysis (Lopez-Rubio *et al.,* 2008), since in this form only a maximum linear portion of three glucose units is available; this is insufficient for complete substrate binding. This suggests that the difference in the extent of hydrolysis between RB and TB (with RB>TB) also could be attributed to differences in their DHC (TB, 37.8 %; RB, 31.1 %, Table 3.4). The above explanations seem plausible, since on the basis of surface area (RB, 0.23 m^2/g; TB, 0.39 m^2/g, Table 3.2), amylose content (RB, 22.1 %; TB, 30.0 %, Table 3.1), and RC (RB, 23.8 %; TB, 21.4 %, Table 3.4), TB should have been hydrolysed to a greater extent than RB. This suggests that in RB and TB starches, cracks on the granule surface and DHC may have reduced the influence of surface area, composition and crystallinity on hydrolysis. The difference in hydrolysis between LB and NB (with LB>NB) was due to surface area (LB, 0.38 m^2/g; NB, 0.30 m^2/g, Table 3.2) and amylose content (LB, 32.1 %; NB, 26.5 %, Table 3.1) being higher, and molecular order (LB, 0.813; NB, 0.860, Table 3.4) and RC (LB, 19.9 %; NB, 20.7 %, Table 3.4) being lower in LB. The combined effect of the above parameters may have reduced the influence of higher DHC and B-type unit cells (present only in LB) on LB hydrolysis. The presence of B-type unit cells has been shown to resist PPA hydrolysis compared to A-type unit cells (Gérard *et al*., 2002). The higher resistance of VB towards amylolysis could be attributed to RC, molecular order, and DHC being higher than that of the other starches.

3.1.13 Pasting properties

Pasting occurs after gelatinization in the process of dissolution of starch. The granules become very susceptible to shear, resulting in disintegration. The paste that is obtained on gelatinization is a viscous mass consisting of a continuous phase of solubilized amylose and/or amylopectin, and granule remnants embedded in the leached amylose network (BeMiller, 2011). The pasting properties are presented in Table 3.6. The pasting temperature, peak viscosity (PV), viscosity breakdown (during the holding cycle at 95˚C) and set-back (during the cooling cycle) followed the order of VB>NB>LB>TB~RB, TB>NB>RB>LB>VB, TB~NB>RB>LB~VB and RB~LB>VB~NB>TB, respectively. PV is influenced by the interplay of friction between swollen granules, the extent of AML and RC (Chung *et al*., 2009a). The higher PV (5311 cP) of TB (Table 3.6) is mainly due to its higher extent of AML (Figure 3.4B). This seems plausible, since the RC (21.4 %, Table 3.4) and granule size (21.9 μm, Table 3.2) of TB were comparable and lower, respectively, than those of RB, LB, and NB. The higher RC (26.5 %, Table 3.4) of VB may have been the main causative factor (restricts granular swelling during heating) responsible for its peak viscosity (3283 cP) being lower than that of other starches. Among RB, LB and NB, the PV of NB (Table 3.6) was higher than that of RB due to its higher tendency to leach amylose (Figure 3.4b) and lower RC (Table 3.4). The PV of LB was lower than that of RB and NB, due to its smaller granule size (21.94 μm, Table 3.2). The lower PV of LB (3612 cP) and VB (3283 cP) may have been responsible for the extent of viscosity breakdown (during the holding cycle at 95°C) in LB (1131 cP) and VB (1175 cP), being much lower than those of the other starches (Table 3.6). The breakdown viscosity among the starches was most pronounced in TB (3036 cP) due to its higher PV (Table 3.6).

Table 3.6: Pasting properties of pulse starches[1]

Starch source	Pasting temp. (°C)	Peak time (min)	Peak viscosity (cP)	Trough viscosity (cP)	Breakdown viscosity (cP)	Final viscosity (cP)	Set-back viscosity (cP)
Lablab bean	75.7±0.3^{a}	7.1±0.0^{a}	3612±35^{a}	2301±42^{a}	1311±77^{a}	5056±26^{a}	2755±016^{a}
Navy bean	78.3±0.0^{b}	7.2±0.0^{b}	4831±09^{b}	1922±09^{b}	2909±18^{b}	3780±13^{b}	1858±023^{b}
Rice bean	72.3±0.0^{c}	6.8±0.0^{c}	4583±03^{c}	2820±61^{c}	1763±58^{c}	5750±27^{c}	2930±034^{a}
Tepary bean	72.5±0.4^{c}	7.0±0.0^{d}	5311±19^{d}	2275±10^{a}	3036±09^{b}	3883±49^{b}	1608±039^{c}
Velvet bean	79.8±0.0^{d}	7.7±0.0^{e}	3283±76^{e}	2108±23^{d}	1175±53^{a}	4029±13^{b}	1921±114^{b}

[1]All data represent the mean of triplicates. Values followed by different superscripts in each column for each starch source are significantly different ($P < 0.05$) by Tukey's HSD test.

Among the starches, viscosity breakdown during the holding cycle at 95°C, which reflects granule disintegration due to shear, was less pronounced in RB, due to stronger interactions that minimize granule breakdown between amylose-amylose and/or amylose-amylopectin chains (Figure 3.4b) within native granules. The set-back (SB) viscosity reflects interactions between leached amylose chains (resulting in amylose network formation) during the cooling cycle, and the presence of intact and/or fragmented granules embedded in the amylose net-work (Ambigaipalan *et al.,* 2011). The SB viscosities of RB (2930 cP) and LB (2755 cP) were not significantly different (Table 3.6), and they were much higher compared to those of the other starches. This could be attributed to a higher extent of AML (Figure 3.4b) in LB and to the presence of larger granules (intact and/or fragmented) embedded in the amylose network in RB. Among the starches, the lower SB viscosity of TB (Table 3.6) reflects extensive granule disruption during the heating cycle; this is reflected in the high extent of viscosity breakdown (3036 cP). Consequently, the resistance to the stirring action of the paddles during the cooling cycle would be minimal in TB as evidenced by the absence of granule fragments or to the presence of only very small granule fragments. As seen in Table 3.6, both VB and NB exhibited comparable SB viscosity values in spite of large differences in viscosity breakdown [NB (2909 cP) and VB (1175 cP)] during the holding cycle at 95°C. Theoretically, the SB viscosity of NB should have been much lower than that of VB due to higher extent of granule disintegration in the NB starch (Table 3.6). This suggests that the higher AML of NB (Figure 3.4b) may have reduced the influence of viscosity breakdown on SB viscosity. This seems plausible, since VB and NB did not differ significantly in granule size (Table 3.2).

3.1.14 Retrogradation characteristics

3.1.14.1 Turbidity

Turbidity effects have their origin in refractive index fluctuations over a distance scale comparable to the wavelength of observation (Craig *et al.,* 1989). In a polymer-solvent system, this is caused by density fluctuations over the same distance scale and is mostly due to aggregation between polymer chains. Craig *et al.* (1989) have shown that turbidity associated with a starch paste is influenced by the size and number of interactions between and among starch chains that reflect or scatter incident light, and the nature and number of swollen and fragmented granules that refract incident light. The first stage of retrogradation (completed during the first few hours of storage) has been shown to involve mainly interactions between amylose chains leading to the formation of junction zones (Ambigaipalan *et al.,* 2013). These junction zones, being larger compared to the wavelength of illumination, reduce light transmittance by scattering and/or reflecting the incident light (Craig *et al.,* 1989). Jacobson *et al.* (1997) have shown, by studies on starches from various botanical origins by monitoring changes in absorbance and the rapid initial rate of turbidity development in stored starch pastes is related to the loss of networked amylose, the development of amylose aggregates, and binding of granule remnants into assemblies by amylose and amylose aggregates.

In this study, the rate of retrogradation was monitored by changes in transmission. As shown in Figure 3.7, the percentage transmission (%T), measured after heating 2 % aqueous suspensions of pulse starches at 100°C for 60 min, followed by cooling to 25°C for 50 min (indicated as day 0 in Figure 3.7), followed the order TB>VB>NB>LB>RB.

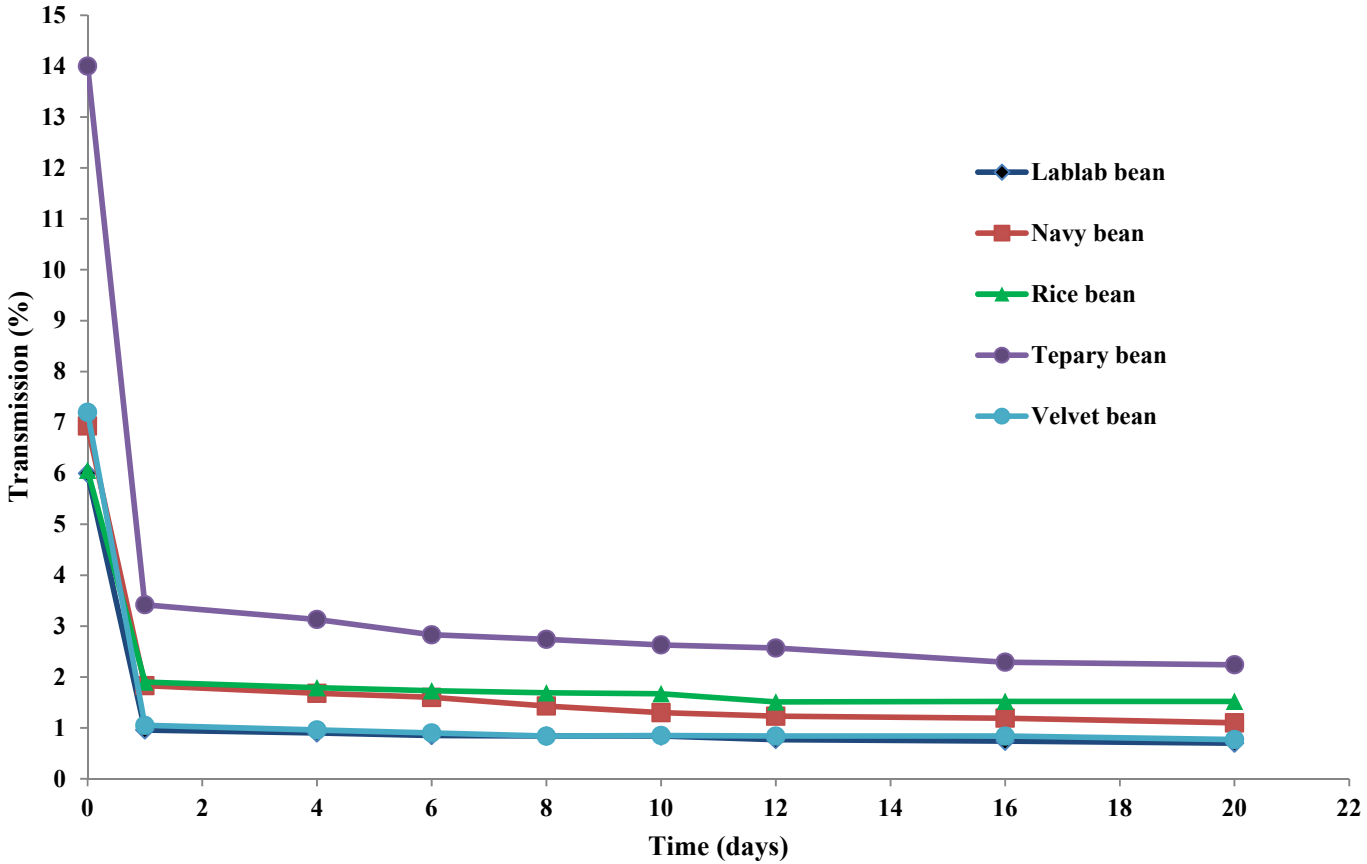

Figure 3.7: Turbidity profile of pulse starches stored at 4ºC for one day and then kept at 25ºC for 20 days.

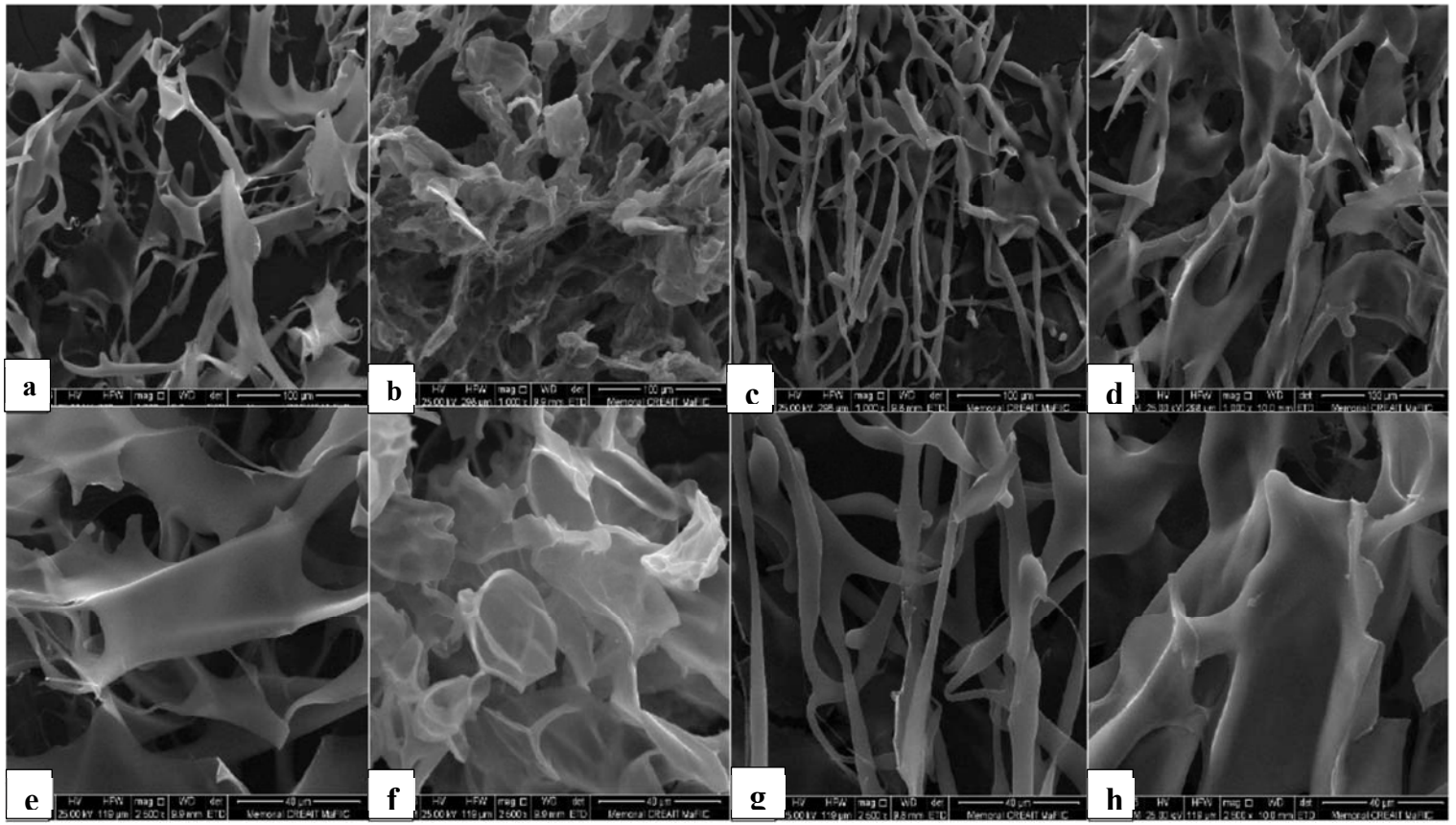

Figure 3.8: SEM images of freshly gelatinized and stored (24 h at 4°C) starch pastes at lower and higher magnifications: freshly gelatinized lablab bean starch *(a,e),* stored lablab bean starch *(b,f)*, freshly gelatinized tepary bean starch *(c,g)* and stored tepary bean starch *(d,h)*.

This suggests that at the end of the heating period (100°C for 60 min), swollen and fragmented granules were present in lesser amount in TB than in the other starches. SF (Figure 3.4a) and viscosity measurements (Table 3.6) showed the granules of TB to be more prone to disintegration than granules of VB, NB, LB and RB. This would explain the %T being more pronounced in TB. The rapid reduction in light transmittance during the first 24 h after gelatinization reflects network formation as a result of the extensive interaction between leached amylose chains (amylose-amylose) during the gelatinization process (Lewen *et al.,* 2003). The SEM micrographs (Figure 3.8) of LB and TB starches show the polymer network formation between leached amylose chains during retrogradation.

The extent of decrease in %T during storage the period (at 25°C) from day 2-20 (TB>RB~NB~VB~LB) reflects reduced the transmission of light due to interaction between and among leached amylose and amylopectin chains. These interactions would be stronger and occur more rapidly in TB, due to higher amount of leached amylose (Figure 3.4b) and to a lower viscosity of the reaction medium (due to reduced amounts of fragmented and swollen granules). This seems plausible, since studies have shown that the presence of large amounts of fragmented and swollen granules embedded in the network formed by leached amylose chains hinder amylose chain aggregation (Ambigaipalan *et al.,* 2013). This would then explain the extent of the decrease in %T of TB from day 1-20 (11.80 %) being higher than the % T in LB (5.30 %), NB (5.80 %), RB (4.57 %) and VB (6.43 %). The results indicate that differences in the rate at which pulse starches retrograde during the storage period is mainly influenced by the sequence of process that occured during gelatinization.

3.1.14.2 Differential scanning calorimetry of retrograded starches (DSC)

The DSC parameters of the starch gels stored at 4°C for 24 h and then at 25°C for 2-25 days are presented in Table 3.7. In all pulse starches, the retrogradation endotherm displayed a broader endothermic peak (increased Tc-To) after 2 days. Marginal differences were observed in gelatinization parameters among the pulse starches. In all pulse starches, the retrogradation enthalpy (ΔH_R) at the end of the storage period (25th day) was marginally increased. The gelatinization parameters of retrograded starches were much lower than those of their native counterparts (Table 3.5) due to the improper alignment of starch chains during retrogradation. The differences in Tc-To between the native and retrograded starches could be attributed to variation in the size, stability and extent of crystallite perfection (Ambigaipalan *et al.*, 2014). However, the DSC data indicate that the crystallites formed in LB, NB, RB, TB and VB starches were similar in size, perfection and crystallite stability. This seems plausible since the amylopectin chain length distribution of these starches was similar.

Table 3.7: Retrogradation transition parameters of pulse starches[1]

Starch source	Days of storage	Retrogradation transition parameters (°C)				Enthalpy[4] (J/g)[4]
		To[2]	Tp[2]	Tc[2]	Tc-To[3]	
Lablab bean	2	51.0±0.1^{a}	60.1±0.1^{a}	75.4±0.3^{a}	24.4±0.2^{a}	5.3±0.0^{a}
Navy bean		50.7±0.5^{ab}	60.0±0.4^{a}	73.2±0.9^{ab}	22.4±0.5^{ab}	4.0±0.1^{b}
Rice bean		49.2±0.5^{b}	59.2±0.7^{a}	70.0±1.4^{b}	20.8±0.9^{b}	4.3±0.2^{b}
Tepary bean		50.4±0.1^{ab}	59.7±0.2^{a}	70.3±0.9^{b}	19.8±0.9^{b}	4.2±0.0^{b}
Velvet bean		51.1±0.7^{a}	62.4±0.0^{b}	75.6±0.4^{a}	24.5±0.2^{a}	5.0±0.3^{a}
Lablab bean	10	52.7±0.4^{a}	62.0±0.1^{ab}	76.5±0.5^{a}	23.8±0.8^{a}	7.2±0.0^{a}
Navy bean		52.5±0.0^{a}	61.8±0.1^{ab}	75.9±0.2^{a}	23.2±0.2^{a}	6.5±0.2^{ab}
Rice bean		52.5±0.1^{a}	61.1±0.1^{a}	75.3±0.4^{a}	22.7±0.4^{a}	6.5±0.0^{ab}
Tepary bean		52.7±0.1^{a}	61.5±0.5^{ab}	76.2±0.4^{a}	23.5±0.3^{a}	6.5±0.2^{ab}
Velvet bean		52.9±0.0^{a}	62.2±0.2^{b}	76.2±0.4^{a}	23.3±0.4^{a}	6.2±0.5^{b}
Lablab bean	17	52.3±0.1^{a}	62.2±0.2^{a}	76.6±0.6^{a}	24.3±0.7^{a}	8.4±0.0^{a}
Navy bean		53.0±0.6^{a}	62.2±0.0^{a}	76.6±0.3a	23.6±0.3^{a}	7.1±0.4^{ab}
Rice bean		53.3±0.2^{a}	62.2±0.0^{a}	76.4±0.1^{a}	23.2±0.3^{a}	6.3±0.7^{b}
Tepary bean		53.4±0.2^{a}	62.6±0.0^{a}	76.2±0.1^{a}	22.8±0.1^{a}	6.6±0.1^{b}
Velvet bean		54.8±0.1^{b}	63.6±0.2^{b}	78.2±0.4^{b}	23.4±0.3^{a}	6.1±0.1^{b}
Lablab bean	25	52.8±0.6^{a}	62.4±0.1^{ab}	76.1±0.0^{a}	23.4±0.6^{a}	7.6±0.8^{a}
Navy bean		53.9±0.1^{a}	62.9±0.4^{ac}	76.1±0.4^{a}	22.2±0.3^{a}	6.6±0.4^{a}
Rice bean		52.9±0.1^{a}	62.1±0.1^{b}	76.0±0.3^{a}	23.2±0.4^{a}	7.6±0.0^{a}
Tepary bean		52.7±0.7^{a}	62.5±0.0^{ab}	75.9±0.5^{a}	23.3±0.2^{a}	7.0±0.1^{a}
Velvet bean		54.2±0.1^{a}	63.4±0.0^{c}	78.2±0.7^{b}	24.0±0.8^{a}	7.5±0.2^{a}

[1]All data represent the mean of triplicates. Values followed by different superscripts in each column for each starch source are significantly different ($P < 0.05$) by Tukey's HSD test.
[2] To, Tp, Tc represents the onset, peak and end temperature, respectively.
[3](Tc-To) represents the gelatinization temperature range.
[4]Enthalpy of retrogradation expressed in J/g of dry starch**.**

The work presented in chapter 3.1 (excluding sections 3.1.11 and 3.1.14) have been published in *Food Chemistry, 2014 (152):* 491-499. Co-authors (Q. Liu and E. Donner) contributed to the analysis of HPEAC-PAD, RVA and ATR-FTIR.

3.2 *In vitro* amylolysis of pulse and Hylon®VII starches explained in terms of their composition, morphology, granule architecture and interaction between hydrolysed starch chains

3.2.1 Chemical composition

The chemical composition of native LB, NB, RB, TB and VB starches was discussed in section 3.1.1. Therefore, in this study, only the compositional ranges are listed. The nitrogen content (N), surface lipid (SL), bound lipid (BL), apparent amylose content (AAC), starch damage (SD) and specific surface area (SSA) ranged from 0.02-0.13 % (with the order being RB>LB~NB~TB~VB), 0.03-0.12 % (with the order being TB>LB~VB~NB~RB), 0.40-0.85 % (with the order being RB~NB~TB>LB >VB), 22.1-32.1 % (with the order being LB>TB>NB~VB> RB), 0.00-0.01 % (with all starches being similar) and 0.23-0.39 m^2/g (with the order being LB~TB>VB>NB>RB), respectively. The N, SL, BL, AAC, SD and SSA of wrinkled pea (WP) starch were 0.06 %, 0.08 %, 0.85 %, 79.6 %, 1.21 % and 0.66 m^2/g, respectively. The corresponding values for Hylon®VII (HYVII) were 0.05 %, 0.08 %, 0.59 %, 67.4 %, 0.87 % and 0.77 m^2/g, respectively. Control refers to starches kept in the digestion medium for 24 h without enzyme. High amylose starches such as WP and HYVII were used in this study to better understand whether amylose content per se and/or the packing density of amylose chains within the granule interior (HYVII > WP) play a role in influencing the rate and extent of hydrolysis.

3.2.2 Hydrolysis kinetics

The hydolysis profiles of the pulse and HYVII starches by pancreatin and amyloglucosidase are presented in Figure 3.9. The time taken to reach an equivalent level of hydrolysis (50 %) varied significantly among the starches (WP, 3 h; RB and TB, 8 h; NB, 16 h; LB, 18 h). However, this level of hydrolysis was not reached by either VB or HYVII throughout the progress of hydrolysis. At the end of 30 h, the extents of hydrolysis for the starches were WP, 85.0 %; TB, 83.9 %; RB, 79.0 %; NB, 68.0 %; LB, 60.5 %; HYVII, 50.9 %; and VB, 45.9 %. The difference in the extent of hydrolysis between NB and LB starches (with NB>LB) reflects the interplay among differences in molecular order (with NB>LB), crystallinity (with NB>LB), DHC (with LB>NB), proportion of amorphous material (with NB>LB, see section 3.2.7, Table 3.10), and surface area (LB, 0.38 m^2/g; NB, 0.30 m^2/g). It is likely that differences in DHC (see section 3.2.7, Table 3.10) between NB (36.9 %) and LB (40.7 %) starches may have reduced the impact of differences in molecular order, crystallinity and surface area on hydrolysis. This seems plausible, since double helices are not only too wide to enter the catalytic site of amylolytic enzymes (André *et al*., 1999), but they also need to be disrupted and disentangled before the glycosidic linkages become accessible to enzymatic attack. The marginal difference in hydrolysis between RB and TB starches (Figure 3.9) was surprising, since the surface area of TB (0.39 m^2/g) was higher than that of RB (0.23 m^2/g) and its molecular order (see section 3.2.8, Table 3.11), crystallinity (see section 3.2.7, Table 3.10), and the extent of cracks on the granular surfaces were lower than that of RB (see section 3.2.3, Figure 3.11). Consequently, TB should have been hydrolysed to a greater extent than RB. This suggests that the large difference in DHC between TB (40.2 %) and RB (31.0 %) may have reduced the impact of molecular order, RC, and

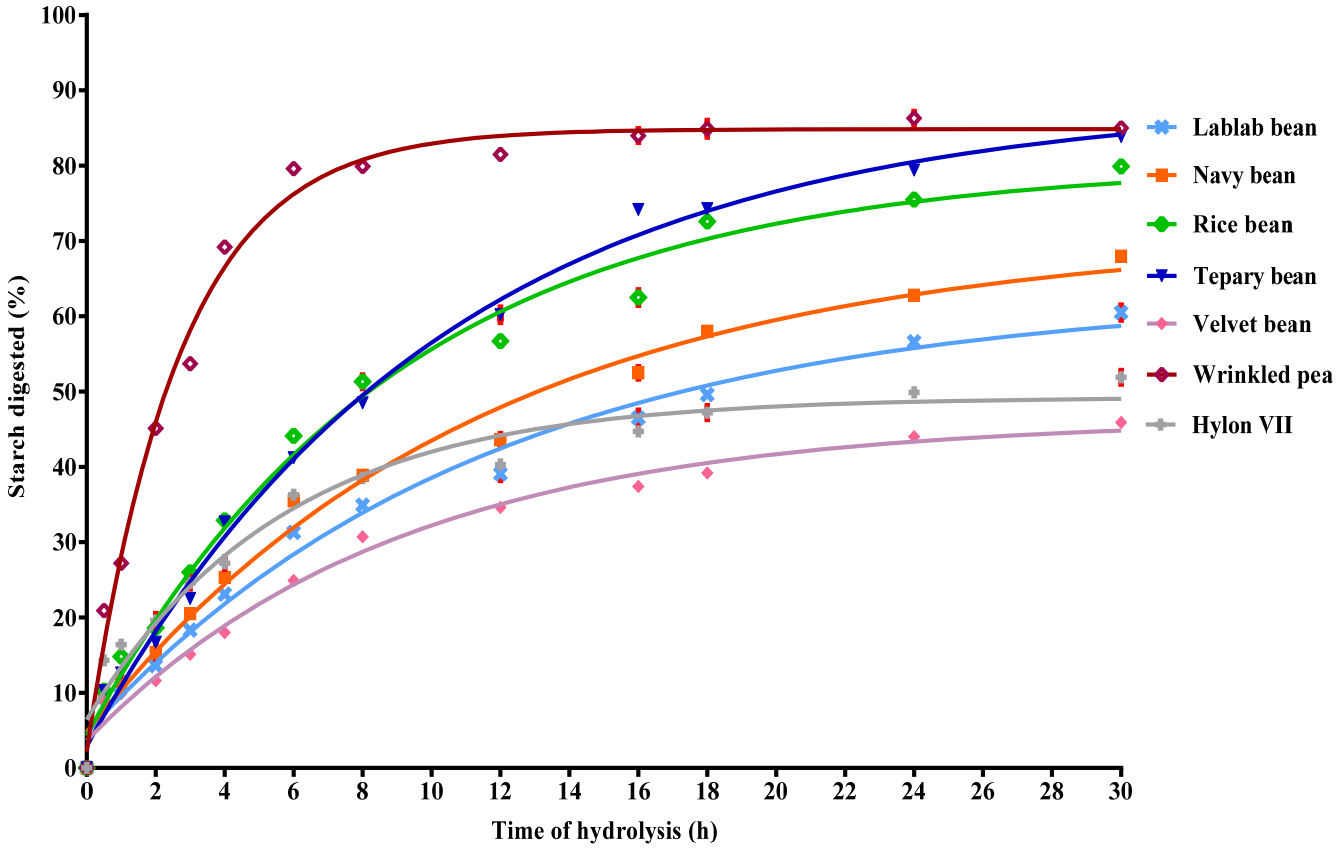

Figure 3.9: Hydrolysis kinetics (37°C) of pulse and Hylon®VII starches by porcine pancreatin and amyloglucosidase.

surface area differences on hydrolysis. The lower susceptibility of VB toward amylolysis could be attributed to its molecular order (see section 3.2.8, Table 3.11), RC and DHC (see section 3.2.6 and 3.2.7, Table 3.10) being higher than that of LB, NB, RB and TB. Between the two high amylose starches (WP and HYVII), the much higher resistance of HYVII toward hydrolysis (Figure 3.9) could be attributed to its molecular order (see section 3.2.8, Table 3.11), RC, DHC (see section 3.2.6 and 3.2.7, Table 3.10), the association between amylose chains (within the amorphous regions) being higher (see section 3.2.10, Figure 3.16) and the granule damage being lower than in WP. Furthermore, intermediate materials are present mainly in high amylose starches, with chain lengths longer than normal amylopectin and a molecular weight intermediate between amylose and amylopectin (Bertoft *et al*., 1993a; Vamadevan *et al*., 2014). It also is likely that structural differences between HYVII and WP in the branching density (with HYVII >WP) and glucan chain length (with HYVII >WP) of the intermediate material may also have contributed to the lower susceptibility of HYVII towards amylolysis. Thus, all of the above factors may have reduced the effect of surface area differences (HYVII >WP) between these two starches on the rate and extent of hydrolysis.

3.2.3 Morphology of control and hydrolysed starch granules

Scanning electron microscopy, which provides topographical data on exposed surfaces of starch granules, showed that control starch granules of LB (Figure 3.10a), NB (Figure 3.10b), RB (Figure 3.10c), TB (Figure 3.10d) and VB (Figure 3.10e) ranged from oval to round to irregular in shape. WP (Figure 3.10f) exhibited simple (small and large) and compound granules (composed of two or more fused sub granules).

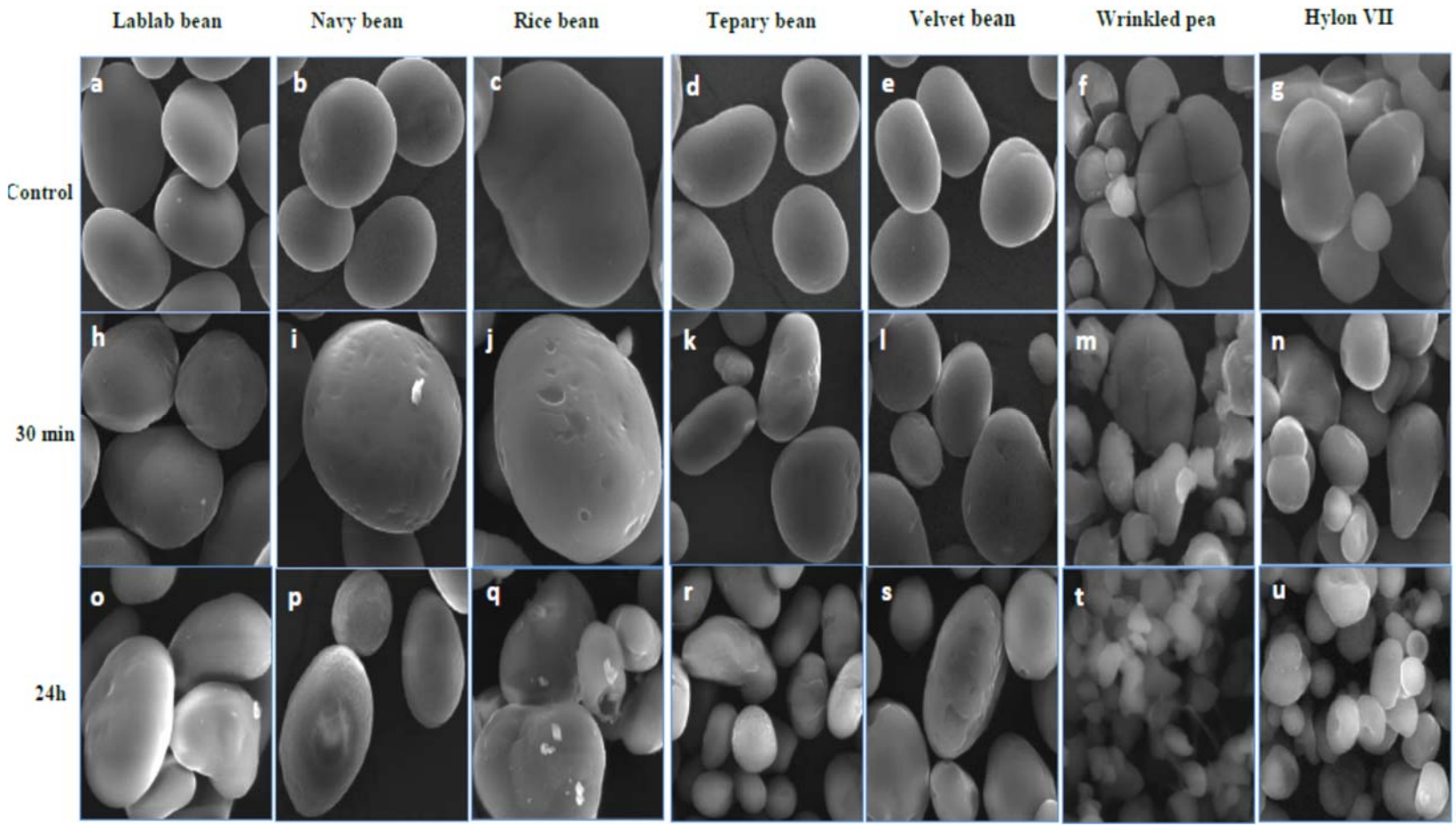

Figure 3.10: Scanning electron micrographs of control *(a-g)* and hydrolysed (30 min *[h-n]*, 24 h *[o-u]*) starches.

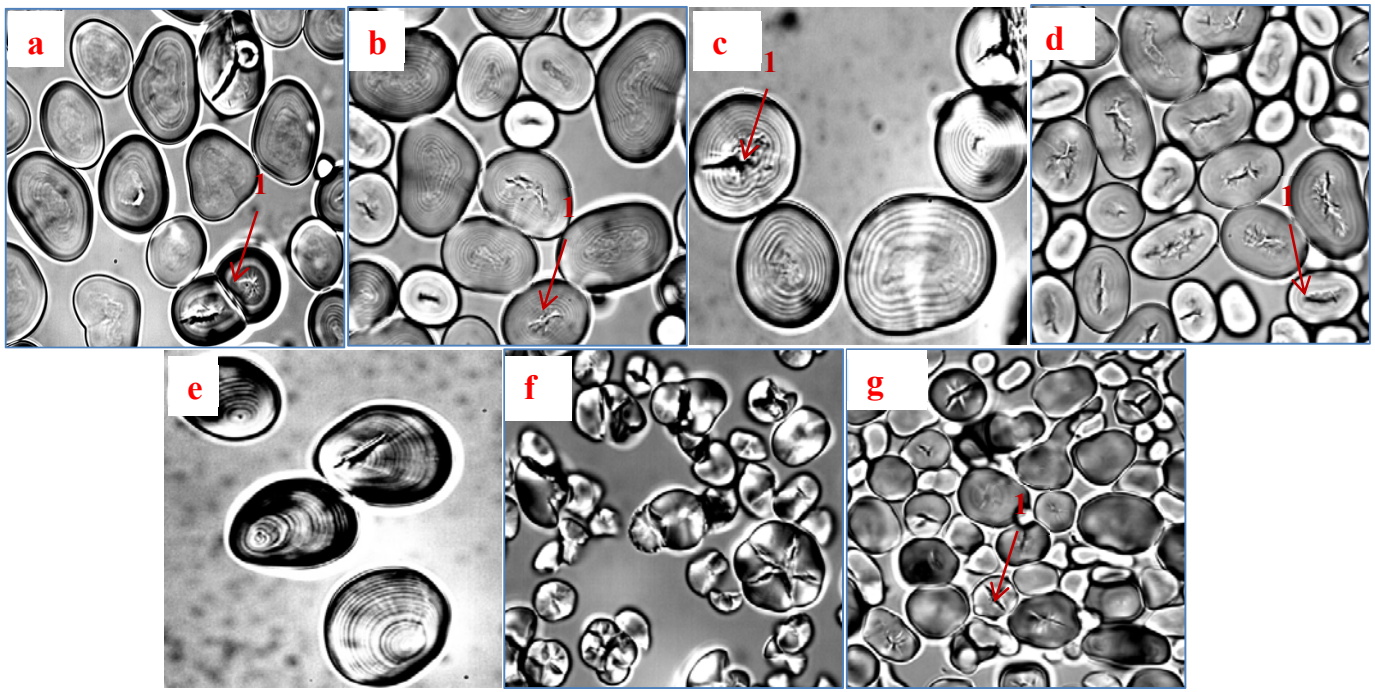

Figure 3.11: Bright field microscopy images of lablab bean *(a)*, navy bean *(b)*, rice bean *(c)*, tepary bean *(d)* velvet bean *(e)*, wrinkled pea *(f)* and HylonHylon®VII *(g)* starches. Arrow 1 indicates cracks on the granule surface.

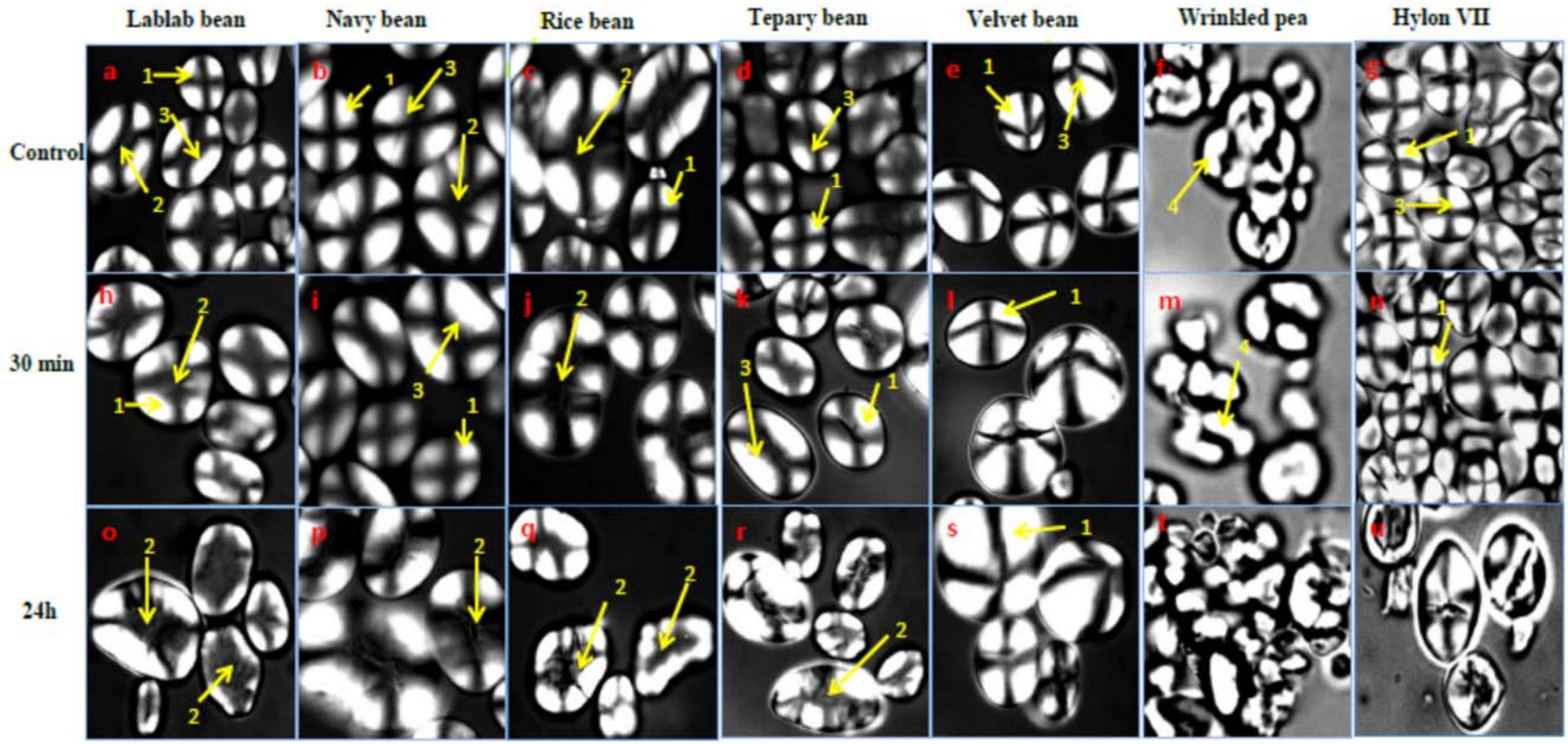

Figure 3.12: Polarized microscopy images of control *(a-g)* and hydrolysed (30 min *[h-n]*, 24 h *[o-u]*) starches. Arrows 1, 2 & 3 indicate quadrants, voids and shape of the quadrants, respectively. Arrow 4 (in panel *f* and *m*) represents the distorted quadrants of wrinkled pea.

Some compound granules of WP were separated (Figure 3.10f). LB (Figure 3.10a), NB (Figure 3.10b), RB (Figure 3.10c) and TB (Figure 3.10d) exhibited indentations, whereas no indentations were present on VB (Figure 3.10e) and HYVII (Figure 3.10g) [Appendix VIII shows a larger number of granules]. The morphology of the residues obtained after 30 min and 24 h of enzyme-catalysed hydrolysis are presented in Figure 3.10(h–n) and Figure 3.10(o–u), respectively. After 30 min of hydrolysis, the surfaces of LB, NB, RB, TB and VB (Figure 3.10h-l) were eroded with disc like depressions. The extent of these changes varied from granule to granule (within and among the starch sources). WP (Figure 3.10m) and HYVII (Figure 3.10n) exhibited only mild surface erosion. WP differed from all other starches in exhibiting extensive granule fragmentation (Figure 3.10m). At the end of hydrolysis (24 h), an increase in surface erosion was evident for all starches (Figure 3.10o-u). Fragmented granules at different stages of fragmentation were seen only with RB (Figure 3.10q), TB (Figure 3.10r) and WP (Figure 3.10t), the extent of fragmentation being more pronounced in WP (Figure 3.10t).

Bright field microscopy (Figure 3.11) of the control starches showed the presence of cracks on the surfaces of some granules of LB (Figure 3.11a), NB (Figure 3.11b), RB (Figure 3.11c) and HYVII (Figure 3.11d). The extent of cracking was more pronounced in RB than in LB. Particle size analysis (Table 3.2) showed that granule size ranged from 4.6-33.8 μm (LB), 10.1-46.9 μm (NB), 19.0-59.8 μm (RB), 6.2-32.5 μm (TB), 7.8-42.6 μm (VB), 2.5-15.3 μm (WP), and 2.1-10.4 μm (HYVII).

The birefringence patterns of the control starches are presented in Figure 3.12. Birefringence patterns under polarized light reflect that the average orientation of polymer chains is radial. The intensity of the pattern is influenced by granule shape

and on the orientation of the granules with respect to the light beam. The quadrants (Figure 3.12, arrow 1) that form the maltese cross were more closely packed in VB (Figure 3.12e) and HYVII (Figure 3.12g) (with VB>HYVII) than in LB (Figure 3.12a), NB (Figure 3.12b), RB (Figure 3.12c) and TB (Figure 3.12d). Large voids (arrow 2) were present between the quadrants in LB, NB, RB and TB. This suggests that polymer chains of VB and HYVII are better radially oriented than those of NB, TB, LB and RB. The shapes of the quadrants varied among and within each starch source (arrow 3). The birefringence pattern and intensity of WP (Figure 3.12f) were different from those of the other starches, and the quadrants appeared distorted (arrow 4). This distortion may not necessarily reflect disrupted crystallites and/or improperly oriented amylose and amylopectin chains. As shown in Figure 3.10f, the size, shape and arrangement of WP granules (clusters containing overlapped granules) were different from those of the other starches. In addition, many compound granules of WP were separated. Consequently, the interactions of polarized light with WP granules may have caused the distorted birefringence pattern (Figure 3.12f).

Birefringence patterns of residues obtained after 30 min and 24 h of hydrolysis are presented in Figure 3.12(h-n) and Figure 3.12(o-u), respectively. During the progress of hydrolysis, birefringence decreased in all starches, as reflected by disorganized quadrants (Figure 3.12 arrow 1) and appearance of voids (Figure 3.12, arrow 2) in the hilum region. The extent of the above changes at 24 h hydrolysis (Figure 3.12 (o-u) was less pronounced in VB (Figure 3.12s) than in the other starches. This suggests greater resistance of VB granules towards amylolysis (Figure 3.9).

3.2.4 HPAEC- PAD of control and hydrolysed starches

The chain length distribution of isoamylase-debranched amylopectin of control pulse and HYVII starches and their enzyme digested (24 h) residues are presented in Table 3.8. The debranched chains were categorized into four groups of different degrees of polymerization (dp): 6-12, 13-24, 25-36 and >37. Among control starches, the proportion of amylopectin chain lengths with the dp in the range 6-12, 13-24, 25-36, and >37 followed the order of RB~TB>NB~HYVII~LB~VB>WP, LB~RB>VB>NB~TB>HYVII>WP, WP>TB~RB~VB~HYVII>NB>LB, and WP~HYVII>NB~TB~RB>LB, respectively. The average chain length ($\overline{CL}$) followed the order of WP~HYVII>VB~LB~NB~TB>RB (Table 3.8).

There was no significant difference in the proportion of dp 6-12 between control and digested starches of LB, NB, RB, TB and VB (Table 3.8). Hydrolysis decreased the proportion of amylopectin chains with dp in the range 6-12 and 13-24, and increased the proportion of long amylopectin chains with dp 25-36 and dp >37 in WP and HYVII starches (with WP>HYVII). However, in RB and TB, significant differences were observed only with respect to dp 13-24 and dp 13-24 and dp >37, respectively. A similar observation was reported by Zhang *et al*. (2006b) for maize starches. The dp of all other starches in the above ranges showed no significant differences. This suggests that crystallites of WP, HYVII, and TB are not well organized within the crystalline lamella. The appearance of a plateau (Figure 3.9) at different time periods of hydrolysis in WP (6 h) and HYVII (12 h) can be attributed to amylose chains within the amorphous domains of HYVII being more densely packed than in WP (AML data, Figure 3.16). This may have restricted the diffusion of the enzymes toward the disorganized crystallites within the crystalline lamella of HYVII.

Table 3.8: Amylopectin chain length distribution of control and hydrolysed pulse and Hylon®VII starches as determined by high performance anion exchange chromatography with pulsed amperometric detection[1]

Starch source	Hydrolysis time	Degree of polymerization[2] (dp) %				
		6-12	13-24	25-36	>37	$\overline{CL}$ [3]
Lablab bean	control[4]	18.9±0.8[a]	58.0±0.0[a]	14.8±0.5[a]	7.9±0.5[a]	16.5±0.3[a]
	24 h	18.8±1.4 [a]	55.5±1.4[a]	16.3±0.9[a]	9.9±0.6[a]	16.6±0.5[a]
Navy bean	control[4]	19.2±1.2[a]	52.9±1.5[a]	16.1±0.3[a]	11.4±2.2[a]	16.7±0.4[a]
	24 h	18.1±0.7[a]	53.1±0.5[a]	17.6±1.1[a]	10.8±0.6[a]	17.1±0.4[a]
Rice bean	control[4]	22.7±0.7[a]	57.4±0.8[a]	17.6±0.2[a]	8.6±0.7[a]	15.2±0.1[a]
	24 h	21.6±0.8[a]	53.1±0.4[b]	16.7±1.0[a]	8.0±0.4[a]	16.2±0.2[b]
Tepary bean	control[4]	21.1±1.0[a]	51.5±0.2[a]	17.9±1.0[a]	9.2±0.1[a]	16.6±0.3[a]
	24 h	20.7±0.6[a]	50.6±0.2[b]	18.5±0.4[a]	10.0±0.1[b]	16.8±0.2[a]
Velvet bean	control[4]	17.7±0.3[a]	54.1±0.5[a]	17.5±0.1[a]	10.3±0.2[a]	17.0±0.1[a]
	24 h	16.8±0.9[a]	53.7±0.2[a]	18.1±0.2[a]	10.8±1.1[a]	17.3±0.3[a]
Wrinkled pea	control[4]	15.6±0.3[a]	46.9±0.9[a]	23.1±0.2[a]	14.0±0.8[a]	18.1±0.1[a]
	24 h	5.2±0.3[b]	37.1±0.5[b]	35.4±1.4[b]	21.9±0.6[b]	23.0±0.3[b]
Hylon®VII	control[4]	19.0±1.0[a]	50.5±0.3[a]	17.1±0.3[a]	13.3±0.6[a]	18.3±0.3[a]
	24 h	10.2±0.4[b]	46.6±1.9[a]	24.6±1.3[b]	18.3±0.1[b]	20.4±0.0[b]

[1]Values followed by different superscripts in each column for each starch source are significantly different ($P < 0.05$) by independent two sample t-test. [2]dp_n: indicates degree of polymerization. Total relative area was used to calculate the percent distribution. [3]Average chain length ($\overline{CL}$) calculated by Σ ($dp_n \times$ peak area)/Σ (peak $area_n$). [4]Control refers to starches kept in the digestion medium for 24 h without enzyme.

3.2.5 Apparent amylose content (AAC) of hydrolysed starches

The AAC of all starches decreased on hydrolysis (Table 3.9). This could be attributed to depolymerisation of amylose chains (factor 1), and the formation of double helices by hydrolysed amylose chains (factor 2). Since AAC was determined by iodine binding, factor 1 may have rendered the degree of polymerization (dp) of hydrolysed amylose chains less than optimal for complexing iodine. However, factor 2 may have restricted the ability of iodine to enter the hydrophobic core of amylose. The extent of decrease in AAC was not significant ($p > 0.05$) in LB, TB and VB starches during the first 2 h. However, during this time period, AAC decreased by 4.2%, 3.9%, 10.5% and 28.4% in NB, RB, Hylon VII and WP. At the end of 24 h, the extent of decrease in AAC followed the order: WP (47.5 %) > Hylon VII (17.9 %) > LB (11.8 %) > NB (8.9 %), VB (8.6 %) > RB (7.1 %) and TB (6.4 %). The variation in AAC decrease among starches could reflect the interplay among the following: (1) rate and extent of depolymerisation of amylose chains, (2) the amount and length of double helices formed between hydrolysed amylose chains and (3) state of aggregation of the formed double helices.

3.2.6 Wide angle X-ray diffraction (WAXS) pattern and relative crystallinities (RC) of control and hydrolysed starches

The WAXS patterns and RC of control and hydrolysed starches are presented in Figure 3.13 and Table 3.10, respectively. NB, RB, TB, and VB exhibited a pure A-type diffraction pattern characterized by strong intensity peaks at 15°, 17°, 18°, 23° 2θ, respectively (Figure 3.13). LB exhibited an A+B pattern; the peak at 5.5° 2θ (arrow 1) is characteristic of B-type crystals.

Table 3.9: Apparent amylose content of control and hydrolysed pulse and Hylon®VII starches

Starch source	Hydrolysis time	Apparent amylose content (%)[1]
Lablab bean	Control	34.8±0.8[a]
	30 min	31.8±1.2[a]
	2 h	33.1±1.0[a]
	24 h	23.0±1.2[b]
Navy bean	Control	28.1±0.6[a]
	30 min	23.9±0.4[b]
	2 h	27.7±0.4[a]
	24 h	19.2±0.8[c]
Rice bean	Control	24.5±0.4[a]
	30 min	20.6±0.8[b]
	2 h	22.6±0.3[ab]
	24 h	17.4±1.2[c]
Tepary bean	Control	34.0±0.2[a]
	30 min	32.7±1.1[a]
	2 h	31.4±1.0[ab]
	24 h	27.6±1.5[b]
Velvet bean	Control	32.6±1.5[a]
	30 min	29.9±0.6[ab]
	2 h	27.0±0.2[bc]
	24 h	24.0±1.0[c]
Wrinkled pea	Control	79.6±0.2[a]
	30 min	51.2±1.2[b]
	2 h	60.4±0.4[c]
	24 h	32.1±0.7[d]
Hylon®VII	Control	67.4±0.8[a]
	30 min	56.9±1.0[b]
	2 h	60.5±0.3[c]
	24 h	49.5±0.8[d]

Values followed by different superscripts in each column for each starch source are significantly different ($P < 0.05$) by Tukey's HSD test.

[1]Determined by iodine binding and reflects the content of true amylose chains + intermediate chains + longer glucan chains of amylopectin.

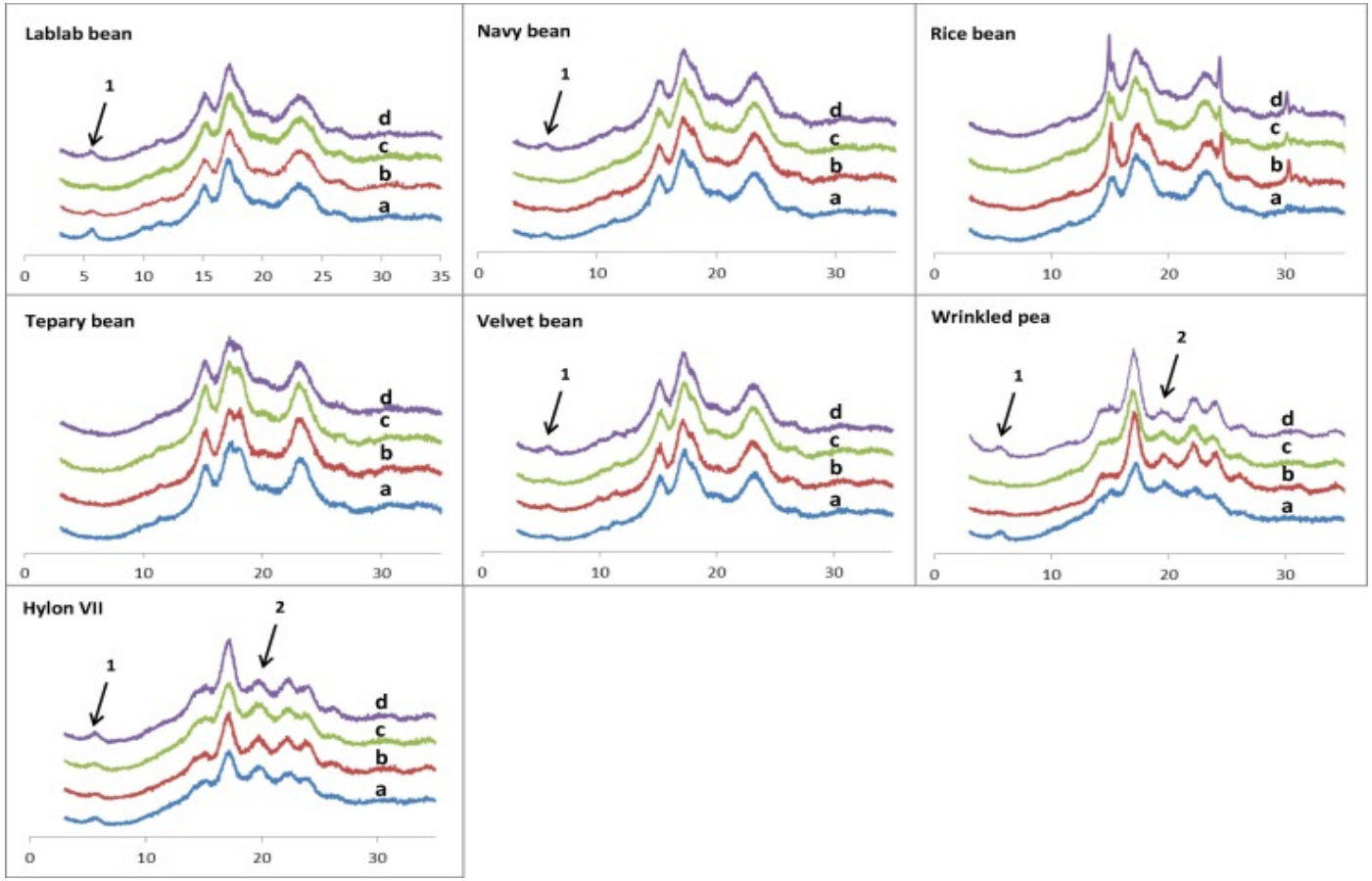

Figure 3.13: X-ray diffraction patterns of control *(a)* and ezyme hydrolysed (30 min *(b)*, 2 h (c) and 24 h *(d)*) pulse and HylonHylon®VII starches. Arrow 1 and 2 shows the characteristic peak (2θ~5.5°) of B-type crystallites and V-type peak (2θ~20°), respectively.

Table 3.10: Relative proportions of double helical and amorphous contents and relative crystallinity of control and hydrolysed pulse and Hylon®VII starches

Starch source	Hydrolysis time	WAXS	^{13}C CP/MAS NMR	
		Crystallinity (%)[1]	Double helix (%)[2]	Amorphous (%)[3]
Lablab bean	Control[4]	25.4	40.7	59.3
	30 min	26.5	39.4	60.6
	2 h	31.2	42.3	57.7
	24 h	45.0	28.9	71.1
Navy bean	Control[4]	25.6	36.9	63.1
	30 min	26.5	37.8	62.2
	2 h	30.0	50.9	49.1
	24 h	45.9	35.4	64.6
Rice bean	Control[4]	27.3	31.0	69.0
	30 min	28.6	39.3	60.7
	2 h	32.5	52.7	47.3
	24 h	28.3	40.5	59.5
Tepary bean	Control[4]	26.4	40.2	59.8
	30 min	27.9	44.8	55.2
	2 h	42.9	49.0	51.0
	24 h	38.3	24.0	76.0
Velvet bean	Control[4]	30.2	42.0	58.0
	30 min	38.7	41.6	58.4
	2 h	47.0	54.8	45.2
	24 h	45.3	40.7	59.3
Wrinkled pea	Control[4]	15.1	14.3	85.7
	30 min	25.3	67.6	32.4
	2 h	38.7	45.4	54.6
	24 h	50.4	70.3	29.7
Hylon®VII	Control[4]	19.2	18.2	81.8
	30 min	20.1	38.1	61.9
	2 h	22.6	29.4	70.6
	24 h	34.5	37.7	62.3

[1]Reflects double helices arranged in a crystalline array.
[2]Reflects double helices arranged in both crystalline and non-crystalline arrays.
[3]Regions devoid of organized structures.
[4]Control refers to starches kept in the digestion medium for 24h without enzyme. Control starches differed marginally from their native counterparts with respect to molecular order, relative crystallinity, double helical content and gelatinization parameters. There was no significant difference ($P < 0.05$) in the above parameters among control starches at 30 min, 2 h and 24 h.
The maximum standard deviation for NMR measurements and crystallinity calculations were ±1.2 % and ±1.4 %, respectively.

Both WP and HYVII exhibited a B+V type pattern; the V-type peak (arrow 2) centered at 20° 2θ is characteristic of single helices packed in a crystalline array and/or amylose-lipid complexes. The intensity of the V-type peak was higher in HYVII (Figure 3.13). This was rather surprising, since the amount of bound lipid (complexed with amylose) in WP (0.85 %) was higher than that in HYVII (0.59 %). This suggests that in WP, the V-amylose lipid complex helical chain segments have poorly developed long range order. The absence of the V-type peak in the other pulse starches (Figure 3.13) may be a reflection of their lower bound lipid content (0.40-0.52 %) and/or to single helices being arranged in a non-crystalline array. It is likely, that the 20° 2θ peak in WP and HYVII mainly reflects lipid-amylose complexes, since this peak disappeared when HYVII was defatted with n-propanol/water 3:1(Appendix VII). The RC of control starches (Table 3.10) ranged from 15.1-30.2 % (with the order being VB>RB>TB>NB>LB>HYVII>WP). RC differences among the starches could reflect the interplay of differences in 1) amylopectin content (with RB (75.5 %)>NB (71.9 %)~VB (67.4 %)>TB (66.0 %)> LB (65.2 %)> HYVII (32.6 %)> WP (20.4 %)), crystallite size, orientation of crystallites to the X-ray beam, and the ratio of splayed double helices (that are not in parallel alignment but within the crystalline register) to organized double helices within the crystalline register.

The intensity of the peak centered at 5.5° 2θ (which represents B-type crystals) decreased progressively in LB, NB, WP and HYVII during the first 2 h but then increased by 24 h. The above peak was prominent in VB at 24 h (Figure 3.13). The V-type peak in WP and HYVII, centred at 20° 2θ, progressively increased in intensity during the first 2 h but then decreased by 24 h. The intensity reduction of the above peak is indicative that B-type crystals of LB, NB, WP and HYVII are susceptible to

amylolysis. The reappearance of this peak at 24 h can be attributed to retrogradation resulting from interactions between hydrolysed amylose chains (Zobel, 1988b). The increase in the V-type peak in WP and HYVII during the first 2 h suggests that free lipid present in the control starches may have complexed with hydrolysed amylose chains to form ordered crystalline V-amylose-lipid complexes. The slight decrease in intensity of this peak at 24 h is indicative of a change in alignment of the V-helix to the X-ray beam and/or to hydrolysis of the amylose-lipid complex. It must be emphasized, that although amylose-lipid complexes hinder interaction between amylose chains and the active site of an enzyme, it does not confer complete resistance to hydrolysis, and they are fully degraded after prolonged hydrolysis (Seneviratne & Biliaderis, 1991). In both WP and HYVII starches, the peaks centred at 22-23° 2θ became well resolved after 24 h. The RC of hydrolysed starches at 2 h was higher than that of control starches by 23.6, 16.8, 16.5, 5.8, 5.2, 4.4, and 3.4 % in WP, VB, TB, LB, RB, NB, and HYVII starches, respectively. This suggests that double helices arranged in a crystalline array within crystalline domains of control starches were not disrupted during this time period. Therefore, the increase in RC on hydrolysis reflects degradation of amorphous regions and formation of double helical structures (resulting from aggregation of hydrolysed amylose chains) arranged into crystalline arrays. The decrease in RC, which reflects a disruption of ordered double helices, that is exhibited by both RB and TB (Table 3.10) beyond 2 h of hydrolysis may have been due to entry of amylolytic enzymes into crystalline regions via cracks on the granule surfaces of these starches (Figure 3.11).

3.2.7 ^{13}C CP/MAS NMR of control and hydrolysed starches

^{13}C CP/MAS NMR measures the structural organization of starch at a shorter distance scale than X-ray diffraction and it gives characteristic spectra for ordered helices and non-ordered chains (Gidley & Bociek, 1988). The multiplicity of the C-1 position of the glucose unit gives information on starch crystallinity and double helical symmetry (Primo-Martin *et al*., 2007). A-type crystals exhibit three peaks at 100, 101 and 102 ppm, whereas in a B-type crystal, the C-1 resonance exhibits two peaks at 100 and 101 ppm (Primo-Martin, *et al.,* 2007). Amylose-lipid complexes (V-amylose helices) have been shown to exhibit a broad resonance at 31 ppm (corresponding to the mid-chain methylene carbon of monoacyl lipids) and a C1 signal (103-104 ppm) attributed to V-conformation (Morrison *et al*., 1993a; Morrison *et al*., 1993c). The intensity of the C4 resonance, which occurs at ~84 ppm, has been attributed solely to the amorphous contributions of the particular starch (Tan *et al.,* 2007). Peaks in the region 68-77 ppm represent chemical shifts for C2, C3 and C5; those in the region 59-62 ppm are representative of C6 (Gidley & Bociek, 1985). The ^{13}C CP/MAS NMR of control and enzyme-hydrolysed starches are shown in Figure 3.14.

The double helical and amorphous contents obtained from the spectra are shown in Table 3.10. It was difficult to ascertain the type of crystalline polymorph from the nature of C1 splitting (doublet or triplet) in control, LB, RB, NB, TB and VB starches (Figure 3.14). However, both control WP and HYVII exhibited doublets at 100 and 101 ppm at C1, and peaks characteristic of V-amylose-lipid complexes at 103 and 32 ppm (Figure 3.14). Peaks at 103 and 32 ppm were not present in the other starches.

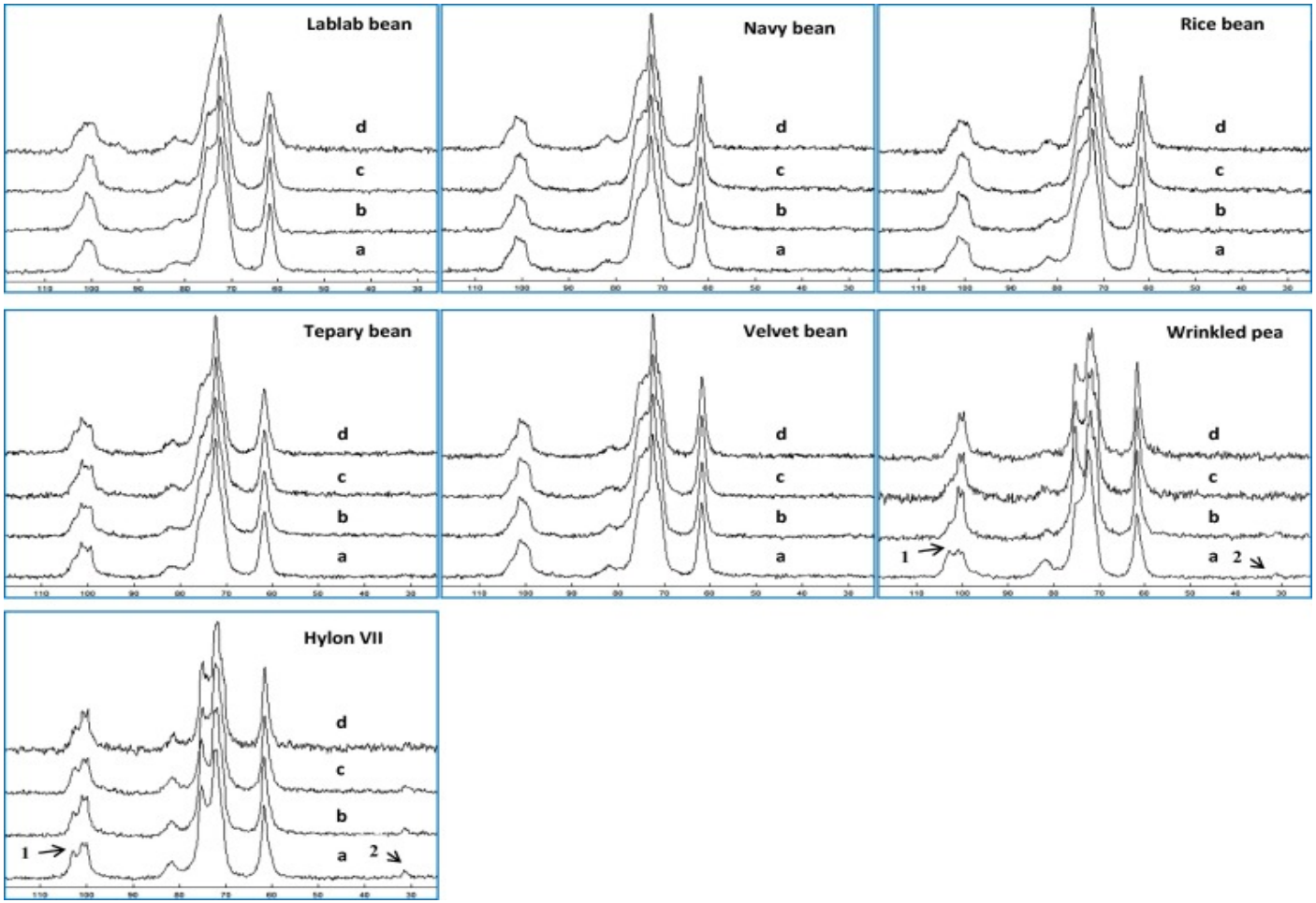

Figure 3.14 ^{13}C CP/MAS NMR spectra of control *(a)* and hydrolysed (30 min *(b)*; 2 h *(c)*; and 24 h *(d)*) pulse and Hylon®VII starches. Arrows 1 and 2 indicate the V-amylose–lipid complex at 103 and 32 ppm, respectively. 161

The resonance at C4, which reflects amorphous contributions, was of a lower order of intensity in LB, RB, NB, TB and VB (Figure 3.14), but was higher in intensity in WP and HYVII (with WP>HYVII) (Figure 3.14). This was not surprising, since the apparent amylose content (Table 3.9) of WP (79.6 %) and HYVII (67.4 %) were higher that of the other starches (24.5-34.8 %). It was interesting to observe that although the bound lipid content of HYVII (0.60 %) was lower than that of WP (0.89 %), the peak intensity at 32 ppm was much stronger in the former (Figure 3.14, arrow 2). These data also suggest that the level of organization and/or state of aggregation of V-amylose-lipid helices is higher in HYVII. The DHC of control starches (Table 3.10), which reflects double helices organized in both crystalline and non-crystalline arrays, followed the order VB~TB~LB>NB>RB>HYVII>WP. The low DHC of WP (14.3 %) and that of HYVII (18.2 %) may reflect their low amylopectin contents (WP, 20.4 %; HYVII, 32.6 %) and/or to disrupted double helices resulting from co-crystallization of amylose with amylopectin A-chains (Yuryev *et al*., 2004).

In WP, the C1 peak after 2 h hydrolysis differed significantly from that of the control with respect to higher intensity (represented by peak height), disappearance of the signal at 103 ppm and narrower peak width. The C1 signal of HYVII after 2 h was similar to that of the control (Figure 3.14). Furthermore, the peak at 32 ppm for WP disappeared completely after 2 h hydrolysis (Figure 3.14), whereas for HYVII, the peak was prominent even after 24 h hydrolysis. In all other starches, the intensity, shape and splitting pattern of the C1 signal did not change significantly throughout the time course of hydrolysis. The above data suggest that in spite of the bound lipid content being higher in WP, the amylose–lipid complex of WP is less stable, due to a lower degree of organization and perfection of ordered domains of aggregated chains [Seneviratne, *et*

al., 1991], and hence more susceptible to hydrolysis by amylolytic enzymes. The disappearance of the V-conformation (103 ppm) after 2 h hydrolysis for WP (Figure 3.14) may have decreased segmental mobility, resulting in a more efficient cross polarization between ^{1}H and ^{13}C (reflected in increased peak height and decreased peak width).

During the first 30 min of hydrolysis, there was no significant change in DHC for LB and VB (Table 3.10). However, DHC increased in all other starches (in the order of WP>RB>HYVII>NB). This increase reflects double helices formed mainly between hydrolysed amylose chains. The data indicate that variations in the extent of change in DHC among the starches are influenced by the interplay between the amount and length of amylose chains participating in double helical formation, and by the rate of amylose chain crystallization and aggregation. The larger DHC (Table 3.10) increase for WP during the above time period is a reflection of more extensive amylose chain hydrolysis, a higher rate of crystallization and aggregation of hydrolysed amylose chains. It is likely that many of the double helices formed in WP and HYVII during the first 30 min may have been arranged in a non-crystalline array, since the extent of increase in DHC did not parallel a similar type of increase in RC (Table 3.10). At the end of 2 h, DHC decreased in WP and HYVII (with WP>HYVII), but increased in all other starches (with VB~RB>NB>TB>LB). In WP and HYVII starches, the increase in amorphous content, RC and apparent amylose content (Table 3.9) at 2 h and the concomitant decrease in DHC (Table 3.10) suggest that double helices formed during the first 30 min may not have had the required stability to resist amylolysis. This suggests that the degree of polymerization (dp) of the hydrolysed chains may have been below the optimum (dp10) for formation of stable helices. In the other starches, the

increase in DHC at 2 h, when considered along with the concomitant decrease in amorphous content, increase in RC and marginal changes in apparent amylose content (Tables 3.9 and 3.10), is indicative that hydrolysed amylose chains involved in double helical formation had the optimum dp, and hence were able to resist amylolysis. As shown in Table 3.10, the increase in DHC at the end of 24 h was more pronounced in WP and HYVII (with WP>HYVII) than in the other starches. This is indicative that the long intermediate chains responsible for the high apparent amylose content of the above starches (Vamadevan *et al*., 2014) may have been partially hydrolysed, resulting in chain lengths capable of forming double helices resistant to amylolysis. This seems plausible, since the decrease in apparent amylose content in WP and HYVII at the end of 24 h (with WP>HYVII) was more pronounced than in the other starches (Table 3.9). In LB and NB, the decrease in DHC at 24 h, when considered along with the concomitant increase in RC (Table 3.10), is indicative that only double helices present in non-crystalline arrays may have been hydrolysed. In RB, TB, and VB, the decrease in DHC at 24 h, when considered along with the concomitant decrease in RC (Table 3.10), is indicative of hydrolysis of double helices present in both non-crystalline and crystalline arrays.

3.2.8 ATR-FTIR of control and hydrolysed starches

The ATR-FTIR spectrum of starch is sensitive to the so-called short range order, defined as the double helical order, as opposed to long range order related to the packing of double helices. The IR spectum has been shown to be representative of the external part of the starch granule (Sevenou *et al*., 2002). In the IR spectrum, the absorbance bands at 1022 cm^{-1} and 1047 cm^{-1} are characteristic of amorphous and ordered structures, respectively (van Soest *et al*., 1995). Thus, molecular order at or

near the granule surface (expressed as the ratio of 1047/1022 cm^{-1}) reflects the amount of ordered domains (amylopectin double helices and single helices) to amorphous domains (linear chains). The molecular order at the granule surface of control and hydrolysed starches is presented in Table 3.11. The FTIR 1047/1022 cm^{-1} ratio (Table 3.11) followed the order of VB>RB~NB~TB>LB~HYVII>WP. The low degree of molecular order seen with HYVII (0.877) and WP (0.778) may be due to their low amylopectin contents (WP, 20.4 %; HYVII, 32.6 %) and/or to the presence of amylose defects located in the crystalline region of the lamellae which may have hindered double helical alignment. The difference in molecular order among the other starches reflects the interplay between differences in amylopectin content (being in order of RB>NB>VB>TB>LB), and/or to differences in double helical alignment.

As shown in Table 3.11 (FTIR data), after 30 min hydrolysis, molecular order increased in WP and HYVII (with HYVII>WP), but decreased in the other starches (with the order being TB~VB>LB~NB>RB). Since FTIR data reflect short range order at the level of individual double and single helices, the decrease in DHC reflects disorganization of helices present at or near the granule surface. The increase in molecular order seen with WP and HYVII reflects the formation of double helices resulting from interaction between hydrolysed amylose chains. Beyond 30 min, molecular order continued to decrease in TB, VB, LB, NB and RB. However, in WP and HYVII, changes in molecular order beyond 30 min (for WP) and 2 h (for HYVII) were not measurable, since the peak at 1022 cm^{-1} characteristic of amorphous starch was not well defined (Figure 3.15). In the other starches, the peak at 1022 cm^{-1} was reduced in intensity, but well defined, at 24 h.

Table 3.11: Molecular order at the granule surface of control and hydrolysed pulse and Hylon®VII starches

Starch source	Hydrolysis time	ATR-FTIR ratio 1048/1022 cm^{-1} [1]
Lablab bean	Control[2]	0.893±0.004[a]
	30 min	0.882±0.007[ab]
	2 h	0.892±0.005[a]
	24 h	0.864±0.002[b]
Navy bean	Control[2]	0.932±0.002[a]
	30 min	0.946±0.000[b]
	2 h	0.944±0.000[b]
	24 h	0.903±0.000[c]
Rice bean	Control[2]	0.944±0.003[a]
	30 min	0.912±0.000[b]
	2 h	0.933±0.000[c]
	24 h	0.923±0.004[c]
Tepary bean	Control[2]	0.918±0.005[a]
	30 min	0.867±0.004[b]
	2 h	0.875±0.000[b]
	24 h	0.852±0.000[c]
Velvet bean	Control[2]	0.982±0.002[a]
	30 min	0.947±0.000[b]
	2 h	0.965±0.000[c]
	24 h	0.917±0.000[d]
Wrinkled pea	Control[2]	0.778±0.001
	30 min	0.881±0.008
	2 h	N/A
	24 h	N/A
Hylon®VII	Control[2]	0.877±0.003[a]
	30 min	0.992±0.011[b]
	2 h	1.000±0.000[b]
	24 h	N/A

Values followed by different superscripts in each column for each starch source are significantly different ($P < 0.05$) by Tukey's HSD test.

[1]The ratio of band intensities (1048/1022 cm^{-1}) measures the relative proportions of crystalline to amorphous regions at or near the granule surface.

[2]Control refers to starches kept in the digestion medium for 24h without enzyme.

Hylon®VII

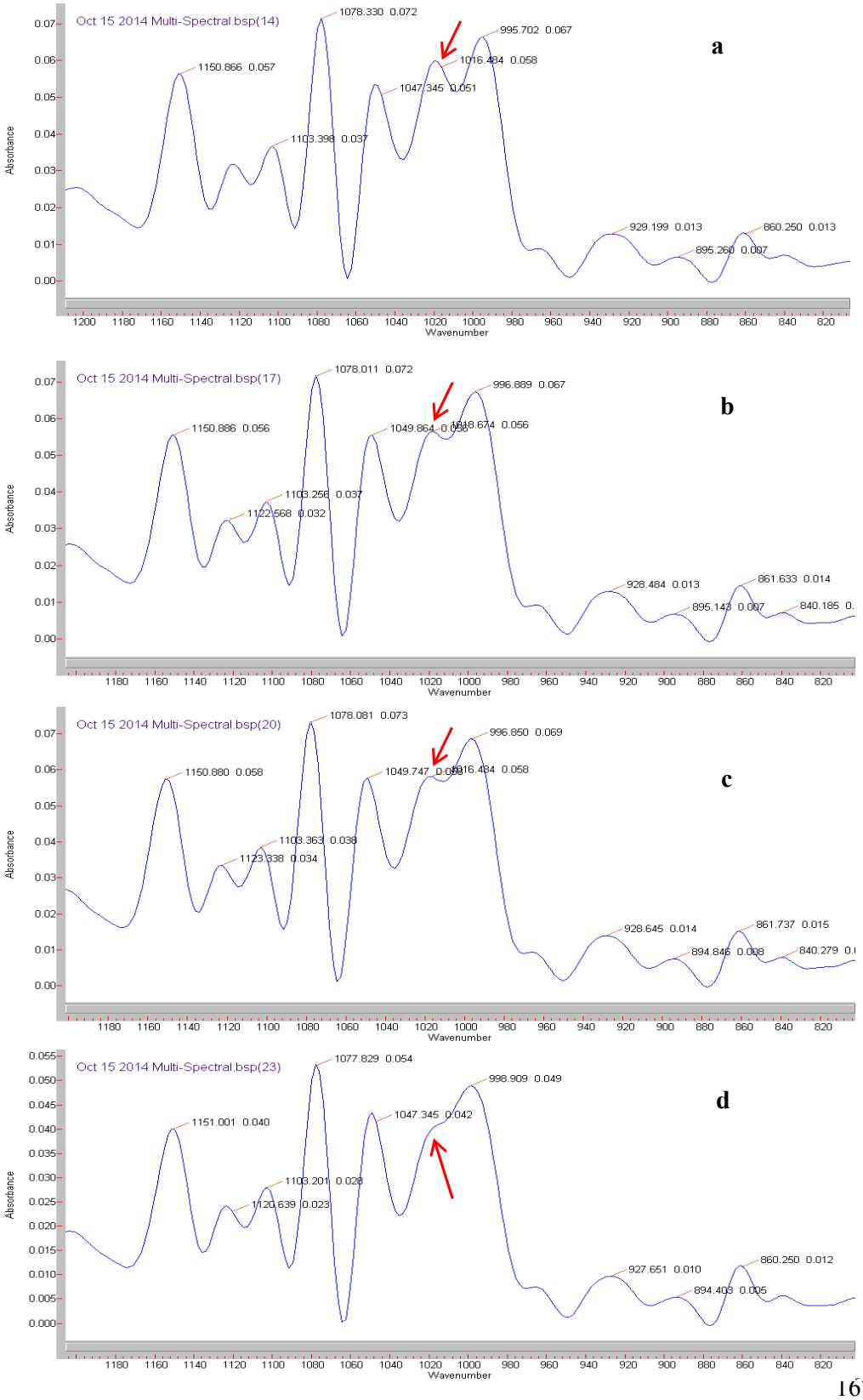
Oct 15 2014 Multi-Spectral.bsp(14)
1078.330 0.072
995.702 0.067
1016.484 0.058
1150.866 0.057
1047.345 0.051
1103.398 0.037
929.199 0.013
860.250 0.013
895.260 0.007
a
Oct 15 2014 Multi-Spectral.bsp(17)
1078.011 0.072
996.889 0.067
1150.886 0.056
1049.864 0.056
1018.674 0.056
1103.256 0.037
1122.568 0.032
928.484 0.013
861.633 0.014
895.143 0.007
840.185 0.
b
Oct 15 2014 Multi-Spectral.bsp(20)
1078.081 0.073
996.850 0.069
1150.880 0.058
1049.747 0.058
1016.484 0.058
1103.363 0.038
1123.338 0.034
928.645 0.014
861.737 0.015
894.846 0.008
840.279 0.
c
Oct 15 2014 Multi-Spectral.bsp(23)
1077.829 0.054
998.909 0.049
1151.001 0.040
1047.345 0.042
1103.201 0.028
1120.639 0.023
927.651 0.010
860.250 0.012
894.403 0.005
d
Absorbance
Wavenumber

Wrinkled pea

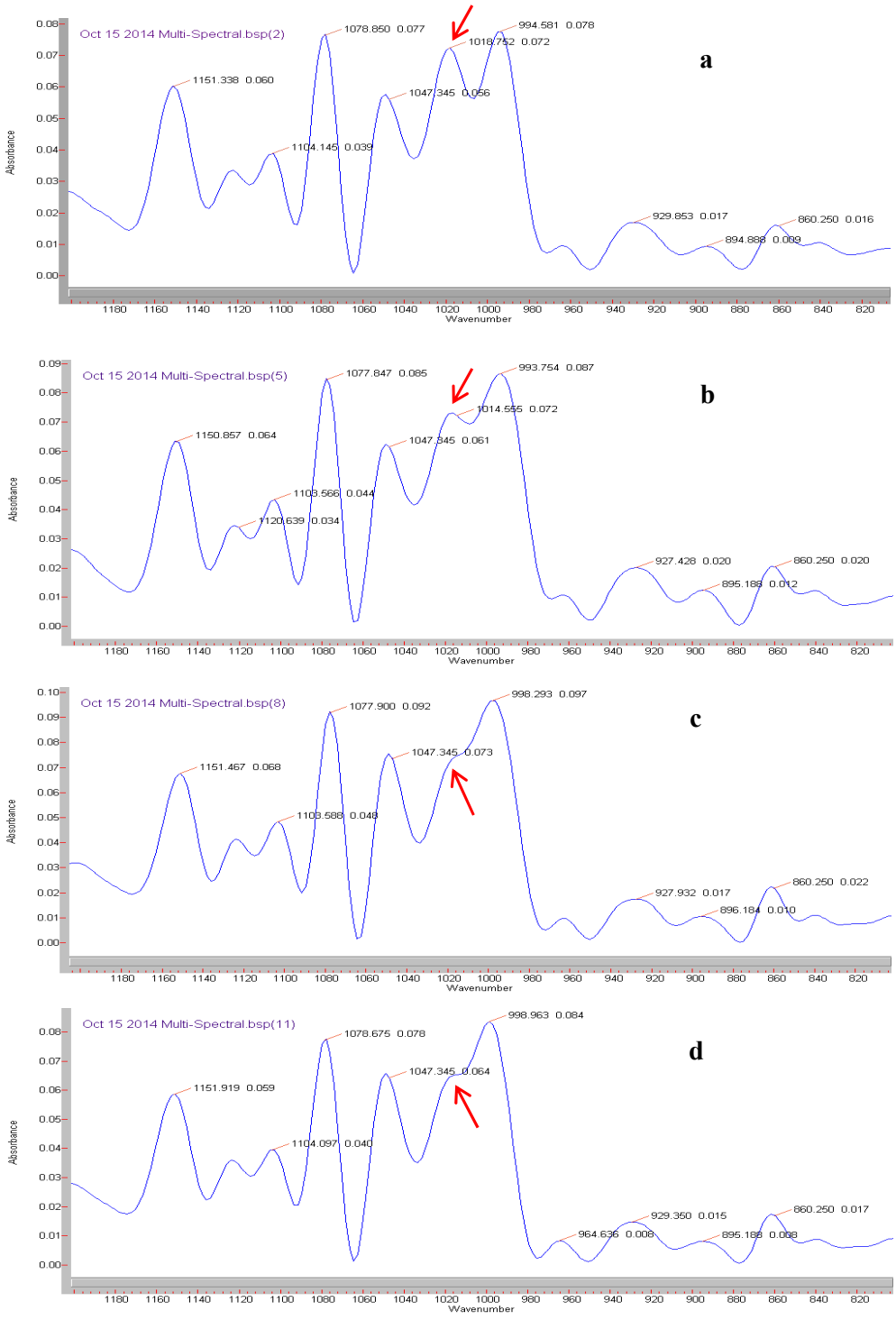

Figure 3.15: FTIR spectra of control *(a)* and enzyme-treated (30 min *(b)*; 2 h *(c)*; and 24 h *(d)*) wrinkled pea and Hylon®VII starches.

3.2.9 DSC of control and hydrolysed starches

The gelatinization transition temperatures (To, Tp and Tc) and ΔHs of the control and hydrolysed starches are presented in Table 3.12. To and Tc represent the melting of the weakest and most stable crystallites, respectively (Nakazawa & Wang, 2004). ΔH reflects the thermal energy associated with crystallite melting and dissociation and unravelling of double helices present in both crystalline and non-crystalline arrays. Tc-To represents variation in crystalline organization amongst granules. The data showed that amongst the starches, To, Tc-To, and ΔH followed the order of VB>TB>NB>RB>LB, LB>NB>RB>TB>VB, and LB>VB>TB>NB>RB, respectively. The To values suggest that the highest proportion of weak and strong crystallites are present in LB (To, 61.8°C) and VB (To, 72.2°C), respectively. The difference in Tc-To is indicative that crystalline heterogeneity is more pronounced in LB (Tc-To, 17.5°C) than in VB (Tc-To, 11.1°C). It was interesting to observe that the ΔH of LB (10.4 J/g) was significantly higher than that of VB (9.9 J/g), in spite of its lower crystallinity (LB, 25.4 %; VB, 30.2 %), weaker crystallites (LB, To = 61.8°C; VB, To = 72.2°C) and lower DHC (LB, 40.7 %; VB, 42.0 %). This suggests that the double helices of LB are probably longer than those of VB, and thus require more thermal energy for disruption of hydrogen bonds within and between double helices. The endotherms of both WP and HYVII were too wide to obtain an accurate value for the gelatinization parameters. The gelatinization parameters of starches hydrolysed for 24 h are presented in Table 3.12. For all starches, To increased (with the order being LB>RB>TB>NB>VB), and Tc-To decreased upon hydrolysis. Changes to Tp and Tc were marginal for all starches. ΔH increased in LB and RB, but remained unchanged in TB, NB and VB.

Table 3.12: Gelatinization parameters of control and hydrolysed pulse starches[1]

Starch source	Hydrolysis time	Gelatinization transition parameters (°C)				ΔH[4] (J/g)
		To[2]	Tp[2]	Tc[2]	Tc-To[3]	
Lablab bean	Control[5]	61.8±0.0^{a}	67.0±0.0^{a}	79.3±0.3^{a}	17.5±0.2^{a}	10.4±0.2^{a}
	30 min	62.6±0.1^{b}	68.2±0.0^{ab}	78.2±0.0^{b}	15.6±0.1^{b}	8.3±0.1^{b}
	2 h	63.7±0.1^{c}	68.7±0.0^{b}	78.2±0.0^{b}	14.5±0.1^{c}	10.4±0.1^{a}
	24 h	66.4±0.3^{d}	71.0±0.7^{c}	78.2±0.4^{b}	11.9±0.1^{d}	11.5±0.3^{c}
Navy bean	Control[5]	65.5±0.0^{a}	72.1±0.1^{a}	79.3±0.5^{a}	13.8±0.6^{a}	8.9±0.0^{a}
	30 min	67.2±0.1^{bc}	72.7±0.2^{a}	79.4±0.1^{a}	12.2±0.0^{ab}	8.7±0.0^{a}
	2 h	67.2±0.3^{b}	72.3±0.3^{a}	79.8±0.1^{a}	12.6±0.2^{ab}	8.5±0.5^{a}
	24 h	67.8±0.0^{c}	72.3±0.5^{a}	79.3±0.5^{a}	11.6±0.5^{b}	8.7±0.6^{a}
Rice bean	Control[5]	63.4±0.1^{a}	68.6±0.4^{a}	76.4±0.2^{a}	13.0±0.3^{a}	7.7±0.0^{a}
	30 min	64.8±0.0^{b}	69.6±0.1^{ab}	77.0±0.4^{a}	12.2±0.4^{ab}	7.4±0.4^{a}
	2 h	65.7±0.3^{c}	69.9±0.5^{bc}	77.2±0.4^{ab}	11.5±0.1^{bc}	8.1±0.0^{ab}
	24 h	67.5±0.1^{d}	71.2±0.2^{c}	78.5±0.4^{b}	11.0±0.3^{c}	8.5±0.1^{b}
Tepary bean	Control[5]	66.9±0.0^{a}	72.0±0.2^{a}	78.6±0.0^{a}	11.7±0.0^{a}	9.3±0.0^{a}
	30 min	68.3±0.2^{b}	72.9±0.1^{b}	79.2±0.0^{b}	10.9±0.2^{a}	7.9±0.1^{b}
	2 h	68.7±0.3^{bc}	73.1±0.0^{b}	79.5±0.2^{bc}	10.9±0.5^{a}	8.5±0.1^{c}
	24 h	69.4±0.0^{c}	73.7±0.0^{c}	80.0±0.0^{c}	10.6±0.0^{b}	9.4±0.2^{a}
Velvet bean	Control[5]	72.2±0.3^{a}	77.8±0.1^{a}	83.2±0.4^{a}	11.1±0.1^{a}	9.9±0.0^{a}
	30 min	73.1±0.1^{ab}	77.6±0.0^{a}	83.3±0.4^{a}	10.3±0.5^{ab}	9.0±0.0^{b}
	2 h	73.9±0.3^{bc}	78.2±0.4^{a}	84.0±0.1^{a}	10.1±0.2^{ab}	9.7±0.1^{a}
	24 h	74.1±0.1^{c}	78.3±0.5^{a}	83.4±0.2^{a}	9.3±0.3^{b}	10.2±0.4^{a}

[1] All data represent the mean of triplicates. Values followed by different superscripts in each column for each starch source are significantly different ($p < 0.05$) by Tukey's HSD test. Starch: water ratio (1:3 w/w. dry basis).

[2]To, Tp and Tc indicate the onset, peak, and conclusion temperatures, respectively.

[3](Tc-To) represents the gelatinization temperature range.

[4] Enthalpy of gelatinization expressed in J/g of dry starch.

[5] Refer to starches kept in the digestion medium for 24 h without enzyme.

The increase in ΔH for LB and RB cannot be explained in terms of changes to crystallinity or DHC during hydrolysis (Table 3.10) for the following reasons: 1) in NB, ΔH remained unchanged upon hydrolysis, although the increase in crystallinity (25.6-45.9 %) was similar to that for LB (25.4-45.0 %); 2) the large crystallinity increase in TB (26.4-38.3 %) and VB (30.2-45.3 %) on hydrolysis did not influence ΔH; 3) in RB, ΔH increased by 0.8 J/g, in spite of the crystallinity increase (27.3-28.3 %) being much smaller than for TB and VB; and 4) ΔH increased in LB (10.4-11.5 J/g) in spite of a decrease in DHC (40.7-28.9 %, Table 3.10). This leads me to conclude that the increase in ΔH on hydrolysis exhibited by LB and RB reflects an increase in crystalline perfection. This seems plausible, since the extent of increase in To (melting of weakest crystallites) and decrease in Tc-To (crystalline heterogeneity) were much higher in LB and RB (with LB>RB) than in other starches (Table 3.12). The increased crystallite perfection on hydrolysis suggests that double helices of control LB and RB may have been less perfectly aligned (within the crystalline domains) than in the other starches. Consequently, upon hydrolysis, these imperfectly aligned double helices may have become better aligned due to an increase in helical mobility (resulting from hydrolysis of the α-(1→6) linkages present within the inter-crystalline amorphous regions). The above data also suggest that crystalline regions were not attacked during the time course of hydrolysis.

3.2.10 Amylose leaching (AML) at 80°C and 90°C

AML data reflect the state of organization (compact or loosely packed) of amylose chains within the granule interior. The extent of AML is influenced by the extent of interplay among the following factors: 1) amylose content; 2) the extent of interaction between amylose chains; 3) amount of amylose chains that are co-

crystallized or intermingled with the repeating lamellae in amylopectin; and 4) amylose-lipid complexes. AML (at 80°C) among control starches (Figure 3.16) followed the order of TB>WP>LB>NB~VB>RB>HYVII. This suggests that AML among the above starches was not influenced by differences in their amylose content (Table 1). This is concluded based on the observation that HYVII, with a high amylose content of 67.4 %, versus LB, NB, RB, TB and VB (with an amylose content of 24.5-34.8 %), exhibited no AML. Also, TB, with a low amylose content (34.0%) versus LB (34.8 %), exhibited a higher amount of AML or by the amount of lipid complexed amylose chains. Whereas, VB with a lower bound lipid content than TB [VB (0.40 %) < TB (0.52 %), Table 3.1) exhibited less AML (Figure 3.16). This indicates that differences in AML among control starches are influenced by the extent of interaction between amylose chains and/or by the presence of amylose tie chains – amylose chains that are associated with amylopectin chains and/or with the loosely branched intermediate chains that are mainly present in WP and HYVII starches (Vamadevan *et al*., 2014).

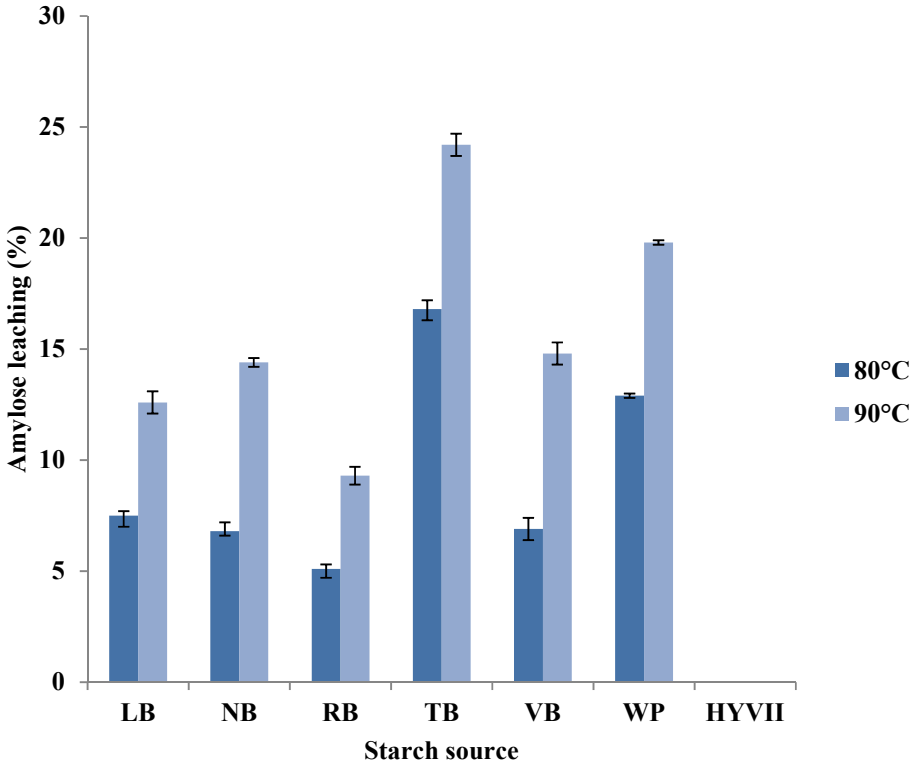

Figure 3.16: Amylose leaching of control starches of pulse and HYVII at 80 and 90°C.

The work presented in chapter 3.2 has been published in *Food Chemistry, 2016 (192):* 1098- 1108. Co-authors (Q. Liu, V. Vamadevan and R. Waduge) contributed to the analysis of HPEAC-PAD and ATR-FTIR.

3.3 Impact of annealing treatment on the molecular structure and properties of pulse and high amylose maize starches

3.3.1 Granule morphology

The granule morphology of native pulse starches has been described in section 3.1.2. The majority of studies have reported that annealing did not cause any major changes to granule morphology of cereal, tuber and root starches (Jayakody & Hoover, 2008; Zavareze & Dias, 2011). In this study, no significant differences were observed between native and annealed starches with respect to their shape or their surface characteristics. However, in HYVII starch, agglomeration of starch granules increased after annealing (Figure 3.17). A similar observation (granule aggregates) was reported for pea starches upon annealing where the granules appeared to adhere to each other (Wang *et al*., 2013).

3.3.2 Impact of annealing on the molecular order at the granule surface

Attenuated total reflectance –Fourier transform infrared spectroscopy spectral data for native and annealed starches are presented in Table 3.13. The ratio of the heights of the bands at 1047 and 1022 cm^{-1} represents the amount of ordered starch versus amorphous starch. Among the native starches, the ratio of the bands at 1047 cm^{-1}/1022 cm^{-1} followed the order of VB~RB>NB>TB>LB>HYVII>WP. These results suggest that the exterior regions of VB and RB starch granules are better organized than in the other pulse starches used in this study. In contrast to normal pulse starches, high amylose starches exhibited a lower ratio, as the double helical arrangement is less compactly organized on the surface of the granule. Sevenou *et al*. (2002) reported that the peripheral regions of B-type starches were more ordered than those of A-type starches, whereas the band representing amorphous structures at 1022 cm^{-1} was more prominent in A-type starches compared to B-type starches.

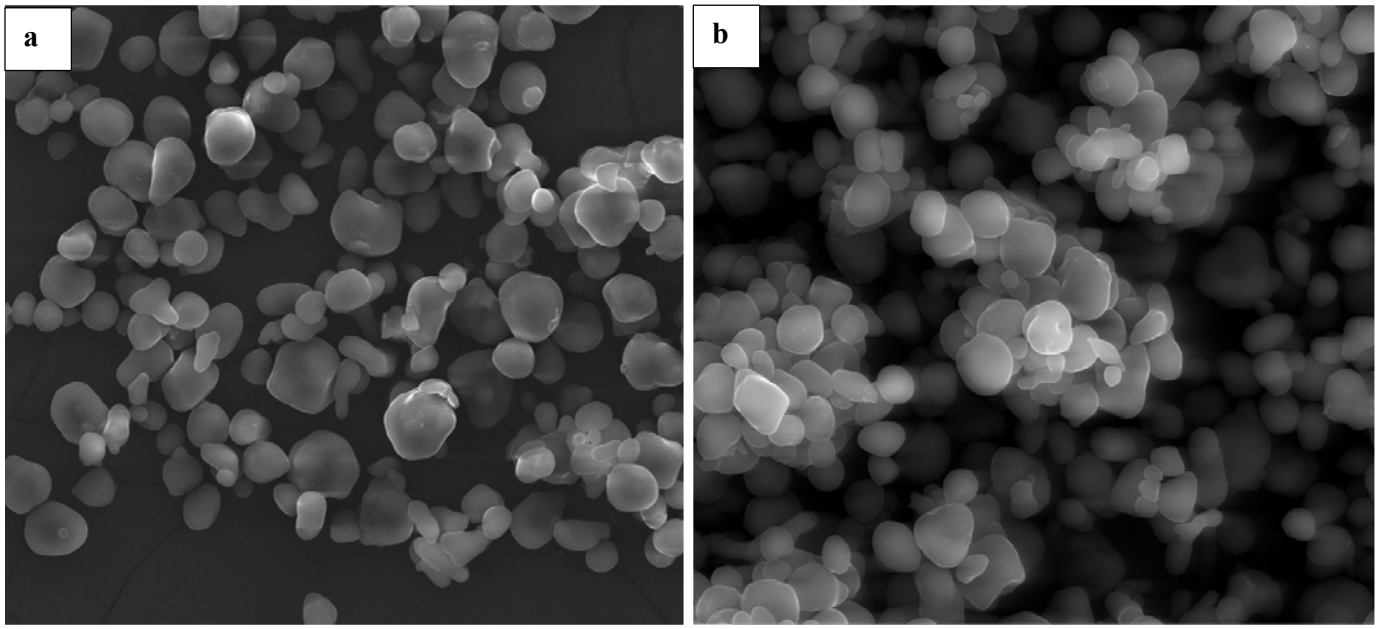

Figure 3.17: Scanning electron micrographs of native *(a)* and annealed *(b)* Hylon®VII starches.

Table 3.13: Short range molecular orders of native and annealed starches determined by attenuated total reflectance –Fourier transform infrared spectroscopy (ATR-FTIR)[1]

Starch Source	Treatment	Ratio (1047/1022 cm^{-1})[2]
Lablab bean	Native	0.879±0.000[a]
	Annealed	0.933±0.003[b]
Navy bean	Native	0.944±0.003[a]
	Annealed	0.974±0.003[b]
Rice bean	Native	0.960±0.004[a]
	Annealed	0.967±0.002[a]
Tepary bean	Native	0.916±0.004[a]
	Annealed	0.922±0.005[a]
Velvet bean	Native	0.963±0.001[a]
	Annealed	0.968±0.007[a]
Wrinkled pea	Native	0.782±0.001[a]
	Annealed	0.816±0.007[b]
Hylon®VII	Native	0.856±0.004[a]
	Annealed	0.898±0.002[b]

[1]All data represent the mean of triplicates.
[2]Ratio of the ordered crystalline (1047 cm^{-1}) to amorphous domains (1022 cm^{-1}). Values followed by different superscripts in each column for each starch source are significantly different ($P < 0.05$).

However, WP and HYVII starches had a higher B polymorphic content than the other pulse starches and exhibited a lower ratio. In spite of theirhigher B-polymorphic content, the lower ratio of 1047 cm^{-1}/1022 cm^{-1} in high amylose starches suggest that the crystallite organization at the granular surface was loosely organized. This may be due to their lower amylopectin content, larger surface area and/or to the presence of amylose tie chains causing crystalline defects which may have hindered the double helical alignment.

No significant differences were observed in the IR ratios (1047 cm^{-1}/1022 cm^{-1}) after annealing of VB, RB and TB starches. This suggests that the crystallites at the granule surface were better organized in their native state and had a less impact on annealing. The 1047/1022 cm^{-1} ratio increased on annealing and the extent of this increase followed the order of LB>HYVII>WP>NB. The increase in molecular order indicates that the double helical packing density (compactness) increased near the vicinity of the granule surface as a result of improved helical alignment upon annealing. The variation in molecular order increase suggests that the packing density at the granule surface may have been different among the starches. The above increase was primarily observed in B-type (HYVII and WP) and C-type (LB) polymorphic starches. The greater increase in molecular order (1047/1022 cm^{-1}) observed in LB starch was a reflection of stronger aggregation between helices and/or partial conversion of the polymorphic pattern (from A- to B-type) at the peripheral regions of the granule. This seems plausible, since Wang *et al.* (2008) reported that in pea starch, the B-type polymorphs are located at the center of the granule, which is surrounded by A-type polymorphs peripherally.

3.3.3 Impact of annealing on X-ray diffraction pattern and crystallinity

The X-ray diffraction patterns and the relative crystallinities (RC) of native and annealed starches are presented in Figure 3.18. The A-type starches exhibited the typical diffraction peak intensities centered at 15^{O} and 23^{O} 2θ, and an unresolved doublet at around 17^{O} and 18^{O} 2θ. The B-type starches displayed the strongest diffraction peak at around 17^{O} 2θ, a few small peaks at 15^{O}, 20^{O}, 22^{O} and 24^{O} 2θ, and a characteristic peak at about 5.6^{O} 2θ. C-type starches typically yield strong diffraction peaks at 17^{O} and 23^{O} 2θ, and a few small peaks at 5.6^{O} and 15^{O} 2θ (Cheetham & Tao, 1998; Cairns *et al*., 1997). NB, RB and TB starches exhibited an A-type crystalline pattern, whereas WP and HYVII starches exhibited typical B-type crystalline patterns. LB starch displayed a C-type crystalline pattern, which was a mixture of A and B-type unit cells in varying proportions. The RCs of normal pulse starches ranged from 23.5-28.4 %; these values were within the range reported for other pulse starches, (being 17.0-34.0 %) (Hoover *et al*., 2010). A comparative study on native maize starches with varying amylose content showed that a polymorphic transition occurred from type A to B via C, with an increase in amylose content. Furthermore, the crystallinity of starch decreases with an increase in amylose content and the long chain fraction of amylopectin (Cheetham & Tao, 1998). In this study, the high amylose starches (WP and HYVII) exhibited a lower value of RC compared to normal pulse starches with typical B-type polymorphic patterns.

The X-ray results indicated that the crystal types and the structures of the pulse starches were unaffected by annealing treatment. Similar X-ray diffraction patterns were obtained for native and annealed starches, which is in agreement with previous studies (Chung *et al*., 2009a; Gomes *et al*., 2005; Rocha *et al*., 2011).

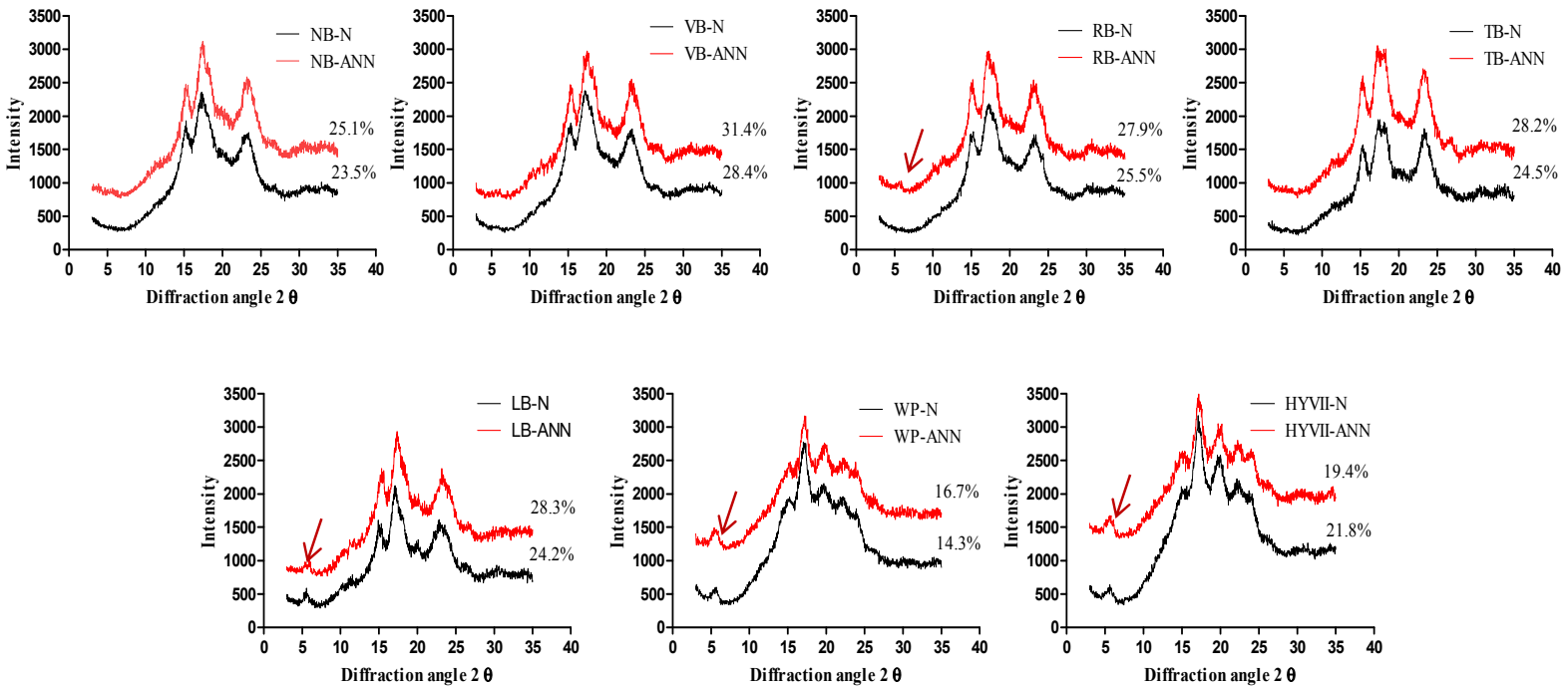

Figure 3.18: X-ray diffraction patterns and relative crystallinities of native (N) and annealed (ANN) pulse and Hylon®VII starches. The arrow shows the characteristic (~5.5^{O} 2θ) of B-type crystallites.

However, a smaller peak centered at 5.5° 2θ was observed in RB starch after annealing, which is a characteristic peak for the B-type polymorphic structure. Furthermore, the peak height at 5.5^{O} 2θ of LB, HYVII and WP starches increased upon annealing. In general, the increase in B-polymorphic content is characterized by the development of peak height and the full width at half maximum (FWHM) at 5.5° 2θ, and the apparent increase in the peak height of the doublet between 22°-24° 2θ (Vamadevan *et al*., 2014). However, the peak heights of the doublet between 22°-24° 2θ remained unchanged in high amylose starches. In LB starch, the peak height at 23° 2θ also remained identical, with a slight shift toward the higher 2θs. It is difficult to ascertain whether the annealing treatment had a significant effect on polymorphic transformation, or if these changes were associated with differences in moisture incorporation among the native and annealed starches. Cheetham and Tao (1998) reported that hydration induces an increase in the degree of crystallinity without changing the crystal type. The increase in peak height at 5.5^{O} 2θ of LB and RB starches could be due to the partial polymorphic transition from A to B rather than disruption of A-type of polymorphs. Wang *et al*. (2013) also reported a similar increase in B-polymorphs in pea starches upon annealing.

The relative crystallinity (RC) of pulse and HYVII starches increased as a result of annealing treatment (Figure 3.18). A similar observation was reported in high amylose barley (Waduge *et al.*, 2006), waxy corn (Rocha *et al*., 2012), Peruvian carrot and potato starches (Rocha *et al*., 2011). The increase in RC of starches post-annealing suggests that the crystallites may have become better aligned due to the more efficient packing of double helices within the crystalline lamellae and/or an increase in crystal size and crystallite reorientation (Tester *et al*., 1998; Genkina *et al*.,

2004; Chung *et al*., 2010). BeMiller and Huber (2015) suggested that the annealing conditions and starch source influence the relative crystallinity of annealed starches, and the increase, decrease or no change depends on the balance between crystallite disruption and reorientation and recrystallization.

3.3.4 Impact of annealing on gelatinization parameters

The gelatinization parameters of the native and annealed starches are presented in Table 3.14. Annealing treatment was performed for various time intervals (24 h, 48 h and 72 h) and their impact on gelatinizations parameters were determined using DSC. The results showed a significant difference between the 24 h annealed and their native counterparts. However, only a marginal difference was observed between the 24 h, 48 h and 72 h annealed samples. In this discussion, the annealed samples subjected to 72 h of incubation time were compared with their native counterparts.

It was assumed that these starches had reached their optimum level of crystalline perfection at the prevailing annealing conditions. To and Tc represents the melting of the weakest and most stable crystallites, respectively, and the crystalline perfection is represented by Tp (Tester, 1997). The DSC traces of all annealed starches produced a single-peaked gelatinization endotherm which was obtained under excess water conditions. Under the same conditions, high amylose starches (WP and HYVII) exhibited a broader endotherm comprised of two overlapping endothermic peaks. In comparison with the pulse starches, HYVII starch exhibited a higher To and Tp, which is associated with the amylose-lipid complexes and a higher proportion of longer glucan chains.

Table 3.14: Gelatinization parameters of native annealed pulse and Hylon®VII starches.

Starch source	Treatment	Gelatinization transition parameters (°C)[1]				
		To[2]	Tp[2]	Tc[2]	Tc-To[3]	ΔH[4](J/g)
Lablab bean	Native	62.6±0.2^{a}	67.9±0.1^{a}	81.9±0.0^{a}	19.3±0.2^{a}	15.4±0.3^{a}
	24H_ANN	69.0±0.0^{b}	71.3±0.0^{b}	77.7±0.1^{b}	8.8±0.1^{b}	14.5±0.1^{a}
	48H_ANN	70.0±0.2^{c}	72.3±0.3^{c}	78.8±0.1^{c}	8.8±0.1^{b}	14.4±0.6^{a}
	72H_ANN	70.5±0.4^{c}	72.9±0.4^{c}	78.5±0.4^{c}	8.0±0.0^{c}	14.7±0.7^{a}
Navy bean	Native	65.5±0.3^{a}	73.6±0.1^{a}	81.9±0.0^{a}	16.4±0.3^{a}	13.1±0.4^{a}
	24H_ANN	73.3±0.0^{b}	75.4±0.0^{b}	80.6±0.3^{b}	7.3±0.3^{b}	13.3±0.1^{a}
	48H_ANN	73.8±0.1^{bc}	75.8±0.0^{c}	80.7±0.2^{b}	7.0±0.1^{b}	13.6±0.2^{a}
	72H_ANN	74.4±0.1^{c}	76.5±0.0^{d}	81.8±0.0^{a}	7.4±0.1^{b}	13.6±0.3^{a}
Rice bean	Native	62.7±0.2^{a}	68.8±0.1^{a}	81.0±1.0^{a}	18.3±0.8^{a}	14.5±0.8^{a}
	24H_ANN	69.5±0.2^{b}	71.8±0.0^{b}	76.9±0.1^{b}	7.4±0.0^{b}	12.8±0.1^{ab}
	48H_ANN	70.8±0.2^{c}	73.2±0.5^{c}	78.3±0.6^{ab}	7.6±0.4^{b}	12.4±0.0^{b}
	72H_ANN	71.2±0.3^{c}	73.4±0.4^{c}	78.9±0.9^{ab}	7.7±0.5^{b}	13.4±0.6^{ab}
Tepary bean	Native	66.9±0.0^{a}	71.4±0.1^{a}	82.5±0.6^{a}	15.6±0.6^{a}	14.5±0.3^{a}
	24H_ANN	74.6±0.0^{b}	76.9±0.0^{b}	82.3±0.2^{a}	7.6±0.2^{b}	14.5±0.1^{a}
	48H_ANN	75.8±0.0^{c}	78.1±0.5^{c}	83.3±0.7^{a}	7.4±0.2^{b}	14.6±0.1^{a}
	72H_ANN	76.3±0.0^{c}	78.5±0.1^{c}	83.8±0.4^{a}	7.5±0.5^{b}	15.7±0.2^{b}
Velvet bean	Native	72.2±0.2^{a}	77.2±0.3^{a}	81.3±0.4^{a}	9.1±0.2^{a}	15.0±0.2^{ab}
	24H_ANN	80.7±0.1^{b}	82.9±0.0^{b}	88.3±0.2^{b}	7.6±0.1^{b}	15.7±0.6^{ab}
	48H_ANN	80.6±0.0^{b}	82.7±0.0^{b}	88.2±0.0^{b}	7.6±0.0^{b}	16.6±0.0^{bc}
	72H_ANN	81.5±0.0^{c}	83.7±0.5^{b}	89.1±0.7^{b}	7.6±0.5^{b}	17.8±0.3^{c}
Wrinkled pea	Native	59.4±0.0^{a}	75.1±0.1^{a}	90.7±0.8^{a}	31.2±0.6^{a}	6.9±0.3^{a}
	24H_ANN	72.1±0.0^{b}	77.9±0.2^{b}	89.9±1.2^{a}	17.7±0.8^{b}	6.1±0.4^{a}
	48H_ANN	72.7±0.0^{bc}	78.2±0.0^{bc}	89.5±0.1^{a}	16.8±0.2^{b}	6.6±0.3^{a}
	72H_ANN	73.4±0.3^{c}	78.9±0.3^{c}	89.8±0.6^{a}	16.4±0.3^{b}	6.4±0.1^{a}
Hylon®VII	Native	70.4±0.2^{a}	91.1±0.2^{a}	101.8±0.7^{a}	31.4±0.5^{a}	10.2±0.1^{a}
	24H_ANN	78.1±0.1^{b}	86.2±0.1^{b}	102.7±0.1^{ab}	24.5±0.2^{b}	13.0±0.8^{b}
	48H_ANN	79.2±0.5^{c}	87.7±0.5^{c}	102.7±0.0^{ab}	23.6±0.5^{b}	13.2±0.6^{b}
	72H_ANN	79.9±0.1^{c}	88.1±0.0^{c}	103.2±0.2^{b}	23.3±0.1^{b}	13.6±0.0^{b}

[1]All data represent the mean of triplicates. Values followed by different superscripts in each column for each starch source are significantly different ($P < 0.05$) by Tukey's HSD test.
[2]To, Tp and Tc indicates the onset, peak, and conclusion temperatures, respectively.
[3](Tc-To) represents the gelatinization temperature range.
[4]Enthalpy of gelatinization expressed in J/g of dry starch.

Irrespective of the starch source or crystal type, annealing significantly increased To and Tp and narrowed the gelatinization temperature range (Tc-To). Therefore, the DSC results indicated that all starch crystal types responded to the annealing treatment, but the extent of variation differed among the starches. The weakest crystallites exhibit the lowest melting temperature and have a greater tendency toward crystallite perfection upon annealing (Jacobs *et al.*, 1998; Gomand *et al*., 2012). The increase in gelatinization temperatures indicated that the crystallites with the lowest stability improved on annealing. Furthermore, the increase in Tp and decrease in gelatinization temperature range suggested that the annealing increased the crystalline perfection (improved double helix register) by decreasing the heterogeneity within the crystalline lamellae (Vamadevan *et al.*, 2014). The lower Tp values of native LB and RB starches could be attributed to the loose packing of amylopectin double helices within the crystallites, whereas long B chains are interspersed into crystalline lamellae and/or the double helices within the crystalline lamella are not in a crystalline register. Tp is primarily determined by the internal structure of amylopectin, which dictates the optimal packing of double helices within the crystalline lamella. Except HYVII starch, all of the other starches exhibited an increase in Tp, which indicates that annealing decreases crystalline defects. Several studies have shown that annealing increased the crystalline thickness and thereby decreases crystalline defects. The following factors influence the increase in crystalline thickness on annealing: 1) improvement in double helical registration; 2) lengthening of double helices through the twisting of unordered ends in pre-existing double helices; and/or 3) an ordering of unordered ends of double

helices (Tester & Debon, 2000; Kiseleva *et al*., 2004; Vermeylen *et al*., 2006; Gomand *et al*., 2012; Vamadevan *et al*., 2014).

High amylose starches possess longer internal chains with few branches (intermediate chains) and longer external chains of amylopectin, which could cause structural defects such as splayed double helices and imperfect double helices with untwisted ends within the crystalline lamellae (Klucinec & Thompson, 2002). Annealing treatment minimizes the structural defects by increasing glucan chain mobility and interactions between the glucan chains.

The gelatinization enthalpy (ΔH) was increased in TB, VB and HYVII starches, whereas it remained unchanged in other pulse starches. The increase in ΔH of TB, VB and HYVII starches after annealing treatment has been attributed to improved double helical register and the lengthening of double helices by twisting of the chain ends. In addition to these factors, the co-crystallization of tie chains with amylopectin chains could have occurred during annealing, contributing to the higher increase in ΔH of HYVII compared to other pulse starches. However, the ΔH of WP starch remained unchanged. In contrast to HYVII, WP starch exhibited a lower To and ΔH, whereas it possessed a higher amylose content (79.6 %, section 3.2.1). However, Vamadevan *et al*. (2014) suggested that the true amylose content of high amylose maize starches (Hylon®V, Hylon®VII and Hylon®VIII) was similar, while the amount of intermediate material was different. Therefore, the presence of higher amount of intermediate material in WP starch contributed to the increased number of tie chains. This caused crystalline defects where it prevented the parallel packing of double helices by restricting the mobility of the amylopectin molecules during annealing treatment. However, WP showed an increase in Tp, and a larger extent of

decrease in Tc-To, suggesting that annealing increased the crystalline perfection and decreased the heterogeneity of crystallites to a larger extent. The largest increase in To of WP starch could be due to the lengthening of double helices and/or co-crystallization of tie chains with amylopectin chains.

3.3.5 Impact of annealing on starch swelling factor

The swelling factors (SFs) of pulse and Hylon®VII starches in the temperature range from 70-90°C are presented in Figure 3.19. The SFs (at 70-80°C) of the native starches followed the order of TB>LB>RB>NB>VB>WP>HYVII. The SFs of native normal pulse starches increased rapidly in the temperature range of 70-85°C, whereas in the native high amylose starches, the increase in SF in the temperature range of 70-85°C was gradual. Thereafter, SF decreased marginally at 90°C in all starches, with the exception of LB and WP starches where the SF remain unchanged at 90°C. The SF has been reported to be influenced by amylopectin structure (Sasaki & Matsuki, 1998), amylose content (Sasaki & Matsuki, 1998), the extent of interaction between starch chains (amylose-amylose and/or amylopectin-amylopectin chains) (Tester *et al*., 2000), and V-amylose lipid content (Tester & Morrison, 1990a). Swelling factor differences cannot be explained in terms of APCLD (Table 3.3) or V-amylose lipid content (Table 3.1), since differences amongst the native normal pulse starches with respect to the above two factors were not significant. Therefore, the differences in SF among these starches could be influenced by the amylose content and the interaction between starch chains, along with differences in RC, DHC, granular size and surface characteristics. The differences in SF between normal pulse starches and high amylose starches (WP and HYVII starches) can be attributed to the lower crystallinity, lower amylopectin

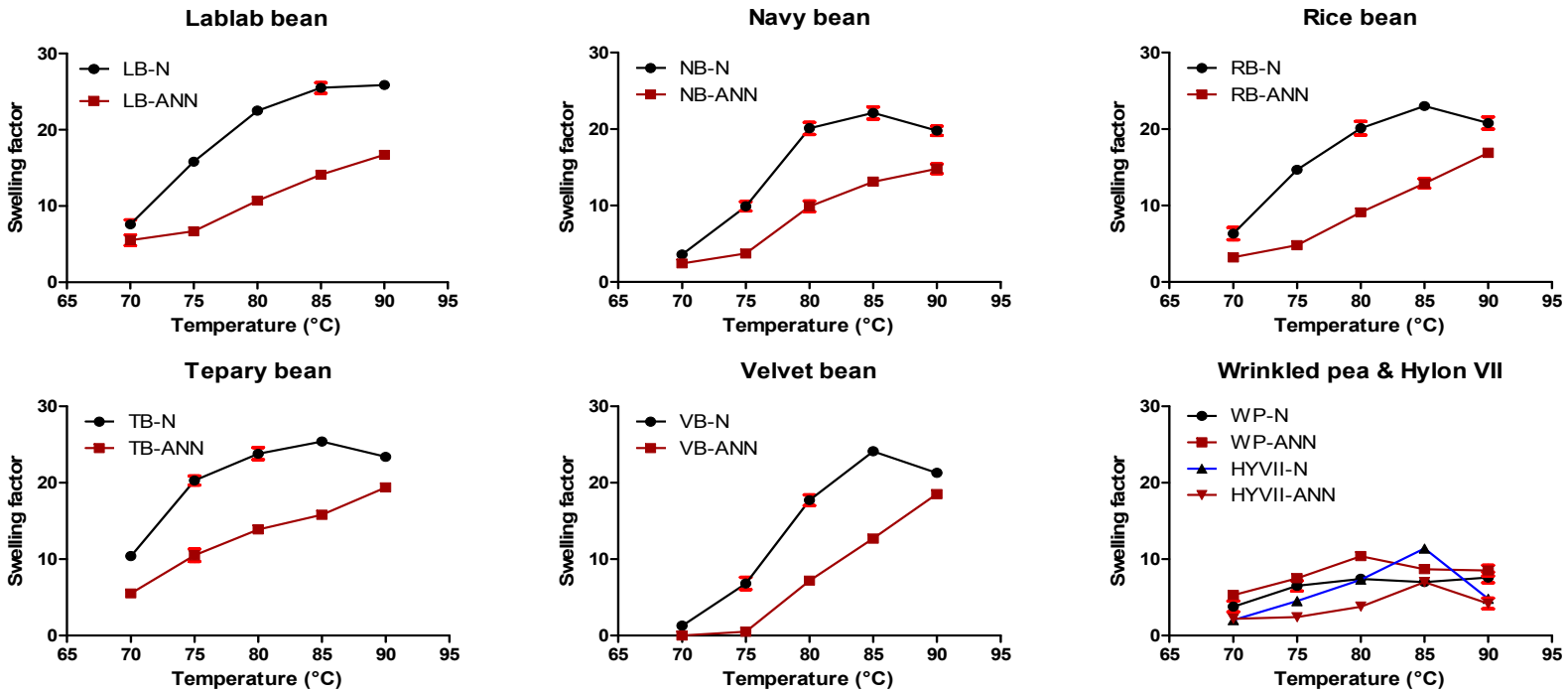

Figure 3.19: Swelling factors of native (N) and annealed (ANN) starches in the temperature range of 70-90^{O}C.

content with a disrupted crystallite structure and relatively higher content of V-amylose-lipid complexes in high amylose starches. Furthermore, Singh *et al*. **(**2009) reported that swelling power was affected by amylopectin and amylose content, and amylose could restrict starch granule swelling. At all temperatures, the SF of annealed starches was lower than their native counterparts, with the exception of WP starch which exhibited either an increase in SF or no change, depending on temperature. The extent of this reduction in SF (at 85°C) among the starches followed the order of LB~VB>RB>TB>NB>HYVII. The extent of decrease in SF on annealing was attributed to the interplay between the extent of crystallite perfection and the additional interaction between amylose-amylose and/or amylose-amylopectin chains (Jayakody *et al.,* 2009). The swelling of starch granules is known to initiate in the bulk amorphous regions and in the restrained amorphous regions, which are adjacent to the crystalline regions (Hoover & Manuel, 1996). The perfection of starch crystallites and the increased interactions between amylose chains on annealing would reduce the extent of hydration of the amorphous regions. Therefore, the movement of water from the amorphous regions into the crystalline area would decrease, which in turn reduce the granular swelling. The extent of this decrease was more pronounced in normal pulse starches than in HYVII starch. In addition to its lower amylopectin content, the swelling of HYVII starch was strongly inhibited by V-amylose-complexes and a relatively higher proportion of amylose double helices which dissociated at higher temperature (Shi *et al*., 1998). It was surprising that the swelling factor of WP starch increased marginally on annealing. This increase may be due to the compound nature of the granule and/or the transformation of amorphous amylose into a helical form that creates a void space in the bulk amorphous region, which in turn facilitates granular

swelling. Decreased granular swelling on annealing also has been reported in lentil, pea (Chung *et al*., 2009b), barley (Waduge *et al.*, 2006), wheat (Lan *et al*., 2008), sweet potato (Song *et al*., 2014) and potato (Nakazawa & Wang 2004) starches.

3.3.6 Impact of annealing on amylose leaching (AML)

The extent of AML in native and annealed starches in the temperature range of 70-90°C is shown in Figure 3.20. AML of native and annealed starches increased with the increase in temperature. AML at 85°C among the native starches followed the order of TB>VB>LB>NB~WP>RB. These data suggest that AML of these starches was not influenced by differences in their amylose content. At all temperatures, AML of annealed starches was lower than that of their native counterparts. Whereas, no AML was observed in either native or annealed HYVII starch. The decrease in AML on annealing could be due to additional interactions between amylose-amylose and/or amylose-amylopectin chains, reduced hydration and restricted granular swelling, and/or enhanced ordering of amylose-lipid complexes (Waduge *et al*., 2006; Lan *et al.*, 2008; Chung *et al*., 2009b). At higher temperatures (85 and 90°C), a greater relative reduction in AML was observed in WP annealed starch compared to the normal pulse starches. However, an increased amount of amylose leaching of native WP starch at higher temperatures ((85 and 90°C)) could be attributed to the weaker interactions between long amylose chains and/or the presence of amylose tie chains that are loosely attached with amylopectin chains within the crystalline lamellae. The reorganization of starch chains during annealing facilitates additional interactions between starch chains, and consequently less AML would occur in annealed starches than in their native counterparts.

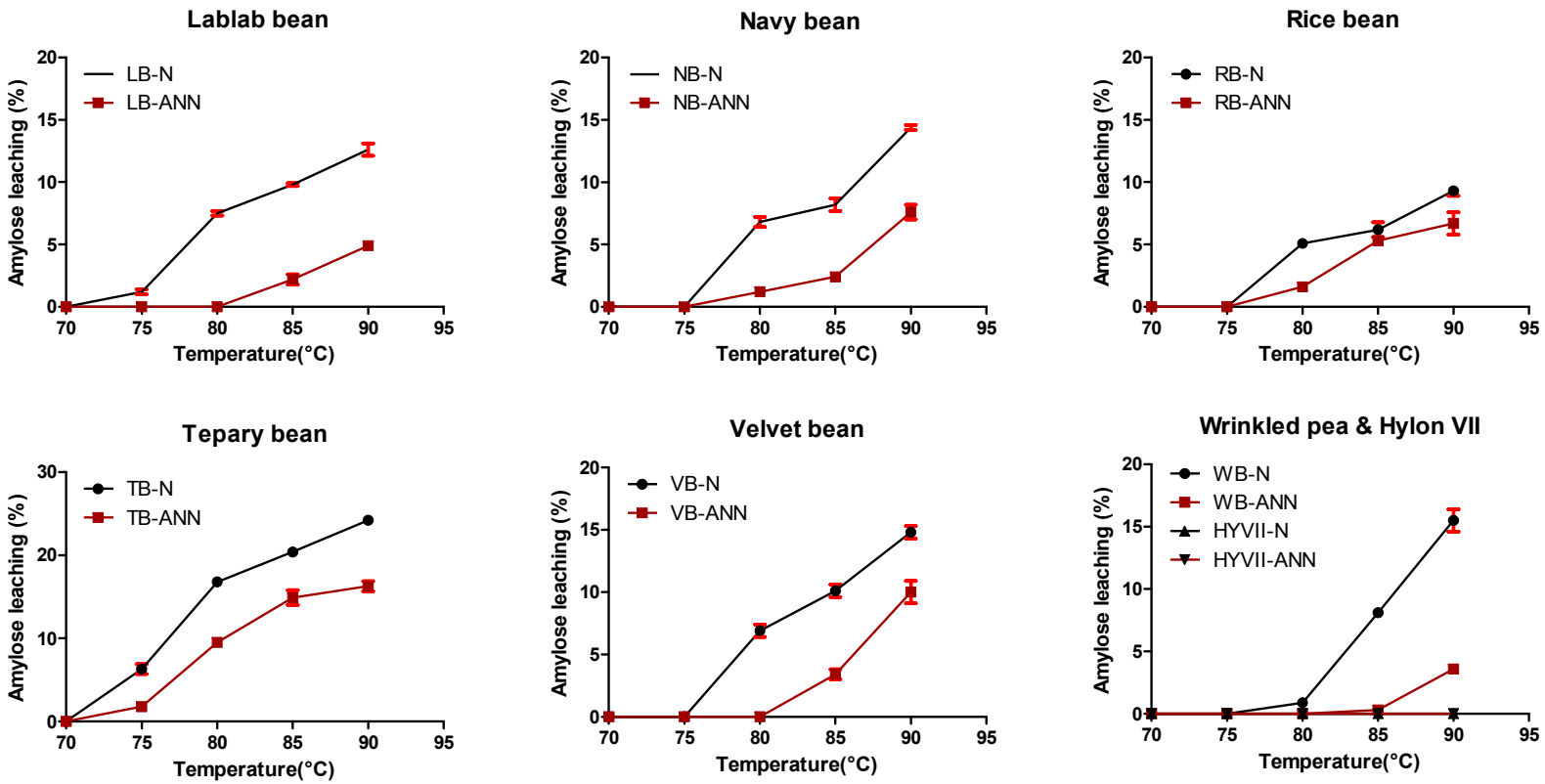

Figure 3.20: Amylose leaching of native (N) and annealed (ANN) starches in the range of 70-90^{O}C.

3.3.7 Impact of annealing on pasting characteristics

The pasting properties of native and annealed starches are presented in Figure 3.21. Differences in RVA parameters (peak viscosity, pasting temperature, breakdown viscosity, final viscosity and set-back) among the native pulse starches were discussed in section 3.1.13. In all of the pulse starches, annealing decreased peak viscosity and breakdown viscosity, but increased peak temperature and peak time. The trough viscosity, final viscosity, and set-back of TB (Figure 3.21b) starch increased, but decreased in other pulse starches on annealing. In normal pulse starches, the reduction in peak viscosity on annealing reflects decreased SF (Figure 3.19) and AML (Figure 3.20), as a result of improved interactions between amylose-amylose, amylopectin-amylopectin and/or amylose-amylopectin chains. The impact of annealing on peak viscosity is more pronounced in the NB (Figure 3.21e) starch than in other pulse starches. This could be attributed to its lower granular swelling and amylose leaching at higher temperatures (>85°C). The increase in pasting temperature of annealed starches and the time taken to reach peak viscosity reflect the improved thermal stability of annealed starches, which is in agreement with the DSC results (Table 3.14). The restricted granular swelling and interactions between starch chains also were responsible for the increase in pasting temperature upon annealing. The decrease in breakdown viscosity of all normal pulse starches indicate that annealed starches were stable during continued heating and shearing (Liu *et al*., 2015).

It has been reported that the extent of set-back is largely influenced by the starch granule size, amylopectin chain length, magnitude of amylose leaching, presence of granule remnants and/or the unfragmented rigid granules embedded in the

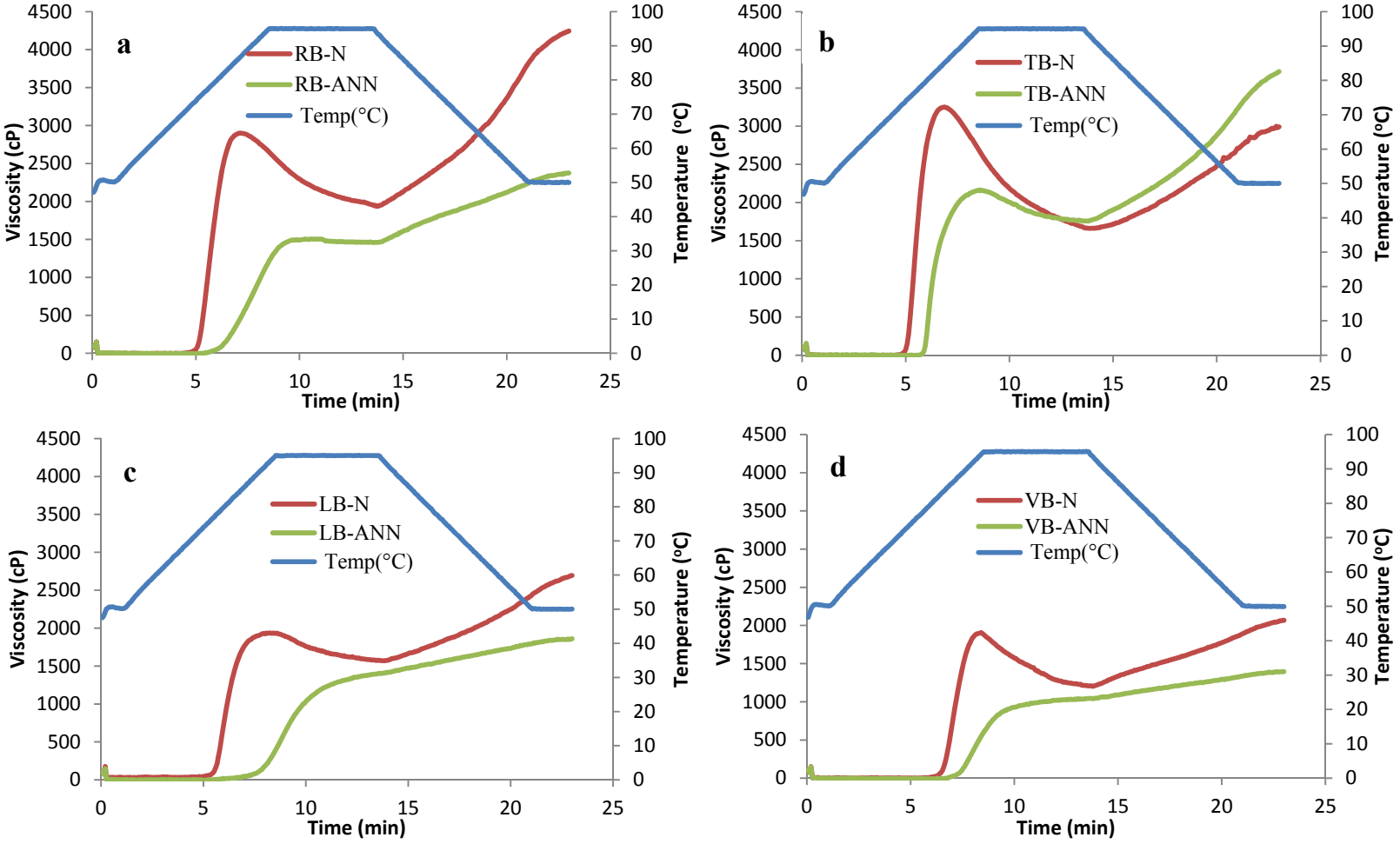
a
RB-N
RB-ANN
Temp(°C)
Viscosity (cP)
Temperature (°C)
Time (min)
b
TB-N
TB-ANN
Temp(°C)
Viscosity (cP)
Temperature (°C)
Time (min)
c
LB-N
LB-ANN
Temp(°C)
Viscosity (cP)
Temperature (°C)
Time (min)
d
VB-N
VB-ANN
Temp(°C)
Viscosity (cP)
Temperature (°C)
Time (min)

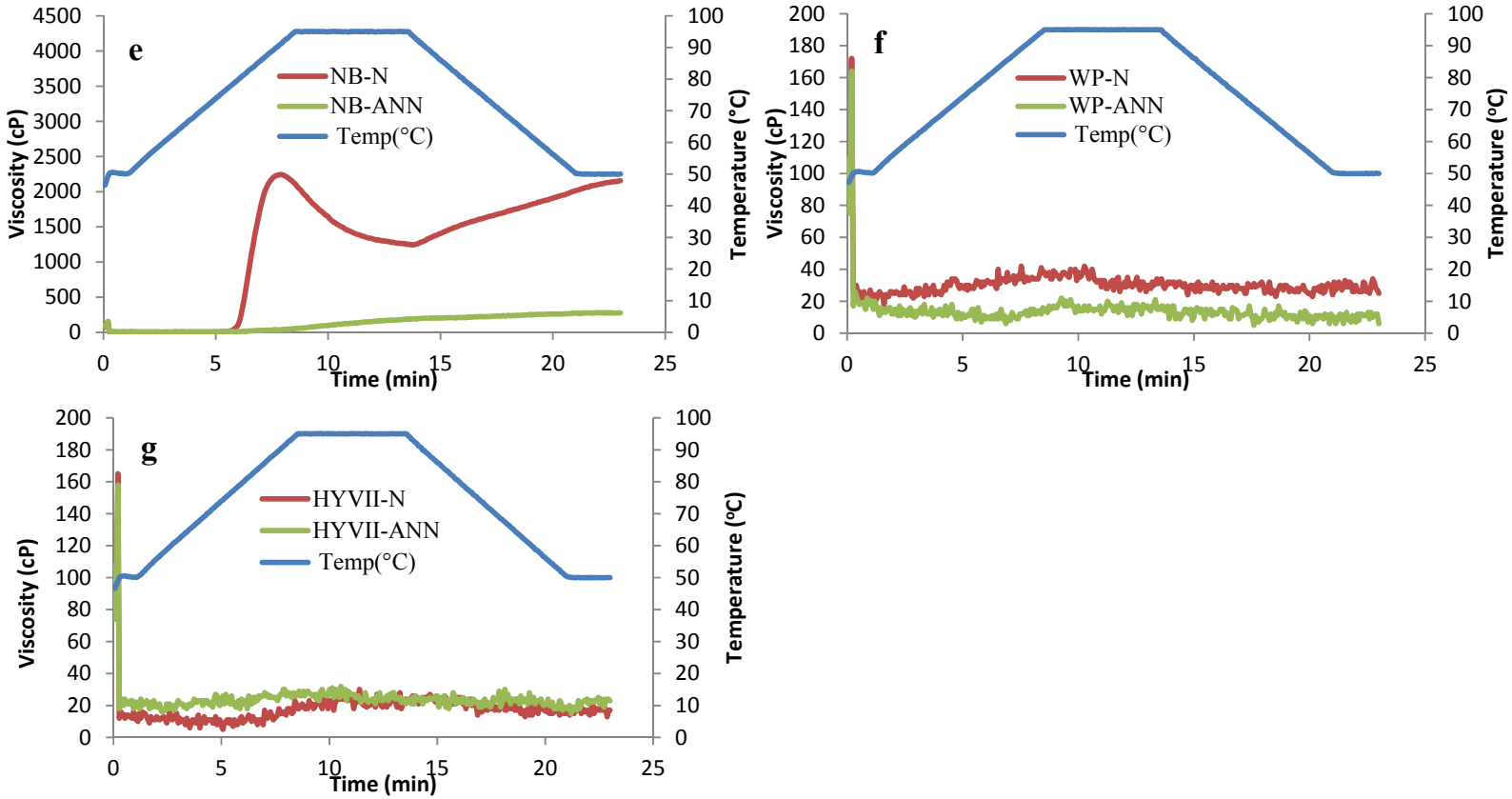

Figure 3.21: Paqsting profiles of native (N) and annealed starches of rice bean *(a)*, tepary bean *(b)*, lablab bean *(c)*, velvet bean *(d)*, navy bean *(e)*, wrinkled pea *(f)* and Hylon®VII *(g)* as determined by rapid visco analyser.

leached amylose complex (Lan *et al*., 2008; Jacobs *et al*., 1995; Hoover & Vasanthan, 1994b). The decrease in set-back cannot be explained in terms of changes in APCLD, since the annealing treatment has no influence on chain length distribution (Kohyama & Sasaki, 2006; Lan *et al*., 2008). Annealing has been shown to increase the stability of the granule by restricting granule swelling and enhancing starch chain interactions inside the granule (BeMiller & Huber, 2015). Therefore, the decrease in set-back on annealing is mainly due to the reduced AML and the presence of more intact granules that are resistant to shear stress at elevated temperatures compared to their native counterparts (Chung *et al*., 2009a). This seems plausible, since the intact granules may have reduced the rapid association of leached amylose chains, which in turn reduced the viscosity development at the end of the cooling cycle. Similar findings were reported by several groups, such that annealed starches commonly display increase pasting temperature or time (Dias *et al*., 2010; Simsek *et al*., 2012; Chen *et al*., 2014) and reduced peak viscosity and breakdown viscosity (Simsek *et al*., 2012; Yadav *et al*., 2013; Song *et al*., 2014).

In contrast to other normal pulse starches, annealed TB (Figure 3.21b) starch exhibited a lower pasting temperature with a greater peak viscosity. This could be attributed to the amount of leached amylose (Figure 3.20) and granule swelling (Figure 3.19) being higher than the other annealed pulse starches. The final viscosity of TB starch also increased on annealing; this suggests that the annealed TB starch was more prone to shear disintegration with extensive amylose leaching. Furthermore, the higher extent of retrogradation during the cooling period is reflected by the increase in set-back viscosity after annealing treatment compared to the other starches. The above results suggest that the extent of interaction between starch chains as a

result of annealing was less in TB starch compared to other starches. Jacobs *et al*. (1996) have reported that annealing increased the peak and final viscosities of pea, wheat and rice starches. The native and annealed HYVII and WP (Figure 3.21 f,g) starches exhibited low viscosity values in their pasting profiles (Figure 3.21). The higher amylose content (>65 %) and lower extent of granular swelling and amylose leaching contributed to the lower viscosity of high amylose starches (Polesi *et al*., 2011).

3.3.8 Impact of annealing on acid hydrolysis

The acid hydrolysis patterns of native and annealed starches are presented in Figure 3.22. Differences in acid hydrolysis among the native normal pulse starches were discussed in section 3.1.11. The native high amylose starches (WP and HYVII, Figure 3.22e,g) were hydrolysed to a lesser extent than were the native normal pulse starches due to their greater amylose content and relatively higher levels of lipid complexed amylose chains (section 3.2.1). Furthermore, the retrogradation resulting from interactions between hydrolysed amylose chains also restricts the accessibility of H_3O^+ to the glyosidic oxygen, which in turn reduces the extent of hydrolysis during the initial stages of hydrolysis. However, in high amylose starches, the structural differences in branching density and glucan chain length and the presence of intermediate material may have contributed to the differences between WP and HYVII starches toward acid hydrolysis. The annealed starches exhibited similar solubilisation patterns to those of their native counterparts. In all starches, with the exception of LB and TB (Figure 3.22d,f) starches, the extent of hydrolysis between day 1 and day 3 was decreased marginally on annealing. However, beyond day 6, differences in hydrolysis between native and annealed starches were more pronounced

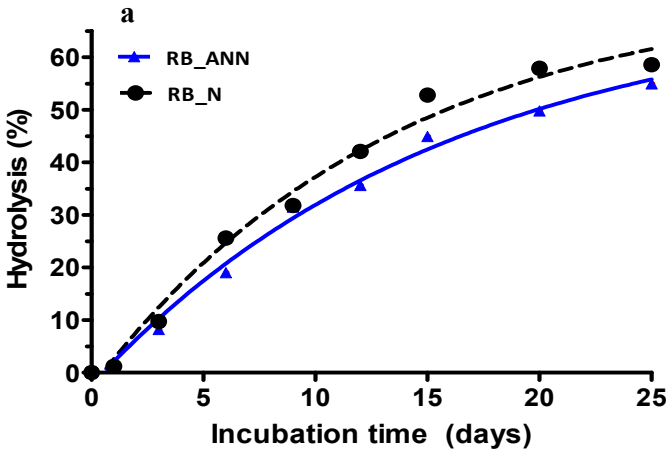
a
RB_ANN
RB_N
Hydrolysis (%)
Incubation time (days)

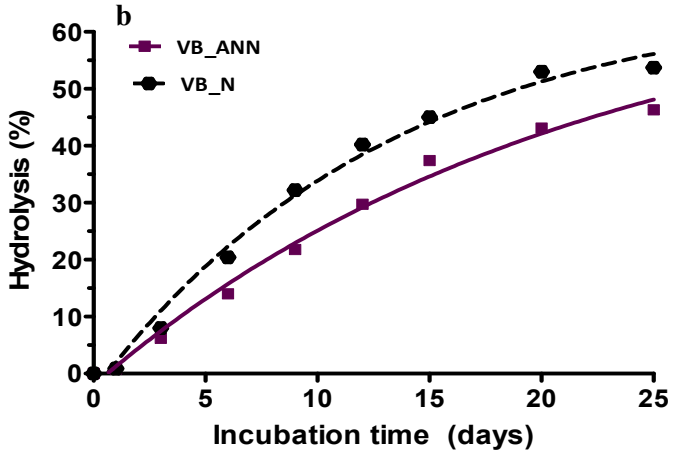
b
VB_ANN
VB_N
Hydrolysis (%)
Incubation time (days)

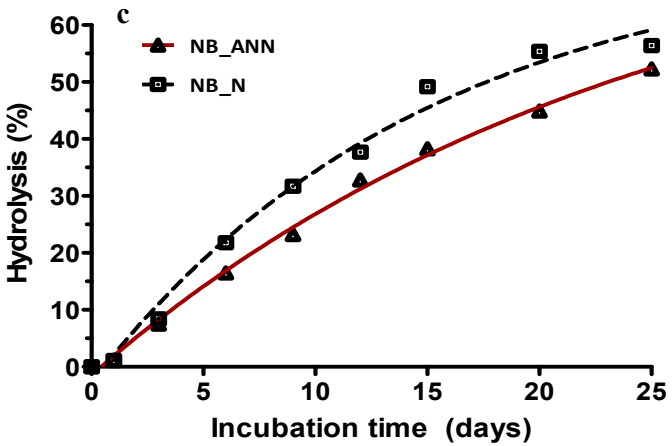
c
NB_ANN
NB_N
Hydrolysis (%)
Incubation time (days)

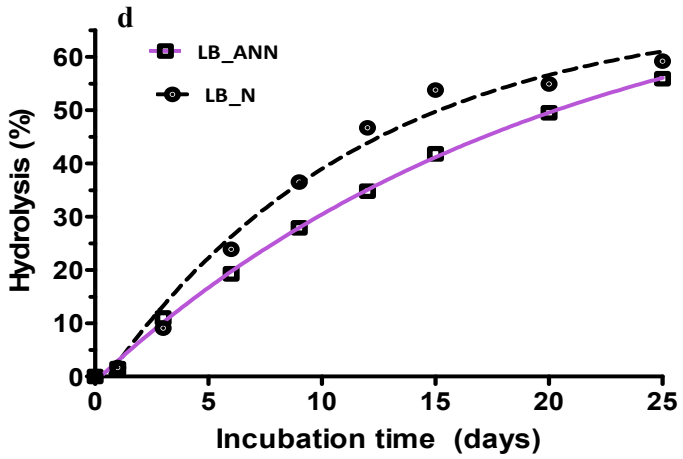
d
LB_ANN
LB_N
Hydrolysis (%)
Incubation time (days)

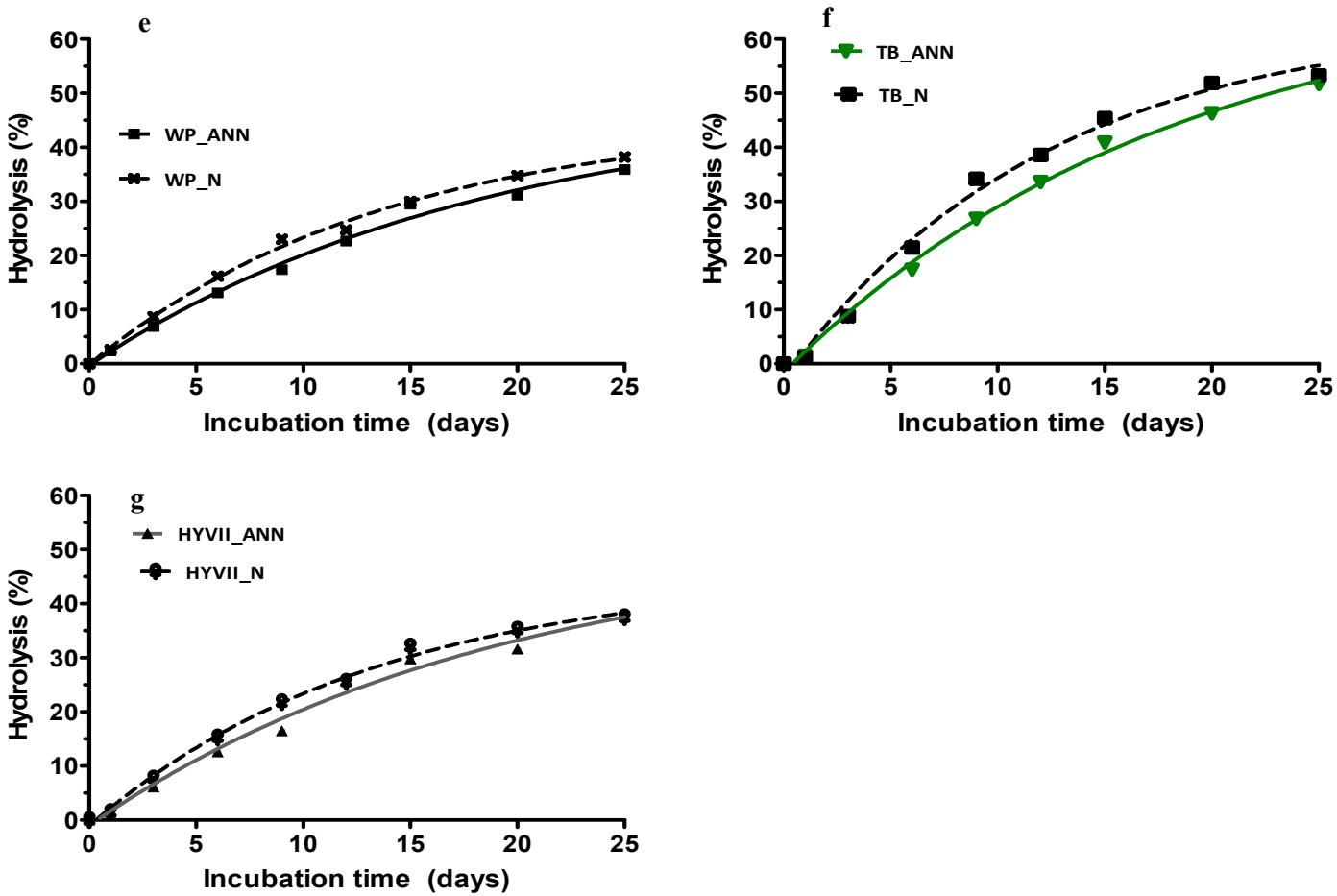

Figure 3.22: Acid hydrolysis (2.2 M hydrochloric acid) profiles of native (N) and annealed (ANN) starches of rice bean *(a)*, velvet bean *(b)*, navy bean *(c)*, lablab bean *(d)*, wrinkled pea *(e)*, tepary bean *(f)* and Hylon®VII *(g)*.

in normal pulse starches than in the high amylose starches (WP and HYVII, Figure 3.22e,g). At the end of day 15, the differences between the hydrolysis of native and annealed starches followed the order of LB>NB>RB>VB>TB>HYVII>WP (Figure 3.22d,c,a,b,f,g,e). Changes in the extent of acid hydrolysis on annealing have been attributed to the interplay of the following factors: 1) perfection and reorientation of starch crystallites; 2) formation of double helices between hydrolysed amylose chains; 3) formation of amylose-lipid complexes; 4) polymorphic changes; and 5) increased embedding of α(1→6) branch points (Hoover & Vasanthan, 1994a; Jacobs *et al.*, 1998; Waduge *et al*., 2006).

In this study, the decrease in the extent of hydrolysis of annealed high amylose starches during the rapid phase (1-9 days) was due to the strong interaction between the amylose chains (formation of amylose double helices) and ordering of amylose lipid complexes in the amorphous regions upon annealing. In normal pulse starches, the amylose leaching data (Figure 3.20) revealed that additional interactions involving amylose chains (amylose-amylose and/or amylose-amylopectin) occurred on annealing. The absence of a V-type peak in these starches reflects their lower bound lipid content and/or single helices being arranged in a non-crystalline array. The variation in the extent of decrease in hydrolysis of normal pulse starches during the initial rapid phase of hydrolysis could reflect interplay among the following: 1) differences in amylose content; 2) the amount and length of double helices formed between hydrolysed amylose chains; 3) the aggregation of formed double helices; and 4) the additional interaction between amylose-amylose and /amylose-amylopectin chains that occurred upon annealing. At the end of the day 3, annealed LB (Figure 3.33d) starch was hydrolysed to a greater extent than its native counterpart. However,

the marginal difference or increase in hydrolysis after annealing has been attributed to the increase in concentration of glucan chains in the amorphous region as a result of the enhanced order of crystalline regions (Tester *et al*., 2000) and the formation of void spaces that facilitates the accessibility of H_3O^+ into the granular interior as a consequence of the more perfect crystalline lamellae (Nakazawa & Wang, 2003).

The second slower phase mainly reflects the hydrolysis of crystalline regions. A marginal decrease/similarity in hydrolysis was observed in annealed high amylose starches (WP and HYVII, Figure 3.22e,g) compared to their native counterparts during the slower phase of hydrolysis (after 9 days). Waduge *et al*. (2006) reported that the similarity in hydrolysis was mainly due to the limited ordering of amylopectin crystallites and the unchanged DHC after annealing. The extent of the decrease in hydrolysis on annealing (beyond day 9) mainly reflects differences in the size and/or number of crystallites, the extent of crystallite perfection and/or the presence of tie chains. Jacobs and Delcour (1998) have suggested that some of the α(1→6) branch points in the amorphous regions become more embedded in the crystalline regions as a result of the perfection of starch crystallites during annealing treatment. The results suggest that the resistance of α(1→6) branch points toward acid hydrolysis was more pronounced in VB starch compared to NB and TB starches. The increase in relative crystallinity, onset temperature of gelatinization and enthalpy of gelatinization of VB and TB (Table 3.14) starches showed that crystallite perfection occurred upon annealing.

3.3.9 Impact of annealing on starch nutritional fractions

The starch nutritional fractions and expected glycemic index (eGI) of native and annealed starches, determined by *in vitro* digestibility with a mixture of pancreatin and α-amyloglucosidase, are presented in Table 3.15. In this study, starch nutritional fractions RDS, SDS and RS are defined as the amount of starch digested within the first 30 min, between 30 min and 16 h, and the residual undigested starch after 16 h, respectively (Ambigaipalan *et al.,* 2013). Among the native starches, RDS, SDS and RS followed the order of WP>HYVII>TB~RB~NB~LB>VB WP~TB>RB>NB>LB>HYVII~VB and VB>HYVII~LB>NB>RB>TB>WP, respectively. Among the native pulse starches, WP starch exhibited higher levels of RDS, SDS and eGI, and lower RS levels (Table 3.15). VB starch exhibited lower levels of RDS, SDS, and eGI, and higher levels of RS. Variations in RDS levels among the normal pulse starches were marginal, but were higher in high amylose starches (WP and HYVII). The RDS content of pulse starches (8.9-20.9 %) was within the range reported for pea (19.2 %), lentil (14.8 %) and chick pea (12.4 %) starches (Chung *et al*., 2008; Hughes *et al*., 2009), but was much higher than that reported for faba bean, black bean, and pinto bean starches (that have a range of 1.6-2.5 %) (Ambigaipalan *et al*., 2011). The SDS levels of WP and TB starches were lower than that reported by Ambigaipalan *et al*. (2011) for faba bean (76.3 %) starch, but much higher than those reported for pea (40.3 %), lentil (41.5 %), chick pea (52.0 %), black bean (43.1 %) and pinto bean (45.4 %) starches (Chung *et al*., 2008; Hughes *et al*., 2009). However, SDS levels in VB and HYVII starches were lower than the levels that were reported previously for other pulse starches (Chung *et al*., 2008; Hughes *et al*., 2009). The RS level of WP starch (5.2 %) was much lower than that reported for

Table 3.15: Nutritional fractions, hydrolysis index and expected glycemic index of native and annealed (ANN) starches determined by *in vitro* enzyme catalysed hydrolysis[1]

Starch source		RDS[2]	SDS[2]	RS[2]	HI[2]	eGI[2]
Lablab bean	Native	9.4±0.4[a]	37.3±0.4[a]	40.7±0.5[a]	42.8±0.2[a]	45.1±0.2[a]
	ANN	2.3±0.1[b]	44.5±0.7[b]	40.6±0.7[a]	47.0±0.3[b]	48.7±0.3[b]
Navy bean	Native	10.1±0.3[a]	42.4±0.9[a]	28.2±0.8[a]	48.0±0.4[a]	49.6±0.3[a]
	ANN	1.1±0.2[b]	44.1±0.4[a]	35.5±0.5[b]	39.8±0.2[b]	42.5±0.2[b]
Rice bean	Native	10.3±0.5[a]	52.3±0.8[a]	15.2±0.7[a]	60.6±0.4[a]	60.4±0.4[a]
	ANN	1.4±0.2[b]	49.9±0.5[b]	26.5±0.5[b]	48.5±0.1[b]	50.0±0.1[b]
Tepary bean	Native	10.3±0.4[a]	63.9±0.4[a]	12.4±0.5[a]	62.7±0.4[a]	62.3±0.3[a]
	ANN	6.7±0.3[b]	71.9±1.0[b]	8.0±0.7[b]	80.5±0.0[b]	77.6±0.0[b]
Velvet bean	Native	8.9±0.2[a]	28.4±0.2[a]	50.3±0.2[a]	35.9±0.2[a]	39.2±0.2[a]
	ANN	1.5±0.1[b]	27.1±0.5[b]	59.1±0.5[b]	26.6±0.2[b]	31.1±0.2[b]
Wrinkled pea	Native	20.9±0.4[a]	63.1±1.2[a]	5.2±0.9[a]	93.6±0.3[a]	88.8±0.3[a]
	ANN	4.9±0.2[b]	51.8±0.4[b]	32.6±0.3[b]	66.0±0.1[b]	65.1±0.1[b]
Hylon®VII	Native	14.3±0.5[a]	30.3±0.9[a]	42.5±0.5[a]	45.9±0.3[a]	47.7±0.2[a]
	ANN	2.6±0.1[b]	29.8±0.9[a]	54.8±0.7[b]	33.9±0.4[b]	37.4±0.4[b]

[1] All data represent the mean of triplicates. Values followed by different superscripts in each column for each starch source are significantly different ($P < 0.05$).
[2]RDS: rapidly digestible starch; SDS: slowly digestible starch; RS: resistant starch; HI: hydrolysis index; eGI: expected glycemic index

pea, lentil, chickpea, black bean, pinto bean, and faba bean starches (that have a range of 11.0-59.4 %). However, RS levels in normal pulse and HYVII starches were comparable to values reported for other pulse starches (Chung *et al*., 2008; Hughes *et al*., 2009; Ambigaipalan *et al*., 2011). The hydrolysis index (HI) and the expected glycemic index (eGI) of native starches followed the order of WP>TB>RB>NB>HYVII>LB>VB and WP>TB>RB>NB>HYVII>LB>VB, respectively. The HI and eGI values of WP starch were much greater than those reported for other pulse starches (with a range of 38.8-70 %) (Ambigaipalan *et al*., 2011; Chung *et al*., 2008). However, HI and GI values of other starches were within the range of reported values by the above authors.

The RDS fraction of granular starches mainly reflects the susceptibility of the starch chains near the vicinity of the granule surface, where the added enzyme initially acts on the surface and gradually diffuses into granule interior. The presence of granular pores, fissures and channels inside the granules facilitates the rapid penetration of enzymes to the granule interior, as obstacles on the surface (such as longer blocklets) are limited, and increases the extent of hydrolysis within a certain time period (Dhital *et al*., 2010). Thus, the RDS content of granular starches is mainly influenced by the surface characteristics and the molecular order at the granule surface. The FTIR data (Table 3.13) of native starches showed that the 1047/1022 cm^{-1} ratio followed the order of VB~RB>NB>TB>LB>HYVII>WP. The low degree of molecular order seen with WP and HYVII starches may be due to their lower amylopectin content, larger surface area (with WP>HYVII – see section 3.2.1) and/or the presence of defective crystallites which may have hindered the double helical alignment. Furthermore, the WP granules appeared extensively damaged, and

the internal layers were exposed with more splitting on the surface with distorted birefringence patterns. Thus, the RDS level of WP was greater than those of HYVII and other pulse starches due to its lower level of molecular order and its surface characteristics facilitated the hydrolytic activity of the enzymes. The marginal differences in RDS levels between TB, RB, NB and LB starches reflects the interplay among differences in molecular order at the granule surface (with RB>NB>TB>LB), specific surface area (with TB~LB>NB>RB) and the extent of cracking on the granular surface (with RB>TB>NB>LB). In contrast to other starches, the lower extent of RDS in VB starch during the first 30 min of hydrolysis could be attributed to its higher molecular order at the granular surface.

The SDS levels in native starches did not follow the same trend as observed in RDS and RS levels. The variation in SDS and RS levels among the native starches reflects the interplay between the double helical organization within the granule, association between the amylose chains within the amorphous regions and the extent of interaction between the hydrolysed starch chains during the progress of hydrolysis. The lower SDS and higher RS levels of VB starch reflects the lower susceptibility of VB toward amylolysis, which was attributed to its relative crystallinity and molecular order and the DHC being higher than that of other starches.

Jane *et al*. (1997) have reported that in B-type starches, the α(1→6) branch points of amylopectin are clustered in the amorphous regions with fewer short branch chains, whereas in A-type starches the branch points are distributed in both amorphous and crystalline regions with more short branch chains. In contrast to B-type starches, the inferior crystalline structure of A-type starch is more susceptible to enzyme-catalysed hydrolysis. Gerald *et al.* (2001) also reported that starches with

predominantly B-type unit cells were more resistant to amylolysis than starches with more A-type unit cells. Furthermore, the extent of hydrolysis followed the order of A-type (>70 %)>C-type (60 %)>B-type (35 %). In this study, HYVII and WP starches contained more B-type unit cells due to their higher amylose content with longer amylopectin branch chains. However, WP starch exhibited a higher level of SDS and a low level of RS than did HYVII starch. The higher resistance of HYVII toward amylolysis could be attributed to its molecular order, relative crystallinity, DHC and the association between amylose chains, with the amorphous regions being higher compared to WP starch. The weaker birefringence patterns and distorted quadrants of WP starch suggest that the amylopectin double helices were more accessible to the hydrolytic enzymes than in the other starches. Furthermore, the extensive granule damage and the fragmentation of compound granules further increased the susceptibility to enzyme-catalysed hydrolysis. TB, RB and NB starches exhibited an A-type polymorphic pattern, and their SDS levels are higher than that of LB starch, which showed a C-type polymorphic pattern (mixture of A- and B-type unit cells). With respect to LB and NB starches, the difference in SDS and RS levels reflected the interplay among the differences in surface area (with LB>NB), amylose content (with LB>NB), molecular order (with LB<NB) and relative crystallinity (with LB<NB). Consequently, the SDS content of LB should have been higher than that of NB. This suggests that the higher DHC (with LB>NB) and the presence of B-type unit cells in LB may reduced the influence of molecular order, relative crystallinity and surface area on the susceptibility of hydrolysis. Thus, both of the above factors contributed to the decreased SDS and increased RS levels in LB starch than NB starch. Variations in

APCLD cannot be considered as a factor influencing the SDS and RS levels, since there was no significant difference among TB, RB and NB starches.

The higher SDS and lower RS levels of TB starch suggest that the surface area of TB (0.39 m^2/g) was higher than that of RB (0.23 m^2/g) and NB (0.30 m^2/g) starches, and its relative crystallinity and molecular order lower compared to RB starch. The mechanism of amylolysis comprises both the preferential disruption of amorphous regions, as well as side-by-side hydrolysis of amorphous and crystalline regions. The preferential hydrolysis of the amorphous growth rings is facilitated by the presence of pores. Therefore, the enzyme easily gets access to the granular interior through surface pores (Blazek & Gilbert, 2010). Thus, the presence of surface cracks in TB and RB starches facilitated the preferential disruption of amorphous regions. Amylose leaching data showed that the extent of AML was higher in TB starch than in the other starches, and this reflected the weaker interactions between amylose-amylose and amylose-amylopectin chains. This would then explain the differences in SDS and RDS levels between TB and RB starches. In my previous study, RB starch was hydrolysed to a greater extent than was TB starch during 72 h of amylolysis (using α-amylase only). This suggests that the difference in DHC between TB starch (37.8 %, Table 3.4) and RB starch (31.1 %, Table 3.4), cracks on the granular surface (with RB>TB, Figure 3.1), and the hydrolytic activity of α-amylase may have contributed to the variation between these starches.

Annealing treatment decreased the RDS levels in all starches compared to their native counterparts. The extent of this decrease on annealing followed the order of WP>HYVII>NB>RB>VB>LB>TB. The decrease in RDS content on annealing reflects the change in molecular (amylose and amylopectin) realignment at the

granular surface on annealing. The FTIR data showed that the molecular order at the granular surface was increased in LB, NB, WP and HYVII starches upon annealing. However, the extent of this increase in these starches (with LB>HYVII>WP>NB) should have theoretically decreased the RDS level in the same order. However, the observed trend in RDS decrease on annealing was attributed to the interplay between the increase in molecular order, extent of interaction between amylose chains, and the crystallite realignment near the granular surface.

In this study, annealing increased SDS levels in LB, NB and TB starches, while it decreased SDS levels in RB, VB, WP and HYVII starches. After annealing, the RS level of TB starch was lower than that of the native counterpart, whereas all the other starches exhibited an increase in their RS levels. However, there was no change in the RS level of LB starch upon annealing. Annealing treatment facilitates the interaction between glucan chains and thus, annealed starches would have shown a greater resistance to enzymatic hydrolysis. However, in the case of annealed TB starch, the amorphous regions were rendered more accessible to amylolytic enzymes after annealing treatment. Chung *et al*. (2010) have reported an increase in RDS and SDS levels, and a decrease in RS levels, in field pea and lentil starches upon annealing. Wang *et al*. (2013) also reported similar results with pea starches upon annealing. The above authors also suggested that the increase in *in vitro* digestibility could be attributed to slight irreversible swelling of starch granules, loss of amylose molecules and the formation of cracks on the granule surface. However, no detectable amylose leaching was observed during the annealing treatment. Thus, irreversible swelling and the formation of cracks could have increased the enzyme susceptibility of TB starch upon annealing. In high amylose starches, the extent of decrease in SDS

and the increase in RS levels were greater in WP than in HYVII starch. Hoover and Vasanthan (1994a,b), and Jacobs *et al*. (1998) have suggested that the mobility of the amylose chains increases during annealing and results in the formation of new double helices between amylose chains, as well as increased interaction between amylose and amylopectin chains. In WP starch, the above interactions were weaker in its native state and as a result of annealing, the enhanced interactions between amylose chains in the amorphous regions would have reduced the susceptibility to enzyme-catalysed hydrolysis. As discussed earlier, the starch chains in HYVII were more densely packed than in WP starch, and the annealing treatment further increased the extent of interaction between the starch chains. Thus, RS levels in HYVII starch increased further upon annealing.

The difference in the extent of decrease in SDS levels and increase in RS levels in RB, VB and LB starches reflects the interplay between increased crystallite perfection, increased crystallinity, enhanced interactions between amylose-amylose and/or amylose-amylopectin chains and the extent of crack formation at the granule surface. Based on the above results, the majority of pulse starches used in this study with their lower extent of hydrolysis have the potential to benefit human health through sustained glycemic and insulinemic response and as a source of prebiotic carbohydrate (Ells *et al*., 2005; Rodríguez-Cabezas *et al*., 2010). The data revealed that among the pulses, velvet bean, lablab bean, and navy bean may be a good source of slowly digestible starch (SDS) and resistant starch (RS). SDS is digested slowly with a moderate glycemic and insulinemic response. RS is considered to have high nutritional value, not only by promoting beneficial microflora and colonic health, but also through reducing energy intake and prolonging satiety.

3.4 The contribution of amorphous regions to structural changes within the crystalline lamellae on annealing

The contribution of amorphous regions to the mechanism of annealing was explored using the following approaches: 1) partial acid hydrolysis and annealing treatment; and 2) cross-linking with sodium trimetaphosphate (STMP) and sodium tripolyphosphate (STPP) before and after annealing treatment.

3.4.1 Partial acid hydrolysis and annealing treatment

Acid treatment preferentially hydrolyses the less compact amorphous regions first, and then the crystalline regions of starch granules (Robin *et al.,* 1974; Biliaderis *et al.,* 1980). Pulse and high amylose maize starches were exposed to partial acid hydrolysis for up to 72 h, during which time the amorphous material was partially hydrolysed and the starch granules remained intact. The acid hydrolysed residues (lintnerised starch) taken at different time intervals were subjected to annealing for 72 h at a temperature below their individual onset of gelatinization temperatures. The annealing temperatures were chosen as a function of onset gelatinization temperature (To) of the lintnerised starches to avoid melting of starch crystallites and to facilitate glucan starch chain mobility within the granule.

3.4.1.1 ^{13}C CP/MAS NMR of native and lintnerised starches

The ^{13}C CP/MAS NMR spectra of native and acid-modified starches after 72 h of hydrolysis are presented in Figure 3.23. Signals at 94-105 and 58-65 ppm corresponded to the C1 and C6 in hexapyranoses, and the overlapping signal occurring around 68-78 ppm is linked to C2, C3, and C5, respectively (Atichokudomchai *et al*., 2004). At 103 and 95 ppm, two broad shoulders could be observed; these might arise possibly from the amorphous domains for C1, whereas the broad resonance appearing at 82 ppm would have resulted from amorphous domains

for C4 (Man *et al*., 2012). The intensities at C1 and C4 amorphous resonance appeared to decrease after 72 h of hydrolysis, and the spectra began to appear sharper. However, normal pulse starches showed a slight decrease in the intensities at C1 and C4 in comparison with WP and HYVII starches. The dramatic reduction in the resonances at 103 and 95 ppm (amorphous shoulders of the C1 peak), and the 82 ppm of C4, are due to the faster degradation of the amylose chains that contributed to the amorphous component in high amylose starches. Generally, amorphous compounds exhibit broad resonances and ordered materials give a narrow resonance.

^{13}C CP/MAS NMR of C1 resonance provides information on the crystalline and non-crystalline chains, and the multiplicity of the C1 resonance refers to the packing type of the starch granule. The C1 peak in spectra of A-type starch is a triplet, whereas it is a doublet in B-type starch (Bogracheva *et al.,* 2001; Atichokudomchai *et al*., 2004). As C-type starch is a mixture of both A- and B-type crystalline structures, the C1 spectra of the C-type starch exhibits a mixed pattern of both A- and B- types. The relative proportion of A- and B-type polymorphic forms determines the resonances in the spectra of C-type starch. C-type starch exhibits a triplet C1 spectra if the A- type crystalline structure remains predominant and a doublet C1 spectra if the B-type crystalline structure is predominant (Bogracheva *et al.,* 2001). It was difficult to ascertain the type of crystalline polymorph from the nature of C1 splitting (doublet or triplet) in native LB, RB, NB, TB and VB starches (Figure 3.14). However, both native WP and HYVII starches exhibited doublets at 100 and 101 ppm at C1, and peaks characteristic of V-amylose-lipid complexes at 103 and 32 ppm (Table 3.14). Peaks at 103 and 32 ppm were not present in the other starches. After 72 h of hydrolysis, the C1 resonance of the acid hydrolysed starches gradually became a

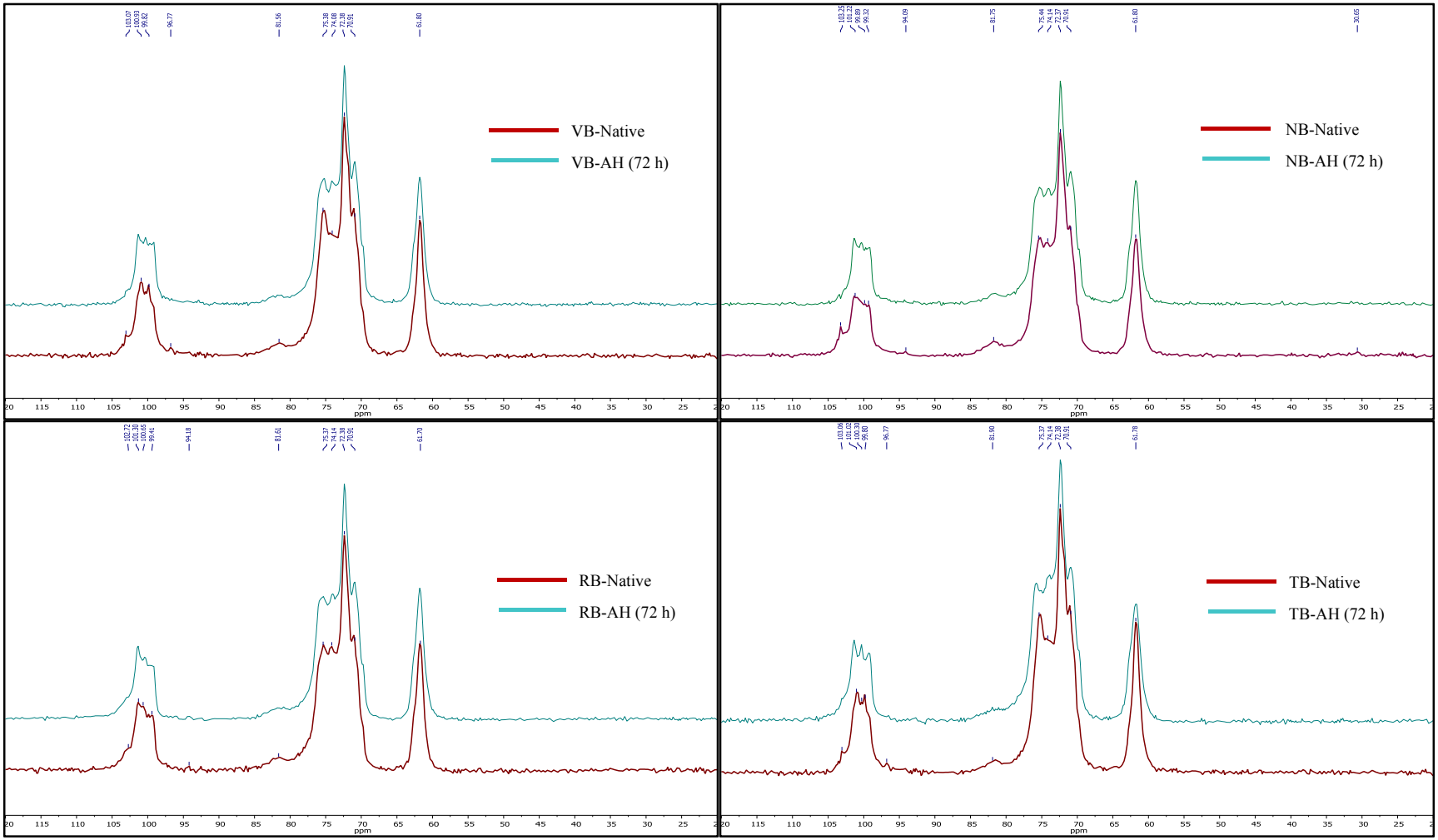
VB-Native
VB-AH (72 h)
NB-Native
NB-AH (72 h)
RB-Native
RB-AH (72 h)
TB-Native
TB-AH (72 h)
ppm

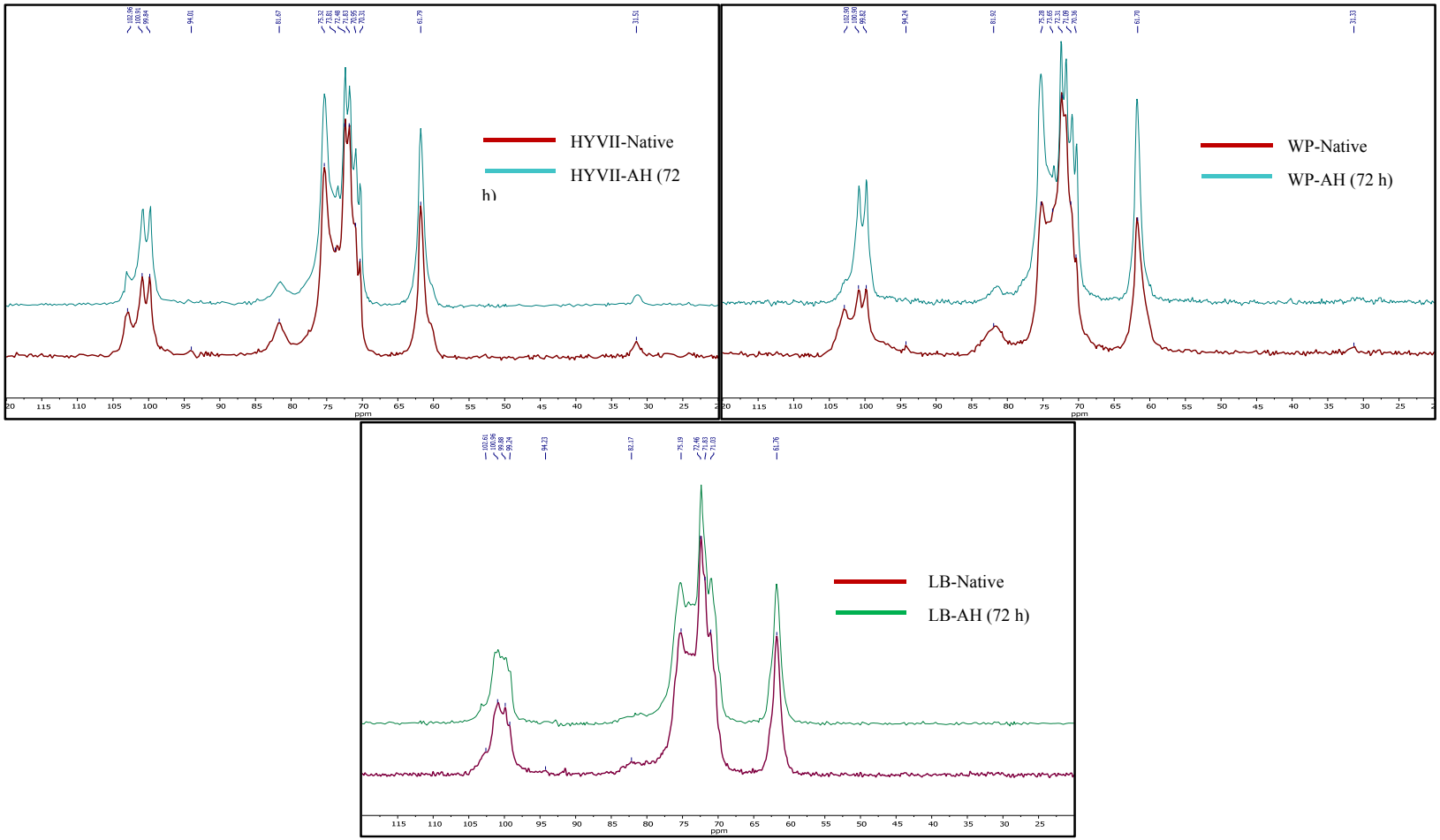

Figure 3.23: ^{13}C CP/MAS NMR spectra of native and acid hydrolysed (AH) pulse and Hylon®VII starches.

triplet in NB, TB and VB starches, whereas in WP and HYVII starches, the doublet became more prominent at 100 and 101 ppm. However, the C1 resonance of acid-hydrolysed LB starch exhibited an inconspicuous doublet or triplet, which is a characteristic feature of C-type starches (Bogracheva *et al*., 2001; Atichokudomchai *et al*., 2004). The NMR spectra of HYVII and WP starches exhibited a broad resonance with a chemical shift at 31.5 ppm, corresponding to mid-chain methylene carbons of fatty acids in the V-amylose lipid complex. In the acid-hydrolysed starches, the resonance at 31.5 ppm disappeared in WP starch, whereas a weak intensity signal was observed in HYVII starch. In contrast to WP starch, the amylose-lipid complexes present in HYVII starch appeared to be resistant to acid hydrolysis after 72 h.

3.4.1.2 Gelatinization properties of lintnerised starches

The gelatinization transition temperatures (To, Tp and Tc) and ΔHs of gelatinization for the lintnerised starches at different hydrolysis times are presented in Figure 3.24. In normal pulse starches, the gelatinization temperatures To and Tp increased up to 24 h with hydrolysis. After 72 h of hydrolysis, the endothermic peak broadened with a shifting to lower To and Tp values compared to their native counterparts (Figure 3.24). However, Tc and the gelatinization temperature range (Tc-To) increased with increasing hydrolysis time. There were only slight differences observed in ΔH during the first 12 h of hydrolysis, but ΔH decreased at the end of the hydrolysis period (at 72 h). WP starch exhibited an increase in To, Tp and Tc, but Tc-To and ΔH decreased with the progress of hydrolysis. In contrast to WP starch, HYVII showed marginal changes in gelatinization temperature with a greater decrease in ΔH after 72 h of hydrolysis.

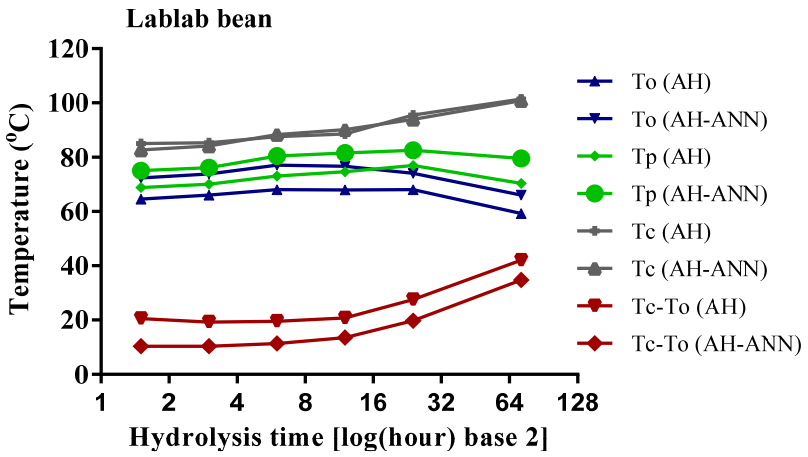
Lablab bean
Temperature (°C)
120
100
80
60
40
20
0
1
2
4
8
16
32
64
128
Hydrolysis time [log(hour) base 2]
To (AH)
To (AH-ANN)
Tp (AH)
Tp (AH-ANN)
Tc (AH)
Tc (AH-ANN)
Tc-To (AH)
Tc-To (AH-ANN)

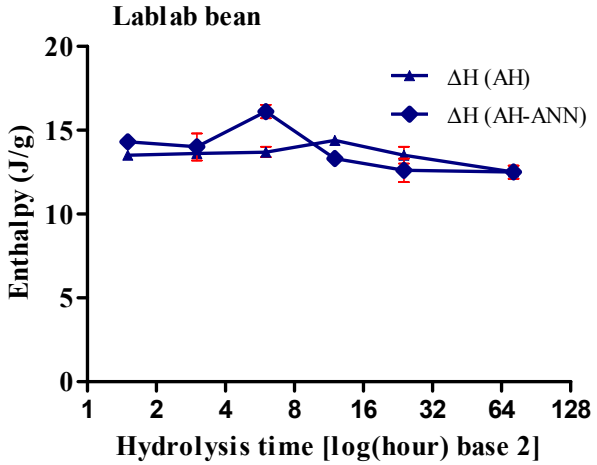
Lablab bean
Enthalpy (J/g)
20
15
10
5
0
1
2
4
8
16
32
64
128
Hydrolysis time [log(hour) base 2]
ΔH (AH)
ΔH (AH-ANN)

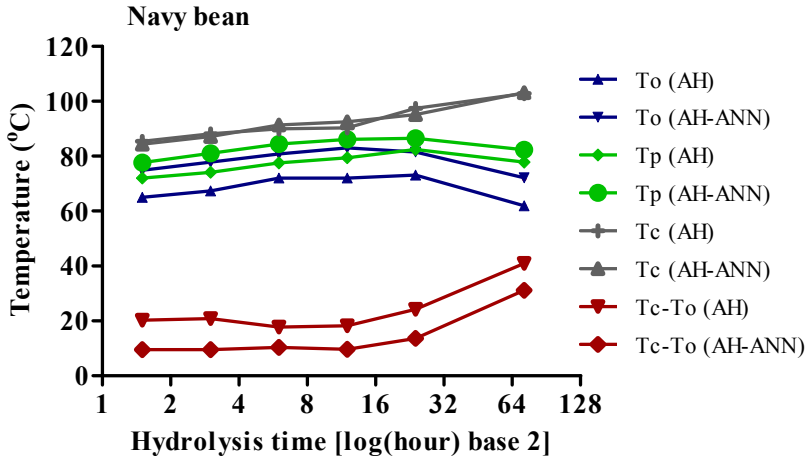
Navy bean
Temperature (°C)
120
100
80
60
40
20
0
1
2
4
8
16
32
64
128
Hydrolysis time [log(hour) base 2]
To (AH)
To (AH-ANN)
Tp (AH)
Tp (AH-ANN)
Tc (AH)
Tc (AH-ANN)
Tc-To (AH)
Tc-To (AH-ANN)

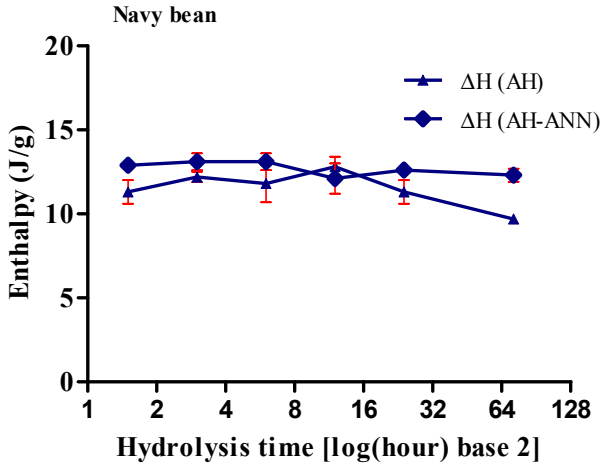
Navy bean
Enthalpy (J/g)
20
15
10
5
0
1
2
4
8
16
32
64
128
Hydrolysis time [log(hour) base 2]
ΔH (AH)
ΔH (AH-ANN)

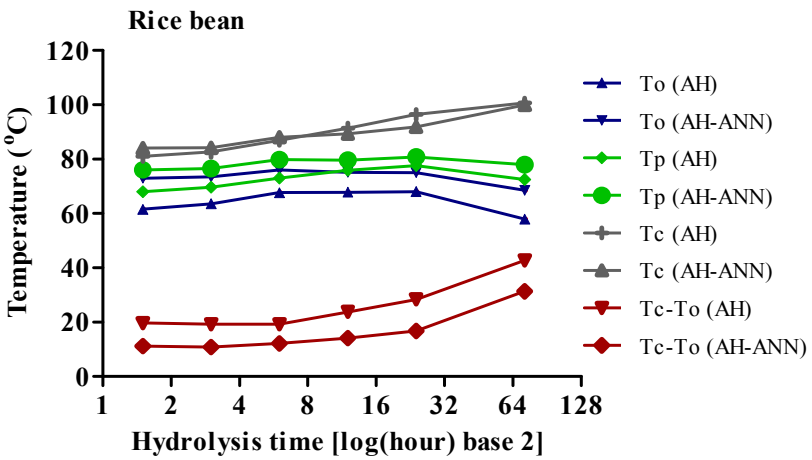
Rice bean
Temperature (°C)
120
100
80
60
40
20
0
1
2
4
8
16
32
64
128
Hydrolysis time [log(hour) base 2]
To (AH)
To (AH-ANN)
Tp (AH)
Tp (AH-ANN)
Tc (AH)
Tc (AH-ANN)
Tc-To (AH)
Tc-To (AH-ANN)

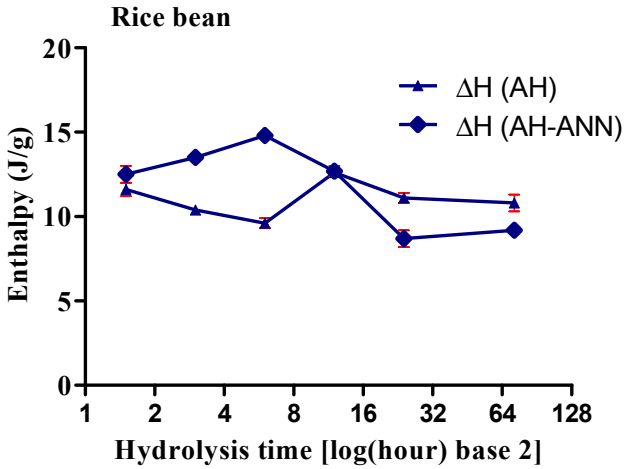
Rice bean
Enthalpy (J/g)
20
15
10
5
0
1
2
4
8
16
32
64
128
Hydrolysis time [log(hour) base 2]
ΔH (AH)
ΔH (AH-ANN)

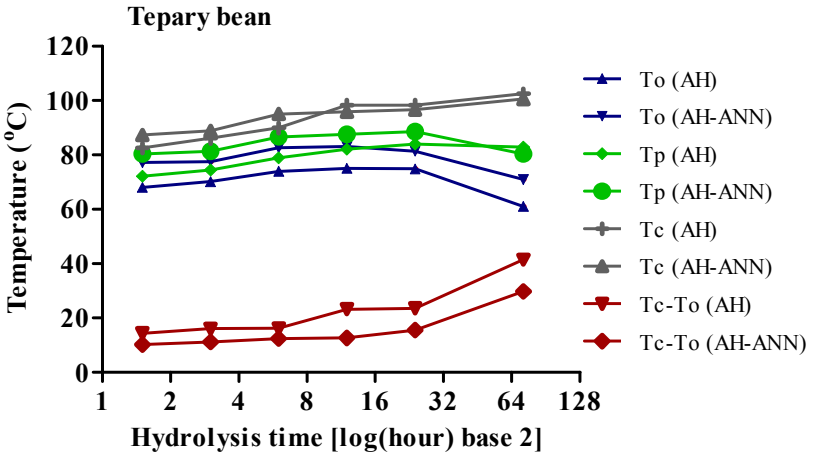
Tepary bean
Temperature (°C)
120
100
80
60
40
20
0
1
2
4
8
16
32
64
128
Hydrolysis time [log(hour) base 2]
To (AH)
To (AH-ANN)
Tp (AH)
Tp (AH-ANN)
Tc (AH)
Tc (AH-ANN)
Tc-To (AH)
Tc-To (AH-ANN)

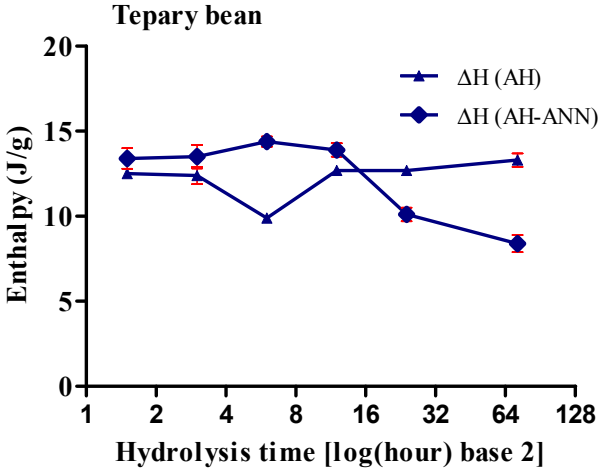
Tepary bean
Enthalpy (J/g)
20
15
10
5
0
1
2
4
8
16
32
64
128
Hydrolysis time [log(hour) base 2]
ΔH (AH)
ΔH (AH-ANN)

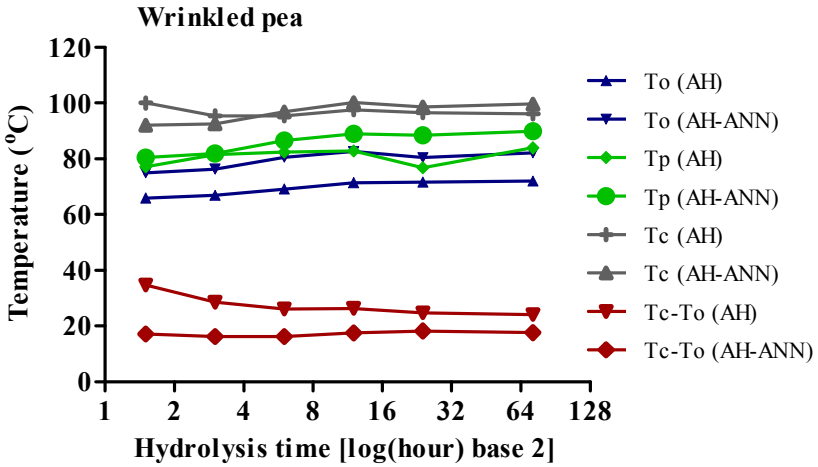
Wrinkled pea
Temperature (°C)
120
100
80
60
40
20
0
1
2
4
8
16
32
64
128
Hydrolysis time [log(hour) base 2]
To (AH)
To (AH-ANN)
Tp (AH)
Tp (AH-ANN)
Tc (AH)
Tc (AH-ANN)
Tc-To (AH)
Tc-To (AH-ANN)

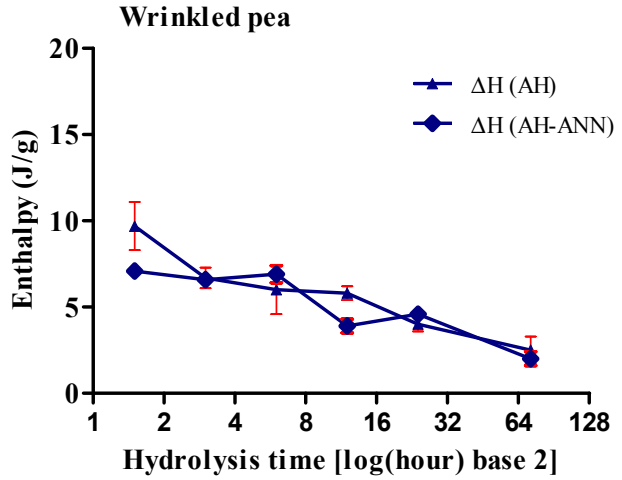
Wrinkled pea
Enthalpy (J/g)
20
15
10
5
0
1
2
4
8
16
32
64
128
Hydrolysis time [log(hour) base 2]
ΔH (AH)
ΔH (AH-ANN)

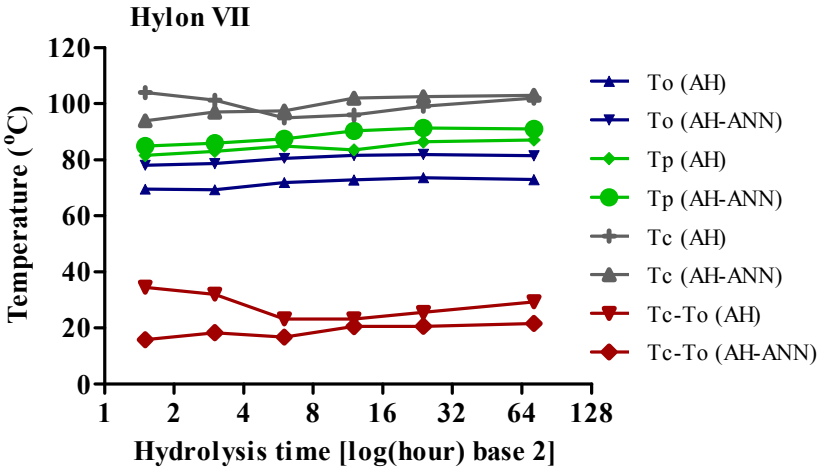
Hylon VII
Temperature (°C)
120
100
80
60
40
20
0
1
2
4
8
16
32
64
128
Hydrolysis time [log(hour) base 2]
To (AH)
To (AH-ANN)
Tp (AH)
Tp (AH-ANN)
Tc (AH)
Tc (AH-ANN)
Tc-To (AH)
Tc-To (AH-ANN)

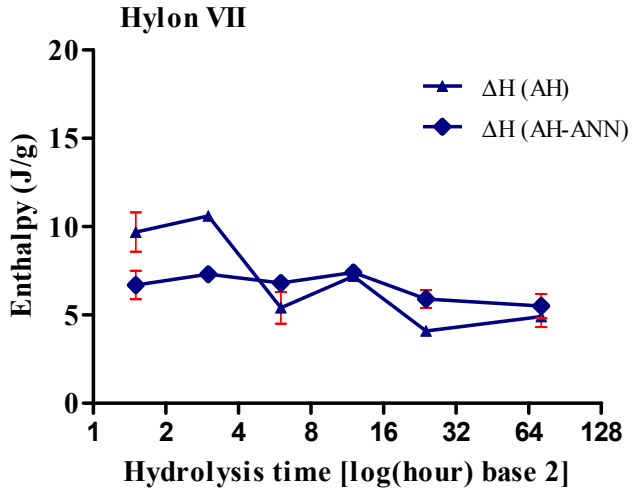
Hylon VII
Enthalpy (J/g)
20
15
10
5
0
1
2
4
8
16
32
64
128
Hydrolysis time [log(hour) base 2]
ΔH (AH)
ΔH (AH-ANN)

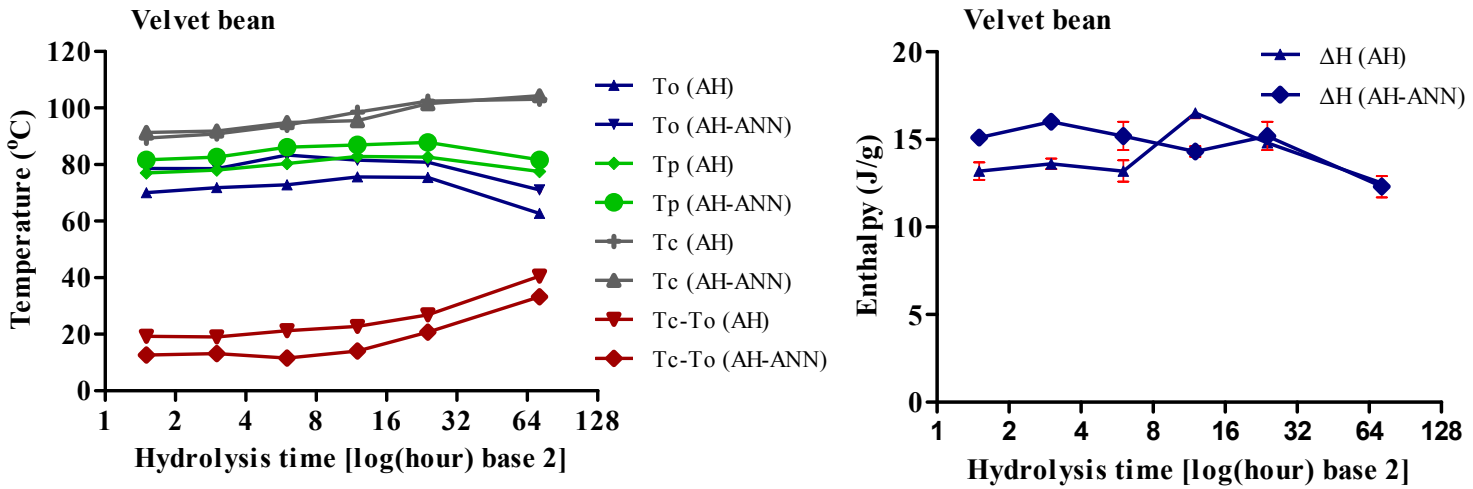

Figure 3.24: Gelatinization parameters of partially acid-hydrolysed (lintnerized) starches before and after annealing. AH: acid hydrolysed; AH-ANN: acid hydrolysed and annealed.

However, in HYVII starch, a greater extent of decrease in Tp was observed after 90 min of hydrolysis, whereas Tc, Tc-To and ΔH showed a steep decrease after 6 h of hydrolysis.

Gelatinization is a swelling driven process that involves unravelling and melting of the double helices that form from the external chains of amylopectin that are packed together in clusters (Coke & Gidley, 1992; Miao *et al*., 2001). Granular swelling is accompanied by water uptake by the amorphous regions, and it exerts stress on the amylopectin crystallites which in turn dissociates the double helices within the starch crystallites (Denovan, 1979). During the initial stages of hydrolysis, acid preferentially attacks the amorphous regions and decreases their destabilizing effect on starch crystallites (Jayakody & Hoover, 2002). In this study, the partial destruction of amorphous regions restricted the cooperative melting of starch crystallites, which was assisted by the water uptake in the amorphous regions of the granule and thus explains the increase in To and Tp upon acid hydrolysis. The higher To and Tp values indicate greater perfection of crystallites or a larger co-operative unit represented by longer chains in the crystallites and/or a larger crystallite size (Miao *et al*., 2001). Palma-Rodriguez *et al.* (2012) also reported that the subsequent reduction in the amorphous regions and rearrangement of shorter chains gave a higher proportion of crystalline material with a more ordered and stable structure, which caused an increase in Tp. Morrison *et al*. (1993a) also suggested that the higher transition temperatures observed due to the preferential hydrolysis of amorphous regions allows the formation of longer amylopectin double helices compared to the unhydrolysed amylopectin molecule, as a result of the

removal of branch points. Furthermore, the broader endothermic transition (Tc-To) shift to higher temperatures following acid hydrolysis indicated the increase in crystallinity or molecular order and greater heterogeneity of the hydrolysed products (Wang & Copeland 2012). This would then explain the increase in Tc-To in the normal pulse starches as the hydrolysis time increased. Jacobs *et al.* (1998) also reported that as a function of hydrolysis time, the endotherm shifted to higher temperatures, together with peak broadening and marginal changes in ΔH.

Native high amylose starches showed variation in their crystalline stability, where the crystallites are made up not only from amylopectin-amylopectin interactions, but also from interactions between amylose-amylose and amylose-amylopectin. Consequently, these starches produce a broader endotherm at higher temperatures. However, the disrupting effect of amylose on crystalline arrangement could be due to co-crystallization between amylose and amylopectin, and the presence of amylose tie-chains that traverse through the inter-crystalline regions. Furthermore, the presence of intermediate material also influences this crystallite disruption. Jane e*t al*. (1997) suggested that the amylopectin branching points of A-type starches scattered in both amorphous and crystalline regions, whereas in B-type starches, the branching points are mainly located in the amorphous regions, making them more susceptible to acid hydrolysis. Therefore, the high amylose starches used in this study exhibited a pure B-type polymorphic pattern. It seems plausible that the cleavage of amylose tie chains and amylopectin branch points located in the amorphous region by acid could lead to a greater realignment and self-association of starch chains forming more double helical structures (Gunaratne & Corke,

2007) and reduce heterogeneity within the crystallites. Thus, Tc-To of WP and HYVII starches was reduced with hydrolysis time compared to their native counterparts. However, the extensive hydrolysis of amylose chains restricted the re-association of these crystallites due to the abundance of the retrograded amylose chains, which in turn produced more crystallites with different stabilities. This would explain the increase in Tc-To of HYVII starch after 24 h of hydrolysis.

Biliaderis *et al*. (1980) reported an increase in To and Tc-To for smooth pea starches, together with a decrease in enthalpy, after acid hydrolysis. Gelatinization enthalpy reflects the disruption of double helical order rather than loss of the crystalline register of the granule (Cooke & Gidley, 1992). The decrease in ΔH on acid hydrolysis has been associated with the loss of some degree of order of amorphous regions and/or the hydrolysis of α(1→6) linkages located in the amorphous lamellae, especially in A-type starches (NB, RB, TB and VB). Scission of α(1→6) branch points of amylopectin would contribute to the increased helical mobility with better alignment and the perfection between adjacent double helices. As a result of this, the number of double helices unravelling and melting during the gelatinization process would decrease after acid treatment (owing to stronger interaction between adjacent double helices) (Gao *et al*., 2012). In comparison with normal pulse starches, high amylose starches exhibited a greater decrease in ΔH. These variations were attributed to a variety of factors, such as longer amylopectin branch chain lengths, higher lipid content and lipid-complexed amylose chains. DSC measures the net endothermic process and the net energy (ΔH) required to form this endotherm is influenced by the presence of free lipids in a starch

water system (Jayakody & Hoover, 2002). Biliaderis *et al*. (1985) have reported that the melting of the V-amylose-lipid complexes decreases ΔH. In this study, WP and HYVII starches contained more free lipids compared to normal pulse starches (section 3.2.1), and the greater reduction in ΔH was associated with the amount of lipid-complexed amylose chains. During the hydrolysis process, the longer amylose chains were fragmented into smaller ones and these chains would have complexed with the available free lipids to form more amylose-lipid complexes at the initial stages of hydrolysis. Furthermore, the hydrolysed amylose chains may have interacted with the double helices present within the crystalline lamella, thereby hindering their dissociation and unravelling during gelatinization. Thus, a gradual decrease in ΔH was observed in lintnerized WP and HYVII starches. The melting endotherm that occurred as a result of interaction between partially hydrolysed amylose chains cannot be detected due to the limitations (using standard aluminum pans) in the DSC analysis range beyond 130^{O}C.

3.4.1.3 Annealing of lintnerized starches

In this study, the lintnernied starches were annealed to ascertain whether, and to what extent, starches with partially or completely removed amorphous parts could still be annealed. It has been reported that the effect of annealing is less pronounced in prolonged acid-treated starches (Jacobs *et al*., 1998; Atichokudumchai *et al.,* 2001). However, the complete removal of amorphous regions would affect the granular morphology and the starch crystallites in the crystalline lamella to a greater extent. Therefore, we decided to perform annealing on partially acid hydrolysed starches with minimal alteration to the granular structure. Figure 3.24 summarizes the susceptibility of lintnerized starches to

annealing with partial removal of amorphous regions. Partially acid-hydrolysed starches exhibited an increase in To and Tp and a decrease in Tc-To upon annealing, whereas Tc and ΔH either remained unchanged or increased after annealing treatment. However, in both WP and HYVII starches, acid hydrolysis increased To and Tp, but decreased Tc-To and ΔH. The Tc values of WP starch increased with the hydrolysis, whereas in HYVII, Tc remained unchanged after 72 h of hydrolysis.

Similar effects were noticed after the annealing treatment of native pulse starches, but the extent of the changes associated with different time intervals of hydrolysis differed among the starches used in this study. The extent of changes after annealing treatment have been influenced by their granule size, their extent of interaction between the starch chains within the amorphous and crystalline regions, the presence of V-amylose-lipid complexes, crystallite organization and polymorphic composition, distribution of α(1→6) branch points between the amorphous, and crystalline regions and the presence/proportion of intermediate chains (Hoover & Vasanthan, 1994a; Morrison *et al*., 1993a; Jane *et al*., 1997; Jayakody & Hoover 2002; Vamadevan *et al*., 2014). The impact of annealing on the lintnerized starches was more pronounced in normal pulse starches than in the high amylose starches. However, both normal and high amylose starches exhibited marginal differences in their rate and extent of hydrolysis after 72 h (Figure 3.22).

Furthermore, during the first 72 h, acid preferentially hydrolysed the longer amylose chains present in the amorphous growth rings and amorphous lamellae into smaller fragments, and the fragmented amylose chains mainly occupied the amorphous

regions. Depending on the hydrolytic activity of H_3O^+, the hydrolysed amylose chains having optimum chain lengths (CL<120) retrograde rapidly and form new double helices during the initial stages of hydrolysis (Gidley & Bulpin 1987; Morrrison *et al*., 1993a). In addition, the long amylopectin chains (B_2, B_3 and B_4) that span to inter-crystalline regions are also susceptible to acid hydrolysis (Morrison *et al*., 1993a). This would destabilize the backbone structure of amylopectin and separate crystallites at the lamellar level. As discussed earlier, A-type starches have relatively fewer branch points of amylopectin located in the amorphous regions compared to B or C-type starches. NB, RB, TB and VB starches exhibited an A-type polymorphic pattern with marginal differences in their amylopectin content (Table 3.1). Therefore, we speculate that the amylopectin branch points of these starches showed a similar extent of susceptibility to mild acid compared to other starches (B or C-type starches). Consequently, the lintnerized starches of NB, RB, TB and VB responded to the annealing treatment in a similar way. WP and HYVII starches exhibited a pure B-type polymorphic pattern and their branching points are mainly located in the amorphous regions. During acid hydrolysis, the branching points of these starches would be more vulnerable and would have yielded similar types of crystallites with long chain lengths, since the proportion of long amylopectin chains is higher in high amylose starches compared to normal pulse starches. Therefore, the extent of variation in their Tc-To was lower during the progress of hydrolysis and showed a similar response to the annealing treatment.

The hydrolysis of amylopectin branch points induces the elongation of double helices due to their increased mobility (Gao *et al*., 2012). Furthermore, the preferential

hydrolysis in the starch granules eliminates the disruptive effect of amylose on the alignment of amylopectin chains within the crystalline lamellae (Gao *et al*., 2012), and this could be more pronounced in high amylose starches. During annealing treatment, the plasticizing effect of water increases the glucan chain mobility within the bulk amorphous regions and then enters the amorphous lamella regions of the semi-crystalline growth rings (Perry & Donald, 2000). Subsequently, the increased mobility in the amorphous regions induces movement in the crystalline lamella and enhances the order of the amylopectin double helices. The gradual erosion of the amorphous regions by acid hydrolysis may reduce the hindrance between double helical chains and facilitate crystallite perfection. Therefore, the crystalline regions are closely packed together, increasing the intermolecular forces, such as van de Waals forces and H-bonding, between the starch chains. In addition, the scission of the α(1→6) amylopectin branch points located in the amorphous regions may also allow the amylopectin branch points to be more mobile during the annealing process, leading to a better realignment within the crystallites and promote the elongation of crystallites. The above changes contributed to the further increase in To, Tp and Tc of the lintnerized annealed starches compared to their native, non-hydrolysed annealed starches. Therefore, the amorphous regions played a significant role in optimising the ordering of double helices in the crystalline regions, increasing the homogeneity and the perfection of the crystalline order, resulting in reduction of the gelatinization temperature range (Tc-To) in lintnerized starches (Tester *et al*., 1998; Tester & debon 2000).

Jacobs *et al*. (1998) found that the partial removal of the amorphous regions within wheat and pea starches decreased their susceptibility to annealing. The structural changes that occurred during acid hydrolysis in the amorphous regions influenced the changes in the crystalline regions during annealing treatment. The results of this study showed that the amorphous regions contributed to the molecular mechanism of annealing by influencing the realignment of glucan chains in the crystalline regions, which in turn produced starches with higher thermal stability, to a certain extent.

3.4.2 Cross-linking with sodium trimetaphosphate and sodium tripolyphosphate

Cross-linking reactions are generally performed using bifunctional or multifunctional reagents that are capable of forming both intramolecular and intermolecular linkages between the hydroxyl groups of adjacent starch chains (Huber & BeMiller, 2009). In this study, normal pulse starches (LB, NB, TB and VB) and high amylose starches (WP and HYVII) were subjected to cross-linking with STMP and STPP to introduce covalent bonds between glucan chains, primarily within the amorphous regions. The cross-linked starches were then annealed at a temperature 6°C below their onset temperature of gelatinization. In order to compare the extent of changes in the crosslinked starches during the annealing treatment, the annealed starches also were cross-linked with the same reagents.

3.4.2.1 The impact of annealing on the extent of cross-linking

The total phosphorous content of control, cross-linked native and annealed starches were quantified using inductively coupled plasma-optical emission spectrometry (ICP-OES), which is sensitive to lower phosphate levels in starch. Table 3.16 shows the

phosphorous content, degree of substitution (DS) and reaction efficiency (RE) of native and annealed cross-linked starches. The total phosphorous content of control starches ranged from 0.001 to 0.027 % (w/w, dwb), which represented the phosphorous content of starches before crosslinking (of which the order was TB>LB~HYVII~WP>VB~NB). The total phosphorus levels of cross-linked starches were higher than those of control starches, indicating that the STMP/STPP reagents reacted with the starch (Table 3.16). In normal pulse starches, the annealed cross-linked starches exhibited a higher level of phosphorous content compared to their native cross-linked starches. In the high amylose starches, an increased level of phosphorous content was observed in native cross-linked samples in comparison to their annealed cross-linked samples. However, LB starch showed only a marginal difference in phosphorous content between the native and annealed cross-linked starches.

On the basis of the phosphorous content in control and cross-linked starches, the degree of substitution (DS) and reaction efficiency (RE) were calculated (Table 3.16). In normal pulse starches, the DS and RE of annealed starches were higher than those of their native counterparts. However, annealed high amylose starches showed lower DS and RE values when cross-linked compared to their native counterparts. In the case of LB starch, no differences in DS and RE were observed between the native and annealed cross-linked starches. Lim *et al.* (1994) reported that cereal starches contain phosphorus, mainly in the form of phospholipids and phosphate monoesters, whereas legume starches contain mainly phosphate monoesters with a trace amount of phospholipids. Therefore, the observed levels of phosphorous in control pulse starches were primarily due to the

Table 3.16: Phosphorous content, degree of substitution (DS) and reaction efficiency (RE) of cross-linked starches

Starch source	Treatment	Phosphorous (%)	DS	RE (%)
Lablab bean	Control[1]	0.013±0.010[a]		
	CL	0.360±0.015[b]	0.0183±0.0003[a]	16.0±0.2[a]
	ANN-CL	0.367±0.001[b]	0.0187±0.0004[a]	16.4±0.4[a]
Navy bean	Control[1]	0.002±0.001[a]		
	CL	0.210±0.002[b]	0.0109±0.0001[a]	9.6±0.1[a]
	ANN-CL	0.353±0.013[c]	0.0185±0.0007[b]	16.2±0.6[b]
Tepary bean	Control[1]	0.027±0.003[a]		
	CL	0.187±0.003[b]	0.0084±0.0000[a]	7.4±0.0[a]
	ANN-CL	0.323±0.005[c]	0.0156±0.0004[b]	13.7±0.4[b]
Velvet bean	Control[1]	0.001±0.000[a]		
	CL	0.300±0.004[b]	0.0158±0.0002[a]	13.8±0.2[a]
	ANN-CL	0.338±0.004[c]	0.0178±0.0002[b]	15.6±0.2[b]
Wrinkled pea	Control[1]	0.009±0.006[a]		
	CL	0.356±0.007[c]	0.0184±0.0001[b]	16.1±0.1[b]
	ANN-CL	0.098±0.010[b]	0.0047±0.0003[a]	4.1±0.2[a]
Hylon®VII	Control[1]	0.010±0.006a		
	CL	0.292±0.013[c]	0.0149±0.0004[b]	13.0±0.3[b]
	ANN-CL	0.221±0.006[b]	0.0111±0.0000[a]	9.7±0.0[a]

Values followed by different superscripts in each column for each starch source are significantly different ($P < 0.05$).

[1]Refer to starches subjected to all cross-linking conditions without STMP and STPP.

ANN-CL-Annealed cross-linked; CL-native cross-linked.

presence of phosphate monoesters, whereas in HYVII starch, phospholipid formed the major component.

According to the Code of Federal Regulations of the U.S. Food and Drug Administration (2016), the residual phosphorous content of starch cross-liked with STMP alone and or combination of STMP/STPP should not exceed 0.04 % and 0.4 %, respectively. In this study, a mixture of STMP/STPP (99:1, weight basis) used for the cross-linking reaction resulted in a residual phosphorous content of 0.098-0.370 %, which was within the maximum allowable limit (0.4 %) of residual phosphorous content. The cross-linking of starches was carried out at a pH of 11.5 and sodium sulfate (Na_2SO_4) was used as a stabilizing salt to enhance the reaction with STMP (Yangsheng & Seib, 1990; Woo & Seib, 1997). The crosslinking reaction using STMP and STPP at pH 11.5 possibly would lead mainly to distarch phosphate cross-links, while monoesters are formed as monostarch monophosphate (MSMP) (Singh *et al.*, 2007). At pH levels below 6, the latter (MSMP) would be expected to predominant (Kasemsuwan & Jane, 1994).

Despite the differential granular reaction patterns observed for the various cross-linking reagents, all cross-linking reactions are thought to occur primarily within the granule amorphous regions. This conclusion was derived from the similarities in X-ray diffraction patterns between cross-linked and unmodified starches (Hoover & Sosulski, 1986; Zheng *et al.*, 1999). Cross-linking, when performed using STMP and STPP, can cause both the reagents to penetrate into the interior of the starch granule and result in better distribution (Hirsch & Kokini, 2002). Differences in the extent of cross-linking (DS and RE) between native and annealed starches suggest that the changes which occurred

mainly in the amorphous regions either increased or reduced the extent of cross-linking. The normal pulse starches used in this study (LB, NB, TB and VB) exhibited a marginal difference in amylopectin chain length distribution and the amylose content being ranged from 26.5 to 32.1 % (Table 3.1). However, these starches differed with respect to the extent of packing of amylose chains within the amorphous domains, double helical organization within the amylopectin crystallites, extent of interaction between starch chains (amylose-amylose, amylose-amylopectin and amylopectin-amylopectin), and the distribution of amylopectin branch points. Consequently, cross-linking of native pulse starches at the same molar concentration resulted in different levels (DS) of cross-linking.

Annealing has been shown to induce structural changes within the amorphous and crystalline regions, thereby facilitating improved alignment and registration of amylopectin double helices within the crystalline domains (Tester & Debon, 2000; Kieseleva *et al.*, 2004; Gomand *et al*., 2012). In addition to this, annealing disrupts the weakest crystallites (Tester *et al*., 1998), allowing for subsequent recrystallization, restructuring or both, for enhancement of higher molecular order to provide greater homogeneity among crystallites (Tester *et al*., 2000; Jayakody & Hoover, 2008; Rocha *et al*., 2011, 2012; Vamadevan *et al*., 2013). Consequently, in normal pulse starches, annealing could have increased the availability of the hydroxyl groups in the adjacent glucan chains, especially in the amorphous regions which, in turn, would increase the extent of cross-linking.

Tester and Debon (2000) have suggested that annealing treatment enables the preferential hydration, chain mobility and structural rearrangement of starch chains within

granule amorphous regions. This results in an increased Tg and rigidity of granule amorphous regions. The close packing of amylose chains (without forming double helices) facilitated the accessibility of cross-linking reagents to the hydroxyl groups of anhydroglucose units and promoted intermolecular cross-linking between the starch chains. These linkages could possibly occur between C_2 and C_2/C_3, C_6 and C_6, or C_6 and C_2/C_3 of anhydroglucose units (Liu *et al*., 2014), thus forming a multidimensional space network structure. It seems plausible that annealed starches of normal pulses (NB, TB and VB) were more highly crosslinked than their native counterparts. However, the annealed high amylose starches exhibited a lower degree of substitution in comparison with normal annealed pulse starches. In high amylose starches, the increase in amylose content could lead to an accumulation of unordered amylose chains in amorphous lamellae, as well as an accumulation of amylose tie chains in crystalline lamellae. These amylose tie chains act as defects within double-helical crystalline packing and, therefore, weaken the crystalline order (Jenkins & Donald, 1995; Tester & Debon, 2000; Genkina *et al*., 2004). Thus, the high amylose starches cross-linked to a greater extent in their native state. However, annealing treatment increased the crystal thickening and co-crystallization between amylose and amylopectin chains. In addition to this, annealing also diminished the crystalline defects by enhancing the mobility of the starch chains in the amorphous regions. These changes restricted the reaction sites for cross-linking and thus reduced the DS in the annealed starches. The extent of this reduction was more pronounced in WP starch than in the HYVII starch. This could be due to the differences in their packing arrangement of amylose chains and the presence of intermediate chains.

3.4.2.2 Gelatinization parameters of control and cross-linked starches

Table 3.17 summarizes the gelatinization transition parameters of the control, annealed (ANN), cross-linked (CL), cross-linked followed by annealing (CL-ANN) and cross-linked after annealing (ANN-CL) samples of normal pulse (LB, NB, TB and VB) and high amylose (WP and HYVII) starches. The control starches of LB, NB, TB, VB and HYVII, which were subjected to all cross-linking conditions without STMP and STPP, exhibited a slightly lower To (within 3°C) and enthalpy of gelatinization (ΔH) compared to their native counterparts (Tables 3.14). However, Tc and Tc-To increased in all of the control starches, whereas in HYVII starch Tc and Tc-To decreased. The extent of decrease in ΔH was more pronounced in control starches of HYVII (4.5 J/g) and TB (3.7 J/g) compared to their native starches (Table 3.14). In contrast to native cross-linked starches (CL), cross-linked and annealed starches (CL-ANN) showed an increase in To and Tp, whereas Tc-To decreased. With the exception of TB and HYVII starches, there was no significant difference in Tc and ΔH observed after the annealing of cross-linked starches. The extent of increase in To and Tp between CL and CL-ANN starches followed the order of WP>LB>NB~VB>TB>HYVII and LB>NB>WP>VB>TB>HYVII, respectively.

For normal pulse starches (NB, TB and VB), the extent of increase in To and Tp between control and annealed starches (ANN) was more pronounced than was observed for CL and CL-ANN starches. Furthermore, the magnitude of decrease in Tc-To was also greater between control and ANN starches versus CL and CL-ANN starches. CL-ANN starches of WP behaved differently from other starches, as they exhibited higher To and

Table 3.17: Gelatinization parameters of control and cross-linked starches[1]

Starch source	Treatment	Gelatinization transition parameters (°C)				
		To[2]	Tp[2]	Tc[2]	Tc-To[3]	ΔH[4](J/g)
Lablab bean	Control[5]	60.5±0.2^{a}	66.4±0.4^{a}	83.0±0.4^{b}	22.5±0.7^{c}	13.2±0.5^{bc}
	ANN	67.9±0.1^{b}	70.9±0.5^{b}	79.3±0.8^{a}	11.4±0.7^{a}	12.1±0.4^{ab}
	CL	60.2±0.4^{a}	66.3±0.1^{a}	87.8±0.3^{c}	27.5±0.0^{d}	14.4±0.3^{c}
	CL-ANN	68.7±0.6^{b}	72.0±0.2^{bc}	86.7±0.4^{c}	18.0±0.2^{b}	12.8±0.5^{ab}
	ANN-CL	69.1±0.0^{b}	72.7±0.0^{c}	88.2±0.1^{c}	19.1±0.1^{b}	11.5±0.0^{a}
Navy bean	Control[5]	64.0±0.0^{a}	72.0±0.1^{b}	87.0±0.5^{b}	22.9±0.6^{d}	11.5±0.4^{a}
	ANN	74.5±0.2^{c}	77.7±0.1^{d}	83.8±0.4^{a}	9.3±0.3^{a}	12.0±0.6^{ab}
	CL	62.8±0.5^{b}	70.6±0.4^{a}	88.5±0.8^{bc}	25.6±0.3^{e}	13.9±0.6^{c}
	CL-ANN	69.9±0.0^{d}	74.8±0.1^{c}	89.4±0.4^{cd}	19.5±0.4^{c}	13.6±0.0^{bc}
	ANN-CL	76.9±0.3^{e}	80.8±0.2^{e}	90.8±0.4^{d}	13.8±0.0^{b}	10.8±0.2^{a}
Tepary bean	Control[5]	65.3±0.9^{a}	70.4±0.0^{a}	84.0±0.1^{ab}	18.7±0.7^{c}	10.8±0.1^{a}
	ANN	74.4±0.0^{c}	77.0±0.0^{d}	83.5±0.1^{a}	9.1±0.0^{a}	13.4±0.2^{c}
	CL	65.2±0.0^{a}	71.6±0.1^{b}	84.7±0.3^{b}	19.5±0.2^{c}	12.3±0.0^{bc}
	CL-ANN	70.4±0.1^{b}	74.5±0.3^{c}	83.2±0.4^{a}	12.8±0.3^{b}	13.0±0.2^{c}
	ANN-CL	77.8±0.1^{e}	80.6±0.3^{e}	87.7±0.3^{c}	10.7±0.6^{a}	11.7±0.7^{ab}
Velvet bean	Control[5]	69.5±0.3^{a}	77.1±0.5^{a}	90.1±0.4^{b}	20.6±0.1^{d}	14.2±0.3^{ab}
	ANN	79.1±0.0^{c}	81.8±0.1^{bc}	88.2±0.6^{a}	9.0±0.6^{a}	14.1±0.7^{ab}
	CL	69.0±0.0^{a}	77.4±0.1^{a}	92.2±0.5^{c}	23.2±0.5^{e}	16.3±0.2^{c}
	CL-ANN	75.9±0.2^{b}	80.7±0.5^{b}	92.1±0.2^{c}	16.2±0.3^{c}	15.4±0.1^{bc}
	ANN-CL	78.2±0.5^{c}	82.6±0.1^{c}	90.4±0.2^{b}	12.2±0.3^{b}	13.2±0.2^{a}
Wrinkled pea	Control[5]	62.6±0.2^{a}	77.5±1.7^{a}	94.1±0.6^{b}	31.4±0.4^{d}	6.0±1.1^{a}
	ANN	72.5±0.4^{c}	78.0±0.3^{a}	90.2±0.2^{a}	17.8±0.1^{a}	5.8±0.2^{a}
	CL	66.8±0.3^{b}	80.7±0.8^{a}	97.2±0.1^{c}	30.4±0.2^{d}	7.2±0.4^{a}
	CL-ANN	78.1±0.0^{d}	84.7±0.2^{b}	96.2±0.7^{c}	18.1±0.6^{a}	6.6±0.7^{a}
	ANN-CL	71.5±0.1^{c}	77.7±0.1^{a}	93.0±0.3^{b}	21.5±0.2^{c}	6.2±0.4^{a}
Hylon®VII	Control[5]	69.6±0.1^{a}	79.7±0.1^{a}	93.7±0.3^{a}	24.1±0.2^{a}	5.7±0.5^{a}
	ANN	75.4±0.0^{c}	84.4±0.6^{ab}	102.6±0.7^{c}	27.2±0.7^{b}	11.5±0.1^{d}
	CL	71.4±0.2^{b}	83.0±2.8^{ab}	94.8±0.3^{a}	23.4±0.5^{a}	8.2±0.3^{bc}
	CL-ANN	76.0±0.3^{c}	83.7±0.0^{ab}	98.2±0.2^{b}	22.2±0.5^{a}	9.6±0.1^{c}
	ANN-CL	78.3±0.2^{d}	85.1±0.5^{b}	102.5±0.4^{c}	24.2±0.5^{a}	7.3±0.7^{ab}

[1]Values followed by different superscripts in each column for each starch source are significantly different ($P < 0.05$). Starch: water ratio (1:3 w/w. dry basis).

[2]To, Tp and Tc indicates the onset, peak, and conclusion temperatures, respectively.

[3](Tc-To) represents the gelatinization temperature range.

[4] Enthalpy of gelatinization expressed in J/g of dry starch.

[5] Refer to starches subjected to all cross-linking conditions without STMP and STPP.

Tp with respect to their annealed starches, whereas these (To and Tp) parameters remained unchanged in LB starch. Tc of CL starches remained unchanged after annealing treatment. It is evident from the data that the gelatinization transition parameters (To and Tp) of ANN-CL starches of NB, TB and VB were higher than that of their CL-ANN samples. This could be attributed to the higher DS in the annealed starches compared to their native counterparts. The DS of NB, TB and VB were significantly higher in ANN-CL starches. It was observed that in LB starch, there was only a marginal difference in the DS values between CL-ANN and ANN-CL treatment (Table 3.16). This is reflected in the DSC results, which indicate a marginal difference between the To, Tp and Tc values of ANN-CL and CL-ANN samples. In the case of high amylose starches, the To, Tp and Tc values decreased in ANN-CL starches versus CL-ANN starches. This also can be explained by the significant differences in the DS between the CL and ANN-CL starches (Table 3.16).

The differences observed in the gelatinization parameters between control and native starches could be attributed to the partial unwinding of double helices during the modification process in the presence of sodium hydroxide at 45°C. It seems plausible that the majority of -OH groups in the anhydrous glucose units were ionized at high pH levels (>11.5) at an elevated temperature (Suortti *et al*., 1998). Therefore, the development of negative charges in the adjacent anhydrous glucose units induced repulsion between glucan chains, which in turn reduced glucan chain interactions within the granular starches. Furthermore, the weakest crystallites were more vulnerable to these changes and melted at lower temperatures. These changes mainly occurred in the bulk amorphous and

intercrystalline amorphous regions where most of the amylose chains were located and had direct contact with the solvent. Since the majority of the cross-linking between the glucan chains occurred in the amorphous regions of starch granules, the mobility of the glucan chains, particularly the amylose chains, was restricted. The results of this study suggest that the cross-linking of starches with STMP/STPP decreased the extent of interaction between starch chains during the annealing treatment, which in turn reduced the perfection of existing crystallites upon annealing. Furthermore, the extent of these changes differed between normal pulse starches and high amylose starches due to the structural differences that exist in both amorphous and crystalline regions.

3.5 Summary and conclusions

Composition, morphology, structure, and physicochemical properties of starches isolated from lablab bean, navy bean, rice bean, tepary bean and velvet bean were determined. The results of this study showed that the starches differed significantly with

	LB	NB	RB	TB	VB
Amylose content					
Granule size					
Specific surface area					
Cracks on granule surface					
Molecular order at the granule periphery					
Relative crystallinity					
Double helical content					
Onset temperature of gelatinization (To)					
Peak temperature of gelatinization (Tp)					
Gelatinization temperature range (Tc-To)					
Swelling factor (60-80°C)					
Amylose leaching (60-80°C)					
Susceptibility to α-amylase (PPA)					
Pasting temperature					
Susceptibility to acid hydrolysis (> 9 days)					
Peak viscosity					
Thermal stability					
Setback					

respect to the following factors:

The colour intensity decreases with the decending order for each factor:

> > > >

However, amylopectin chain length distribution and enthalpy of gelatinization were not significantly different among the starches. Differences in physicochemical properties were influenced by the interplay among differences in morphology, composition and

structure. The results indicated that among the starches, only velvet bean would be suitable in its native state for incorporation into thermally processed and frozen foods, due to its higher thermal stability, higher resistance to shear and lower extent of set-back. All other starches would require physical and/or chemical modification to render them suitable as ingredients in food products.

The *in vitro* amylolysis study revealed the variations in susceptibility of the pulse and high amylose maize (Hylon®VII) starches towards amylolysis by pancreatin and amyloglucosidase. The results showed that predominantly amorphous regions of the granules were degraded during the progress of hydrolysis after 24 h. Differences in hydrolysis among the starches were mainly influenced by differences in molecular order, RC, DHC, organization of amylose chains within the amorphous domains and the extent of interaction among hydrolysed chains. Amylose content, starch damage, surface area and granule size played a secondary role in hydrolysis. Furthermore, the pulse starches used in this study (VB, LB and NB) with their lower extent of hydrolysis have potential to benefit human health through moderation of the glycemic response and as a source of prebiotic carbohydrate. The data obtained in this study will enable food processors to optimize reaction conditions for modifying pulse starch structure to a level that could improve the digestibility characteristics of pulse-starch-based foods. Starches with modified digestibility characteristics can be prepared using physical and/or chemical modification techniques which increase the RS and SDS contents with a substantial reduction of RDS content. Therefore, the development of pulse starches with higher

levels of RS would allow them to be used in unique apllications such as bakery products, noodles and fat replacers.

Granular pulse and Hylon®VII starches were annealed at 10ºC below the onset temperature of gelatinization in excess water (80 %) for 72 h. The effect of annealing on morphology, structure and physicochemical properties of pulse and high amylose maize starches were investigated. In all starches, granular morphology remained unchanged on annealing. The results showed that annealing increased onset (To) and mid-point (Tp) temperatures, whereas the gelatinization temperature range (Tc-To) was decreased. The increase in Tp and decrease in Tc-To suggest that annealing improved the double helix register by decreasing heterogeneity within the crystalline lamellae. However, gelatinization enthalpy (ΔH) remained unchanged in LB, NB, RB and WP starches but increased in others (HVII>VB>TB) upon annealing. Molecular order at the granular surface increased in LB, NB and HVII starches upon annealing, but remained unchanged in other starches. The X-ray diffraction patterns of pulse starches after annealing remained unchanged. However, annealing treatment resulted in more efficient packing of amylopectin double helices within the crystalline lamellae in all starches, which increased the relative crystallinity of the annealed starches. Swelling factor and amylose leaching of annealed starches were lower than their native counterparts in the temperature range of 70-90°C. Annealing treatment decreased peak, breakdown, final and set back viscosities, but increased peak temperature and peak time. However, TB starch showed an increase in final and setback viscosities upon annealing. The changes in the viscosity profile of pulse starches reflect the increased granular stability through restricted granule swelling and the

enhanced glucan chain interactions within the starch granule as a result of annealing. Annealing treatment decreased the RDS, SDS and eGI levels, and increased the RS levels in granular starches. However, the SDS levels of LB, NB and TB starches, the eGI of LB and TB starches, and the RS level of TB starch were increased upon annealing. In comparison to native starches, the relative decrease in RDS and SDS levels and increase in RS levels suggest that the structural changes occurred within amorphous regions, and crystalline regions showed a greater resistance to enzyme-catalysed hydrolysis upon annealing. The annealed starches exhibited similar solubilisation patterns to those of their native counterparts. The susceptibility to acid hydrolysis decreased upon annealing. The results showed that the organization of starch chains within the amorphous and crystalline domains of native starches influenced the reorganization of starch chains on annealing.

The contribution of amorphous regions to the mechanism of annealing was explored using the approaches of partial acid hydrolysis and cross-linking with STMP and STPP. Partial acid hydrolysis would preferentially hydrolyse the amorphous regions of the granule and facilitate starch chain mobility. Furthermore, it may have increased the elongation of the double helices, diminished the disruptive effect of amylose on the arrangement of amylopectin within the crystalline lamellae, and facilitated new double helical formation through the association of hydrolysed amylose chains. As a result of these changes within the granules, annealing treatment further increased the mobility of glucan chains and formed a highly-ordered structure. The above changes contributed to the further increase in To, Tp and Tc of lintnerized (acid hydrolysed) annealed starches versus their native annealed starches. This suggests that the amorphous regions play an

important role in optimizing the ordering of double helices in the crystalline regions by increasing the homogeneity and the perfection of starch crystallites, thus resulting in a reduction in gelatinization temperature range (Tc-To) in lintnerized annealed starches. The results suggest that partially acid hydrolysed starches could still be annealed. However, the susceptibility of lintnerised starches to annealing treatment decreased with increasing hydrolysis time.

In normal pulse starches, the DS and RE of cross-linked annealed starches were higher than those of their native counterparts. However, annealed high amylose starches showed lower DS and RE values in cross-linking versus their native starches. In the case of LB starch, no difference in DS and RE was observed between the native and annealed cross-linked starches. Differences in DS and RE after cross-linking between native and annealed starches suggest that the changes which occurred mainly in the amorphous regions either increased or reduced the extent of cross-linking. Since the majority of the cross-linking between starches chains occurred in the amorphous regions of starch granules, the mobility of the starch chains, particularly the amylose chains, was restricted. The cross-linking of starches with STMP/STPP decreased the extent of interaction between starch chains during the annealing treatment, which in turn reduced the perfection of existing crystallites upon annealing. This study opens up new avenues of dual-modified pulse starches with different substitution levels of cross-linking that can be used in several food applications such as stabilizers and thickeners of baby foods and canned and frozen foods. The data obtained in this study will broden the understanding of pulse starch structure and properties that are useful both for product designers and food

processors to expand the range of functionality and applications of pulse starches in the food industry.

3.6 Directions for further research

This research has provided additional information on the mechanism of annealing (ANN) with respect to starch chain realignment and their interaction within the amorphous and crystalline domains of pulse and high amylose maize starches. Modification of these starches by annealing followed by cross-linking (CL) may lead to the development of ANN-CL starches that have novel properties required for specific food applications. Cross-linking reagents used in this study formed intermolecular linkages between hydroxyl groups on starch molecules mainly within the amorphous regions. The changes occurred during the annealing treatment either facilitated or hindered the accessibility of the cross-linking reagents into the reaction sites. Consequently, the cross-linking of native and annealed starches at the same molar concentration resulted in different levels of cross-linking in these starches. However, the location of cross-links within the amorphous regions and their distribution pattern (with in the amylose and amylopectin molecules) is still in contention. Further research is needed to understand to what extent amylose and amylopectin contribute to the overall degree of substitution in cross-linking. It can be assumed that starches with different amylose and amylopectin contents differ in their susceptibility to cross-linking reagents, since the amorphous regions are more vulnerable to cross-linking and the reaction occurs with the available hydroxyls groups of the glucose moieties of both amylose and amylopectin molecules. The isolation and structural analysis of each component (amylose and

amylopectin) from cross-linked starches will shed light on the extent of distribution (DS) and substitution pattern of cross-linking reagents in the interior of the granule. This will provide a better understanding of the structural changes that influence the availability of reaction sites for cross-linking within the amorphous regions upon annealing.

In addition, factors that determine the ratio of mono- and di-ester bonds, due to cross-linking reaction mechanisms and available starch hydroxyls, include the type of reagents used and the cross-linking conditions (Koch *et al.*, 1982). Therefore, it is worthwhile to investigate the ratio of mono- and di-ester (cross-linked) derivatives of the starches used in this study. ^{31}P NMR can be used to characterize the starch phosphate derivatives and their individual contents (Kasemsuwan and Jane, 1996). This will provide new insight how cross-linking is achieved at the macromolecular level of the granule structure. Furthermore, it would help to reveal the structure-functional property relationship of modified starches.

The impact of annealing on the amylose-lipid complex formation is still in debate. A comprehensive study of the interaction of starches with added fatty acids and/or monoacylglycerols (MG) with different chain lengths prior to and post annealing would provide an understanding of V-amylose-lipid complex formation during annealing. A comparative study of lipid-amylose complexes in native and annealed starches may provide additional information about amylose chain rigidity within the amorphous regions on annealing. Therefore, it can be hypothesized that interactions among amylose chains within the amorphous regions upon annealing will decrease the ability to form amylose-lipid helical inclusion complexes. In this study, the ability of starches to complex with

FFA and/or MG before and after annealing could be monitored by determination of FFA/MG content, ^{13}C CP/MAS NMR and DSC.

3.7 Novelty and significance

The results of this study will expand the knowledge base with respect to pulse starch structure and its impact on physicochemical properties and nutritional fractions. Consequently, researchers will be able to optimize reaction conditions for chemical, physical and enzymatic modifications of underutilized pulse starches. This is the first comprehensive study that compares the structures of native pulse starches with those of their enzyme (α-amylase and amyloglucosidase) digested residues using a multi-technique approach. This study showed that the rate and extent of hydrolysis was influenced by the interplay between the kinetics of enzyme-catalysed hydrolysis and the molecular rearrangement between glucan chains during the progress of hydrolysis. Furthermore, this study would provide the impetus for research into the structural factors that influence resistant starch formation and to modify the rate and extent of starch digestibility in real food matrices. This study will also be invaluable for researchers in understanding the effects of specific mutations on starch structure, and the link between genetically modified characteristics affecting waxiness, high amylose content and digestibility.

Research on annealed starches has involved comparative studies on starches having widely different amylopectin chain length distributions. Consequently, due to the large influence that amylopectin chains have on changes to starch structure on annealing, the role of amylose on structural changes within the amorphous domains has not been

properly ascertained. This study was able to show clearly that starch chain interactions involving amylose chains significantly influenced starch structure. This was made possible due to similar amylopectin chain length distributions among the normal pulse starches. Furthermore, this study provides additional information on the role of amylose and its packing density within the amorphous regions that influence the structural rearrangement of amylopectin crystallites on annealing, especially in high amylose starches. This study would enable food processors to better understand the extent to which annealing conditions of normal and high amylose starches must be manipulated or controlled to achieve the desired properties for food and non-food applications. The data obtained in this study will provide an alternative way of modifying pulse starch structure without the use of chemical reagents that could improve the health-related quality of pulse-starch-based foods.

A combination of physical and chemical modification (dual modification) techniques can be applied to produce starches with wide ranges of functional properties that are required for specific food applications. In terms of thermal processing, annealed pulse starches would require less chemical modification to achieve the required thermal stability that can be used in thermally processed foods. Furthermore, crystalline perfection during annealing could decrease the rapidly digestible starch content and/or increase the resistant starch content, thereby influencing the postprandial blood glucose levels and insulin concentrations. Therefore, pre-treatments like partial acid hydrolysis followed by annealing modify starch structure (extent of crystalline perfection and the

interactions between starch chains) which in turn produce starches with modified digestibility characteristics and higher thermal stability.

The comparative study of cross-linking in native and annealed starches provided a deep insight into how the availability of reaction sites for cross-linking within the amorphous and crystalline domains are influenced by the structural arrangement of amylose and amylopectin chains of normal and high amylose starches. Furthermore, the glucan chain realignment during annealing treatment may open up additional reaction sites which may have not been available in the native granules. Additional reaction sites may result in achieving desired DS levels using lower concentrations of chemical reagents. These additional reaction sites would facilitate the introduction of new chemical substituent groups that are used to modify starch structure and generate a wide range of functionalities.

References

AACC (2000). Approved methods of the American association of cereal chemists (10th ed.). American Association of Cereal Chemists, Inc., St. Paul, MN, USA (2000).

Adebowale, K., Afolabi, T., & Olu-Owolabi, B. (2005). Hydrothermal treatments of finger millet (Eleusine coracana) starch. *Food Hydrocolloids, 19*(6), 974-983.

Adebowale, K., Henle, T., Schwarzenbolz, U., & Doert, T. (2009). Modification and properties of African yam bean (*Sphenostylis stenocarpa Hochst. Ex A. Rich*.) *Harms* starch I: Heat moisture treatments and annealing. *Food Hydrocolloids ,23*(7), 1947-1957.

Ai, Y., Hasjim, J., & Jane, J.-l. (2013). Effects of lipids on enzymatic hydrolysis and physical properties of starch. *Carbohydrate Polymers, 92*(1), 120-127.

Alcázar-Alay, S. C., & Meireles, M. A. A. (2015). Physicochemical properties, modifications and applications of starches from different botanical sources. *Food Science and Technology (Campinas),* 35(2), 215-236.

Allen, O. N., & Allen, E. K. (1981). The Leguminosae: A Source book of characteristics, uses, and nodulation. (p. 812) Madison, Wisconsin, USA:The University of Wisconsin Press.

Alvani, K., Qi, X., & Tester, R. F. (2012). Gelatinisation properties of native and annealed potato starches. *Starch-Stärke, 64*(4), 297-303.

Ambigaipalan, P., Hoover, R., Donner, E., & Liu, Q. (2013). Retrogradation characteristics of pulse starches. *Food Research International, 54*(1), 203-212.

Ambigaipalan, P., Hoover, R., Donner, E., Liu, Q., Jaiswal, S., Chibbar, R., Nantanga, K.

K. M.,& Seetharaman, K. (2011). Structure of faba bean, black bean and pinto bean starches at different levels of granule organization and their physico-chemical properties. *Food Research International, 44*(9), 2962-2974.

Ambigaipalan, P., Hoover, R., Donner, E., Liu, Q., Jaiswal, S., Chibbar, R., Nantanga, K., & Seetharaman, K. (2011). Structure of faba bean, black bean and pinto bean starches at different levels of granule organization and their physicochemical properties. *Food Research International*, 44, 2962-2974.

Anderson, K. (1996). Micro-digestion and ICP-AES analysis for the determination of macro and micro elements in plant tissues. *Atomic Spectroscopy*, *17*(1), 30-33.

André, G., Buléon, A., Haser, R., & Tran, V. (1999). Amylose chain behavior in an interacting context. III. Complete occupancy of the AMY2 barley α-amylase cleft and comparison with biochemical data. *Biopolymers, 50*(7), 751-762.

Ao, Z., & Jane, J.-l. (2007). Characterization and modeling of the A-and B-granule starches of wheat, triticale, and barley. *Carbohydrate Polymers, 67*(1), 46-55.

Apinan, S., Yujiro, I., Hidefumi, Y., Takeshi, F., Myllärinen, P., Forssell, P., & Poutanen, K. (2007). Visual observation of hydrolysed potato starch granules by α-amylase with confocal laser scanning microscopy. *Starch-Stärke*, 59(11), 543-548.

Atichokudomchai, N., Varavinit, S., & Chinachoti, P. (2002a). A study of annealing and freeze-thaw stability of acid-modified tapioca starches by differential scanning calorimetry (DSC). *Starch - Stärke, 54*(8), 343-349.

Atichokudomchai, N., Varavinit, S., & Chinachoti, P. (2002b). Gelatinization transitions of acid-modified tapioca starches by differential scanning calorimetry

(DSC). *Starch-Stärke*, *54*(7), 296-302.

Atichokudomchai, N., Varavinit, S., & Chinachoti, P. (2004). A study of ordered structure in acid-modified tapioca starch by ^{13}C CP/MAS solid-state NMR. *Carbohydrate Polymers*, *58*(4), 383-389.

Atkin, N. J., Cheng, S. L., Abeysekera, R. M., & Robards, A. W. (1999). Localisation of amylose and amylopectin in starch granules using enzyme-gold labelling.*Starch-Stärke, 51*(5), 163-172.

Atwell, W., Hood, L., Lineback, D., Varriano-Marston, E., & Zobel, H. (1988). The terminology and methodology associated with basic starch phenomena. *Cereal Foods World*. 33, pp. 306–311.

Augustin, M. A., Sanguansri, P., & Htoon, A. (2008). Functional performance of a resistant starch ingredient modified using a microfluidiser. *Innovative Food Science and Emerging Technologies, 9*(2), 224-231.

Bajka, B. H., Topping, D. L., Cobiac, L., & Clarke, J. M. (2006). Butyrylated starch protects colonocyte DNA against dietary protein-induced damage in rats. *British Journal of Nutrition*, 96(02), 276-282.

Baks, T., Ngene, I. S., Van Soest, J. J., Janssen, A. E., & Boom, R. M. (2007). Comparison of methods to determine the degree of gelatinisation for both high and low starch concentrations. *Carbohydrate Polymers, 67*(4), 481-490.

Baldwin, P. M. (2001). Starch granule-associated proteins and polypeptides.*Starch-Stärke, 53*(10), 475-503.

Ball, S. G., & Morell, M. K. (2003). From bacterial glycogen to starch: understanding the

biogenesis of the plant starch granule. *Annual Review of Plant Biology, 54*(1), 207-233.

Ball, S., Guan, H. P., James, M., Myers, A., Keeling, P., Mouille, G., Buleon, A., Colonna, P., & Preiss, J. (1996). From glycogen to amylopectin: a model for the biogenesis of the plant starch granule. *Cell, 86*(3), 349-352.

Ballicora, M. A., Iglesias, A. A., & Preiss, J. (2004). ADP-glucose pyrophosphorylase: a regulatory enzyme for plant starch synthesis. *Photosynthesis Research, 79*(1), 1-24.

Banks, W. and Greenwood, C. T. (1975). Starch and its components (pp. 309-325). Edinburgh, UK: Edinburgh University Press.

Barry, J. L., Hoebler, C., Macfarlane, G. T., Macfarlane, S., Mathers, J. C., Reed, K. A., & Rumney, C. J. (1995). Estimation of the fermentability of dietary fibre in vitro: a European interlaboratory study. *British Journal of Nutrition, 74*(03), 303-322.

Beckles, D. M., Smith, A. M., & Rees, T. (2001). A cytosolic ADP-glucose pyrophosphorylase is a feature of graminaceous endosperms, but not of other starch-storing organs. *Plant Physiology*, *125*(2), 818-827.

Bemiller, J. N. (1997). Starch modification: Challenges and prospects. *Starch - Stärke, 49*(4), 127-131.

BeMiller, J. N. (2011). Pasting, paste, and gel properties of starch–hydrocolloid combinations. *Carbohydrate Polymers, 86*(2)*,* 386–423.

BeMiller, J. N., & Huber, K. C. (2015). Physical modification of food starch

functionalities. *Annual Review of Food Science and Technology, 6*, 19-69.

Bertoft, E., Piyachomkwan, K., Chatakanonda, P., & Sriroth, K. (2008). Internal unit chain composition in amylopectins. *Carbohydrate Polymers*, *74*(3), 527-543.

Bertoft, E., Qin, Z., & Manelius, R. (1993). Studies on the structure of pea starches part 4: Intermediate material of wrinkled pea starch. *Starch-Stärke, 45*(12), 420-425.

Biliaderis, C. G. (1991). The structure and interactions of starch with food constituents. *Canadian Journal of Physiology and Pharmacology, 69*(1), 60-78.

Biliaderis, C. G. (1998). Structures and phase transitions of starch polymers. Walter R. H (Ed): *Polysaccharide Association Structures in Foods* (pp. 57-168). New York, NY: Marcel Dekker Inc.

Biliaderis, C. G., & Galloway, G. (1989). Crystallization behavior of amylose-V-complexes: structure-property relationships. *Carbohydrate Research, 189*, 31-48.

Biliaderis, C. G., & Tonogai, J. R. (1991). Influence of lipids on the thermal and mechanical properties of concentrated starch gels. *Journal of Agricultural and Food Chemistry,39*(5), 833-840.

Biliaderis, C. G., Grant, D. R., & Vose, J. R. (1981). Structural characterization of legume starches .1. Studies on amylose, amylopectin, and beta-limit dextrins. *Cereal Chemistry, 58*(6), 496-502.

Biliaderis, C., Grant, D., & Vose, J. (1981). Structural characterization of legume starches II. Studies on acid-treated starches. *Cereal Chemistry*, *58*(6), 502-507.

Biliaderis, C. G., Maurice, T. J., & Vose, J. R. (1980).

Starch gelatinization phenomena studied by differential scanning calorimetry. *Journal of*

Food Science, *45*(6), 1669-1674.

Biliaderis, C., Page, C., Slade, L., & Sirett, R. (1985). Thermal behavior of amylose-lipid complexes. *Carbohydrate Polymers*, *5*(5), 367-389.

Bingham, S. A., Day, N. E., Luben, R., Ferrari, P., Slimani, N., Norat, T., Clavel-Chapelon, F., Kesse, E., Nieters, A., & Boeing, H. (2003). Dietary fibre in food and protection against colorectal cancer in the European prospective investigation into cancer and nutrition (EPIC): an observational study. *The Lancet*, *361*(9368), 1496-1501.

Birkett, A. M., Mathers, J. C., Jones, G. P., Walker, K. Z., Roth, M. J., & Muir, J. G. (2000). Changes to the quantity and processing of starchy foods in a Western diet can increase polysaccharides escaping digestion and improve in vitro fermentation variables. *British Journal of Nutrition*, *84*(01), 63-72.

Blazek, J., & Copeland, L. (2010). Amylolysis of wheat starches. II. Degradation patterns of native starch granules with varying functional properties. *Journal of Cereal Science 52*(2), 295-302.

Blazek, J., & Gilbert, E. P. (2010). Effect of enzymatic hydrolysis on native starch granule structure. *Biomacromolecules, 11*(12), 3275-3289.

Blennow, A., Bay-Smidt, A. M., Olsen, C. E., & Møller, B. L. (2000). The distribution of covalently bound phosphate in the starch granule in relation to starch crystallinity. *International Journal of Biological Macromolecules, 27*(3), 211-218.

Blennow, A., Hansen, M., Schulz, A., Jørgensen, K., Donald, A. M., & Sanderson, J.

(2003). The molecular deposition of transgenically modified starch in the starch granule as imaged by functional microscopy. *Journal of Structural Biology, 143*(3), 229-241.

Blennow, A., Nielsen, T. H., Baunsgaard, L., Mikkelsen, R., & Engelsen, S. B. (2002). Starch phosphorylation: a new front line in starch research. *Trends in Plant Science, 7*(10), 445-450.

Bligh, E. G., & Dyer, W. J. (1959). A rapid method of total lipid extraction and purification. *Canadian Journal of Biochemistry and Physiology*, *37*(8), 911-917.

Bogracheva, T. Y., Morris, V., Ring, S., & Hedley, C. (1998). The granular structure of C-type pea starch and its role in gelatinization. *Biopolymers*, *45*(4), 323-332.

Bogracheva, T. Y., Wang, Y., & Hedley, C. (2001). The effect of water content on the ordered/disordered structures in starches. *Biopolymers, 58*(3), 247-259.

Brand, J. C., Colagiuri, S., Crossman, S., Allen, A., Roberts, D. C., & Truswell, A. S. (1991). Low-glycemic index foods improve long-term glycemic control in NIDDM. *Diabetes Care, 14*(2), 95-101.

Brown, I. L. (2004). Applications and uses of resistant starch. *Journal of AOAC International, 87*(3), 727-732.

Brown, I., Warhurst, M., Arcot, J., Playne, M., Illman, R. J., & Topping, D. L. (1997). Fecal numbers of bifidobacteria are higher in pigs fed *Bifidobacterium longum* with a high amylose cornstarch than with a low amylose cornstarch. *The Journal of Nutrition*, *127*(9), 1822-1827.

Brumovsky, J. O., & Thompson, D. B. (2001). Production of boiling-stable granular

resistant starch by partial acid hydrolysis and hydrothermal treatments of high-amylose maize starch. *Cereal chemistry, 78(6)*, 680-689.

Bruner, R.L. (1964). Determination of reducing value. Whistler R. L (Ed), Methods in Carbohydrate Chemistry: *Starch (Vol. IV)*. 4, (pp. 67-71). New York: Academic Press.

Buléon, A., Colonna, P., Planchot, V., & Ball, S. (1998). Starch granules: structure and biosynthesis. *International Journal of Biological Macromolecules, 23*(2), 85-112.

Burrell, M. (2003). Starch: the need for improved quality or quantity—an overview. *Journal of Experimental Botany, 54*(382), 451-456.

Burton, R. A., Bewley, J. D., Smith, A. M., Bhattacharyya, M. K., Tatge, H., Ring, S., Bull, V., Hamilton, W., & Martin, C. (1995). Starch branching enzymes belonging to distinct enzyme families are differentially expressed during pea embryo development. *The Plant Journal, 7*(1), 3-15.

Cai, J., Cai, C., Man, J., Zhou, W., & Wei, C. (2014). Structural and functional properties of C-type starches. *Carbohydrate Polymers*, *101*, 289-300.

Cairns, P., Bogracheva, T. Y., Ring, S., Hedley, C., & Morris, V. (1997). Determination of the polymorphic composition of smooth pea starch. *Carbohydrate Polymers*, *32(3)*, 275-282.

Carlson, T. G., Larsson, K., Dinh-Nguyen, N., & Krog, N. (1979). A study of the amylose-monoglyceride complex by Raman spectroscopy. *Starch-Stärke, 31*(7), 222-224.

Chauhan, F., & Seetharaman, K. (2013). On the organization of chains in amylopectin. *Starch-Stärke, 65*(3-4), 191-199.

Cheetham, N. W. H., & Tao, L. (1998). Solid state NMR studies on the structural and conformational properties of natural maize starches. *Carbohydrate Polymers, 36(4)*, 285-292.

Chen, X., He, X., & Huang, Q. (2014). Effects of hydrothermal pretreatment on subsequent octenylsuccinic anhydride (OSA) modification of cornstarch. *Carbohydrate Polymers, 101*,493-498.

Chung, H. J., Hoover, R., & Liu, Q. (2009a). The impact of single and dual hydrothermal modifications on the molecular structure and physicochemical properties of normal corn starch. *International Journal of Biological Macromolecules, 44*(2), 203-210.

Chung, H. J., Jeong, H.Y., & Lim, S.T. (2003). Effects of acid hydrolysis and defatting on crystallinity and pasting properties of freeze-thawed high amylose corn starch. *Carbohydrate Polymers, 54*(4), 449-455.

Chung, H. J., Liu, Q., & Hoover, R. (2009b). Impact of annealing and heat-moisture treatment on rapidly digestible, slowly digestible and resistant starch levels in native and gelatinized corn, pea and lentil starches. *Carbohydrate Polymers, 75*(3), 436-447.

Chung, H. J., Liu, Q., & Hoover, R. (2010). Effect of single and dual hydrothermal treatments on the crystalline structure, thermal properties, and nutritional fractions of pea, lentil, and navy bean starches. *Food Research International*,

43(2), 501-508.

Chung, H. J., Liu, Q., Hoover, R., Warkentin, T. D., & Vandenberg, B. (2008). *In vitro* starch digestibility, expected glycemic index, and thermal and pasting properties of flours from pea, lentil and chickpea cultivars. *Food Chemistry*, *111*(2), 316-321.

Colonna, P., & Buleon, A. (2009). Thermal transitions of starches. In A. C. Bertolini, (Ed), *Starches: Characterization, properties, and applications* (pp. 71-102). Boca Raton, FL: CRC Press.

Colonna, P., Buléon, A., & Lemarié, F. (1988). Action of Bacillus subtilis α-amylase on native wheat starch. *Biotechnology and Bioengineering, 31*(9), 895-904.

Commuri, P. D., & Keeling, P. L. (2001). Chain-length specificities of maize starch synthase I enzyme: studies of glucan affinity and catalytic properties. *The Plant Journal, 25*(5), 475-486.

Comparot-Moss, S., & Denyer, K. (2009). The evolution of the starch biosynthetic pathway in cereals and other grasses. *Journal of Experimental Botany, 60*(9), 2481-2492.

Conde-Petit, B., Nuessli, J., Arrigoni, E., Escher, F., & Amado, R. (2001). Perspectives of starch in food science. *CHIMIA International Journal for Chemistry*, *55*(3), 201-205.

Cooke, D., & Gidley, M. J. (1992). Loss of crystalline and molecular order during starch gelatinisation: origin of the enthalpic transition. *Carbohydrate Research, 227*, 103-112.

Copeland, L., Blazek, J., Salman, H., & Tang, M. C. (2009). Form and functionality of starch. *Food Hydrocolloids, 23*(6),1527-1534.

Craig, S. A., Maningat, C. C., Seib, P. A., & Hoseney, R. (1989). Starch paste clarity. *Cereal Chemistry, 66*(3), 173-182.

Cui, R., & Oates, C. (1999). The effect of amylose–lipid complex formation on enzyme susceptibility of sago starch. *Food Chemistry, 65*(4), 417-425.

Cummings, J. H., Beatty, E. R., Kingman, S. M., Bingham, S. A., & Englyst, H. N. (1996). Digestion and physiological properties of resistant starch in the human large bowel. *British Journal of Nutrition, 75*(05), 733-747.

Dauvillée, D., Mestre, V., Colleoni, C., Slomianny, M.-C., Mouille, G., Delrue, B., d'Hulst, C., Bliard, C., Nuzillard, J.-M., & Ball, S. (2000). The debranching enzyme complex missing in glycogen accumulating mutants of *Chlamydomonas reinhardtii* displays an isoamylase-type specificity. *Plant Science, 157*(2), 145-156.

Davis, J. P., Supatcharee, N., Khandelwal, R. L., & Chibbar, R. N. (2003). Synthesis of novel starches in planta: opportunities and challenges. *Starch-Stärke, 55*(3-4), 107-120.

Davydova, N., Leont'v, S. P., Genin, Y. V., Sasov, A. Y., & Bogracheva, T. Y. (1995). Some physicochemical properties of smooth pea starches. *Carbohydrate Polymers*, *27*(2), 109-115.

Debet, M. R., & Gidley, M. J. (2006). Three classes of starch granule swelling: Influence of surface proteins and lipids. *Carbohydrate Polymers, 64*(3), 452-465.

Deffenbaugh, L., & Walker, C. (1989). Use of the rapid visco analyzer to measure starch pasting properties. Part I: Effect of sugars. *Starch-Stärke, 41*(12), 461-467.

Donovan, J. W. (1979). Phase transitions of the starch–water system. *Biopolymers, 18*(2), 263-275.

Denyer, K., Waite, D., Motawia, S., Møller, B. L., & Smith, A. M. (1999). Granule-bound starch synthase I in isolated starch granules elongates malto-oligosaccharides processively. *Biochemical Journal*, *340*(1), 183-191.

Dhital, S., Shrestha, A. K., & Gidley, M. J. (2010). Relationship between granule size and *in vitro* digestibility of maize and potato starches. *Carbohydrate Polymers, 82*(2), 480-488.

Dhital, S., Warren, F. J., Butterworth, P. J., Ellis, P. R., & Gidley, M. J. (2017). Mechanisms of starch digestion by α-amylase-Structural basis for kinetic properties. *Critical Reviews in Food Science and Nutrition*, *57*(5), 875-892.

Dias, A. R. G., Zavareze, E. R., Spier, F., de Castro, L. A. S., & Gutkoski, L. C. (2010). Effects of annealing on the physicochemical properties and enzymatic susceptibility of rice starches with different amylose contents. *Food Chemistry, 123*(3), 711-719.

Dona, A. C., Pages, G., Gilbert, R. G., & Kuchel, P. W. (2010). Digestion of starch: *In vivo* and *in vitro* kinetic models used to characterise oligosaccharide or glucose release. *Carbohydrate Polymers, 80*(3), 599-617.

Donovan, J. W. (1979). Phase transitions of the starch–water system. *Biopolymers, 18*(2), 263-275.

Eerlingen, R., & Delcour, J. (1995). Formation, analysis, structure and properties of type III enzyme resistant starch. *Journal of Cereal Science, 22*(2), 129-138.

Eerlingen, R. C., Crombez, M., & Delcour, J. (1993). Enzyme-resistant starch. 1. Quantitative and qualitative influence of incubation-time and temperature of autoclaved starch on resistant starch formation. *Cereal Chemistry, 70*(3), 339-344.

Eliasson, A. C. and Gudmundsson, M. (1996). Starch: physicochemical and functional aspects. Eliasson A. C (Ed), *Carbohydrates in Food* (pp. 431- 503), New York, NY; Marcel Dekker Inc.

Eliasson, A. C., & Kim, H. R. (1992).Changes in rheological properties of hydroxypropyl potato starch pastes during freeze-thaw treatments I. A rheological approach for evaluation of freeze-thaw stability. *Journal of Texture Studies, 23*(3), 279-295.

EI-Faki, H. A., Desikachar, H. S. R., Tareen, J. A. K. and Tharanathan, R. N. (1983).Scanning electron microscopy of in vivo and in vitro digested starch granules ofchickpea, cowpea and horse gram. *Journal of Food Science and Technology*, 17, 276-281.

Ellis, R. P., Cochrane, M. P., Dale, M. F. B., Duffus, C. M., Lynn, A., Morrison, I. M., Prentice, R. D. M., Swanston, J. S., & Tiller, S. A. (1998). Starch production and industrial use. *Journal of the Science of Food and Agriculture, 77*(3), 289-311.

Ells, L. J., Seal, C. J., Kettlitz, B., Bal, W., & Mathers, J. C. (2005). Postprandial glycaemic, lipaemic and haemostatic responses to ingestion of rapidly and slowly digested starches in healthy young women. *The British Journal of Nutrition*, *94*(6), 948.

Emes, M., Bowsher, C., Hedley, C., Burrell, M., Scrase-Field, E., & Tetlow, I. (2003). Starch synthesis and carbon partitioning in developing endosperm. *Journal of Experimental Botany, 54*(382), 569-575.

Englyst, K. N., Englyst, H. N., Hudson, G. J., Cole, T. J., & Cummings, J. H. (1999). Rapidly available glucose in foods: an in vitro measurement that reflects the glycemic response. *The American Journal of Clinical Nutrition, 69*(3), 448-454.

Englyst, H. N., Kingman, S. M., Hudson, G. J., & Cummings, J. H. (1996). Measurement of resistant starch *in vitro* and *in vivo*. *British Journal of Nutrition, 75*(05), 749-755.

Englyst, H. N., Kingman, S., & Cummings, J. (1992). Classification and measurement of nutritionally important starch fractions. *European Journal of Clinical Nutrition, 46*, S33-50.

Evans, I., & Haisman, D. (1982). The effect of solutes on the gelatinization temperature range of potato starch. *Starch-Stärke, 34*(7), 224-231.

Faki, H. E., Desikachar, H., Paramahans, S., & Tharanathan, R. (1983). Physico-chemical characteristics of starches from chick pea, cow pea and horse gram. *Starch-Stärke, 35*(4), 118-122.

Fanta, G., Shogren, R., & Salch, J. (1999). Steam jet cooking of high-amylose starch–fatty acid mixtures; An investigation of complex formation. *Carbohydrate Polymers, 38*(1), 1-6.

Fardet, A., Hoebler, C., Baldwin, P., Bouchet, B., Gallant, D., & Barry, J. L. (1998). Involvement of the protein network in thein vitro degradation of starch from

spaghetti and lasagne: a microscopic and enzymic study. *Journal of Cereal Science, 27*(2), 133-145.

Ferguson, L. R., Tasman-Jones, C., Englyst, H., & Harris, P. J. (2000). Comparative effects of three resistant starch preparations on transit time and short-chain fatty acid production in rats. *Nutrition and Cancer*, 36(2), 230-237.

Fredriksson, H., Silverio, J., Andersson, R., Eliasson, A. C., & Åman, P. (1998). The influence of amylose and amylopectin characteristics on gelatinization and retrogradation properties of different starches. *Carbohydrate Polymers, 35*(3–4), 119-134.

French, D. (1972). Fine structure of starch and its relationship to the organization of starch granules. *Journal of the Japanese Society of Starch Science, 19*(1), 8-25.

Frias, J., Fornal, J., Ring, S. G., & Vidal-Valverde, C. (1998). Erffect of germination on physico- chemical properties of lentil starch and its components. *LWT-Food Science and Technology, 31*(3), 228-236.

Fuentes-Zaragoza, E., Riquelme-Navarrete, M., Sánchez-Zapata, E., & Pérez-Álvarez, J. (2010). Resistant starch as functional ingredient: A review. *Food Research International, 43*(4), 931-942.

Fujita, N., & Taira, T. (1998). A 56-kDa protein is a novel granule-bound starch synthase existing in the pericarps, aleurone layers, and embryos of immature seed in diploid wheat (*Triticum monococcum L.*). *Planta, 207*(1), 125-132.

Gallant, D. J., Bouchet, B., & Baldwin, P. M. (1997). Microscopy of starch: evidence of a new level of granule organization. *Carbohydrate Polymers, 32*(3), 177-191.

Gallant, D., Bouchet, B., Buleon, A., & Perez, S. (1992). Physical characteristics of starch granules and susceptibility to enzymatic degradation. *European Journal of Clinical Nutrition, 46*(2), S3-S16.

Galliard, T. and Bowler, P. (1987). Morphology and composition of starch. In T.Galliard, (Ed), *Starch, Properties and Potential* (pp. 55-78). Chichester, UK: John Wiley.

Gao, J., Vasanthan, T., Hoover, R., & Li, J. (2012). Structural modification of waxy, regular, and high-amylose maize and hulless barley starches on partial acid hydrolysis and their impact on physicochemical properties and chemical modification. *Starch-Stärke, 64*(4), 313-325.

Gao, M., Wanat, J., Stinard, P. S., James, M. G., & Myers, A. M. (1998). Characterization of dull1, a maize gene coding for a novel starch synthase. *The Plant Cell, 10*(3), 399-412.

Genkina, N. K., Kiseleva, V. I., & Noda, T. (2009). Comparative investigation on acid hydrolysis of sweet potato starches with different amylopectin chain-length. *Starch-Stärke, 61*(6), 321-325.

Genkina, N. K., Wasserman, L. A., Noda, T., Tester, R. F., & Yuryev, V. P. (2004). Effects of annealing on the polymorphic structure of starches from sweet potatoes (Ayamurasaki and Sunnyred cultivars) grown at various soil temperatures. *Carbohydrate Research, 339*(6), 1093-1098.

Genkina, N. K., Wikman, J., Bertoft, E., & Yuryev, V. P. (2007). Effects of structural imperfection on gelatinization characteristics of amylopectin starches with A-and B-type crystallinity. *Biomacromolecules, 8*(7), 2329-2335.

Gerard, C., Colonna, P., Buleon, A., & Planchot, V. (2001). Amylolysis of maize mutant starches. *Journal of the Science of Food and Agriculture, 81*(13), 1281-1287.

Gérard, C., Colonna, P., Buléon, A., & Planchot, V. (2002). Order in maize mutant starches revealed by mild acid hydrolysis. *Carbohydrate Polymers*, *48*(2), 131-141.

Gernat, C., Radosta, S., Damaschun, G., & Schierbaum, F. (1990). Supramolecular structure of legume starches revealed by X-ray scattering. *Starch-Stärke, 42*(5), 175-178.

Ghosh, H. P., & Preiss, J. (1966). Adenosine diphosphate glucose pyrophosphorylase a regulatory enzyme in the biosynthesis of starch in spinach leaf chloroplasts. *Journal of Biological Chemistry, 241*(19), 4491-4504.

Gidley, M. J., & Bociek, S. M. (1985). Molecular organization in starches: a carbon ^{13}C CP/MAS NMR study. *Journal of the American Chemical Society, 107*(24), 7040-7044.

Gidley, M. J., & Bociek, S. M. (1988). ^{13}C CP/MAS NMR studies of amylose inclusion complexes, cyclodextrins, and the amorphous phase of starch granules: relationships between glycosidic linkage conformation and solid-state carbon-13 chemical shifts. *Journal of the American Chemical Society, 110*(12), 3820-3829.

Gidley, M. J., & Bulpin, P. V. (1987). Crystallisation of malto-oligosaccharides as models of the crystalline forms of starch: minimum chain-length requirement for the formation of double helices. *Carbohydrate Research, 161*(2), 291-300.

Gilbert, E. P., Lopez-Rubio, A. & Gidley, M. J. (2012) Characterisation techniques in

food materials science. In B. Bhandari & Y. H. Roos (Eds.), *Food Materials Science and Engineering* (pp. 52-93). Oxford, UK: Wiley-Blackwell.

Glaring, M. A., Koch, C. B., & Blennow, A. (2006). Genotype-specific spatial distribution of starch molecules in the starch granule: a combined CLSM and SEM approach. *Biomacromolecules, 7*(8), 2310-2320.

Godet, M., Bizot, H., & Buléon, A. (1995). Crystallization of amylose—fatty acid complexes prepared with different amylose chain lengths. *Carbohydrate Polymers, 27*(1), 47-52.

Godet, M., Tran, V., Delage, M., & Buléon, A. (1993). Molecular modelling of the specific interactions involved in the amylose complexation by fatty acids. *International Journal of Biological Macromolecules*, *15*(1), 11-16.

Goesaert, H., Slade, L., Levine, H., & Delcour, J. A. (2009). Amylases and bread firming–an integrated view. *Journal of Cereal Science, 50*(3), 345-352.

Gomand, S. V., Lamberts, L., Gommes, C. J., Visser, R. G., Delcour, J. A., & Goderis, B.(2012). Molecular and morphological aspects of annealing-induced stabilization of starch crystallites. *Biomacromolecules, 13*(5), 1361-1370.

Gomand, S., Lamberts, L., Visser, R., & Delcour, J. (2010). Physicochemical properties of potato and cassava starches and their mutants in relation to their structural properties. *Food Hydrocolloids, 24*(4), 424-433.

Gomes, A. M., da Silva, C. E. M., & Ricardo, N. M. (2005). Effects of annealing on the physicochemical properties of fermented cassava starch ("polvilho azedo"). *Carbohydrate Polymers, 60*(1), 1-6.

Gomes, A. M., da Silva, C. E. M., Ricardo, N. M., Sasaki, J. M., & Germani, R. (2004). Impact of annealing on the physicochemical properties of unfermented cassava starch ("polvilho doce"). *Starch-Stärke, 56*(9), 419-423.

Granfeldt, Y., Bjorck, I., Drews, A., & Tovar, J. (1992). An in vitro procedure based on chewing to predict metabolic response to starch in cereal and legume products. *European Journal of Clinical Nutrition, 46*, 649-660.

Guan, H. P., & Preiss, J. (1993). Differentiation of the properties of the branching isozymes from maize (*Zea mays*). *Plant Physiology, 102*(4), 1269-1273.

Gunaratne, A., & Corke, H. (2007). Influence of unmodified and modified cycloheptaamylose (β-cyclodextrin) on transition parameters of amylose–lipid complex and functional properties of starch. *Carbohydrate Polymers, 68*(2), 226-234.

Haase, N. U., & Shi, H. L. (1991). A characterization of faba bean starch (*Vicia faba L.*). Starch-Stärke, *43(6)*, 205-208.

Hahn, D., & Hood, L. (1987). Factors influencing corn starch-lipid complexing. *Cereal Chemistry, 64*(2), 81-85.

Han, K. H., Fukushima, M., Kato, T., Kojima, M., Ohba, K., Shimada, K. I., & Nakano, M. (2003). Enzyme-resistant fractions of beans lowered serum cholesterol and increased sterol excretions and hepatic mRNA levels in rats. *Lipids*, *38*(9), 919-924.

Han, J. J., Janz, J. A., & Gerlat, M. (2010). Development of gluten-free cracker snacks using pulse flours and fractions. *Food Research International, 43*(2), 627-633.

Han, X. Z., & Hamaker, B. (2002). Location of starch granule-associated proteins revealed by confocal laser scanning microscopy. *Journal of Cereal Science, 35*(1), 109-116.

Han, X. Z., Campanella, O. H., Guan, H., Keeling, P. L., & Hamaker, B. R. (2002). Influence of maize starch granule-associated protein on the rheological properties of starch pastes. Part II. Dynamic measurements of viscoelastic properties of starch pastes. *Carbohydrate Polymers, 49*(3), 323-330.

Hanashiro, I., Abe, J. I., & Hizukuri, S. (1996). A periodic distribution of the chain length of amylopectin as revealed by high-performance anion-exchange chromatography. *Carbohydrate Research, 283*, 151-159.

Hanashiro, I., Tagawa, M., Shibahara, S., Iwata, K., & Takeda, Y. (2002). Examination of molar-based distribution of A, B and C chains of amylopectin by fluorescent labeling with 2-aminopyridine. *Carbohydrate Research, 337*(13), 1211-1215.

Hasjim, J., & Jane, J. L. (2009). Production of resistant starch by extrusion cooking of acid-modified normal maize starch. *Journal of Food Science, 74*(7), C556-C562.

Hasjim, J., Lee, S. O., Hendrich, S., Setiawan, S., Ai, Y., & Jane, J. L. (2010). Characterization of a novel resistant-starch and its effects on postprandial plasma-glucose and insulin responses. *Cereal Chemistry, 87*(4), 257-262.

Helbert, W., & Chanzy, H. (1994). Single crystals of V-amylose complexed with n-butanol or n-pentanol: structural features and properties. *International Journal of Biological Macromolecules, 16*(4), 207-213.

Hermansson, A.-M., & Svegmark, K. (1996). Developments in the understanding of

starch functionality. *Trends in Food Science & Technology, 7*(11), 345-353.

Hernández, J. M., Gaborieau, M., Castignolles, P., Gidley, M. J., Myers, A. M., & Gilbert, R. G.(2008). Mechanistic investigation of a starch-branching enzyme using hydrodynamic volume SEC analysis. *Biomacromolecules, 9*(3), 954-965.

Higgins, J. A., Higbee, D. R., Donahoo, W. T., Brown, I. L., Bell, M. L., & Bessesen, D. H. (2004). Resistant starch consumption promotes lipid oxidation. *Nutrition & Metabolism*, *1*(1), 8-19.

Hirsch, J. B., & Kokini, J. L. (2002). Understanding the mechanism of cross-linking agents ($POCl_3$, STMP, and EPI) through swelling behavior and pasting properties of cross-linked waxy maize starches. *Cereal Chemistry, 79*(1), 102-107.

Hizukuri, S. (1985). Relationship between the distribution of the chain length of amylopectin and the crystalline structure of starch granules. *Carbohydrate Research, 141*(2), 295-306.

Hizukuri, S. (1986). Polymodal distribution of the chain lengths of amylopectins, and its significance. *Carbohydrate Research, 147*(2), 342-347.

Hizukuri, S., Kaneko, T., & Takeda, Y. (1983). Measurement of the chain length of amylopectin and its relevance to the origin of crystalline polymorphism of starch granules. *Biochimica et Biophysica Acta (BBA)-General Subjects, 760*(1), 188-191.

Hizukuri, S., Tabata, S., & Nikuni, Z. (1970). Studies on Starch Phosphate Part 1. Estimation of glucose-6-phosphate residues in starch and the presence of other bound phosphate (s).*Starch-Stärke, 22*(10), 338-343.

Hizukuri, S., Takeda, Y., Shitaozono, T., Abe, J., Ohtakara, A., Takeda, C., & Suzuki, A. (1988). Structure and properties of water chestnut (*Trapa natans L*. var. *bispinosa* Makino) starch. *Starch-Stärke, 40*(5), 165-171.

Hizukuri, S., Takeda, Y., Yasuda, M., & Suzuki, A. (1981). Multi-branched nature of amylose and the action of debranching enzymes. *Carbohydrate Research, 94*(2), 205-213.

Hong, J. S., Gomand, S. V., & Delcour, J. A. (2015). Preparation of cross-linked maize (*Zea mays L.*) starch in different reaction media. *Carbohydrate Polymers, 124*, 302-310.

Hoover, R. & Ratnayake, W.S. (2004). Determination of total amylose content of starch. In Wrolstad *et al*. (Eds), *Handbook of Food Analytical Chemistry– Water, protein, enzymes, lipids, and carbohydrates* (pp. 689-691), Hoboken, NJ, USA: Wiley-Interscience.

Hoover, R. (1995). Starch retrogradation. *Food Reviews International, 11*(2), 331-346.

Hoover, R. (2000). Acid-treated starches. *Food Reviews International, 16*(3), 369-392.

Hoover, R. (2001). Composition, molecular structure, and physicochemical properties of tuber and root starches: a review. *Carbohydrate Polymers, 45*(3), 253-267.

Hoover, R. (2010). The impact of heat-moisture treatment on molecular structures and properties of starches isolated from different botanical sources. *Critical Reviews in Food Science and Nutrition, 50*(9), 835-847.

Hoover, R., & Manuel, H. (1996). The effect of heat–moisture treatment on the structure and physicochemical properties of normal maize, waxy maize, dull waxy maize

and amylomaize V starches. *Journal of Cereal Science*, *23*(2), 153-162.

Hoover, R., & Ratnayake, W. (2002). Starch characteristics of black bean, chick pea, lentil, navy bean and pinto bean cultivars grown in Canada. *Food Chemistry*, *78*(4), 489-498.

Hoover, R., & Sosulski, F. (1985). Studies on the functional characteristics and digestibility of starches from *Phaseolus vulgaris* biotypes. *Starch-Stärke, 37*(6), 181-191.

Hoover, R., & Sosulski, F. (1986). Effect of cross-linking on functional properties of legume starches. *Starch-Stärke, 38*(5), 149-155.

Hoover, R., & Sosulski, F. (1991). Composition, structure, functionality, and chemical modification of legume starches: a review. *Canadian Journal of Physiology and Pharmacology, 69*(1), 79-92.

Hoover, R., & Vasanthan, T. (1994a). The effect of annealing on the physicochemical properties of wheat, oat, potato and lentil starches. *Journal of Food Biochemistry, 17*(5), 303-325.

Hoover, R., & Vasanthan, T. (1994). The flow properties of native, heat-moisture treated, and annealed starches from wheat, oat, potato and lentil. *Journal of Food Biochemistry, 18*(2), 67-82.

Hoover, R., & Zhou, Y. (2003). *In vitro* and *in vivo* hydrolysis of legume starches by α-amylase and resistant starch formation in legumes. *Carbohydrate Polymers*, *54*(4), 401-417.

Hoover, R., Hughes, T., Chung, H. J., & Liu, Q. (2010). Composition, molecular

structure, properties, and modification of pulse starches: A review. *Food Research International, 43*(2), 399-413.

Hoover, R., Swamidas, G., & Vasanthan, T. (1993). Studies on the physicochemical properties of native, defatted, and heat-moisture treated pigeon pea (*Cajanus cajan L.*) starch. *Carbohydrate Research*, *246*(1), 185-203.

Huang, J., Schols, H. A., van Soest, J. J., Jin, Z., Sulmann, E., & Voragen, A. G. (2007). Physicochemical properties and amylopectin chain profiles of cowpea, chickpea and yellow pea starches. *Food Chemistry, 101*(4), 1338-1345.

Huber, K. C., & BeMiller, J. N. (2001). Location of sites of reaction within starch granules. *Cereal Chemistry, 78*(2), 173-180.

Huber, K. C., & BeMiller, J. N. (2009). Modified starch. In A. C. Bertolini, (Ed), *Starches: Characterization, properties, and applications* (pp. 145-203). Boca Raton, FL, USA: CRC Press.

Huber, K., & BeMiller, J. (2000). Channels of maize and sorghum starch granules. *Carbohydrate Polymers, 41*(3), 269-276.

Hughes, T., Hoover, R., Liu, Q., Donner, E., Chibbar, R., & Jaiswal, S. (2009). Composition, morphology, molecular structure, and physicochemical properties of starches from newly released chickpea (*Cicer arietinum L.*) cultivars grown in Canada. *Food Research International, 42*(5), 627-635.

Imberty, A., & Perez, S. (1988). A revisit to the three-dimensional structure of B-type starch. *Biopolymers, 27*(8), 1205-1221.

Immel, S., & Lichtenthaler, F. W. (2000). The hydrophobic topographies of amylose and

its blue iodine. *Starch-Staerke, 52*(1), 1-8.

International starch institute (2017), Statistic on starch raw materials, composition and worldwide use. URL http://www.starch.dk/isi/stat/index.asp. Accessed 25 June 2017.

Israkarn, K., Hongsprabhas, P., & Hongsprabhas, P. (2007). Influences of granule-associated proteins on physicochemical properties of mungbean and cassava starches. *Carbohydrate Polymers, 68*(2), 314-322.

Jacobs, H., & Delcour, J. A. (1998). Hydrothermal modifications of granular starch, with retention of the granular structure: A review. *Journal of Agricultural and Food Chemistry, 46*(8), 2895-2905.

Jacobs, H., Eerlingen, R. C., & Delcour, J. A. (1996). Factors affecting the visco amylograph and rapid visco analyzer evaluation of the impact of annealing on starch pasting properties. *Starch-Stärke, 48*(7-8), 266-270.

Jacobs, H., Eerlingen, R. C., Rouseu, N., Colonna, P., & Delcour, J. A. (1998). Acid hydrolysis of native and annealed wheat, potato and pea starches—DSC melting features and chain length distributions of lintnerised starches. *Carbohydrate Research, 308*(3–4), 359-371.

Jacobs, H., Eerlingen, R. C., Spaepen, H., Grobet, P. J., & Delcour, J. A. (1997). Impact of annealing on the susceptibility of wheat, potato and pea starches to hydrolysis with pancreatin. *Carbohydrate Research, 305*(2), 193-207.

Jacobs, H., Eerlingen, R., Clauwert, W., & Delcour, J. (1995). Influence of annealing on the pasting properties of starches from varying botanical sources. *Cereal*

Chemistry, 72(5), 480-487.

Jacobson, M. R., Obanni, M., & Bemiller, J. N. (1997). Retrogradation of starches from different botanical sources. *Cereal Chemistry, 74*(5), 511-518.

James, M. G., Denyer, K., & Myers, A. M. (2003). Starch synthesis in the cereal endosperm. *Current opinion in plant biology, 6*(3), 215-222.

Jane, J. L., & Shen, J. J. (1993). Internal structure of the potato starch granule revealed by chemical gelatinization. *Carbohydrate Research*, *247*, 279-290.

Jane, J. L., Kasemsuwan, T., Leas, S., Zobel, H., & Robyt, J. F. (1994). Anthology of starch granule morphology by scanning electron microscopy. *Starch-Stärke, 46*(4), 121-129.

Jane, J., Chen, Y., Lee, L., McPherson, A., Wong, K., Radosavljevic, M.,& Kasemsuwan, T. (1999). Effects of amylopectin branch chain length and amylose content on the gelatinization and pasting properties of starch 1. *Cereal Chemistry, 76*(5), 629-637.

Jane, J.L, Wong, K.S., & McPherson, A. E. (1997). Branch-structure difference in starches of A-and B-type X-ray patterns revealed by their Naegeli dextrins. *Carbohydrate Research*, *300* (3), 219-227.

Jane, J. J. M. S. (1995). Starch properties, modifications, and applications. *Journal of Macromolecular Science, Part A: Pure and Applied Chemistry*, *32*(4), 751-757.

Jane, J. L. (2006). Current understanding on starch granule structures. *Journal of Applied Glycoscience, 53*(3), 205-213.

Jane, J. L. (2007). Structure of starch granules. *Journal of Applied Glycoscience, 54*(1),

31-36.

Jane, J. L., & Robyt, J. F. (1984). Structure studies of amylose-V-complexes and retrograded amylose by action of alpha amylases, and a new method for preparing amylodextrins. *Carbohydrate Research, 132*(1), 105-118.

Jane, J. L., Ao, Z., Duvick, S. A., Wiklund, M., Yoo, S. H., Wong, K. S., & Gardner, C. (2003). Structures of amylopectin and starch granules: how are they synthesized? *Journal of Applied Glycoscience*, *50*(2), 167-172.

Jane, J. L., Atichokudomchai, N., Park, J. H., & Suh, D.S. (2006). Effects of amylopectin structure on the organization and properties of starch granules. In *Advances in Biopolymers*, vol. 935 (pp. 146-164): Washington, DC, USA: American Chemical Society.

Jane, J. L., Xu, A., Radosavljevic, M., & Seib, P. (1992). Location of amylose in normal starch granules. I. Susceptibility of amylose and amylopectin to cross-linking reagents. *Cereal Chemistry, 69*(4), 405-409.

Jayakody, L., & Hoover, R. (2002). The effect of lintnerization on cereal starch granules. *Food Research International, 35*(7), 665-680.

Jayakody, L., & Hoover, R. (2008). Effect of annealing on the molecular structure and physicochemical properties of starches from different botanical origins – A review. *Carbohydrate Polymers, 74*(3), 691-703.

Jayakody, L., Hoover, R., Liu, Q., & Donner, E. (2009). Studies on tuber starches III. Impact of annealing on the molecular structure, composition and physicochemical properties of yam (*Dioscorea sp*.) starches grown in Sri Lanka. *Carbohydrate*

Polymers, 76(1), 145- 153.

Jayakody, L., Lan, H., Hoover, R., Liu, Q. and Donner, E. (2007). Composition, molecular structure and physicochemical properties of starches from two grass pea (*Lathyrus sativus L.*) cultivars grown in Canada. *Food Chemistry*, *105*, 116-125

Jenkins, D., Wolever, T., Jenkins, A., Thorne, M., Lee, R., Kalmusky, J., Reichert, R., & Wong, G. (1983). The glycaemic index of foods tested in diabetic patients: a new basis for carbohydrate exchange favouring the use of legumes. *Diabetologia, 24*(4), 257-264.

Jenkins, D. J., Wolever, T. M., Taylor, R. H., Ghafari, H., Jenkins, A. L., Barker, H., & Jenkins, M. J. (1980). Rate of digestion of foods and postprandial glycaemia in normal and diabetic subjects. *British Medical Journal*, *281*(6232), 14-17.

Jenkins, D., Wolever, T., Taylor, R. H., Barker, H., Fielden, H., Baldwin, J. M., Bowling, A. C., Newman, H. C., Jenkins, A. L., & Goff, D. V. (1981). Glycemic index of foods: a physiological basis for carbohydrate exchange. *The American Journal of Clinical Nutrition, 34*(3), 362-366.

Jenkins, P. J., & Donald, A. M. (1998). Gelatinisation of starch: a combined SAXS/ WAXS /DSC and SANS study. *Carbohydrate Research, 308*(1), 133-147.

Jenkins, P., & Donald, A. (1995). The influence of amylose on starch granule structure. *International Journal of Biological Macromolecules, 17*(6), 315-321.

Jeon, J. S., Ryoo, N., Hahn, T.-R., Walia, H., & Nakamura, Y. (2010). Starch biosynthesis in cereal endosperm. *Plant Physiology and Biochemistry, 48*(6), 383-392.

Jood, S., Chauhan, B., & Kapoor, A. (1988). Contents and digestibility of carbohydrates of chickpea and black gram as affected by domestic processing and cooking. *Food Chemistry, 30*(2), 113-127.

Joshi, M., Aldred, P., McKnight, S., Panozzo, J., Kasapis, S., Adhikari, R., & Adhikari, B. (2013). Physicochemical and functional characteristics of lentil starch. *Carbohydrate Polymers, 92*(2), 1484-1496.

Jyothi, A. N., Sajeev, M. S., & Sreekumar, J. (2011). Hydrothermal modifications of tropical tuber starches–Effect of ANN on the physicochemical, rheological and gelatinization characteristics. *Starch-Stärke, 63*(9), 536-549.

Kainuma, K., & French, D. (1971). Nägeli amylodextrin and its relationship to starch granule structure. I. Preparation and properties of amylodextrins from various starch types. *Biopolymers, 10*(9), 1673-1680.

Kasemsuwan, T., & Jane, J. L. (1996). Quantitative method for the survey of starch phosphate derivatives and starch phospholipids by ^{31}P nuclear magnetic resonance spectroscopy. *Cereal Chemistry 73*(6),702-707

Keeling, P. L., & Myers, A. M. (2010). Biochemistry and genetics of starch synthesis. *Annual Review of Food Science and Technology*, *1*, 271-303.

Kim, H. Y., Lee, J. H., Kim, J. Y., Lim, W. J., & Lim, S. T. (2012). Characterization of nanoparticles prepared by acid hydrolysis of various starches. *Starch-Stärke, 64*(5), 367-373.

Kim, R. E., & Ahn, S.Y. (1996). Gelling properties of acid-modified red bean starch gels. *Journal of the Korean Society for Applied Biological Chemistry, 39*(1), 49-53.

Kimura, A., & Robyt, J. F. (1995). Reaction of enzymes with starch granules: kinetic products of the reaction with glucoamylase. *Carbohydrate Research, 277*(1), 87-107.

Kiseleva, V. I., Krivandin, A. V., Fornal, J., Błaszczak, W., Jeliński, T., & Yuryev, V. P. (2005). Annealing of normal and mutant wheat starches. LM, SEM, DSC, and SAXS studies. *Carbohydrate Research, 340*(1), 75-83.

Kiseleva, V., Genkina, N., Tester, R., Wasserman, L., Popov, A., & Yuryev, V. (2004). Annealing of normal, low and high amylose starches extracted from barley cultivars grown under different environmental conditions. *Carbohydrate Polymers, 56*(2), 157- 168.

Kishida, T., Nogami, H., Himeno, S., & Ebihara, K. (2001). Heat moisture treatment of high amylose cornstarch increases its resistant starch content but not its physiologic effects in rats. *The Journal of Nutrition*, *131*(10), 2716-2721.

Klein, B., & Foreman, J. A. (1980). Amylolysis of a chromogenic substrate, Cibachron Blue F3GA-amylose: kinetics and mechanism. *Clinical Chemistry, 26*(2), 250-253.

Klucinec, J. D., & Thompson, D. B. (2002). Structure of amylopectins from *ae*-containing maize starches. *Cereal Chemistry, 79*(1), 19-23.

Knutson, C. (1990). Annealing of maize starches at elevated temperatures. *Cereal Chemistry, 67* (4), 376-384.

Kohyama, K., & Sasaki, T. (2006). Differential scanning calorimetry and a model calculation of starches annealed at 20 and 50°C. *Carbohydrate Polymers*, 63(1),

82-88.

Koroteeva, D. A., Kiseleva, V. I., Krivandin, A. V., Shatalova, O. V., Błaszczak, W., Bertoft, E., Piyachomkwan, K., & Yuryev, V. P. (2007). Structural and thermodynamic properties of rice starches with different genetic background: Part 2. Defectiveness of different supramolecular structures in starch granules. *International Journal of Biological Macromolecules*, *41*, 534-547.

Kosar-Hashemi, B., Li, Z., Larroque, O., Regina, A., Yamamori, M., Morell, M. K., & Rahman, S. (2007). Multiple effects of the starch synthase II mutation in developing wheat endosperm. *Functional Plant Biology, 34*(5), 431-438.

Kubo, A., Fujita, N., Harada, K., Matsuda, T., Satoh, H., & Nakamura, Y. (1999). The starch debranching enzymes isoamylase and pullulanase are both involved in amylopectin biosynthesis in rice endosperm. *Plant physiology, 121*(2), 399-410.

Kweon, M., & Bhirud, P. (1996). An aqueous alcoholic-alkaline process for cationization of corn and pea starches. *Starch-Stärke, 48*(6), 214-220.

Lan, H., Hoover, R., Jayakody, L., Liu, Q., Donner, E., Baga, M., Asare, E. K., Hucl, P., & Chibbar, R. N. (2008). Impact of annealing on the molecular structure and physicochemical properties of normal, waxy and high amylose bread wheat starches. *Food Chemistry, 111*(3), 663-675.

Langton, M., & Hermansson, A. (1989). Microstructural changes in wheat starch dispersions during heating and cooling. *Food Structure, 8*(1), 29-39.

Lee, B.H., Bello-Pérez, L. A., Lin, A. H.M., Kim, C. Y., & Hamaker, B. R. (2013). Importance of location of digestion and colonic fermentation of starch related to

its quality. *Cereal Chemistry, 90*(4), 335-343.

Lehmann, U., Jacobasch, G., & Schmiedl, D. (2002). Characterization of resistant starch type III from banana (*Musa acuminata*). *Journal of Agricultural and Food Chemistry, 50*(18), 5236-5240.

Leszczyñski, W. A. (2004). Resistant starch–classification, structure, production. *Polish Journal of Food and Nutrition Sciences, 13*(54), 37-50.

Lewen, K. S., Paeschke, T., Reid, J., Molitor, P., & Schmidt, S. J. (2003). Analysis of the retrogradation of low starch concentration gels using differential scanning calorimetry, rheology, and nuclear magnetic resonance spectroscopy. *Journal of Agricultural and Food Chemistry, 51*(8), 2348-2358.

Li, Q., Xie, Q., Yu, S., & Gao, Q. (2013). New approach to study starch gelatinization applying a combination of hot-stage light microscopy and differential scanning calorimetry. *Journal of Agricultural and Food Chemistry*, *61*(6), 1212-1218.

Li, C., & Gilbert, R. G. (2016). Progress in controlling starch structure by modifying starch-branching enzymes. *Planta, 243*(1), 13-22.

Lim, S.T., Kasemsuwan, T., & Jane, J. L., (1994). Characterization of phosphorus in starch by 31P-nuclear magnetic resonance spectroscopy. *Cereal Chemistry 71*(5), 488-493.

Lin, J.-H., Wang, S.-W., & Chang, Y.-H. (2009). Impacts of acid-methanol treatment and annealing on the enzymatic resistance of corn starches. *Food Hydrocolloids, 23*(6), 1465-1472.

Lindeboom, N., Chang, P. R., & Tyler, R. T. (2004). Analytical, biochemical and

physicochemical aspects of starch granule size, with emphasis on small granule starches: a review. *Starch-Stärke, 56*(3-4), 89-99.

Liu, H., Guo, X., Li, W., Wang, X., Peng, Q., & Wang, M. (2015). Changes in physicochemical properties and in vitro digestibility of common buckwheat starch by heat-moisture treatment and annealing. *Carbohydrate Polymers, 132*, 237-244.

Liu, H., Yu, L., Simon, G., Dean, K., & Chen, L. (2009). Effects of annealing on gelatinization and microstructures of corn starches with different amylose/ amylopectin ratios. *Carbohydrate Polymers, 77*(3), 662-669.

Liu, J., Wang, B., Lin, L., Zhang, J., Liu, W., Xie, J., & Ding, Y. (2014). Functional, physicochemical properties and structure of cross-linked oxidized maize starch. *Food Hydrocolloids, 36*, 45-52.

Liu, Q., Gu, Z., Donner, E., Tetlow, I., & Emes, M. (2007). Investigation of digestibility in vitro and physicochemical properties of A-and B-type starch from soft and hard wheat flour. *Cereal Chemistry*, *84*(1), 15-21.

LMC International, 2002. Evaluation of the Community Policy for Starch and Starch Products (Evaluation report prepared for European Commission – DG Agriculture) LMC International Limited., Oxford, England.

Lopez-Rubio, A., Flanagan, B. M., Gilbert, E. P., & Gidley, M. J. (2008). A novel approach for calculating starch crystallinity and its correlation with double helix content: A combined XRD and NMR study. *Biopolymers, 89*(9), 761-768.

Lopez-Rubio, A., Flanagan, B. M., Shrestha, A. K., Gidley, M. J., & Gilbert, E. P. (2008). Molecular rearrangement of starch during in vitro digestion: toward a better

understanding of enzyme resistant starch formation in processed starches. *Biomacromolecules*, 9, 1951-1958.

Ludwig, D. S. (2002). The glycemic index: physiological mechanisms relating to obesity, diabetes, and cardiovascular disease. *The Journal of the American Medical Association, 287*(18), 2414-2423.

Ludwig, D. S., Majzoub, J. A., Al-Zahrani, A., Dallal, G. E., Blanco, I., & Roberts, S. B. (1999). High glycemic index foods, overeating, and obesity. *Pediatrics, 103*(3), e26-e26.

Maaran, S., Hoover, R., Donner, E., & Liu, Q. (2014). Composition, structure, morphology and physicochemical properties of lablab bean, navy bean, rice bean, tepary bean and velvet bean starches. *Food Chemistry, 152*, 491-499.

Maaran, S., Hoover, R., Vamadevan, V., Waduge, R. N., & Liu, Q. (2016). *In vitro* amylolysis of pulse and Hylon®VII starches explained in terms of their composition, morphology, granule architecture and interaction between hydrolysed starch chains. *Food Chemistry, 192*, 1098-1108.

Malhotra, S. (1968). Epidemiological study of cholelithiasis among railroad workers in India with special reference to causation. *Gut, 9*(3), 290-295.

Man, J., Cai, J., Cai, C., Xu, B., Huai, H., & Wei, C. (2012). Comparison of physico-chemical properties of starches from seed and rhizome of lotus. *Carbohydrate Polymers, 88*(2), 676-683.

Mariotti, M., Zardi, M., Lucisano, M., & Pagani, M. A. (2005). Influence of the heating rate on the pasting properties of various flours. *Starch-Stärke, 57*(11), 564-572.

Martin, C., & Smith, A. M. (1995). Starch biosynthesis. *The Plant Cell, 7*(7), 971-985

Martinez-Flores, H. E., Chang, Y. K., Martinez-Bustos, F., & Sgarbieri, V. (2004). Effect of high fiber products on blood lipids and lipoproteins in hamsters. *Nutrition Research, 24*(1), 85-93..

McPherson, A., & Jane, J.-l. (1999). Comparison of waxy potato with other root and tuber starches. *Carbohydrate Polymers, 40*(1), 57-70.

Miao, M., Jiang, B., Zhang, T., Jin, Z., & Mu, W. (2011). Impact of mild acid hydrolysis on structure and digestion properties of waxy maize starch. *Food Chemistry*, *126*(2), 506-513.

Miles, M. J., Morris, V. J., Orford, P. D., & Ring, S. G. (1985). The roles of amylose and amylopectin in the gelation and retrogradation of starch. *Carbohydrate Research, 135*(2), 271-281.

Mitchell, C. R. (2009). Rice starches: production and properties. In J. N. BeMiller, & R. L. Whistler (Eds.), Starch: Chemistry and technology (pp. 569-577). New York, NY,USA: Academic Press.

Morais, M. B., Feste, A., Miller, R. G., & Lifschitz, C. H. (1996). Effect of resistant and digestible starch on intestinal absorption of calcium, iron, and zinc in infant pigs. *Pediatric Research, 39*(5), 872-876.

Morell, M. K., Kosar-Hashemi, B., Cmiel, M., Samuel, M. S., Chandler, P., Rahman, S., Buleon, A., Batey, I. L., & Li, Z. (2003). Barley sex6 mutants lack starch synthase IIa activity and contain a starch with novel properties. *The Plant Journal, 34*(2), 173-185.

Morita, T., Kasaoka, S., Hase, K., & Kiriyama, S. (1999). Psyllium shifts the fermentation site of high-amylose cornstarch toward the distal colon and increases fecal butyrate concentration in rats. *Journal of Nutrition, 129*(11), 2081-2087.

Morrison, W. (1981). Starch lipids: A reappraisal. *Starch-Stärke, 33*(12), 408-410.

Morrison, W. (1995). Starch lipids and how they relate to starch granule structure and functionality. *Cereal Foods World, 40*(6), 437-446.

Morrison, W. R. (1988). Lipids in cereal starches: A review. *Journal of Cereal Science, 8*(1), 1-15.

Morrison, W. R., Tester, R. F., Gidley, M. J., & Karkalas, J. (1993a). Resistance to acid hydrolysis of lipid-complexed amylose and lipid-free amylose in lintnerised waxy and non-waxy barley starches. *Carbohydrate Research, 245*(2), 289-302.

Morrison, W. R., Tester, R. F., Snape, C. E., Law, R., & Gidley, M. J. (1993b). Swelling and gelatinization of cereal starches. IV. Some effects of lipid-complexed amylose and free amylose in waxy and normal barley starches. *Cereal Chemistry*, *70*(4), 385-391.

Morrison, W. R., Law, R. V., & Snape, C. E. (1993c). Evidence for inclusion complexes of lipids with V-amylose in maize, rice and oat starches. *Journal of Cereal Science*, *18*(2), 107-109.

Morrison, W.R., & Gadan, H. (1987). The amylose and lipid contents of starch granules in developing wheat endosperm. *Journal of Cereal Science*, *5*(3), 263-275.

Mua, J. P., & Jackson, D. S. (1998). Retrogradation and gel textural attributes of corn starch amylose and amylopectin fractions. *Journal of Cereal Science, 27*(2), 157-

166.

Muhrbeck, P., & Wischmann, B. (1998). Influence of phosphate esters on the annealing properties of starch. *Starch-Stärke, 50*(10), 423-426.

Mukerjea, R., Mukerjea, R., & Robyt, J. F. (2009). Starch biosynthesis: experiments on how starch granules grow in vivo. *Carbohydrate Research, 344*(1), 67-73.

Myers, A. M., Morell, M. K., James, M. G., & Ball, S. G. (2000). Recent progress toward understanding biosynthesis of the amylopectin crystal. *Plant Physiology, 122*(4), 989-998.

Nakamura, Y. (2002). Towards a better understanding of the metabolic system for amylopectin biosynthesis in plants: rice endosperm as a model tissue. *Plant and Cell Physiology, 43*(7), 718-725.

Nakazawa, Y., & Wang, Y.-J. (2003). Acid hydrolysis of native and annealed starches and branch-structure of their Naegeli dextrins. *Carbohydrate Research, 338*(24), 2871-2882.

Nakazawa, Y., & Wang, Y.-J. (2004). Effect of annealing on starch–palmitic acid interaction. *Carbohydrate Polymers, 57*(3), 327-335.

Nielsen, T. H., Baunsgaard, L., & Blennow, A. (2002). Intermediary glucan structures formed during starch granule biosynthesis are enriched in short side chains, a dynamic pulse labeling approach. *Journal of Biological Chemistry, 277*(23), 20249-20255.

Nielsen, T. H., Wischmann, B., Enevoldsen, K., & Moller, B. L. (1994). Starch

phosphorylation in potato tubers proceeds concurrently with de novo biosynthesis of starch. *Plant Physiology, 105*(1), 111-117.

Nikuni, Z. (1978). Studies on starch granules. *Starch-Stärke, 30*(4), 105-111.

Nuessli, J., Putaux, J. L., Le Bail, P., & Buléon, A. (2003). Crystal structure of amylose complexes with small ligands. *International Journal of Biological Macromolecules, 33*(4), 227-234.

Nugent, A. P. (2005). Health properties of resistant starch. *Nutrition Bulletin, 30*(1), 27-54.

Oates, C. G. (1997). Towards an understanding of starch granule structure and hydrolysis. *Trends in Food Science and Technology, 8*(11), 375-382.

Olu-Owolabi, B. I., Afolabi, T. A., & Adebowale, K. O. (2011). Pasting, thermal, hydration, and functional properties of annealed and heat-moisture treated starch of sword bean (*Canavalia gladiata*). *International Journal of Food Properties, 14*(1), 157-174.

O'Shea, M. G., Samuel, M. S., Konik, C. M., & Morell, M. K. (1998). Fluorophore-assisted carbohydrate electrophoresis (FACE) of oligosaccharides: efficiency of labelling and high-resolution separation. *Carbohydrate Research, 307*(1), 1-12.

Ozcan, S., & Jackson, D. S. (2002). The impact of thermal events on amylose-fatty acid complexes. *Starch-Stärke, 54*(12), 593-602.

Ozcan, S., & Jackson, D. S. (2003). A response surface analysis of commercial corn starch annealing. *Cereal Chemistry, 80*(2), 241.

Palma-Rodriguez, H. M., Agama-Acevedo, E., Mendez-Montealvo, G., Gonzalez-Soto,

R. A., Vernon-Carter, E. J., & Bello-Pérez, L. A. (2012). Effect of acid treatment on the physicochemical and structural characteristics of starches from different botanical sources. *Starch-Stärke, 64*(2), 115-125.

Paris, M., Bizot, H., Emery, J., Buzaré, J., & Buléon, A. (1999). Crystallinity and structuring role of water in native and recrystallized starches by 13 C CP/MAS NMR spectroscopy: 1: Spectral decomposition. *Carbohydrate Polymers, 39*(4), 327-339.

Paschall, E. F. (1964). Phosphation with inorganic phosphate salts. *Methods in Carbohydrate Chemistry, 4*, 294-296.

Perera, A., Meda, V., & Tyler, R. (2010). Resistant starch: A review of analytical protocols for determining resistant starch and of factors affecting the resistant starch content of foods. *Food Research International, 43*(8), 1959-1974.

Pérez, S., & Bertoft, E. (2010). The molecular structures of starch components and their contribution to the architecture of starch granules: A comprehensive review. *Starch-Stärke, 62*(8), 389-420.

Perry, P., & Donald, A. (2000). The role of plasticization in starch granule assembly. *Biomacromolecules, 1*(3), 424-432.

Planchot, V., Colonna, P., & Buleon, A. (1997). Enzymatic hydrolysis of α-glucan crystallites. *Carbohydrate Research, 298*(4), 319-326.

Planchot, V., Colonna, P., Gallant, D. J., & Bouchet, B. (1995). Extensive degradation of native starch granules by alpha-amylase from *Aspergillus fumigatus*. *Journal of Cereal Science, 21*(2), 163-171.

Polesi, L., Sarmento, S., & Anjos, C. (2011). Composition and characterization of pea and chickpea starches. *Brazilian Journal of Food Technology, 14*, 74-81.

Primo-Martin, C., Van Nieuwenhuijzen, N., Hamer, R., & Van Vliet, T. (2007). Crystallinity changes in wheat starch during the bread-making process: starch crystallinity in the bread crust. *Journal of Cereal Science, 45*(2), 219-226.

Putaux, J.-L., Molina-Boisseau, S., Momaur, T., & Dufresne, A. (2003). Platelet nanocrystals resulting from the disruption of waxy maize starch granules by acid hydrolysis. *Biomacromolecules, 4*(5), 1198-1202.

Raben, A., Tagliabue, A., Christensen, N. J., Madsen, J., Holst, J. J., & Astrup, A. (1994). Resistant starch: the effect on postprandial glycemia, hormonal response, and satiety. The *American Journal of Clinical Nutrition, 60*(4), 544-551.

Radchuk, V. V., Borisjuk, L., Sreenivasulu, N., Merx, K., Mock, H. P., Rolletschek, H., & Weschke, W. (2009). Spatiotemporal profiling of starch biosynthesis and degradation in the developing barley grain. *Plant Physiology, 150*(1), 190-204.

Ratnayake, W. S., Hoover, R., & Warkentin, T. (2002). Pea starch: composition, structure and properties. *Starch-Stärke*, *54*(6), 217-234.

Ratnayake, W., Hoover, R., Shahidi, F., Perera, C., & Jane, J. (2001). Composition, molecular structure, and physicochemical properties of starches from four field pea (*Pisum sativum L.*) cultivars. *Food Chemistry, 74*(2), 189-202.

Reader, A. (1997). Response of resistant starch in a food bar vs two commercially available bars in persons with type II diabetes mellitus. *Diabetes, 46*, 254A.

Riley, C. K., Wheatley, A. O., & Asemota, H. N. (2006). Isolation and characterization of starches from eight *Dioscorea alata* cultivars grown in Jamaica. *African Journal of Biotechnology, 5*(17), 1528-1536.

Roach, R., & Hoseney, R. (1995). Effect of certain surfactants on the swelling, solubility and amylograph consistency of starch. *Cereal Chemistry, 72*(6), 571-577.

Robin, J. (1974). Lint-nerized starches. Gel filtration and enzymatic studies of insoluble residues from prolonged acid treatment of potato starch. *Cereal Chemistry, 51*, 389-406.

Robyt, J.F. (1984) Enzymes in the hydrolysis and synthesis of starch. In R. L. Whistler, & J. N. BeMiller & E. F. Paschell (Eds), *Starch Chemistry and Technology (2nd edn)* (pp. 87-123). New York,NY, USA: Academic Press.

Robyt, J., & French, D. (1963). Action pattern and specificity of an amylase from Bacillus subtilis. *Archives of Biochemistry and Biophysics, 100*(3), 451-467.

Robyt, J. F., & French, D. (1967). Multiple attack hypothesis of α-amylase action: action of porcine pancreatic, human salivary, and *Aspergillus oryzae* α-amylases. *Archives of Biochemistry and Biophysics, 122*(1), 8-16.

Robyt, J. F., & French, D. (1970). The action pattern of porcine pancreatic α-amylase in relationship to the substrate binding site of the enzyme. *Journal of Biological Chemistry, 245*(15), 3917-3927.

Rocha, T. S., Cunha, V. A. G., Jane, J.-l., & Franco, C. M. L. (2011). Structural characterization of Peruvian carrot (*Arracacia xanthorrhiza*) starch and the effect of annealing on its semicrystalline structure. *Journal of Agricultural and Food*

Chemistry, 59(8), 4208-4216.

Rocha, T. S., Felizardo, S. G., Jane, J.-l., & Franco, C. M. (2012). Effect of annealing on the semicrystalline structure of normal and waxy corn starches. *Food Hydrocolloids, 29*(1), 93-99.

Rodríguez-Cabezas, M. E., Camuesco, D., Arribas, B., Garrido-Mesa, N., Comalada, M., Bailón, E., & Gálvez, J. (2010). The combination of fructooligosaccharides and resistant starch shows prebiotic additive effects in rats. *Clinical Nutrition*, *29*(6), 832-839.

Ryan, S. M., Fitzgerald, G. F., & van Sinderen, D. (2006). Screening for and identification of starch-, amylopectin-, and pullulan-degrading activities in bifidobacterial strains. *Applied and Environmental Microbiology, 72*(8), 5289-5296.

Saibene, D., & Seetharaman, K. (2010). Amylose involvement in the amylopectin clusters of potato starch granules. *Carbohydrate Polymers, 82*(2), 376-383.

Sajilata, M. G., Singhal, R. S., & Kulkarni, P. R. (2006). Resistant starch–a review. *Comprehensive Reviews in Food Science and Food Safety, 5*(1), 1-17.

Sandhu, K. S., & Lim, S.-T. (2008). Digestibility of legume starches as influenced by their physical and structural properties. *Carbohydrate Polymers, 71*(2), 245-252.

Sarko, A., & Wu, H. C. (1978). The crystal structures of A-, B-and C-polymorphs of amylose and starch. *Starch-Stärke, 30*(3), 73-78.

Sasaki, T., & Matsuki, J. (1998). Effect of wheat starch structure on swelling power. *Cereal Chemistry*, *75*(4), 525-529.

Sasaki, T., Yasui, T., & Matsuki, J. (2000). Effect of amylose content on gelatinization, retrogradation, and pasting properties of starches from waxy and nonwaxy wheat and their F1 seeds. *Cereal Chemistry, 77*(1), 58-63.

Satin, M. (1998). Functional properties of starches. *Spolight tropical starch misses market. AGSI report, Agriculture21. FAO-Magazine*, 11.

Schweizer, T., Andersson, H., Langkilde, A., Reimann, S., & Torsdottir, I. (1990). Nutrients excreted in ileostomy effluents after consumption of mixed diets with beans or potatoes. II. Starch, dietary fibre and sugars. *European Journal of Clinical Nutrition, 44*(8), 567-575.

Seneviratne, H., & Biliaderis, C. (1991). Action of α-amylases on amylose-lipid complex superstructures. *Journal of Cereal Science, 13*(2), 129-143.

Seow, C., & Teo, C. (1993). Annealing of granular rice starches—interpretation of the effect on phase transitions associated with gelatinization. *Starch-Stärke, 45*(10), 345-351.

Sevenou, O., Hill, S., Farhat, I., & Mitchell, J. (2002). Organisation of the external region of the starch granule as determined by infrared spectroscopy. *International Journal of Biological Macromolecules, 31*(1), 79-85.

Shi, Y. C., & Seib, P. A. (1992). The structure of four waxy starches related to gelatinization and retrogradation. *Carbohydrate Research, 227*, 131-145.

Shi, Y. C., Capitani, T., Trzasko, P., & Jeffcoat, R. (1998). Molecular structure of a low-amylopectin starch and other high-amylose maize starches. *Journal of Cereal Science, 27*(3), 289-299.

Shrestha, A. K., Blazek, J., Flanagan, B. M., Dhital, S., Larroque, O., Morell, M. K., Gilbert, E. P., & Gidley, M. J. (2015). Molecular, mesoscopic and microscopic structure evolution during amylase digestion of extruded maize and high amylose maize starches. *Carbohydrate Polymers, 118*, 224-234.

Shujun, W., Jinglin, Y., Jiugao, Y., Jiping, P., & Hongyan, L. (2008). Structure characterization of C-type starch granule by acid hydrolysis. *Food Hydrocolloids , 22*(7), 1283-1290.

Shure, M., Wessler, S., & Fedoroff, N. (1983). Molecular identification and isolation of the Waxy locus in maize. *Cell*, *35*(1), 225-233.

Silverio, J., Fredriksson, H., Andersson, R., Eliasson, A. C., & Åman, P. (2000). The effect of temperature cycling on the amylopectin retrogradation of starches with different amylopectin unit-chain length distribution. *Carbohydrate Polymers, 42*(2), 175-184.

Simsek, S., Ovando-Martínez, M., Whitney, K., & Bello-Pérez, L. A. (2012). Effect of acetylation, oxidation and annealing on physicochemical properties of bean starch. *Food Chemistry, 134*(4), 1796-1803.

Singh, H., Chang, Y. H., Lin, J.-H., Singh, N., & Singh, N. (2011). Influence of heat–moisture treatment and annealing on functional properties of sorghum starch. *Food Research International, 44*(9), 2949-2954.

Singh, J., Kaur, L., & McCarthy, O. (2007). Factors influencing the physico-chemical, morphological, thermal and rheological properties of some chemically modified starches for food applications. *Food Hydrocolloids, 21*(1), 1-22.

Singh, N. (2011). Functional and physicochemical properties of pulse starches. In B.K. Tiwari, A.Gowen & B. McKenna (Eds), *Pulse Foods: Processing, quality and nutraceutical applications* (pp. 91-120). London. UK: Academic Press.

Singh, N., Chawla, D., & Singh, J. (2004). Influence of acetic anhydride on physico-chemical, morphological and thermal properties of corn and potato starch. *Food Chemistry, 86*(4), 601-608.

Singh, N., Singh, J., Kaur, L., Sodhi, N. S., & Gill, B. S. (2003). Morphological, thermal and rheological properties of starches from different botanical sources. *Food Chemistry, 81*(2), 219-231.

Singh, S., Singh, N., Isono, N., & Noda, T. (2009). Relationship of granule size distribution and amylopectin structure with pasting, thermal, and retrogradation properties in wheat starch. *Journal of Agricultural and Food Chemistry, 58*(2), 1180-1188.

Singh, H., Sodhi, N. S., & Singh, N. (2009). Structure and functional properties of acid thinned sorghum starch. *International Journal of Food Properties*, *12*(4), 713-725.

Siswoyo, T. A., & Morita, N. (2010). Influence of annealing on gelatinization properties, retrogradation and susceptibility of breadfruit starch (*Artocarpus communis*). *International Journal of Food Properties, 13*(3), 553-561.

Skerritt, J. H., Frend, A. J., Robson, L. G., & Greenwell, P. (1990). Immunological homologies between wheat gluten and starch granule proteins. *Journal of Cereal Science, 12*(2), 123-136.

Smith, A. M., Denyer, K., & Martin, C. R. (1995). What controls the amount and structure of starch in storage organs? *Plant physiology, 107*(3), 673.

Snow, P., & O'Dea, K. (1981). Factors affecting the rate of hydrolysis of starch in food. *The American Journal of Clinical Nutrition, 34*(12), 2721-2727.

Socorro, M., Levy-Benshimol, A., & Tovar, J. (1989). *In vitro* digestibility of cereal and legume (*Phaseolus vulgaris*) starches by bovine, porcine and human pancreatic α-amylases effect of dietary fiber. *Starch-Stärke, 41*(2), 69-71.

Song, H. Y., Lee, S. Y., Choi, S. J., Kim, K. M., Kim, J. S., Han, G. J., & Moon, T. W. (2014). Digestibility and physicochemical properties of granular sweet potato starch as affected by annealing. *Food Science and Biotechnology, 23*(1), 23-31.

Srichuwong, S., Sunarti, T. C., Mishima, T., Isono, N., & Hisamatsu, M. (2005a). Starches from different botanical sources I: Contribution of amylopectin fine structure to thermal properties and enzyme digestibility. *Carbohydrate Polymers, 60*(4), 529-538.

Srichuwong, S., Sunarti, T. C., Mishima, T., Isono, N., & Hisamatsu, M. (2005b). Starches from different botanical sources II: Contribution of starch structure to swelling and pasting properties. *Carbohydrate Polymers, 62*(1), 25-34.

Stute, R. (1992). Hydrothermal Modification of Starches: The difference between annealing and heat/moisture-treatment. *Starch-Stärke, 44*(6), 205-214.

Sujka, & Jamroz, J. (2009). α-Amylolysis of native potato and corn starches–SEM, AFM, nitrogen and iodine sorption investigations. *LWT-Food Science and Technology, 42*(7), 1219-1224.

Sujka, M., & Jamroz, J. (2007). Starch granule porosity and its changes by means of amylolysis. *International Agrophysics, 21*(1), 107-113.

Suortti, T., Gorenstein, M., & Roger, P. (1998). Determination of the molecular mass of amylose. *Journal of Chromatography A*, *828*(1), 515-521.

Szydlowski, N., Ragel, P., Raynaud, S., Lucas, M. M., Roldán, I., Montero, M., Muñoz, F. J., Ovecka, M., Bahaji, A., & Planchot, V. (2009). Starch granule initiation in Arabidopsis requires the presence of either class IV or class III starch synthases. *The Plant Cell, 21*(8), 2443-2457.

Tabata, S., & Hizukuri, S. (1971). Studies on Starch Phosphate. Part 2. Isolation of Glucose 3-Phosphate and maltose phosphate by acid hydrolysis of potato starch. *Starch-Stärke, 23*(8), 267-272.

Takahashi, S., & Seib, P. (1988). Paste and gel properties of prime corn and wheat starches with and without native lipids. *Cereal Chemistry, 65*(6), 474-483.

Takata, H., Takaha, T., Okada, S., Takagi, M., & Imanaka, T. (1996). Cyclization reaction catalyzed by branching enzyme. *Journal of Bacteriology, 178*(6), 1600-1606.

Takeda, Y., & Hizukuri, S. (1981). Re-examination of the action of sweet-potato beta-amylase on phosphorylated (1→ 4)-χ-d-glucan. *Carbohydrate Research, 89*(1), 174-178.

Takeda, Y., Guan, H.-P., & Preiss, J. (1993). Branching of amylose by the branching isoenzymes of maize endosperm. *Carbohydrate Research, 240*, 253-263.

Takeda, Y., Hizukuri, S., Takeda, C., & Suzuki, A. (1987). Structures of branched

molecules of amyloses of various origins, and molar fractions of branched and unbranched molecules. *Carbohydrate Research, 165*(1), 139-145.

Takeda, Y., Shibahara, S., & Hanashiro, I. (2003). Examination of the structure of amylopectin molecules by fluorescent labeling. *Carbohydrate Research, 338*(5), 471-475.

Takeda, Y., Shibahara, S., & Hanashiro, I. (2003). Examination of the structure of amylopectin molecules by fluorescent labeling. *Carbohydrate Research, 338*(5), 471-475.

Takeda, Y., Tokunaga, N., Takeda, C., & Hizukuri, S. (1986). Physicochemical properties of sweet potato starches. *Starch-Stärke, 38(10)*, 345-350.

Tamaki, S., Hisamatsu, M., Teranishi, K., Adachi, T., & Yamada, T. (1998). Structural change of maize starch granules by ball-mill treatment. *Starch-Stärke, 50*(8), 342-348.

Tan, I., Flanagan, B. M., Halley, P. J., Whittaker, A. K., & Gidley, M. J. (2007). A method for estimating the nature and relative proportions of amorphous, single, and double-helical components in starch granules by ^{13}C CP/MAS NMR. *Biomacromolecules, 8*(3), 885-891.

Tang, M. C., & Copeland, L. (2007). Analysis of complexes between lipids and wheat starch. *Carbohydrate Polymers, 67*(1), 80-85.

Tatge, H., Marshall, J., Martin, C., Edwards, E., & Smith, A. (1999). Evidence that amylose synthesis occurs within the matrix of the starch granule in potato tubers. *Plant, Cell and Environment, 22*(5), 543-550.

Tester, R. F. (1997). Influence of growth conditions on barley starch properties. *International Journal of Biological Macromolecules, 21*(1), 37-45.

Tester, R. F., & Debon, S. J. J. (2000). Annealing of starch — a review. *International Journal of Biological Macromolecules, 27*(1), 1-12.

Tester, R. F., & Morrison, W. R. (1990a). Swelling and gelatinization of cereal starches. I. Effects of amylopectin, amylose, and lipids. *Cereal Chemistry, 67*(6), 551-557.

Tester, R. F., & Morrison, W. R. (1990b). Swelling and gelatinization of cereal starches. II. Waxy rice starches. *Cereal Chemistry, 67*(6), 558-563.

Tester, R. F., Debon, S. J. J., & Karkalas, J. (1998). Annealing of wheat starch. *Journal of Cereal Science, 28*(3), 259-272.

Tester, R. F., Debon, S. J. J., & Sommerville, M. D. (2000). Annealing of maize starch. *Carbohydrate Polymers, 42*(3), 287-299.

Tester, R. F., Karkalas, J., & Qi, X. (2004). Starch-composition, fine structure and architecture. *Journal of Cereal Science, 39*(2), 151-165.

Tester, R., Qi, X., & Karkalas, J. (2006). Hydrolysis of native starches with amylases. *Animal Feed Science and Technology, 130*(1), 39-54.

Tetlow, I. J. (2011). Starch biosynthesis in developing seeds. *Seed Science Research, 21*(01), 5-32.

Tetlow, I. J., & Emes, M. J. (2014). A review of starch-branching enzymes and their role in amylopectin biosynthesis. *IUBMB Life, 66*(8), 546-558.

Tetlow, I. J., Morell, M. K., & Emes, M. J. (2004). Recent developments in understanding the regulation of starch metabolism in higher plants. *Journal of Experimental*

Botany, 55(406), 2131-2145.

Tiwari, B. K., & Singh, N. (2012). Pulse starch. In B.K. Tiwari & N. Singh (Eds), *Pulse Chemistry and Technology (*pp. 107-129*)*. Cambridge. UK: Royal Society of Chemistry.

Topping, D. L., & Clifton, P. M. (2001). Short-chain fatty acids and human colonic function: roles of resistant starch and nonstarch polysaccharides. *Physiological Reviews*, *81*(3), 1031-1064.

Tovar, J., Duan, R.-D., Erlanson-Albertsson, C., & Björck, I. M. (1991). Starch digestibility in the diabetic rat. *Nutrition research, 11*(11), 1329-1334.

Tufvesson, F., Wahlgren, M., & Eliasson, A. C. (2003). Formation of amylose-lipid complexes and effects of temperature treatment. Part 1. Monoglycerides. *Starch-Stärke, 55*(2), 61-71.

Vamadevan, V., & Bertoft, E. (2015). Structure-function relationships of starch components. *Starch-Stärke, 67*(1-2), 55-68.

Vamadevan, V., Bertoft, E., Soldatov, D. V., & Seetharaman, K. (2013). Impact on molecular organization of amylopectin in starch granules upon annealing. *Carbohydrate Polymers, 98*(1), 1045-1055.

Vamadevan, V., Hoover, R., Bertoft, E., & Seetharaman, K. (2014). Hydrothermal treatment and iodine binding provide insights into the organization of glucan chains within the semi-crystalline lamellae of corn starch granules. *Biopolymers, 101*(8), 871-885.

van de Velde, F., van Riel, J., & Tromp, R. H. (2002). Visualisation of starch granule

morphologies using confocal scanning laser microscopy (CSLM). *Journal of the Science of Food and Agriculture, 82*(13), 1528-1536.

van Soest, J. J., Tournois, H., de Wit, D., & Vliegenthart, J. F. (1995). Short-range structure in (partially) crystalline potato starch determined with attenuated total reflectance Fourier-transform IR spectroscopy. *Carbohydrate Research*, 279, 201-214.

Vandeputte, G., Vermeylen, R., Geeroms, J., & Delcour, J. (2003). Rice starches. III. Structural aspects provide insight in amylopectin retrogradation properties and gel texture. *Journal of Cereal Science, 38*(1), 61-68.

Varavinit, S., Shobsngob, S., Varanyanond, W., Chinachoti, P., & Naivikul, O. (2003). Effect of amylose content on gelatinization, retrogradation and pasting properties of flours from different cultivars of Thai rice. *Starch-Stärke, 55*(9), 410-415.

Vasanthan, T., & Bhatty, R. (1996). Physicochemical properties of small-and large-granule starches of waxy, regular, and high-amylose barleys. *Cereal Chemistry, 73*(2), 199-207.

Vasanthan, T., & Hoover, R. (1992a). A comparative study of the composition of lipids associated with starch granules from various botanical sources. *Food Chemistry, 43*(1), 19-27.

Vasanthan, T., & Hoover, R. (1992b). Effect of defatting on starch structure and physico-chemical properties. *Food Chemistry, 45*(5), 337-347.

Veregin, R., Fyfe, C., Marchessault, R., & Taylor, M. (1986). Characterization of the crystalline A and B starch polymorphs and investigation of starch crystallization

by high-resolution carbon-13 CP/MAS NMR. *Macromolecules, 19*(4), 1030-1034.

Vermeylen, R., Goderis, B., & Delcour, J. A. (2006). An X-ray study of hydrothermally treated potato starch. *Carbohydrate Polymers, 64*(2), 364-375.

Vrinten, P. L., & Nakamura, T. (2000). Wheat granule-bound starch synthase I and II are encoded by separate genes that are expressed in different tissues. *Plant Physiology, 122*(1), 255-264.

Waduge, R. N., Hoover, R., Vasanthan, T., Gao, J., & Li, J. (2006). Effect of annealing on the structure and physicochemical properties of barley starches of varying amylose content. *Food Research International, 39*(1), 59-77.

Waigh, T. A., Gidley, M. J., Komanshek, B. U., & Donald, A. M. (2000). The phase transformations in starch during gelatinisation: a liquid crystalline approach. *Carbohydrate Research, 328*(2), 165-176.

Waigh, T. A., Jenkins, P. J., & Donald, A. M. (1996). Quantification of water in carbohydrate lamellae using SANS. *Faraday Discussions, 103*, 325-337.

Waigh, T. A., Kato, K. L., Donald, A. M., Gidley, M. J., Clarke, C. J., & Riekel, C. (2000). Side-chain liquid-crystalline model for starch. *Starch-Stärke, 52*(12), 450-460.

Wang, L., & Seib, P. A. (1996). Australian salt-noodle flours and their starches compared to US wheat flours and their starches. *Cereal Chemistry, 73*(2), 167-175.

Wang, S., & Copeland, L. (2012). New insights into loss of swelling power and pasting profiles of acid hydrolyzed starch granules. *Starch-Stärke*, *64*(7), 538-544.

Wang, S., & Copeland, L. (2013). Molecular disassembly of starch granules during

gelatinization and its effect on starch digestibility . *Food and Function, 4*(11), 1564-1580.

Wang, S., & Copeland, L. (2015). Effect of acid hydrolysis on starch structure and functionality: A review. *Critical Reviews in Food Science and Nutrition, 55*(8), 1081-1097.

Wang, S., Blazek, J., Gilbert, E., & Copeland, L. (2012). New insights on the mechanism of acid degradation of pea starch. *Carbohydrate Polymers, 87*(3), 1941-1949.

Wang, S., Jin, F., & Yu, J. (2013). Pea starch annealing: New insights. *Food and Bio-process Technology, 6*(12), 3564-3575.

Wang, S., Wang, J., Yu, J., & Wang, S. (2014). A comparative study of annealing of waxy, normal and high-amylose maize starches: The role of amylose molecules. *Food Chemistry, 164*, 332-338.

Wang, T. L., Bogracheva, T. Y., & Hedley, C. L. (1998). Starch: as simple as A, B, C? *Journal of Experimental Botany, 49*(320), 481-502.

Wang, W., Powell, A., & Oates, C. (1997). Effect of annealing on the hydrolysis of sago starch granules. *Carbohydrate Polymers, 33*(2), 195-202.

Wang, S., Yu, J., & Yu, J. (2008). Conformation and location of amorphous and semi-crystalline regions in C-type starch granules revealed by SEM, NMR and XRD. *Food Chemistry, 110*(1), 39-46

Waterschoot, J., Gomand, S. V., Fierens, E., & Delcour, J. A. (2015). Starch blends and their physicochemical properties. *Starch-Stärke, 67*(1-2), 1-13.

Weill, C. E., Burch, R. J., & Vandyk, J. W. (1954). An alpha-amyloglucosidase that

produces beta-glucose. *Cereal Chemistry, 31*(2), 150-158.

Whistler, R. L., & BeMiller, J. N. (1997). Starch. In R.L. Whisler, J.N. BeMiller (Eds.), *Carbohydrate Chemistry for Food Scientists*, (pp. 117–151) St. Paul, MN, USA: American Association of Cereal Chemists.

Whittam, M. A., Orford, P. D., Ring, S. G., Clark, S. A., Parker, M. L., Cairns, P., & Miles, M. J. (1989). Aqueous dissolution of crystalline and amorphous amylose-alcohol complexes. *International Journal of Biological Macromolecules, 11*(6), 339-344.

Witt, T., & Gilbert, R. G. (2014). Causal relations between structural features of amylopectin, a semicrystalline hyperbranched polymer. *Biomacromolecules, 15*(7), 2501-2511.

Wolever, T. M., & Bolognesi, C. (1996). Source and amount of carbohydrate affect postprandial glucose and insulin in normal subjects. *The Journal of Nutrition*, *126*(11), 2798-2806.

Wolf, B. W., Bauer, L. L., & Fahey, G. C. (1999). Effects of chemical modification on in vitro rate and extent of food starch digestion: an attempt to discover a slowly digested starch. *Journal of Agricultural and Food Chemistry, 47*(10), 4178-4183.

Woo, K., & Seib, P. (2002). Cross-linked resistant starch: preparation and properties 1. *Cereal Chemistry, 79*(6), 819-825.

Woo, K., & Seib, P. A. (1997). Cross-linking of wheat starch and hydroxypropylated wheat starch in alkaline slurry with sodium trimetaphosphate. *Carbohydrate Polymers, 33*(4), 263-271.

Woolnough, J. W., Bird, A. R., Monro, J. A., & Brennan, C. S. (2010). The effect of a brief salivary α-amylase exposure during chewing on subsequent in vitro starch digestion curve profiles. *International Journal of Molecular Sciences*, 11(8), 2780-2790.

Wu, A. C., Witt, T., & Gilbert, R. G. (2014). Characterization methods for starch-based materials: state of the art and perspectives. *Australian Journal of Chemistry, 66*(12), 1550-1563.

Wurzburg, O. B. (1986). Converted starches. In O. B. Wurzburg (Ed), *Modified starches: Properties and uses* (pp. 17–40). Boca Raton, FL,USA: CRC Press.

Xia, L., Wenyuan, G., Juan, W., Qianqian, J., & Luqi, H. (2010). Comparison of the morphological, crystalline, and thermal properties of different crystalline types of starches after acid hydrolysis. *Starch-Stärke, 62*(12), 686-696.

Xie, X. S., Liu, Q., & Cui, S. W. (2006). Studies on the granular structure of resistant starches (type 4) from normal, high amylose and waxy corn starch citrates. *Food Research International, 39*(3), 332-341.

Yadav, B. S., Guleria, P., & Yadav, R. B. (2013). Hydrothermal modification of Indian water chestnut starch: Influence of heat-moisture treatment and annealing on the physicochemical, gelatinization and pasting characteristics. *LWT-Food Science and Technology, 53*(1), 211-217.

Yangsheng, W., & Seib, A. (1990). Acetylated and hydroxypropylated distarch phosphates from waxy barley paste properties and freeze-thaw stability. *Cereal Chemistry, 67*(2), 202-208.

Yoshimoto, Y., Tashiro, J., Takenouchi, T., & Takeda, Y. (2000). Molecular structure and some physicochemical properties of high-amylose barley starches. *Cereal Chemistry, 77*(3), 279-285.

Yuryev, V.P., Kozlov, S.S., Noda, T., Bertoft, E., and Blennow, A. (2007). Influence of different GBSS 1 and GWD combinations on the amylose localization within wheat and potato starch granules. In V. P. Yuryev, P. Tomasik and E. Bertoft, (Eds): *Starch: Achievements in Under-standing of Structure*, (pp. 1-47). New York, NY,USA: Nova Science Publishers Inc.

Yuryev, V. P., Krivandin, A. V., Kiseleva, V. I., Wasserman, L. A., Genkina, N. K., Fornal, J., Blaszczak, W., & Schiraldi, A. (2004). Structural parameters of amylopectin clusters and semi-crystalline growth rings in wheat starches with different amylose content. *Carbohydrate Research*, 339(16), 2683-2691.

Yusuph, M., Tester, R. F., Ansell, R., & Snape, C. E. (2003). Composition and properties of starches extracted from tubers of different potato varieties grown under the same environmental conditions. *Food Chemistry, 82*(2), 283-289.

Zavareze, E. d. R., & Dias, A. R. G. (2011). Impact of heat-moisture treatment and annealing in starches: A review. *Carbohydrate Polymers, 83*(2), 317-328.

Zeeman, S. C., Smith, S. M., & Smith, A. M. (2007). The diurnal metabolism of leaf starch. *Biochemical Journal, 401*(1), 13-28.

Zeeman, S. C., Umemoto, T., Lue, W.-L., Au-Yeung, P., Martin, C., Smith, A. M., & Chen, J. (1998). A mutant of Arabidopsis lacking a chloroplastic isoamylase accumulates both starch and phytoglycogen. *The Plant Cell, 10*(10), 1699-1711.

Zeng, F., Ma, F., Kong, F., Gao, Q., & Yu, S. (2015). Physicochemical properties and digestibility of hydrothermally treated waxy rice starch. *Food Chemistry, 172*, 92-98.

Zhang, B., Dhital, S., & Gidley, M. J. (2013). Synergistic and antagonistic effects of α-amylase and amyloglucosidase on starch digestion. *Biomacromolecules, 14*(6), 1945-1954.

Zhang, S., Fan, X., Lin, L., Zhao, L., Liu, A., & Wei, C. (2017). Properties of starch from root tuber of Stephania epigaea in comparison with potato and maize starches. *International Journal of Food Properties, 20*(8), 1740-1750.

Zhang, G., & Hamaker, B. R. (2009). Slowly digestible starch: concept, mechanism, and proposed extended glycemic index. *Critical Reviews in Food Science and Nutrition, 49*(10), 852-867.

Zhang, G., Ao, Z., & Hamaker, B. R. (2006a). Slow digestion property of native cereal starches. *Biomacromolecules, 7*(11), 3252-3258.

Zhang, G., Ao, Z., & Hamaker, B. R. (2008). Nutritional property of endosperm starches from maize mutants: A parabolic relationship between slowly digestible starch and amylopectin fine structure. *Journal of Agricultural and Food Chemistry, 56*(12), 4686-4694.

Zhang, G., Venkatachalam, M., & Hamaker, B. R. (2006b). Structural basis for the slow digestion property of native cereal starches. *Biomacromolecules, 7*(11), 3259-3266.

Zheng, G. H., Han, H. L., & Bhatty, R. S. (1999). Functional properties of cross-linked

and hydroxypropylated waxy hull-less barley starches. *Cereal Chemistry, 76*(2), 182-188.

Zhou, Y., Hoover, R., & Liu, Q. (2004). Relationship between α-amylase degradation and the structure and physicochemical properties of legume starches. *Carbohydrate Polymers, 57*(3), 299-317.

Ziegler, G. R., Thompson, D. B., & Casasnovas, J. (1993). Dynamic measurement of starch granule swelling during gelatinization. *Cereal Chemistry 70*(3), 247-251.

Zobel, H. (1988a). Molecules to granules: a comprehensive starch review. *Starch-Stärke, 40*(2), 44-50.

Zobel, H. (1988b). Starch crystal transformations and their industrial importance. *Starch - Stärke, 40*(1), 1-7.

APPENDICES

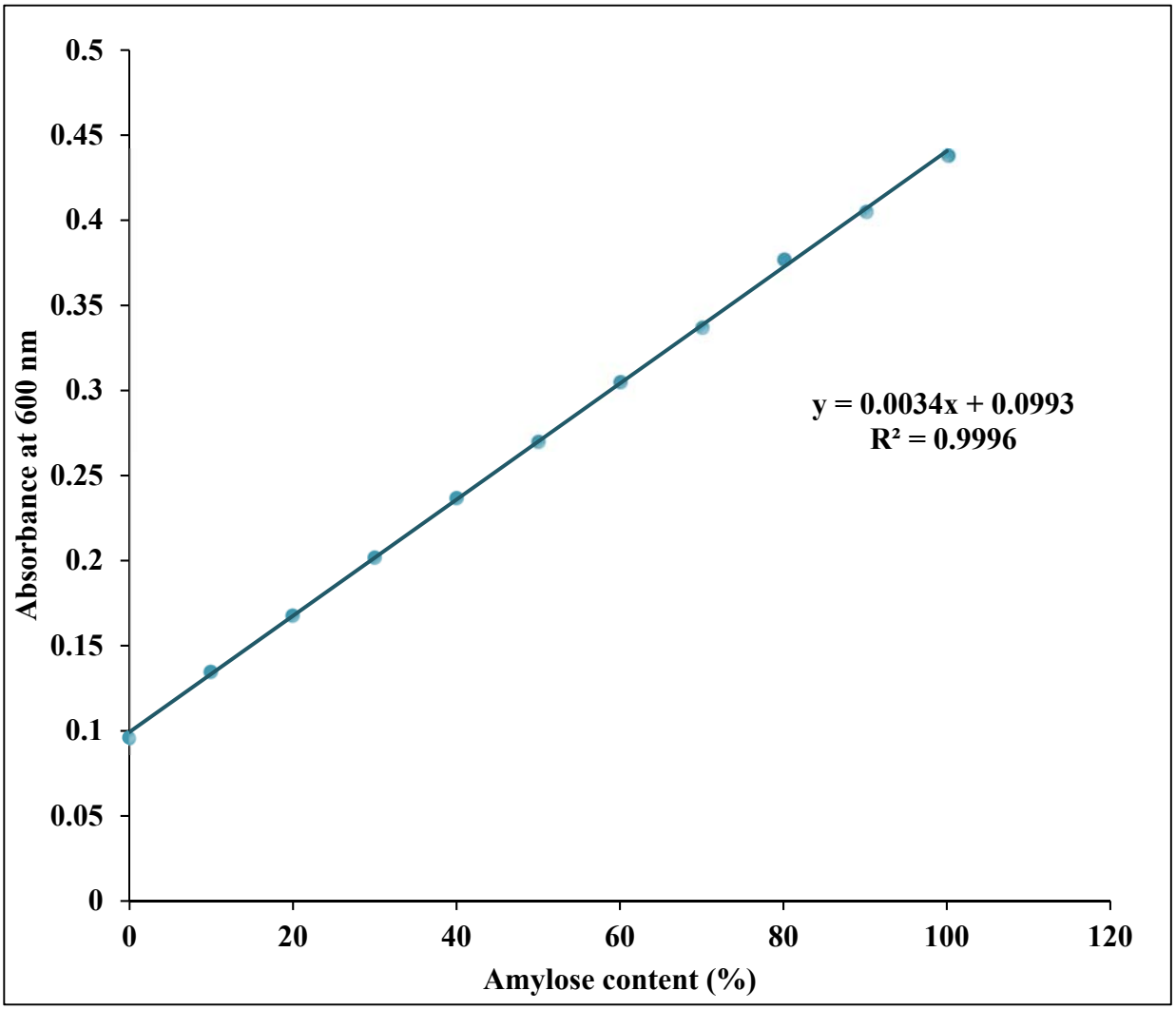

Appendix I: Standard curve for the determination of amylose content (Hoover and Ratnayake, 2004).

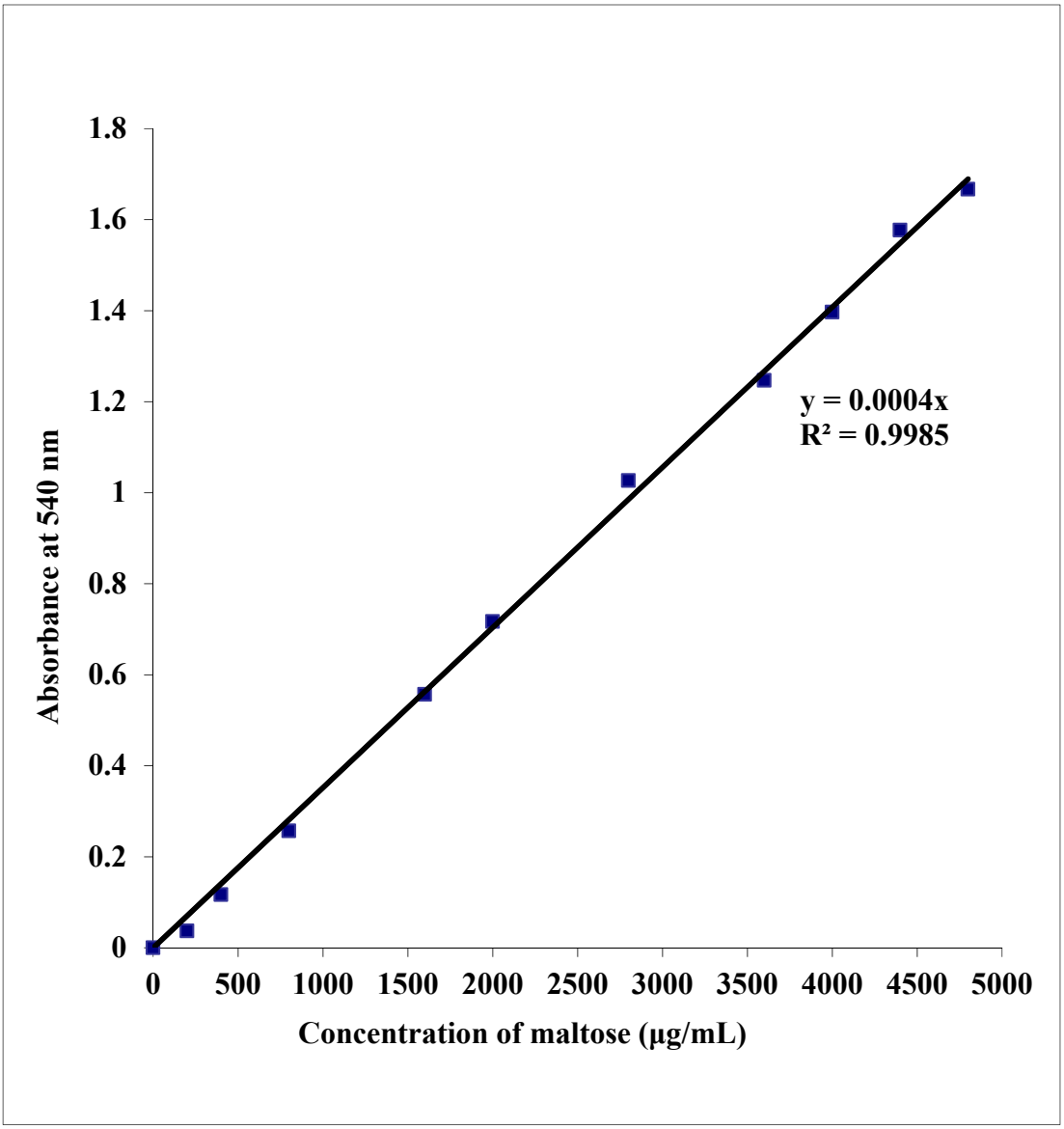

Appendix II: Standard curve for the determination of reducing sugar as maltose.

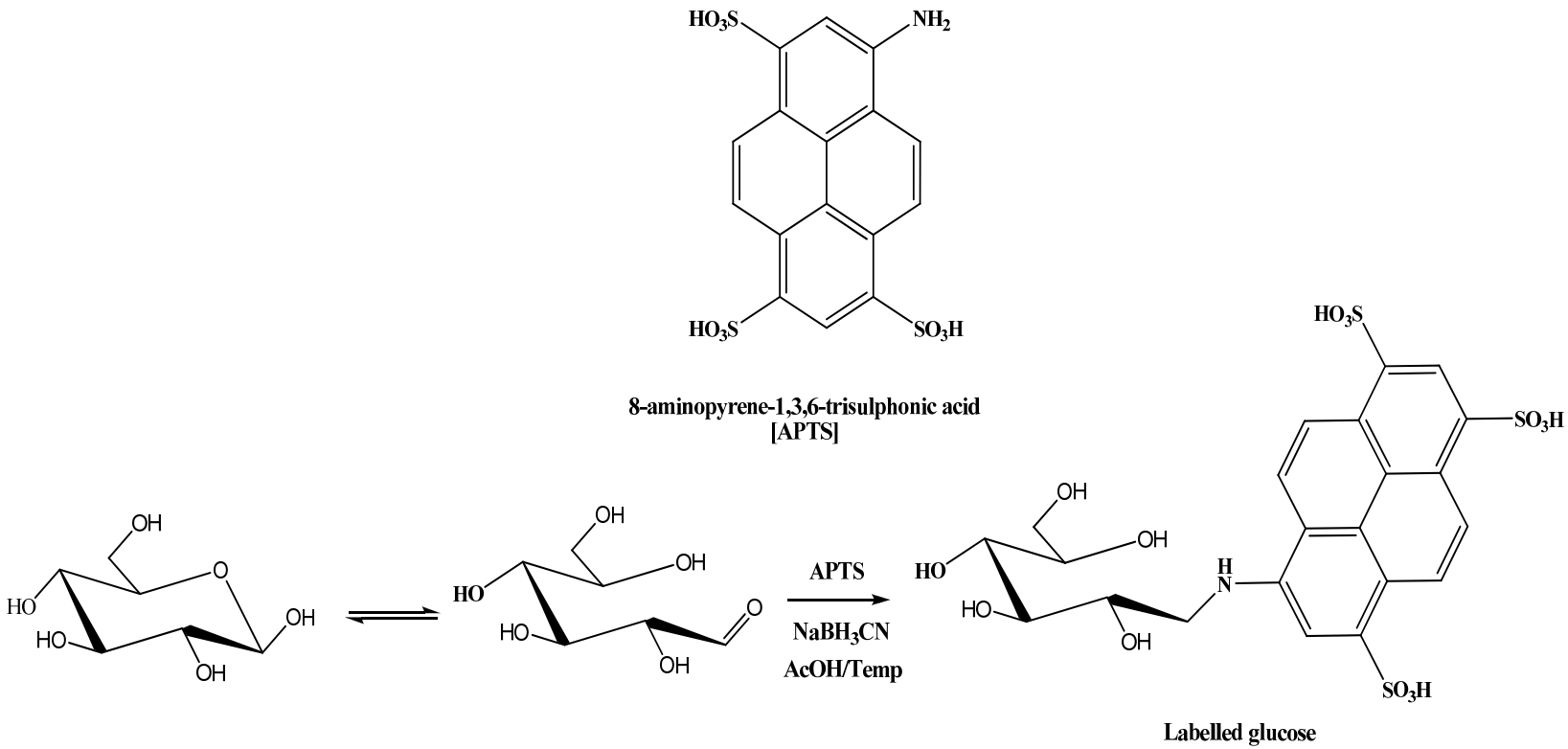

Appendix III: The labelling reaction of 8-amino-1,3,6-pyrene trisulfonic acid (APTS) with a glucose molecule. (Adapted from O'Shea *et al*., 1998).

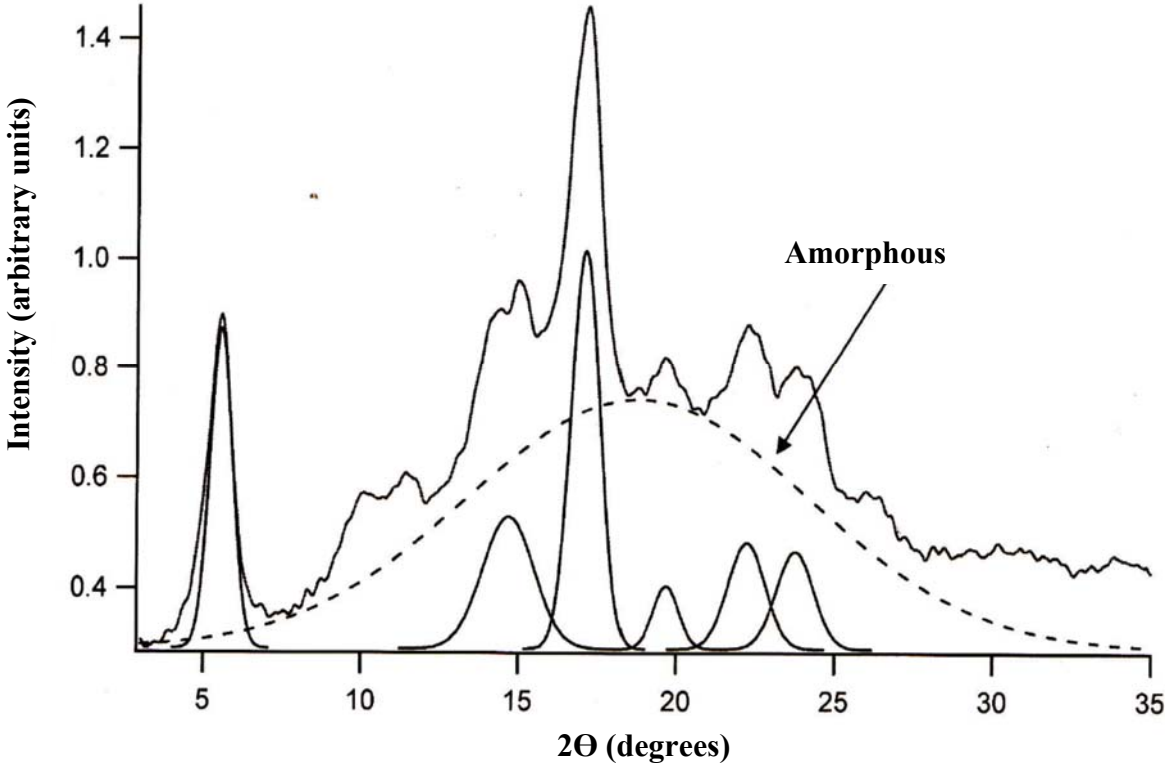

Relative crystallinity of a starch will be calculated after subtracting the amorphous background from the total area.

$$Relative\ crystallinity\ \% = \frac{Total\ peak\ area - Amorphous\ peak\ area}{Total\ peak\ area} \times 100$$

Appendix IV: Curve fitting for XRD using Gaussian function.

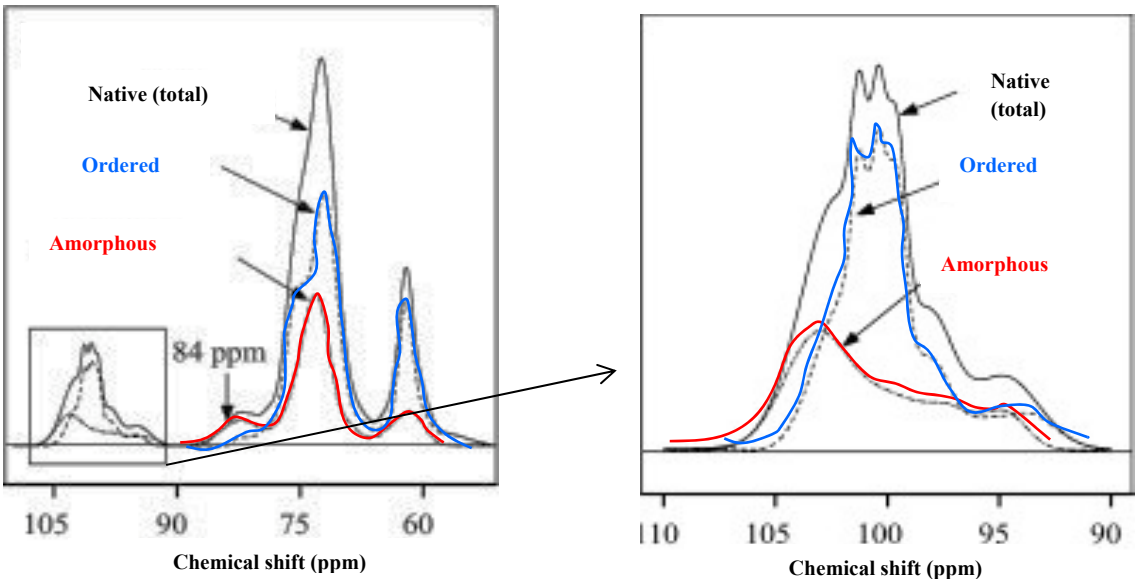

$$\text{Double helix \%} = \frac{\text{Area for the C1 signals in the ordered subspectrum}}{\text{Area for the C1 signals in the native spectrum}} * 100$$

$$\text{Amorphous \%} = 100 - (\text{double helix} + \text{V type helix})\ \%$$

Appendix V: Decomposition of the 13C NMR spectrum into contributions from the amorphous and ordered phases (a) and (b) (Tan *et al*., 2007).

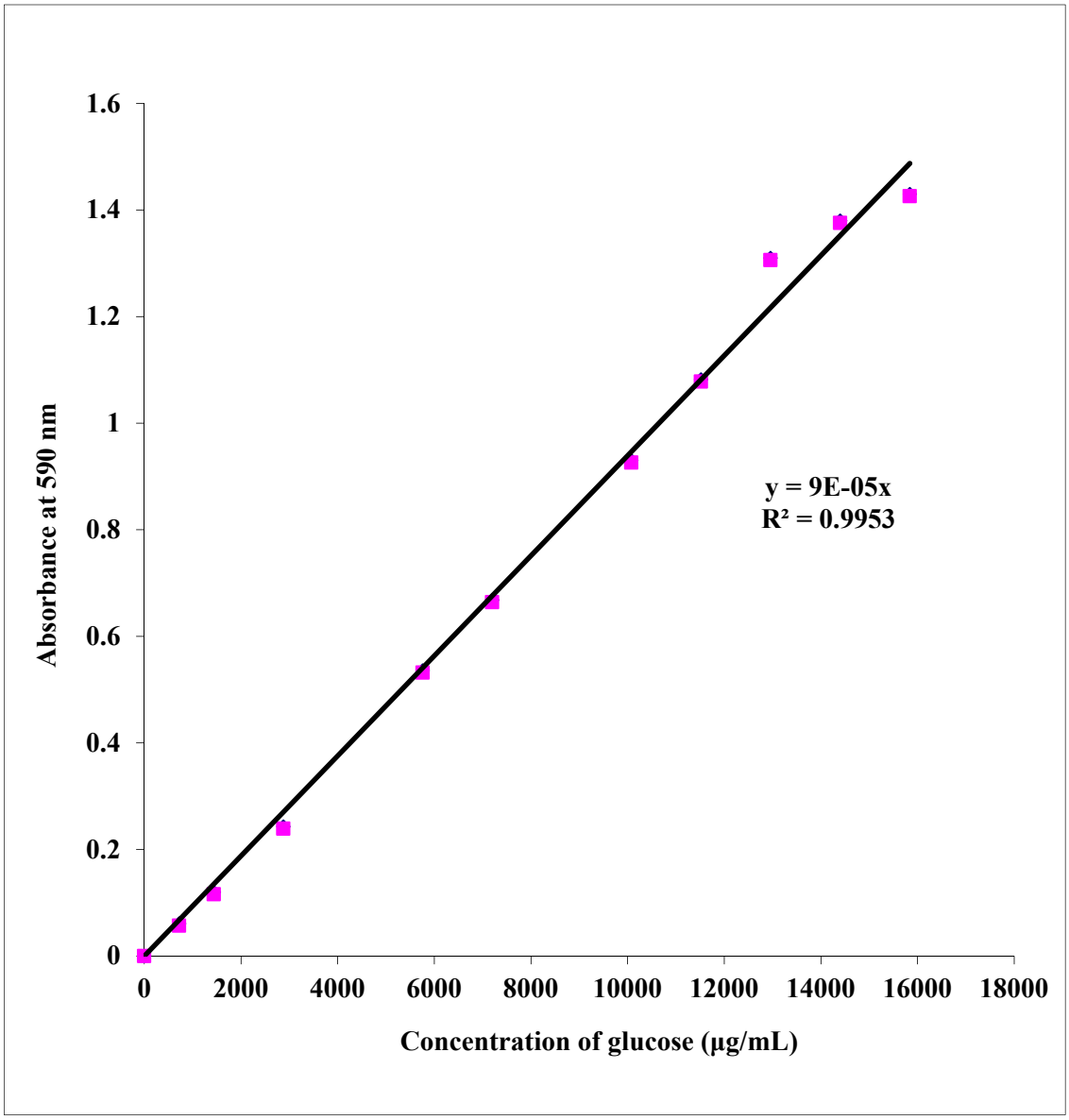

Appendix VI: Standard curve for the determination of reducing sugar as glucose.

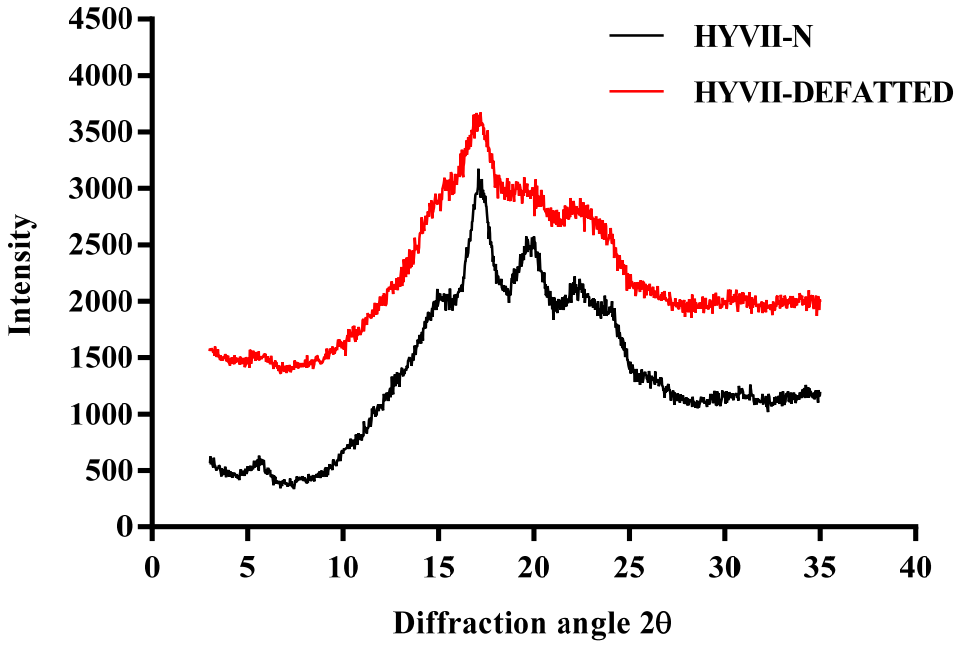

Appendix VII: X-ray diffraction patterns of native (N) and defatted samples of Hylon®VII starch.

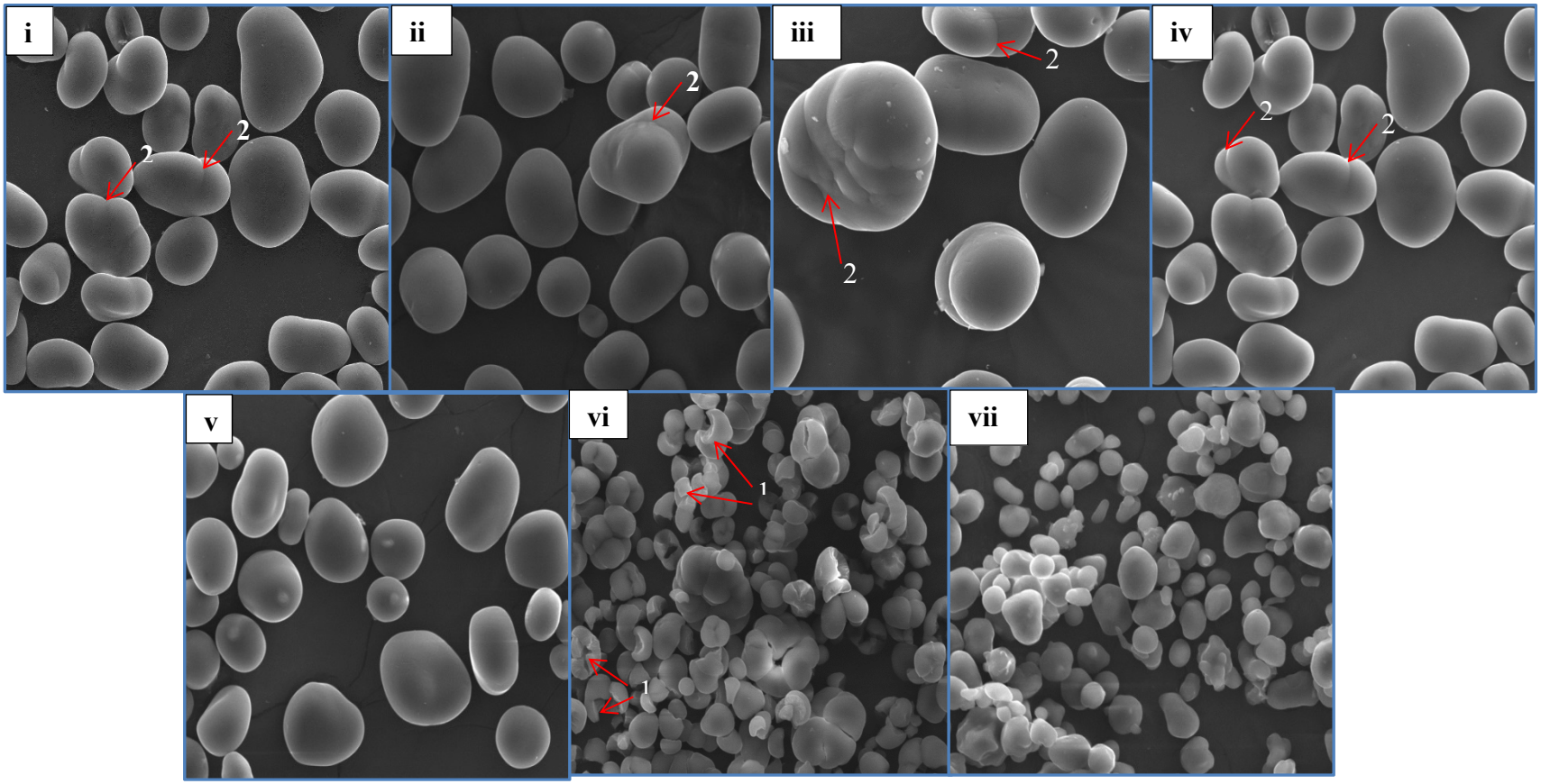

Appendix VIII: SEM images (×1250) of native pulse and HHylon®VII starches. Lablab bean *(i)*, navy bean *(ii)*, rice bean *(iii)*, tepary bean *(iv)*, velvet bean *(v)*, wrinkled pea *(vi)* and HHylon®VII *(vii)* starches. Arrow 1 indicates separated granules of WP. Arrow 2 indicates indentations present on the granule surfaces.

Graduate Program (Memorial University of Newfoundland)

Publications

Maaran, S., Hoover, R., Vamadevan, V., Waduge, R. N., and Liu, Q. (2016). In vitro amylolysis of pulse and Hylon®VII starches explained in terms of their composition, morphology, granule architecture and interaction between hydrolysed starch chains. *Food Chemistry, 192*: 1098-1108.

Maaran, S., Hoover, R., Donner, E., and Liu, Q. (2014). Composition, structure, morphology and physicochemical properties of lablab bean, navy bean, rice bean, tepary bean and velvet bean starches. *Food Chemistry, 152*:491-499.

Conference Presentations

Maaran, S., Hoover, R., Waduge, R. N., and Liu, Q. (2016). Unravelling the mechanism of annealing in pulse and high amylose maize starches. 13th International Hydrocolloids Conference, Guelph, ON, CA, May 16-20, 2016.

Maaran, S., Hoover, R., Vamadevan, V. Waduge, R. N., and Liu, Q. (2015). Structural changes within the amorphous and crystalline domains of high amylose starches on annealing. Starch Round Table Conference, Minneapolis, MN, USA, October 15-17, 2015.

Maaran, S., Hoover, R., Vamadevan, V., and Liu, Q. (2015). How does the hierarchical structure of pulse starches spanning different length scales influence the rate and extent of amylolysis? IFT Annual meeting & Expo, Chicago, IL, USA, July 11-14, 2015.

Maaran, S., Hoover, R., Donner, E. and Liu, Q. (2014). Impact of molecular and supramolecular structure of under-utilized pulse starches on their thermal, rheological and digestibility properties. IFT Annual meeting & Expo, New Orleans, LA, USA, June 21-24, 2014.

Maaran, S., Hoover, R., Donner, E., and Liu, Q. (2014). How is pulse starch digestibility influenced by their molecular and supramolecular structure? Canadian Nutrition Society Annual Meeting, St. John's, NL, CA, June 5-7, 2014.

Symposium Presentations

Hoover, R., **Maaran, S.**, Poudel, A., Raghunathan, R., Ambigaipalan, P., and Liu., Q . (2016). Structure, properties and modification of pulse starches. The Pulse Ingredient Workshop Series, Saskatoon, SK, CA, September 21–23, 2016.

Maaran, S. and Hoover, R. (2015). The effect of annealing on the molecular structure and physicochemical properties of pulse starches. Fifth Annual Biochemistry Summer Symposium, MUN, St. John's, NL, CA, August 11, 2015.

Maaran, S., and Hoover, R. (2015). The relationship between structure, physicochemical properties and nutritional fractions of pulse starches. Aldrich Conference 2015, MUN, St. John's, NL, CA, March 20-22, 2015.

Maaran, S., and Hoover, R. (2014).The impact of morphology, molecular architecture and interaction between hydrolysed starch chains on *in vitro* amylolysis of pulse and high amylose maize starches. Fourth Annual Biochemistry Summer Symposium, MUN, St. John's, NL, CA, August 13, 2014.

Maaran, S., and Hoover, R. (2013). Molecular and supramolecular structure of pulse starches and their impact on physicochemical properties. Third Annual Biochemistry Summer Symposium, MUN, St. John's, NL, CA, August 13, 2013.